A Chemical Based Wet Cold Flow Approach for Addressing Hydrate Flow Assurance Problems

Roghieh Azarinezhad-Mohammadi

Submitted for the degree of Doctor of Philosophy

Heriot-Watt University

Institute of Petroleum Engineering

September 2010

Abstract

Current gas hydrate flow assurance methods are becoming less economical and/or practical for deepwater operations, long tiebacks and ageing reservoirs. The industry thus needs novel flow assurance techniques to address these challenging conditions. An alternative approach called *HYDRAFLOW*, a *chemical based wet Cold Flow* method, has been presented in this thesis in which gas hydrate management, rather than prevention, is the aim. The idea is to convert most of the gas phase into hydrates and transfer it in the form of hydrate-slurry in the pipeline.

This study investigates the concept, i.e. the transportability of hydrate slurries, for different systems (low and high GOR oil systems in the presence and absence of AAs) in different operating conditions, especially in conditions where the other flow assurance solutions either cannot be applied or are not economically viable, e.g. at high watercuts or under very high degree of subcoolings. The experiments involve investigating the rheological behaviour and flow properties of hydrate slurries using the HTI-set up (Helical Tube Impeller, an apparatus designed and build in-house for measuring viscosity of hydrate slurries at high pressures). Additionally, the rate of hydrate formation in low and high oil systems and also at subzero conditions has been measured. Furthermore, the effect of key variables, (e.g. heat transfer, mass transfer, degree of subcooling, salt, anti-agglomerants (AAs) and thermodynamic inhibitors) on the rate of hydrate formation and also on the rheology of hydrate suspensions have been studied in this work. The partitioning of a commercial AA between hydrate, oil and aqueous phases and its performances in each phase have also been determined which can help for decision making about recovering and/or recycling all or part of AAs. And finally, it has been shown that hydrate flow can potentially reducing wax deposition problems in pipeline by abrasion of the deposited wax.

Dedicated to my parents

Acknowledgements

I would like to express my sincere gratitude to Professor Bahman Tohidi for providing me the opportunity to do this research and also for his outstanding supervision, guidance and support throughout my thesis. He was always accessible and willing to help me with my study. On personal side, he did not hesitate to invite me to become an extended part of his family.

I wish to deeply thank Dr. Antonin Chapoy for his technical advice and helpful discussions during the course of this thesis and furthermore for his critical comments on this thesis. My profound thanks are also extended to Ross Anderson, Rod Burgess, Dr. Joanna Lachwa-Langa and Dr. Jinhai Young who helped me constantly with their valuable suggestions and patiently dealt with all my questions. I am also grateful to all my friends and colleagues at the Centre for Gas Hydrate Research and Hydrafact Ltd who made my stay in Edinburgh very pleasant and memorable. Special thanks go to Saied Mazloum who has been a friend and was there whenever I needed his help no matter time or day.

I greatly appreciate the reviewers and examiners of this thesis, Dr. Per Fotland and Dr. Mehran Sohrabi for their precious times and valuable suggestions.

Additionally, I would like to thank the members of mechanical and electrical workshop who were responsible for manufacture and maintenance of the experimental equipments designed and used as part of this study. Other thanks go to Alastair Reid for his assistance in compositional measurements and analysis of the crude oils tested in this work.

The financial support from Dorothy Hodgkin Postgraduate Awards (DHPA) and Heriot-Watt University through their scholarship to conduct this study is gratefully acknowledged.

This study is a part of two research Projects “HYDRAFLOW”, sponsored by Scottish Proof of Concept and “Evaluation of Low Dosage Hydrate Inhibitors” JIP (Joint Industrial Project). The JIP programme is jointly sponsored by Baker Hughes, BASF,

Champoin Technologies, Clariant Oil Services UK Ltd, DONG Energy, Petrobras, Petronas, OMV, Shell/NAM and TOTAL, whose support is gratefully acknowledged.

Last but not least, I express my heartfelt appreciation to my family for their love, moral support and patience during my absence. Special and invaluable thanks go to my sister's family here in the UK: Fariba, Morteza and Holly. I cannot thank them enough for all the unconditional support they provided me while I was facing the most stressful times. They kept me going and never let me feel that I am away from our family and country.

Table of Contents

List of Tables

List of Figures

List of Publications by the Candidate

Some of the results of this research have been published in the following peer reviewed journals and conferences. All the conference papers were orally presented by the candidate.

Azarinezhad, R., Chapoy, A., Anderson, R. and Tohidi, B., 2010. A Wet Cold-Flow Technology for Tackling Offshore Flow-Assurance Problems. *SPE Project, Facilities & Construction Journal*, **5** (No. 2), pp:58-64.

Azarinezhad, R., Valko, I., Chapoy, A. and Tohidi, B., 2008. Can Gas Hydrates Provide a Solution to Gas Utilisation Challenges in Russian Oil Field? *SPE Russian Oil and Gas Technical Conference and Exhibition.* Moscow, Russia, 28-30 October 2008.

Azarinezhad, R., Chapoy, A., Anderson, R. and Tohidi, B., 2008. HYDRAFLOW: A Novel Approach in Addressing Flow Assurance Problems. *6th International Conference on Gas Hydrates*. Vancouver, British Columbia, CANADA, 6-10 July 2008.

Azarinezhad, R., Chapoy, A., Anderson, R. and Tohidi, B., 2008. HYDRAFLOW: A Multiphase Cold Flow Technology for Offshore Flow Assurance Challenges. *Offshore Technology Conference*. Houston, Texas, USA, 5-8 May 2008.

Azarinezhad, R., Valko, I., Tohidi, B. and Glazkov, O., 2008., HYDRAFLOW: A New Approch for Associated Gas Capturing. *Oil Industry Journal*, No.11, pp.93-97. (Азаринежат Р., Валько И., Тохиди Б. and Глазков О., 2008. Концепция HYDRAFLOW: новый подход к утилизации газа на российских месторождениях, *Нефтяное хозяйство журнал*, No 11, сс. 93-97).

Haghighi, H., Azarinezhad, R., Chapoy, A., Anderson, R. and Tohidi, B., 2007. HYDRAFLOW: Avoiding Gas Hydrate Problems. *Europec/EAGE Annual Conference and Exhibition.* London, 11-14 June 2007.

Chapter 1. Introduction

1.1. Introduction

Flow assurance is a term in petroleum industry which refers to ensuring economical and uninterrupted production of oil and gas. It usually involves effective handling or preventing solid deposits like, wax, asphaltene, natural gas hydrates and scale. When water is produced along with petroleum fluids, there are other potential problems such as corrosion and emulsion that also reduce the profitability of oil and gas production. However, gas hydrate management is considered to be the most critical aspect of flow assurance design strategies because hydrate plugs can have major safety and economical impacts on oil and gas production operations and can completely stop production for several days or months and even in the worst case result in pipeline abandonment (Sinquin et al., 2004).

Generally, most of existing gas hydrate flow assurance techniques are based on one or a combination of the following techniques: 1) maintaining pipeline operating conditions outside the hydrate stability zone (e.g. by insulation and/or active heating), 2) preventing hydrate formation by injecting thermodynamic inhibitors (e.g. methanol, ethylene glycol), 3) sufficiently delaying hydrate nucleation/growth by injecting kinetic hydrate inhibitors (KHIs), and 4) reducing water content. However, all of these methods are becoming less practical due to their high cost and/or limitation

particularly in deep waters and high water-cuts (Azarinezhad et al., 2008). Therefore the industry is moving to managing hydrate formation and transportation rather than prevention. These techniques are generally regarded as cold flow, which have several common characteristics, including, 1) no heating or insulation, 2) hydrates are not prevented but allowed to form, and 3) their agglomeration is avoided by various techniques. Several research groups are working on various cold flow concepts, most notably SINTEF-BP (Lund et al., 2000; Lund and Larsen, 2000; Larsen et al., 2001; Larsen et al., 2003; Lund et al., 2004; Wolden et al., 2005; Larsen et al., 2009) and NTNU (Gudmundsson, 2002). IFP has also studied hydrate slurries in flowing conditions and particularly in multiphase flow lines (Peysson, 2003; Singuin et al., 2004).

This thesis will investigate some aspect of *HYDRAFLOW* concept, which is a new patented (Tohidi, 2006) cold flow assurance technology, developed at the Centre for Gas Hydrate Research, Heriot-Watt University. The *HYDRAFLOW* concept is based on allowing gas hydrate formation but preventing their agglomeration and pipeline blockage. The idea is to convert most or all of the gas phase into hydrates and transfer them in the form of hydrate slurry in the pipeline. Where possible, it is proposed to use a "Loop" concept, which allows circulating the liquid phase (totally or partially) and its associated additives. The recycled fluid acts as carrier fluid, transferring produced hydrocarbons to their destination (e.g. platform). In this case, all or part of the additives including anti-agglomerants (AAs) can be recycled, hence reducing the operational cost and potential environmental impacts. Where produced water is the limiting factor for hydrate formation, excess water (either produced or added seawater) can be added. It is also possible to adjust the hydrate slurries viscosity by adjusting the amount of water. AAs might be necessary to control the hydrate crystal size and prevent solid blockage in these systems. They are a type of Low Dosage Hydrate Inhibitor (LDHI), which do not prevent the formation of hydrates, but work by changing the properties of the forming hydrate slurries to ensure that hydrate crystals do not agglomerate and potentially block flowlines. The main advantage of AAs over KHIs is that they are able to inhibit hydrates at higher subcoolings, and can be effective even at subcoolings over 20 °C (Kellant, 2006). Therefore, they have a much wider range of pressure-temperature applications and can be used for deepwater application.

Chapter 2 provides a basic definition of gas hydrates and reviewing the existing gas hydrate flow assurance methods, advantages/disadvantages attached to each method and limitation of the current solutions. A specific attention has been devoted to presenting different types of AA chemicals and the mechanism of their inhibition because AAs have been widely used in this study for controlling the rheological behaviour of hydrate slurries. The rest of the chapter introduces the most notable Cold Flow concepts including *HYDRAFLOW*. And finally, the chapter closes with an economic evaluation of *HYDRAFLOW* concept and providing selection criteria for flow assurance methods. It will be shown that there is a high potential for *HYDRAFLOW* to be adopted by the oil and gas industry due to its economical and technical benefits.

In order to design properly the production systems to implement this Cold Flow technology, it is critical that the rheological behaviour of hydrate slurries in flowing and shut-in/restarts conditions is well understood. While hydrate thermodynamic properties such as equilibrium temperature, pressure and composition, i.e. required for conventional methods of preventing hydrate formation, have reached a good degree of reliability, studies on the rheological behaviour and time dependent phenomena of formation and aggregation of hydrates are, however, at relatively early stages of development. A better understanding of flow properties and time dependent aspects of hydrates is essential if the industry is to be move towards hydrate management through plug prevention. This is an area where there is still little published information. Chapter 3 summarises studies and ideas surrounding hydrate plugging and rheology and discuss the effect of key variables on flow characteristics of hydrate slurries. The lessons learned from this chapter will be used in conducting the experiment for demonstrating the *HYDRAFLOW* concept in Chapters 5 to 7.

Another factor, which is crucial to the successful development of hydrate risk management methods is to have a device and methodology that can accurately measure and evaluate the flow properties of hydrate slurries. If such a readily measurable and repeatable rheological data existed for hydrate transport properties, then the application of cold flow technology could be greatly increased. Currently, there is neither a standard device nor methodology for measuring rheological properties of hydrate slurries. Generally, devices used are custom-built by some research groups with particular research requirements. Therefore, a purpose-built apparatus called the

Helical Tube Impeller (HTI) setup, designed and built in-house, was calibrated and validated for studying the flow properties of hydrate slurries, i.e. viscosity of hydrate slurries. The HTI Set-up is a high pressure autoclave cell with a typical volume of about 2.5 litres equipped with a magnetic stirrer with adjustable rotational speed and voltmeter/ampere-meter to measures the voltage and current needed to calculate the torque, shear rate and viscosity. Chapter 4 presents the description, calibration and validation of this apparatus. The various apparati available for visual and rheological studies of hydrate suspensions have been also reviewed in this chapter. To examine the transferability of data from small scale to large scale experiments, a limited number of tests were performed in parallel both in the HTI Set-up and in an in-house flow loop (C–FAR (Centre for Flow Assurance Research)). The flow loop set-up comprises of a 1" (2.5 cm) diameter, 40 m length loop driven by a Moineau pump system. The results will confirm that viscosity values in the C-FAR flow loop and laboratory scale HTI-set up are comparable, validating the laboratory scale data. The study continues with demonstrating the HYYDRAFLOW concept for different oil and gas systems at different operating conditions. The experiments are focused on investigating the rheological behaviour and flow properties of hydrate slurries using the HTI-set up.

Chapter 5 has three major parts. The first part will describe the evaluation procedures and the results of the investigation on the transportability of hydrate slurries in low and high GOR oil systems and the effect of AAs on the rheological behaviour of the above systems. The second part of the Chapter 5 focuses on the time-dependent behaviour of hydrate slurries. One of the important time-dependent challenges regarding hydrates is their growth rate which can be controlled by heat and mass transfer. As detailed in this chapter, to investigate the effect of heat and mass transfer on hydrate formation and growth, different systems (e.g., low and high GOR oil systems) under different heat and mass transfer scenarios were investigated in this study. The principles can be extended to hydrate formation in a pipeline. In addition, experiments were carried out at two different subcoolings to investigate the effect of driving force on hydrate growth rate. Finally, the last part of the chapter examines the effect of salt on the performance of AAs and consequently on the rheological behaviour and flow properties of water/oil/hydrate slurries as produced water is normally saline in nature and this could affect the performance of different additives including AAs.

In Chapter 6, the *HYDRAFLOW* concept will be demonstrated in conditions where other flow assurance solutions either cannot be applied or are not economically viable, e.g. at high watercuts (>50%) or under very high degree of subcoolings. In these cases large amount of thermodynamic inhibitors are required (in conventional methods) to either shift the hydrate phase boundary to conditions where KHIs can work or to achieve total hydrate inhibition at operating conditions. Furthermore it has been generally accepted by the hydrate community that AAs are not effective at high water-cuts. However, very recently, some chemical companies have developed new AA formulations and they are claiming that their AAs are now effective up to 80-90% watercut. Therefore, in order to obtain a transportable slurry at watercuts >60 % the onus in this chapter will be on testing suitable AAs for high water-cut systems. In the case of high degree of subcoolings, e.g. across a choke with subcooling higher than 20 °C, ultra-deep offshore, permafrost and Arctic, systems may experience sub zero conditions and potential ice formation. Under this condition, the concern can be the potential negative effect of ice on the AA performance at subzero conditions. The approaches which can be adopted to address this challenge will be also examined in this chapter.

The results of the work in Chapter 5 and 6 have proved that *HYDRAFLOW* concept is viable (at least under laboratory conditions). Chapter 7 will examine a number of practical aspects of the concept. The specific objectives are:

- Demonstrating the reduced wax deposition problems in the presence of hydrates
- Measuring partitioning of AA between phases (hydrate, water and oil) and examining the efficiency of distributed AA in each phase for recycling purpose – Application of the *HYDRAFLOW* 'loop' concept
- Testing the performance of biodegradable (green) AAs – Application of the *HYDRAFLOW* 'loop' concept

The thesis will be finished with some conclusions of the work and remarks and suggestions on how to develop and further improve the *HYDRAFLOW* concept. The lessons learned from this study will provide valuable information on the application of the concept. However, as in most cases in the oil and gas industry, further studies for a specific case will often be required for accurate decision-making.

1.2. References

Azarinezhad, R., Chapoy, A., Anderson, R. and Tohidi, B., 2008. HYDRAFLOW: A Novel Approach in Addressing Flow Assurance Problems. *6th International Conference on Gas Hydrates*. Vancouver, British Columbia, CANADA, 6-10 July 2008.

Gudmundsson, J. S., 2002. Cold Flow Hydrate Technology. *4th International Conference on Gas Hydrates*. Yokohama, 19-23 May 2002.

ITI Energy, 2004. Foresighting Report – Maximising Value of Mature Oil and Gas Assets. Scotland, October 2004.

Kelland, M. A., 2006. History of the Development of Low Dosage Hydrate Inhibitors. *Energy and Fuels*, **20**, pp.825–847

Larsen, R., Lund, A., Andersson, V. and Hjarbo, K. W., 2001. Conversion of Water to Hydrate Particles. *SPE Annual Technical Conference and Exhibition*. New Orleans, Louisiana, 30 September-3 October 2001.

Larsen, R., Lund, A. and Argo, C.B., 2003. Cold Flow - A Practical Solution. *11th International Conference "Multiphase 03", BHR group*. San Remo, Italy, 11-13 June 2003.

Larsen, R., Lund, A., Hjarbo, K. W and Wolden, M., 2009. Robustness Testing of Cold Flow. *20th International Oil Field Chemistry Symposium*. Geilo, Norway, 22-25 March 2009.

Lund, A., Lysne, D., Larsen, R. and Hjarbo, K. W, 2004. *Method and System for Treansporting a Flow of Fluid Hydrocarbons Containing Water*. US Pat. 6,774, 276, B1.

Lund, A., Hjarbo, K. W, Larsen, R. and Lysne, D., 2000. Method and System for Treansporting a Flow of Fluid Hydrocarbons Containing Water. CA. Pat. 2 569 693.

Lund, A. and Larsen, R., 2000. Conversion of Water to Hydrate Particles – Theory and Application. 14th Symposium on Thermophysical Properties, Boulder, CO. USA, June 2000.

Palermo, T., Mussumeci, A. and Leporcher, E., 2004. Could Hydrate Plugging Be Avoided Because of Surfactant Properties of the Crude and Appropriate Flow Condition?. *Offshore Technology Conference*. Houston, Texas, U.S.A. 3-6 May 2004.

Peysson, Y., Nuland, S., Maurel, P. and Vilagines, R.: 2003. Flow of Hydrate Dispersed in Production Lines. *SPE Annual Technical Conference and Exhibition*. Denver, Colorado, US, 5–8 October 2003.

Sinquin, A., Palermo, T. and Prysson, Y., 2004. Rheological and Flow Properties of Gas Hydrate Suspensions. *Oil & Gas Science and Technology-Rev. IFP*, **59**(No. 1), pp.41-57.

Tohidi, B., 2006. *Novel Hydrate Based Systems*. International Pat. WO 2006/048666.

Chapter 2. Hydrates and Strategies for avoiding their problem

2.1. Introduction

The purpose of this chapter is to give an overview of gas hydrate, their problems in oil and gas industry and review the existing flow assurance solutions and their limitations for tackling these problems. A further objective of this chapter is to introduce the "Cold Flow" concept, an emerging alternative solution for addressing gas hydrate flow assurance problems. Several major cold flow approaches/methods will be discussed as well.

2.2. What are gas hydrates?

Natural gas hydrates are ice-like crystalline structures formed by hydrogen bonded water molecules and stabilised by the presence of guest molecules within the lattice cavities. Without the support of the trapped molecules, the lattice structure of hydrate clathrates would collapse into conventional ice crystal structure or liquid water. The molecules commonly found in natural gas that occupy the cavities are light alkanes (C_1-C_4), carbon dioxide, nitrogen and hydrogen sulphide. A schematic illustration of one of the possible gas hydrate structure is shown in Figure 2.1

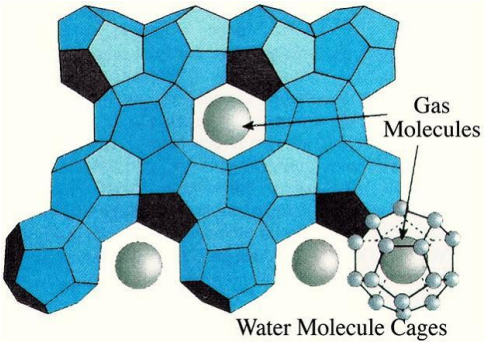

Figure 2.1 Schematic of one of the possible gas hydrate structure (Monicore website)

Three main structural types of gas hydrates, named sI, sII, and sH, have been characterized using neutron or X-ray diffraction techniques. Structural details of sI and sII appeared in 1951 when Claussen (Claussen, 1951) proposed a structure based on ab initio calculations that was soon proven to be correct by von Stackelberg (von Stackelberg and Muller, 1951). Structure H was determined more recently by Ripmeester (Ripmeester 1987). The type of the structure formed depends primarily on the size of the guest molecules. Small and round molecules like methane and carbon dioxide form structure I. While typical natural gas mixture containing C_1-C_4 components will preferentially form structure II hydrate. For inclusion of larger molecules such as n-butane which can go into the large cavities of sII, the presence of a smaller 'help' gas such as methane is required to fill small cavities and stabilise the structure. sH is capable of trapping much larger molecules, such as methylcyclohexane. Figure 2.2 (Sloan, 2003) shows the three common hydrate unit crystal structures and geometry of the cages. Each structure is a combination of small and larger cages. When a minimum number of cavities are occupied, crystals become stable and hydrate forms. Gas hydrates can form at temperatures well above the freezing point of water depending on the pressure. If all the cages are occupied, the ratio of water molecules to hydrocarbon molecules would be 5.67 to 5.75 depending on the formed structure. A detailed description of the molecular structure has been given by (Sloan and Koh, 2008).

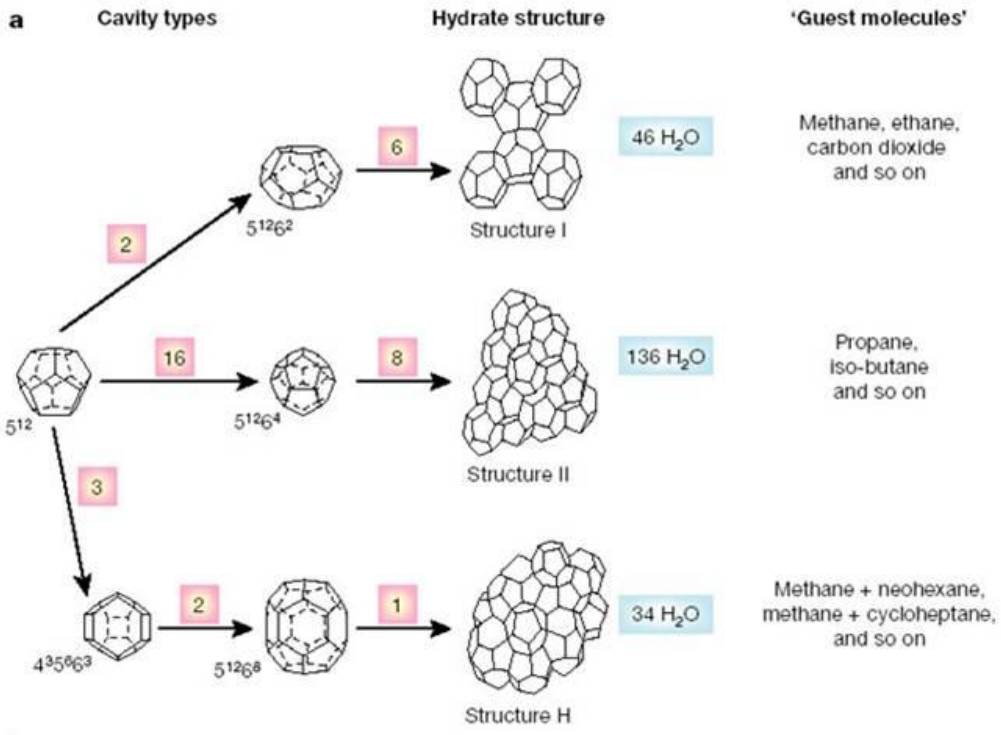

b

Hydrate crystal structure	I		II		H		
Cavity	Small	Large	Small	Large	Small	Medium	Large
Description	5^{12}	$5^{12}6^2$	5^{12}	$5^{12}6^4$	5^{12}	$4^35^66^3$	$5^{12}6^8$
Number of cavities per unit cell	2	6	16	8	3	2	1
Average cavity radius (Å)	3.95	4.33	3.91	4.73	3.91†	4.06†	5.71†
Coordination number*	20	24	20	28	20	20	36
Number of waters per unit cell	46		136		34		

*Number of oxygens at the periphery of each cavity.
†Estimates of structure H cavities from geometric models.

Nomenclature: $5^{12}6^4$ indicates a water cage composed of 12 pentagonal and four hexagonal faces. The numbers in squares indicate the number of cage types. For example, the structure I unit crystal is composed of two 5^{12} cages, six $5^{12}6^2$ cages and 46 water molecules.

Figure 2.2 The three common hydrate unit crystal structures and geometry of cages.

2.3. Gas hydrate stability zone

Natural gas hydrate form when natural gas molecules are in contact with water and the pressure is above a certain point at a given temperature or the temperature is below a certain point at a given pressure. For a given composition of hydrocarbons, a curve of temperature and pressure can be measured and/or predicted from statistical thermodynamics using modern thermodynamic computer programmes such as HWHYD (Heriot-Watt University), CSMGem (Colorado School of Mines), PVTSim (Calsep), ECLIPSE PVTi (Schlumberger), Hysys (AspenTech), etc. These

programmes are usually based upon the solid solution theory of van der Waals and Platteeuw. The hydrate phase boundary will generally have an upward curvature. The area to the right of the curve will be free of hydrates, whereas the area to the left represents conditions where hydrates can form. This is illustrated in Figure 2.3 where curves for natural gas–water system and natural gas–aqueous systems with 10 mass% of different thermodynamic inhibitors are plotted. The effect of presence of heavier components is also shown in the gas condensate phase boundary. The lines represent predictions calculated using HWHYD 2.1 software, which is developed by the Centre for Gas Hydrate Research at Heriot-Watt University. The points are experimental data published by Ng et al (Ng et al, 1985) and Haghighi et al. (Haghighi et al., 2009 a, b). As can be seen, the addition of thermodynamic inhibitors such as salt, methanol and ethylene glycol to the aqueous phase shifts the curves to lower temperatures (or higher pressures). This is the most straightforward way of preventing the formation of gas hydrates. This will be discussed in more detail later in Section 2.5.1, entitled, "Injecting thermodynamic inhibitors". In contrast, the increase in the proportion of heavier/rounder components (propane and butanes) in the gas phase shifts the curves to right hand side (higher temperatures or lower pressures) and cause hydrates to become more stable.

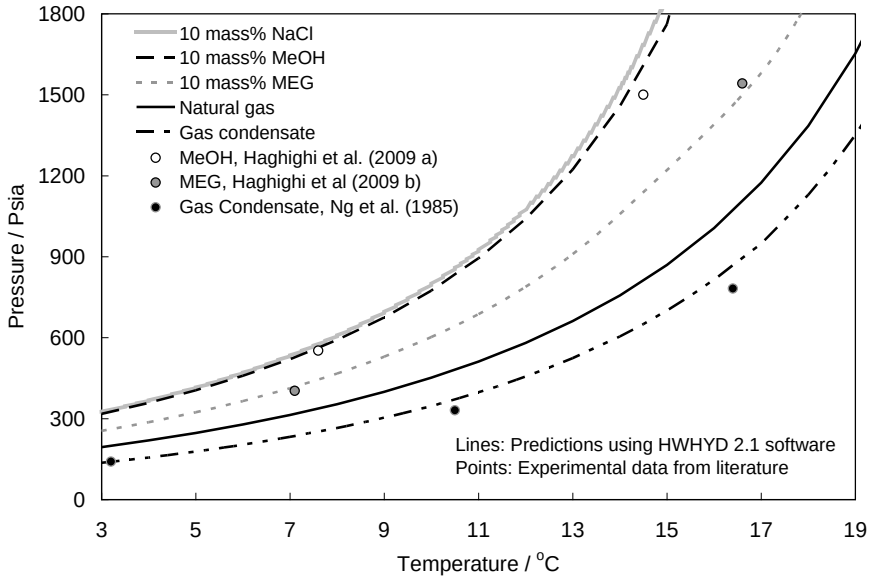

Figure 2.3 Hydrate phase boundary for natural gas and a gas condensate and effect of thermodynamic inhibitors and heavier hydrocarbons on hydrate forming condition

2.4. Gas hydrate problems

Hydrates are a major challenge to the petroleum industry because uncontrolled formation of hydrate may result in plugging of transport pipeline and may cause considerable production loss and safety hazard. Figure 2.4 shows gas hydrates recovered after pigging of a subsea transfer line.

Pressure and temperature conditions favourable for gas hydrate formation are commonly encountered during winter in onshore and in shallow water offshore fields, and regularly in deepwater fields offshore. Hydrates not only can form in transfer lines and tiebacks, but they can also form across gas expansion valves (rapid cooling) and during drilling following a gas kick. Moreover, avoiding gas hydrate problems in shut-in and start-up is a major consideration during pipeline design and operation. On shut-in, the line temperature cools to that of the ocean floor. The seafloor temperature is usually around 4 °C and provides an infinite cooling medium for the warm fluids from the reservoir.

Figure 2.4 Gas hydrate removed from a subsea transfer line (courtesy of Petrobras)

In general, when the produced multiphase fluids flow through the cold pipelines; they become colder and hydrates may form. As solid hydrates forms, they can deposit on the pipe walls or agglomerate into larger solid masses. They can eventually prevent production. The removal of hydrate plugs is generally difficult to achieve. A shutdown of several days or weeks may be required and pipeline abandonment may occur in the worst case scenario. In addition, hydrate plug removal could also cause considerable damage to production facilities such as line rupture and could create a serious safety and environmental hazard.

Upstream pressure in pipeline can cause hydrate plug to move at high velocity. When a hydrate plug moves down a flow line at high velocities, it can fracture the pipe where the pipe bends. Also when gas is compressed at a pipeline obstruction (flange or valve) or restriction (orifice) if the velocity is high enough, the momentum of the plug can cause the pressure to raise enough to rupture the flow line. Another safety problem can occur when high differential pressure is trapped between plugs as there is no method to predict if a single or multiple plugs have formed. And finally, when hydrate plugs are dissociated by heating, any confinement will cause a rapid gas pressure increase because hydrates contain 164 volumes (STP) of gas per volume of hydrate (Sloan and Koh, 2008).

For these reasons, hydrate plug formation (not necessarily hydrate formation) should be prevented effectively and economically to guarantee that pipelines operate normally.

2.5. Current gas hydrate flow assurance strategies

The traditional gas hydrate flow assurance methods rely on the idea of avoiding hydrate formation while the new methods are based on delaying hydrate formation and/or preventing hydrate agglomeration by controlling solid hydrate particle sizes. These two flow assurance methods can be categorised as follows:

- Avoiding hydrate formation
- Controlling hydrate formation by means of Low Dosage Hydrate Inhibitors (LDHIs)

2.5.1. Avoiding hydrate formation

The traditional gas hydrate flow assurance methods rely on removing or modifying one of the essential elements required for hydrate formation, e.g. water or conditions suitable for hydrate formation. Hydrate can be avoided by dehydration which reduces the amount of water available for hydrate formation or by keeping operating pressure and temperature outside the hydrate formation region.

The later method is based on shifting the hydrate phase boundary outside the operating conditions (pressure and temperature of production facility) during normal production (as illustrated in Figure 2.5). This can be achieved by either pushing the hydrate phase boundary of the system to the left by adding chemical compounds such as

thermodynamic inhibitors, by shifting the operating line to the right by heating and/or insolating the flow line. It may also be possible to shift the operating line outside the hydrate stability zone by controlling the operation pressure (though this option is normally used for hydrate plug dissociation by depressurisation).

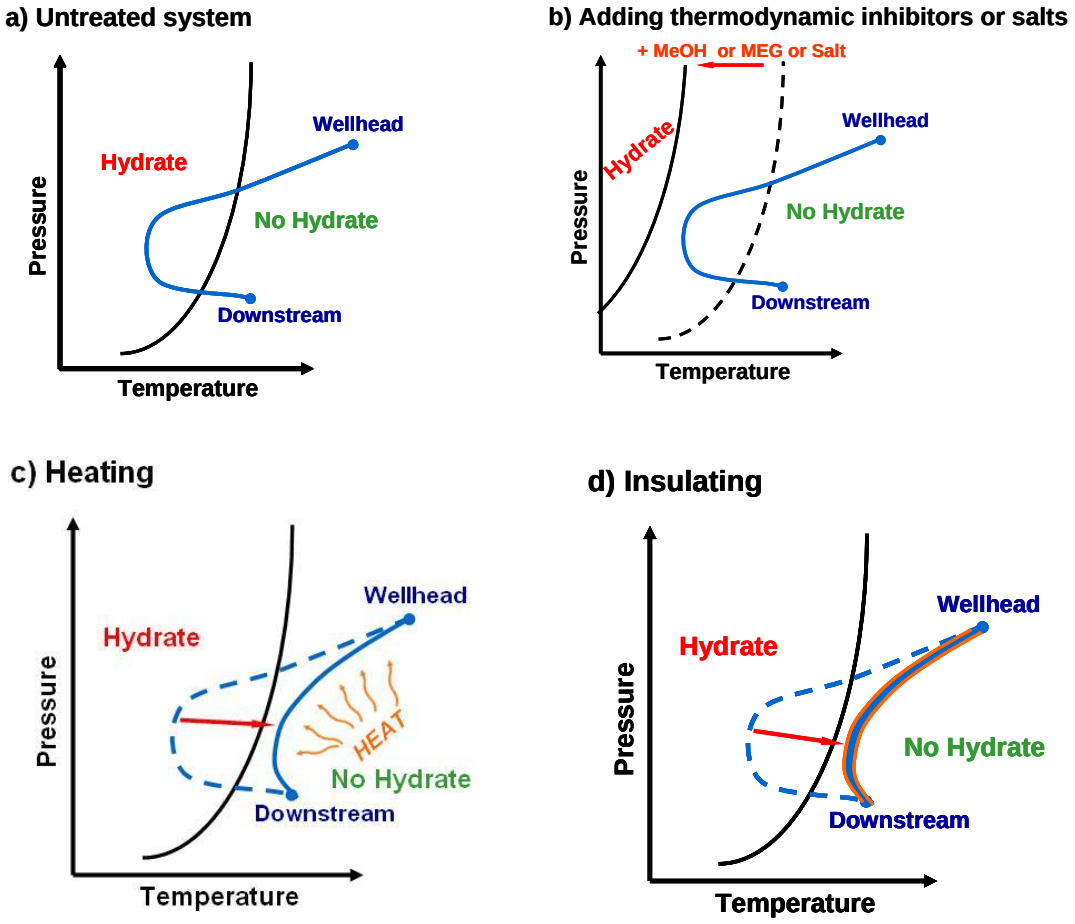

Figure 2.5 Location of operating line and hydrate phase boundary in different flow assurance strategies

All the above mentioned methods will be detailed in the following parts.

Dehydration: This is a permanent solution which removes water from the system so the amount of water left in the system is not enough to form hydrate blockages under operating pressure and temperature conditions. Water content of gas phase can be lowered either through molecular sieve or glycol dehydration plant. Technical disadvantage of this method is that the water left in the fluid stream might build up over time and lead to hydrate formation. From an economic view point, this method requires significant capital expenditure. Obviously, it will need large dehydration unit and relevant personnel which is very costly in offshore environment.

Injection of thermodynamic inhibitors: The addition of thermodynamic inhibitors (typically alcohols, glycols) is an indirect way of removing the free water so that much of the free water is hydrogen bonded to the inhibitor. This reduces the water activity hence lower temperatures at a given pressure are required to form hydrates (Sloan and Koh, 2008). Therefore, the system can be operated safely outside the hydrate stability region. The most commonly used substances are methanol and mono-ethylene glycol (MEG). Methanol is the most widely used inhibitor in the Gulf of Mexico and West Africa while MEG tends to be used more widely in the North Sea and Asia-Pacific region. Both methanol and MEG are used in onshore and shallow water offshore field in North and South America and in the Middle East. In Brazil, ethanol is the thermodynamic inhibitor of choice because of its wide availability. Other alcohols such as diethylene glycol DEG and polypropylene glycol (PPG) are used to a lesser extend for hydrate inhibition, but are used sometimes in the field for plug remediation (Metha et al., 2005).

Another natural thermodynamic inhibitor is the salt that is present in the produced brine. The salt ionises in solution and interacts with the dipoles of the water molecules with a much stronger Coulombic bond than either the hydrogen bond or the van der Waals forces that cause clustering around a polar solute molecule. The stronger bonds of water with salt ions inhibit hydrate formation; water is attracted to ion more than water is attracted to the hydrate structure (Sloan and Koh, 2008). Chevron Texaco (now Chevron) has patented a method for inhibiting hydrate blockage in a flow line by adding water and/or salt to a system. Sufficient water may be added such that the fluid is converted from a water-in-oil emulsion to an oil-in-water emulsion (Matthews et al., 2005).

In some Gulf of Mexico cases the water is naturally saturated with salt and adding other chemical inhibitors like methanol or glycol to the aqueous phase can cause problems such as salt precipitation (rather than hydrate prevention) (Kini et al., 2005). Ethylene glycol has a much lesser adverse impact on the salt deposition than methanol and ethanol (Masoudi et al., 2006).

Selection of the thermodynamic inhibitors often involves comparison of many factors including required dosage, possibility of regeneration, safety and environmental issues, capital/operating cost, physical properties (such as viscosity, volatility and solubility in liquid hydrocarbon phase), gas dehydration capacity and corrosion inhibition effect.

The required inhibitor dosage (injection rate) to prevent hydrate formation is the amount of inhibitor required to treat the free water, plus the amount of inhibitor lost to the vapour phase and the hydrocarbon liquid phase. The appropriate injection rate for each inhibitor depends on how far the phase boundary needs to be shifted for a specific system at a given pressure. For accurate estimation of thermodynamic inhibitor effect, computer programmes should be used (See section 2.3).

Figure 2.6 illustrates the effect of different dosages of MEG and methanol on the hydrate stability zone of a natural gas system (composition given in Table A.6).

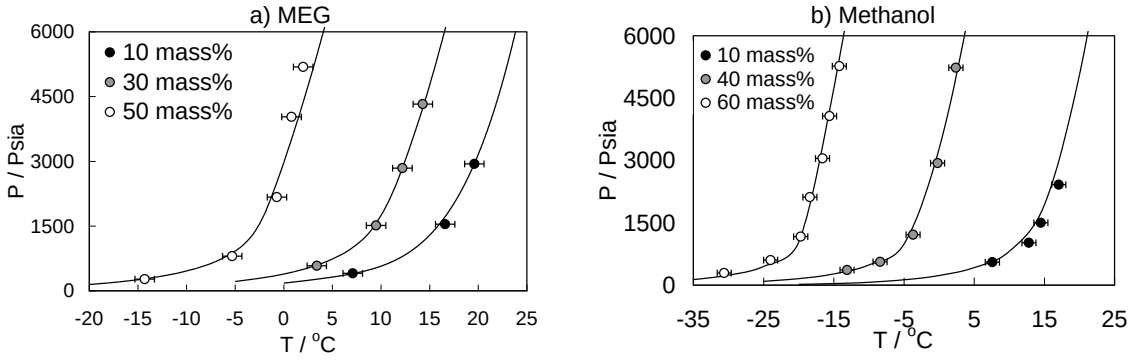

Figure 2.6 Experimental and predicted hydrate phase boundary for natural gas in the presence of a) MEG and b) methanol aqueous solutions (error bars: ±1 °C). Lines: Predictions using HWHYD 2.1 software (Experimental data from Haghighi et al., 2005 a, b)

As can be seen in this figure and also Figure 2.3, methanol inhibits hydrate formation more than an equivalent mass percentage of glycol in the aqueous phase. Though more effective, methanol does have safety issues as it is a volatile and flammable liquid and is known to be toxic to living organisms. From an industrial view point, methanol increases the corrosion tendencies of pipes and equipment because it can deactivate some corrosion inhibitors (CI) and adds oxygen to the system. As a result, if hydrates are controlled with methanol, the system requires extra amount of properly selected corrosion inhibitors to counteract the oxygen induced corrosion (Hoppe et al, 2006). In practice, there is a significant push from refineries to limit the allowable concentration of methanol in the produced oil or condensate arriving at the refinery. It causes upset in the biotreaters in the effluent stream and also poisons catalysts and molecular sieves that are routinely used in the refinery. Refineries have consequently imposed stiff penalties for crude contaminated with methanol that can range from $0.5 to $5.0 /bbl of oil (Metha et al., 2005). Producers have to also reduce methanol

content in gas in order to avoid sever penalties for deviating from gas plants specifications.

Typically, methanol is not recovered due to its high volatility and low costs, therefore, the economic of methanol recovery are not favourable in most cases. But since glycols are expensive inhibitors, there is a definite need for extra, costly and space consuming, onshore or offshore plants for their regeneration (Mokhatab et al., 2007). Methanol injection leads to a high operational expenditure and also needs large storage facilities. MEG injection needs installation of reboilers for regeneration as well as storage requirement.

Glycol is non-flammable. In addition to hydrate inhibition, MEG can act as a dehydration means for gas system. Only a negligible amount of MEG is lost to the gas phase as it is not very volatile. It does not also contaminate the oil due to its low solubility. But it is significantly more viscous than methanol, especially at low temperatures. This means that a MEG injection system requires stronger pumps and larger diameter lines.

When reviewing the advantages, limitations and cost elements of MEG versus methanol, it seems evident that MEG is the preferred inhibitor. This is supported by the choices made by the operators for recently built and planned long distance gas condensate tiebacks. The list of MEG based developments includes record breaking developments like Ormen Lange (Norsk Hydro – Norway), Snohvit (Statoil – Norway), KG-D6 (Reliance Industries – India), Scarab-Safron (Burullus – Egypt), South Pars (Total – Iran), Shah Deniz (BP – Azerbaijan), Britannia Satellites (ConocoPhilips – UK), Gorgon (Chevron Texaco – Australia) and Shtokman (Gazprom – Russian Barents Sea) (Brustad, 2005)

The effectiveness of thermodynamic inhibitors is well known, but they usually require large quantities especially for sever condition, i.e., mature field with increasing water cuts. The volume demand creates logistic problems and safety concerns for the safe handling, transportation and storage of these chemicals. For example, if a field is producing 50,000 BPD (barrel/day) oil and the water cut rises to 70%, then one would need to inhibit 35,000 BPD water. This would roughly require 35,000 BPD methanol or 50,000 BPD ethylene glycol for hydrate prevention. This represents a huge cost and safety issues particularly for a deepwater development.

Active heating and or insulation: Thermal methods, i.e. insulation and active heating, help to prevent both hydrate formation and wax deposition on pipe walls by preserving heat in the system so that the flowing mixture remains outside the hydrate formation zone and wax appearance temperature. These methods can be applied for normal operation and/or shut-downs.

Conventional insulation techniques such as covering the outer surface of the pipe or pipe-in-pipe insulations still are the preferred methods worldwide due to their simplicity; however, more economical/advanced thermal loss methods are also being used in the industry. For instance, a pipeline burial method has been used in an offshore field in the Gulf of Mexico as an economical thermal loss reduction method. Application of thermal methods for subsea installations is a function of the tie back distance. The decision to use insulation is a compromise between the possible high cost of the insulation, and the likely added value of insulation. It should also be highlighted that insulation generally only prevents hydrate formation during normal operation conditions but not during long-term plant shutdowns (Mokhatab, 2007).

If a flow line is well insulated to cope with shutdowns, then conversely restricts heat flow from the surrounding into the flow line while dissociating/removing hydrate blockage. This negative impact of insulation on blockage remediation times can be so significant that one may require months or years to dissociate hydrate plug in a highly insulated flow line depending on the temperature driving force, insulations amount and extend of depressurisation (Kini, 2005).

Several methods are in use for heating up a pipeline system. Actively heated systems generally use hot fluid or electrical heat tracing. The main attraction of active heating is its flexibility. It can be used to extend the cooling down time indefinitely. It is also capable of warming up a line from seawater temperature to a target operating level to avoid risky restarts.

Active heating by circulation of hot fluid is generally more suited to a bundle configuration because large pipeline cross sections are required. There is a length limitation to hot fluid heating because it generally involves a fluid circulation loop along which the temperature of the heating medium decreases. In order to have an adequate efficiency, it is necessary to inject large flow of fluid at a relatively high temperature. This involves storage facilities and significant energy to heat the fluid and

to maintain the flow. Electrical heating does not needs these storage facilities and is applicable to smaller size pipeline systems such as pipe-in-pipe or wet insulated flow lines. A number of electrically based systems are available in the market with a wide range of specifications. The most efficient electrical heating systems can provide the heat input to be as close to the flow line bore as possible and have minimum heat losses to the environment. Trace heating is believed to provide the highest level of heating efficiency and can be applied to bundles (skin effect tubes) or to pipe-in-pipe system (trace heating cables). The length capability of an electrical system depends on the linear heat input required and the admissible voltage. Trace heating can be applied for very long tie-backs (several 10's of kilometres) by either using higher voltage or by introducing intermediate power feeding locations, fed by power umbilical via step down transformers (Denniel et al., 2004).

Figure 2.7 shows different pipe insulation types as a function of temperature and tie-back distance in deep waters (1,500 m) – Courtesy of Doris, June 2007. It shows that wet and bundle insulations could be used in higher temperature and shorter tie-back distance while electrical heating systems are more suitable for lower temperatures and longer tie-back systems (Taxy, 2007).

The drawback to all of these thermal solutions is that they are inherently very expensive and in deepwater, cost escalates rapidly.

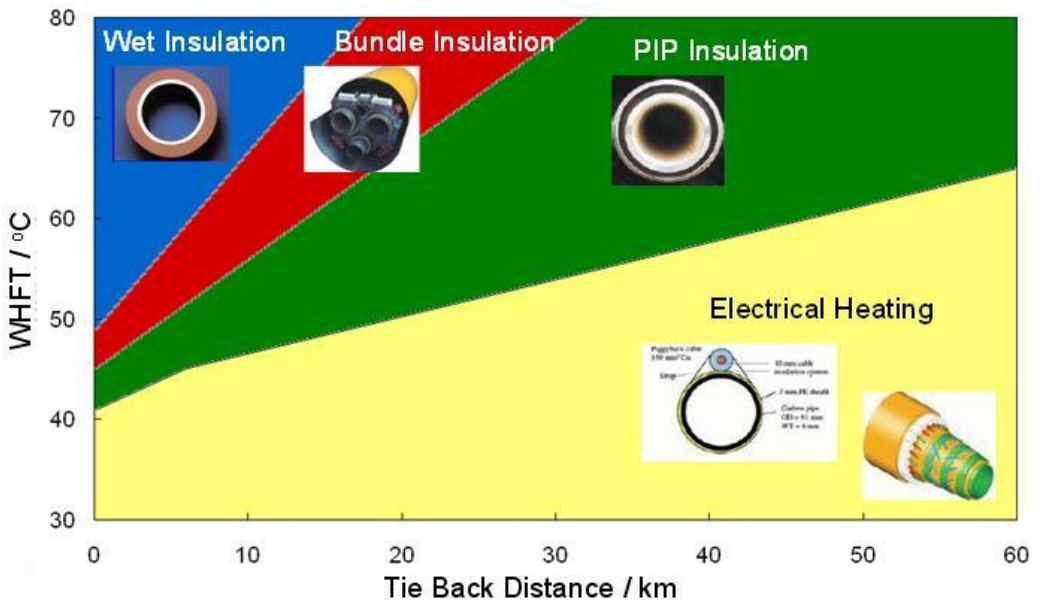

Figure 2.7 Different Pipe Insulation Types as a Function of Temperature and Tie-Back Distance in Deep water (1500 m) – Courtesy Doris, June 2007.

Controlling the operation pressure: This method is not generally practised under normal operating conditions (especially in long and high pressure gas pipelines) as pressure is energy and any loss in energy results in operational problems/costs. However, various depressurisation methods such as single or two sided depressurisation are often used for plug remediation.

2.5.2. Controlling hydrate formation by means of Low Dosage Hydrate Inhibitors

During the last two decades, Low Dosage Hydrate Inhibitors (LDHIs) have emerged as the most promising option of the new flow assurance methods. LDHIs are so called as they can be efficiently used at dosages far lower than those of thermodynamic hydrate inhibitors. Generally they are effective at 0.5 – 3 mass% in water, where as methanol and glycol are generally used between 10 – 60 mass% in water. Therefore, the most interesting economic advantage expected from LDHIs should have been the reduction of OPEX. But it is not the case because their price is still very high (4 to 5 Euros/l), so that their dosage multiplied by their price results in the same OPEX cost as for methanol. In fact, the main economic aspect of using LDHIs currently is the large reduction of CAPEX due to the reduction in the size of the storage, injection rate, pumping requirements and piping facilities. Their other benefit is that that they are far less volatile and flammable than methanol, resulting in a reduction in HSE risks (Peytavy et al., 2008). By 2005 there were 50-70 field applications of LDHIs, the majority of them related to KHIs (Kelland, 2006). The commercial deployment of AA started a little later than KHI due to environmental and operational concerns. However, the number of AA applications is now increasing rapidly.

These new hydrate inhibitors form the basis of a technique that allows the system to operate inside the hydrate stability zone, contrary to the previous described methods. In fact, LDHIs act at the early stages of hydrate formation by interfering with the process of nucleation/growth and/or modifying the rheological properties of the system. Different mechanisms have been proposed to explain these interactions that classify LDHIs into two main groups:

- Kinetic Hydrate Inhibitors (KHIs)
- Anti-Agglomerants (AAs)

Figure 2.8 illustrates a simplified method by which LDHIs prevents hydrate plug formation. Each of these methods is described in the subsequent parts.

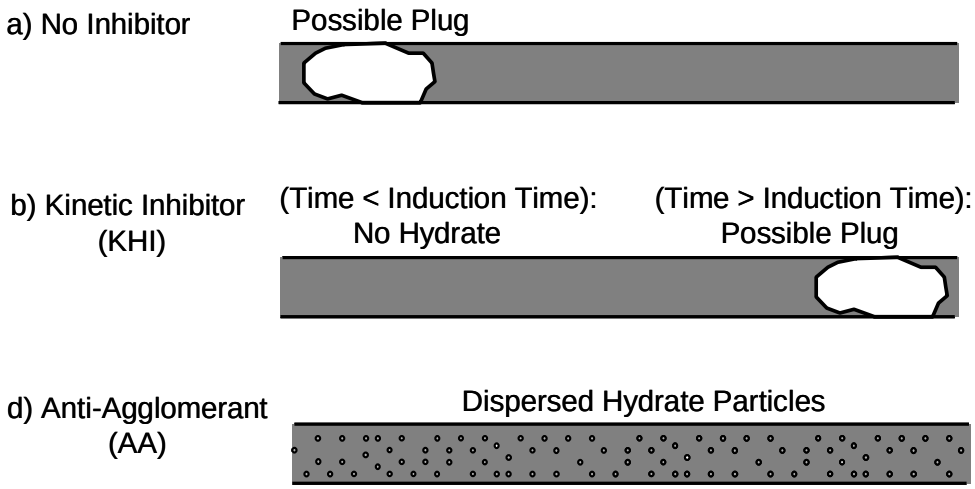

Figure 2.8 Simplified methods by which LDHIs prevent hydrate plug formation. Modified after Frostman (2000)

Kinetic Hydrate Inhibitors (KHIs): The general understanding within the industry and academia is that KHIs interact kinetically with the hydrate nucleation step and the crystal growth process, resulting in an increased 'induction' or 'hold' time for hydrate formation. Induction time is the period of time that passes at a specific subcooling (ΔT_{sub} at pressure P) within the hydrate stability zone for a specific system before critical nuclei are achieved and hydrate nucleation occurred (Kelland, 2006; Sloan and Koh, 2008). In theory, if the KHI–induced induction time at ΔT_{sub} (subcooling) and P is greater than the pipeline fluid residence time at that condition, then the KHI should be able to prevent hydrate nucleation/growth, whereby avoiding plugging. Subcooling is usually considered as the driving force for hydrate formation and is the difference between the operating temperature and the hydrate equilibrium temperature at the operating pressure. The deeper a system operate in the hydrate region, the shorter the time during which KHIs can delay hydrate formation. The earlier generations of KHI are very effective in controlling hydrates up to 8 °C subcooling while some commercial KHIs when dosed at more 5000 ppm have been used in the fields at subcoolings up to approximately 15 °C. Other KHIs have been shown to work at much higher subcoolings, but they are not commercially available (Kelland, 2006).

KHIs are based on specific classes of water soluble polymers. Since the initial discovery of KHI polymers in the early 1990s, a considerable number of compounds

have been developed (and patented) as supposedly kinetic hydrate inhibitors (e.g. Colle et al., 1999; Sinquin et al., 1998). However, the most well known, studied, and arguably still the best performing (when combined with synergist chemicals/solvents), are the poly-n-vinylamides, including poly-n-vinylcaprolactam (PVCap), poly-n-vinylpyrrolidone (PVP) and their co-polymers (Kelland, 2006). PVP and PVCap have been patented by Sloan (Sloan 1995 a, b; Sloan and et al, 1997). While the precise mechanisms by which these (and other) KHIs inhibit hydrate nucleation/growth is still poorly understood, the generally accepted mechanism is crystal surface adsorption.

Molecular dynamic simulations suggest that PVCap/PVP adsorb onto growing hydrate crystal surfaces, with the general consensus that this occurs through partial enclathration of the pendant group (into large $5^{12}6^2$ or $5^{12}6^4$ cavities) coupled with hydrogen bonding of the amide group oxygen with the water lattice (e.g. Freer and Sloan, 2000; Makogon and Sloan, 2002; Anderson et al., 2005; Kvamme, 2005).

Typically, KHI formulations are developed and tested based on the results of induction/hold time studies (Kelland, 2006). The same applies for determining the effects of various parameters including pressure, presence of synergists, salts, liquid hydrocarbons (condensate, oil) and other oilfield chemicals (e.g. corrosion and scale inhibitors). However, there is an inherent problem with the measurement of induction times. Results are almost invariably quite stochastic, poorly repeatable and commonly non-transferable (e.g. Kelland, 2006; Sloan and Koh, 2008; Duchateau et al., 2009).

The main technical drawback of using KHI inhibitors is their limitation in inhibiting the systems with high degree of subcoolings which is the case in deepwater productions. Another limitation of KHIs is that their performance is affected by presence of liquid hydrocarbon phase and other chemicals, e.g. corrosion inhibitors, and also the composition of the gas phase.

Anti-Agglomerants (AAs): While KHIs prevent the formation of hydrae crystal by disrupting the crystal growth, AAs do not prevent the crystals to form, but keep them small and well dispersed in the fluid, thus hydrate crystals can be transported as a slurry at reasonable viscosity. AAs are generally surface active agents combined with synergist chemicals/solvents. They can be either water or oil soluble depending on their formulation and application.

The main advantage of AAs over the KHIs is that AAs are able to control hydrate problems at higher subcoolings and can be effective even at subcoolings (ΔT_{sub}) over 20 ºC (Kelland, 2006). Therefore, they have a much wider range of pressure and temperature application and could be used for ultra deepwater applications. Another useful characteristic of AA is that their performance is relatively independent of time and can inhibit hydrate agglomeration for longer time periods, and as such they can be used for extended shut-ins (Behar et al., 1991; Sloan 2000).

There are some limitations in the use of AAs. Firstly, it is commonly accepted that AAs act as dispersants of the hydrate particles in the liquid hydrocarbon phase and therefore liquid hydrocarbon must be present. Typically water cut should not be greater than 50% to ensure that there is enough hydrocarbon to contain the dispersed hydrate particles. This requirement may be related to w/o emulsion formation, but other reasons such as high slurry viscosity with high hydrate volume fraction are also cited in the literature (Kelland, 2006; Sloan, 2005). Unfortunately, this limitation is generally believed to reduce its deployment in maturing fields with increasing water cut. However, there are still ongoing research studies in this area and a recent study/patent by Nalco showed that a newly developed AA inhibitor is effective at water cuts as high as 80% (Alapati, 2008). This patent claims the use of ion pair amphiphilic, which is a combination of cationic and anionic surfactants. Secondly, the performance of AAs is affected by the type of oil/condensate, nature of the oil (acidic, asphaltenic, etc) and the salinity of the water (Kelland, 1995) which may vary in the lifetime of a field. Finally, there is a major concern regarding the environmental impact of AAs. Most of the available AAs are both toxic and non-biodegradable, which has limited their application. To a degree, this limitation can be addressed by exploring greener version of LDHIs. For example, Rogaland Research in collaboration with Elf have tested natural and biodegradable surfactants as AAs (Kelland et al. 1995 a,b, Kelland et al. 1996). The best product discovered was an alkyle glucoside called Plantaren 600 CPUS. York and Firoozabadi have also shown some promising initial results for Rhamnolipid bio-surfactant (York and Firoozabadi, 2008). However, the cost of bio-surfactants is not comparable with chemical surfactants at the moment. Another solution for this limitation can be mitigation of the environmental impacts of chemical AAs. Two methods have been patented for reducing the impacts if quaternary surfactant AAs. Shell has patented a method to phase separate a quaternary

AA by adding sufficient inorganic salt to the produced water to render the AA insoluble in the aqueous phase (Blytas and Kruka, 2002). Baker Petrolite has patented methods to detoxify quaternary AA surfactants by the addition of anionic polymers or anionic surfactants (Rivers and Downs, 2004; Rivers et al., 2003).

Different types of AAs and mechanism of their inhibition:

Anti-agglomerants inhibitors can be categorized into three main groups according to their inhibition mechanism.

- Dispersant AAs
- Quaternary Ammonium Salts (QAS)
- Gas Well AAs (GWAA)

The first category of AA discovered was called dispersant AAs. The first mention of controlling hydrates with surfactants was by Kuliev (Kuliev et al., 1972) who added commercial surfactants to his well and controlled hydrate problems. The next paper on dispersant AAs was published 15 years later. In the late 1980s, L'Institut Français du Pétrole (IFP) patented a wide range of surfactants including diethanolamides, dioctylsulfosuccinates, sorbitans, ethoxylated polyols, ethoxylated fatty acids and ethoxylated amines as LDHIs (Sugier et al. 1989 a, b, c). Some of these chemical structures are shown in Figure 2.9. Although not described in the early work, it was later discovered that the mechanism of inhibition involves the creation of emulsion by the surfactant which confines the hydrates inside water droplets and do not agglomerate (Kelland, 2006). By mid 1990s, IFP patented various polymeric emulsifiers (Sugier et al. 1993, Durand et al. 1995, Delion et al. 1998) by focusing on polyglycol derivatives of polyalkenylsuccinic anhydrides. Claims were made by Pierrot et al. (1992) that their dispersant additives could be used at 0.5 to 2.0 mass%., and later results showed successful inhibition using 0.8 mass% (Behar 1994). Although IFP was very persistent with their research, there has been no reported application of dispersant AAs to date. A variety of classes of surfactants have been patented by other research groups, however, they gave a limited AA performance (e.g. Reijnhout et al., 1993). Rogaland Research in collaboration with Elf have also tested various commercial monosurfactants as AAs but none of them were useful AAs; however, this work did highlight the fact that surfactants that create a water-in-oil emulsion do not necessarily perform as effective AAs. In fact many studies have

shown that the addition of surfactants can lead to a significant increase in hydrate growth by reducing the interfacial tension, and thus increasing the mass transfer of hydrate forming gas into the aqueous phase (Kalogerakis *et al.* 1993, Irvin *et al.* 2000, Karaaslan and Parlaktuna 2000). Yolsim and Englezos have studied the effect of one commercial anionic surfactant on the formation/dissociation of hydrate and have concluded that the presence and the concentration of surfactant affect both the rate and morphology of growing crystals. These results show that in the presence of surfactant, branches of porous fibre-like crystals are formed instead of needle-like crystals in the absence of any additive (Youlsim and Englezos, 2008).

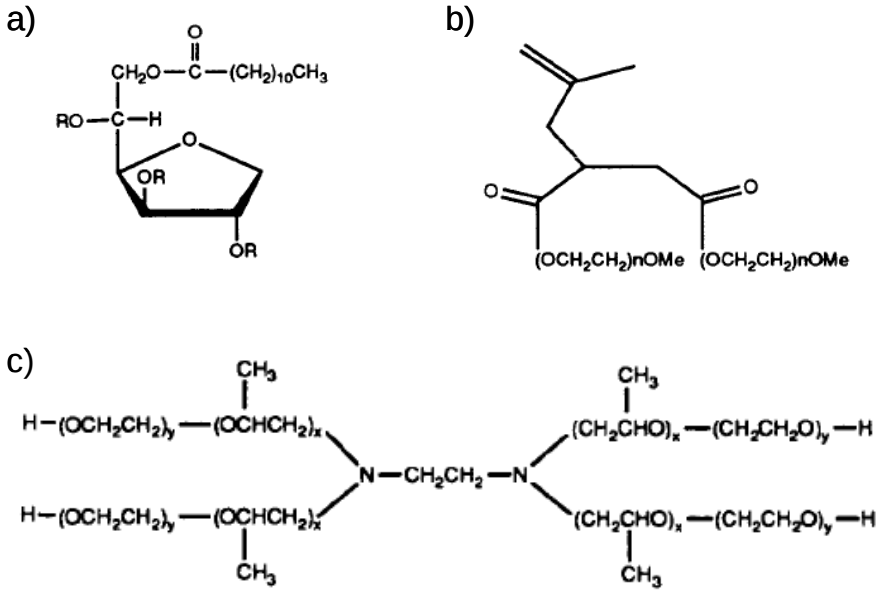

a) Ethoxylated sorbitan monolaurate [R=$(CH_2CH_2O)_nH$]

b) Monomer unit of isobutylene succinate diester of monomethylpolyethylene glycol

c) Ethylene diamine-based block PO-EO copolymers

Figure 2.9 Some chemical structures of IFP's dispersant AAs (Kelland et al., 1995)

The second type of AAs are the quaternary ammonium salts (QAS) AA and were discovered by Shell and are to date still the most effective AAs. This type of AA inhibits hydrate agglomeration via a different mechanism to the dispersant AAs. It is believed that the effectiveness of QAS is due to the semi-clathrate forming nature of the salts. They incorporate themselves into the hydrate by being both the guest molecule and part of the hydrate cage structure. In the case of QAS, the quaternary centre occupies the cage as a guest and becomes embedded in the hydrate structure, where the hydrophobic tails reduce the wettability of the hydrate to water. This

eliminates the possibility of a water bridge with another hydrate particle and also disperses the hydrate particles in the oil phase. It is believed that the AA discovered by Huo et al. (2001) involving the use of KHI head group also works by changing the wettability of hydrates. Another important aspect of the nature of semi-clathrates is that they form at higher temperatures and/or lower pressures than equivalent natural gas hydrates. The surfactant nature of the QAS ensures that they are located at the interface of a water oil mixture, which is the initial location of hydrate formation. For these reasons, it is expected that the semi-clathrate hydrates form first, which may have a benefit in controlling the agglomeration process (Kelland, 2006). Some of the AA QAS are also used as corrosion inhibitor, which is anticipated to help prevent the adherence of hydrate to the pipeline surface, due to a modification in wettability of the pipeline wall (Hoppe et al., 2006).

Shell tested a large range of quaternary salts and found that salts with two or more n-butyl, n-pentyl, and iso-pentyl groups were the best at delaying the growth of THF hydrate crystals (Figure 2.10 a). Shell's next study was to replace one or two of the small alkyl groups with a long hydrophobic tail containing 8-18 carbon atoms (Klomp et al., 1995). These materials are not anti-nucleators, so they are poor KHIs. In fact, some of these small quaternary ammonium and also phosphonium salts can promote hydrate nucleation by being templates. Shell called these chemicals "hydrate growth inhibitors" (HGIs). These quaternary surfactant salts with two or three *n*-butyl, *n*-pentyl, and isopentyl groups performed extremely well as hydrate AAs (Figure 2.10 b).

Recently, Baker Petrolite found that the effective concentration of a quaternary surfactant AA could be reduced by the addition of a minor amount of an anionic, nonionic, or amphoteric compound. The mixture, called an ion pair, allows lower concentrations of the quaternary surfactant to be used in practice, which reduces the treatment cost as well as the environmental impact. For example, the effective concentration of quaternary ammonium surfactant AA was reduced from 0.75 mass % to 0.15 mass % by the addition of 0.12 mass % alcohol ether sulfate (AES) for AA tests with a GoM condensate (Crosby, et al., 2005).

Several research groups, chemical and oilfield service companies have patented their own variation on the existing quaternary ammonium salt technology. Some examples of them are Champion (Panchalingham *et al.* 2005 a, b, c, d; Panchalingham *et al.*

2006), Clariant (Dahlmann *et al.* 2004 a, b, Dahlman *et al.* 2005), Goldschmidt (Milburn *et al.* 2000, Milburn *et al.* 2002).

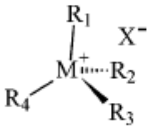

a) Structure of Shell's good quaternary ammonium or phosphonium hydrate growth inhibitors, where M=N or P and at least two of the R groups are n-butyl, n-pentyl, or isopentyle

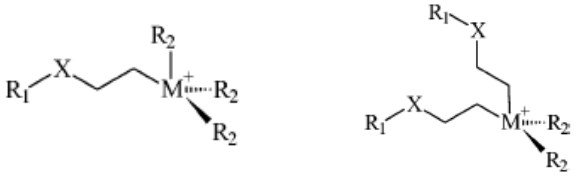

b) Structure of Shell's quaternary AAs (R1=long chain hydrocarbon tail; R2=n-butyl, n-pentyl, or isopentyle; M=N or P; X is an optional spacer group

Figure 2.10 Some chemical structures of Shell's quaternary AAs (Kelland et al., 2006)

The most recent class of AA discovered by BJ Unichem (BJ) are gas well anti agglomerants (GWAAs) (Pakulski, 1997). This class of AAs mainly includes quaternised polyetherpolyamines (Figure 2.11).

$$[R'R'R''N{-}(CHRCH_2\ (OCH_2CHR)_n\ NR'{-})_m\ R']^+\ [X]^-$$

where R=H or CH_3;
R'=H or C_aH_{2a+1}, where a=1 to 4;
R''=C_bH_{2b+1}, where b=4 to 20;
m=1 to 4;
and n=2 to 6.
The anion $[X]^-$ may be freely substituted

Figure 2.11 General structure of polyether ammonium compounds (BJ's GWAAs) (Pakulski, 1997)

These AAs do not require a hydrocarbon liquid phase to disperse hydrates and they actually disperse hydrates in the unconverted water. They are also synergists for KHI polymers such as PVCap. The mechanism is still under debate. However, the quaternary centre works by incorporating themselves into the hydrate in the same way

as the wettability modifier AAs. The main difference is that the wettability of the hydrates do not change but the polyether amines prevent the hydrate particles from agglomerating by inhibiting further hydrate growth in the associated water on the surface of the hydrates.

Natural Anti-Agglomerants in crude oils: Some "natural surfactants" such as resins and asphaltenes have been found to have properties similar to synthetic surfactants. Acid fractions extracted from certain non-plugging crude oils have shown to be able to alter hydrate behaviour from plugging to non-plugging at operationally relevant pressure/temperature conditions. However, some acid fractions, fail to do so, though they were also extracted from non-plugging oils. Several workers have attempted to address these subjects, as detailed below.

Laboratory experiments and field operations experience have both suggested that some oils contain naturally inhibiting components acting as kinetic inhibitors or anti-agglomerants. The nature of these components is not well known but they seem to be associated with biodegraded oils. Experiments show that if the acidic components in non-plugging oil are extracted and added to plugging oil, they will in some cases change the hydrate morphology to form components easily carried by the flow dispersion. However, certain combinations of oil type and concentration of additives are required for the effect of naturally inhibiting components to be sufficient to prevent plugging (Genov and Skaar, 2008).

Leporcher et al. performed a series of lab experiments which showed paraffins may have a positive interaction with the natural surfactants of the oil in order to stabilise the slurry. Their tests on a North Sea crude oil showed that if the amount of asphaltenes in the mixture is high enough (1.5-2.0 % by weight) the system can transport up to 30% of water under hydrate conditions (Leporcher, et al., 1998).

Sinquin, A. et al. showed that whatever the compounds (paraffin, resin or asphaltenes) which have an important role on the kinetic of hydrate formation, it is very difficult to isolate one class from the others in high pressure tests. The hypothesis of the asphaltenes state of dissolution seems a good track and need further investigations but specific action of resins and/or paraffins (alone or together) cannot be draw aside (Sinquin et al., 2001).

Fadnes presented procedures for evaluating the plugging potential of crude oils and tentatively identifying and extracting naturally hydrate inhibiting components in crude oils. He concluded that crude oils have varying degree of plugging potential and the oil content of polar components reflect the potential of emulsion - and hydrate plug formation. Oils not forming stable emulsion have a higher potential of forming hydrate plugs. Components having an inhibiting effect on hydrate plug formation can be extracted from crude oils (Fadnes, 1996).

Genov et al. presented a method for classifying different crude oils with respect to biodegradation levels and gas hydrate plugging potential, based on whole-oil gas chromatography and multivariate data analysis. Samples of ten crude oils from the Norwegian continental shelf were investigated. A clear separation of the oil samples into two groups, biodegraded and non-biodegraded, was achieved. Additional separation of oils with high gas hydrate plugging potential and those with low gas hydrate plugging potential was observed within the group of the biodegraded oils (Genov and Skaar, 2008).

Borgund et al. identified crude oil compositional parameters that impact the anti-agglomerating properties of crude oils. They showed that biodegradation together with a relatively large amount of acids are characteristic for non-plugging crude oils, while excess of basic compounds is characteristic for plugging crude oils. The multivariate data analysis showed a division of the non-biodegraded oils, which are all plugging, and the biodegraded oils. In addition, the biodegraded oils seemed to be divided into two groups, one with plugging oils and one with mostly non-plugging oils (Figure 2.12).

Their results showed that the wettability can be predicted from the variables biodegradation level, density, asphaltene content and the amount of titratable acids (Borgund, et al., 2008).

Petroleum acids derived from some crude oils have been found to be able to convert systems with initially high risk of plugging into easily flowable dispersions. Erstad et al. have isolated acid fractions from three oils with low tendency to form hydrate plugs and from two oils associated with high risk of hydrate plugging by using an ion-exchange resin. The extracts were further separated into four sub-fractions by solid phase extraction. The chemical composition of the fractions was studied by means of

several spectroscopy and elemental analysis techniques. The distribution of chemical compound classes in the fractions differed between the non-plugging and plugging oils, and the differences were most distinctive in one of the sub-fractions. The results imply that acid sub-fractions holding a significant proportion of more weakly polar compounds, like ester functionalities, are important for how the hydrate surfaces and the oil phase interact (Erstad et al., 2008).

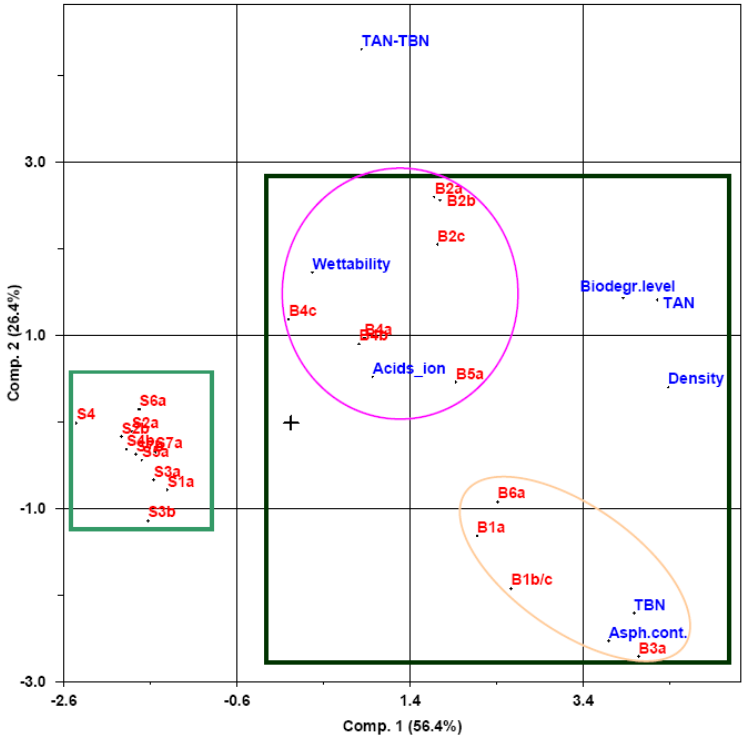

Figure 2.12 A PCA (Principal Component Analysis) plot of all the samples (red) and the variables (blue). The non-biodegraded oils (plugging) are found in the small green square to the left, and the biodegraded oils are found in the large dark green square to the right. The biodegraded oils are separated into two groups: oval in the lower right corner – plugging oils and higher circle - mostly non-plugging oils (Borgund, et al., 2008).

2.6. Limitation of the current gas hydrate flow assurance strategies

As forecasted by ITI Energy (2004), global oil and gas production is increasingly being dominated by exploitation of mature fields where water cuts can be very high. Moreover, offshore oil and gas industry moves into deeper water, harsher environments and longer tie backs which may soon include the Arctic. Gulf of Mexico, offshore Brazil, West Africa, west of Shetland and offshore Mid-Norway are the regions where deepwater production have started and it is likely to expand considerably in the coming decades. These high water cuts, new depths, longer riser

lengths and longer tie backs have brought new challenges for hydrate flow assurance. These aspects combined with the safety hazards and environmental issues like demand for reducing the contamination of the disposed water have made the existing flow assurance techniques less economic and practical. Therefore, the industry needs new and improved ways of tackling these problems. This has resulted in the introduction of novel technique where hydrates are not prevented, but managed to prevent their agglomeration and pipeline blockage. This technique is generally called as "cold flow" and has the potential to deliver significant costs savings and/or enable new field development options.

2.7. What is cold flow?

Cold flow is an emerging risk management tool for preventing gas hydrate blockage in oil and gas production operations. It can provide an economical alternative solution to the current flow assurance methods and can potentially fill the gap that the current methods are not able to handle. Cold flow technology aims to find a reliable method which allows field development based on ultra long cold multiphase flow transport, i.e. un-insulated pipeline. Efficient use of such a tool requires the transition from conventional hydrate avoidance methods to new hydrate control and management techniques. These techniques have several common characteristics: (a) There is no heating or insulation, 2) hydrates are not prevented but allowed to form and 3) their agglomeration is avoided by various techniques. Cold flow methods improve the economics and practicalities of multiphase fluid transports by eliminating the need for expensive thermal/chemical inhibitions.

Few research groups are/have been working on various cold flow concepts, most notably SINTEF-BP (Lund et al., 2000; Lund and Larsen, 2000; Larsen et al., 2001; Larsen et al., 2003; Lund et al., 2004; Wolden et al., 2005; Larsen et al., 2009) and NTNU (Gudmundsson, 2002). IFP has also studied hydrate slurries in flowing conditions and particularly in multiphase flow lines (Peysson, 2003; Singuin et al., 2004). CSIRO/IFP are/have been investigating hydrate transport in continuous gas phase. Shell and ExxonMobil have also studied its own version of cold flow. However, they have not published their results in the open literature. The most important cold flow concepts been investigated so far for addressing gas hydrate flow assurance problems are as follow.

2.7.1. The SINTEF cold Flow concept – CONWHYP or SATURN

SINTEF (Norway), in partnership with BP, are developing a patented cold flow technology named CONWHYP (CONversion of Water to HYdrate Particles) or SATURN cold flow concept (Lund et al., 2000; Lund et al., 2004). The basis of this concept is the argument that 'dry' gas hydrates can be formed under certain conditions, and that these would be able to flow as slurry in a continuous oil phase without agglomerating and blockage. Therefore, the main objective is to convert all the water phase into hydrates. This concept recycles a part (certain fraction) of the cooled hydrates and oil present in the system back up stream using a pump and recirculating loop to act as hydrate growth seeds for the water from the hot new production well-stream. Thus the cold recirculation stream acts both as a heat sink to quickly achieve hydrate forming temperature, and as a nucleation sites to facilitate non-sticky (dry) hydrate growth (Larsen et al., 2001).

Lund and Larsen have described their hypothesis of "seeding and growing" as follows (Larsen et al., 2003). Hydrates normally start to nucleate close to the hydrocarbon phase on a water droplet in gas, oil, or condensate phases. Hydrates grow along the surface of the water droplet until it is completely covered with a thin hydrate layer. Water then penetrates from the inside the droplet to hydrate surface through micro perforations and small cracks in the hydrate films and converts to hydrate (Figure 2.13). The migration of water depends on the hydrate formation driving force and shear forces on hydrate droplets. After a relatively short time, no further conversion of water to hydrate is observed. If a water droplet covered by hydrate film hits e.g. another particle or pipe wall in a turbulent system, the cracks will get larger under the kinetic forces of droplet. Cold trapped water inside the droplet will then drain out through these cracks and spread on the hydrophilic hydrate film. This water may convert to hydrate, often resulting in agglomeration of particles and/or deposition of the droplet on the wall as illustrated in (Figure 2.14). They therefore conclude that if water is to be transported as stable hydrate slurry, the hydrate particles must be dry (no free water inside). These dry particles do not stick to each other and/or deposit later on the pipe wall and hence avoid hydrate blockage. To achieve this, they have proposed to convert all the free water to hydrate near the wells.

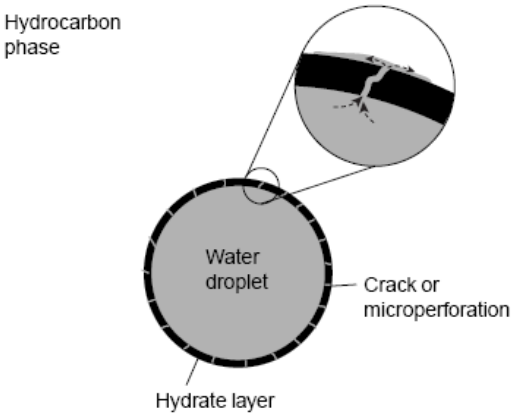

Figure 2.13 Growth of hydrate layer on a water droplet surrounded by hydrocarbons

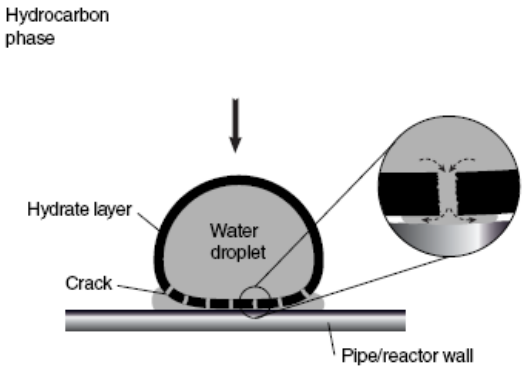

Figure 2.14 Deposition of hydrate particle on pipe wall (Lund and Larsen, 2000)

They argue that if a warm well-stream is mixed with a cooled recycled stream containing dry hydrate particles, the water from the well will quickly coat the pre-formed hydrate particles with a thin water film. If the temperature is right, the water will be converted to hydrate by growing from existing hydrate surfaces from inside to outside as shown in Figure 2.15.

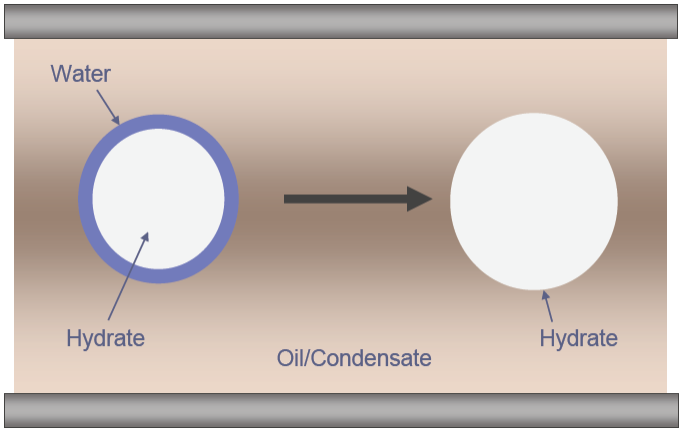

Figure 2.15. Formation of a dry hydrate particle from the existing hydrate surface and outward. Initially, a water droplet wets a dry hydrate particle (Larsen et al., 2003).

This hypothesis forms the basis of the SINTEF's cold flow concept and it is assumed that by formation of dry hydrate particles near wells, no further hydrate agglomeration and/or deposition should occur in the rest of the pipeline.

One of the limitations of the "seeding and growing" idea is water content restriction in the warm well-stream. After cooling and condensation, no more than a certain amount of water (~ 10 vol%) should be present in the fluid stream. Therefore, a water

knockout drum should be used to reduce the water content from the production stream. **Error! Reference source not found.** and **Error! Reference source not found.** show a schematic illustration of the SINTEF cold flow (CONWHYP) process.

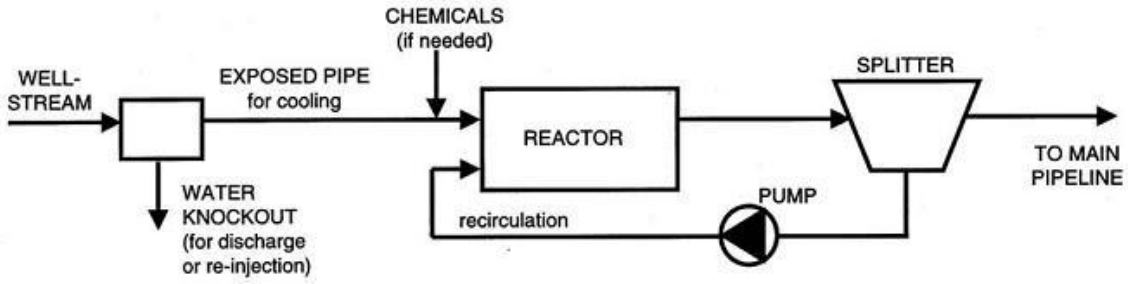

Figure 2.16 Schematic description of the SINTEF cold flow process (Larsen et al., 2001)

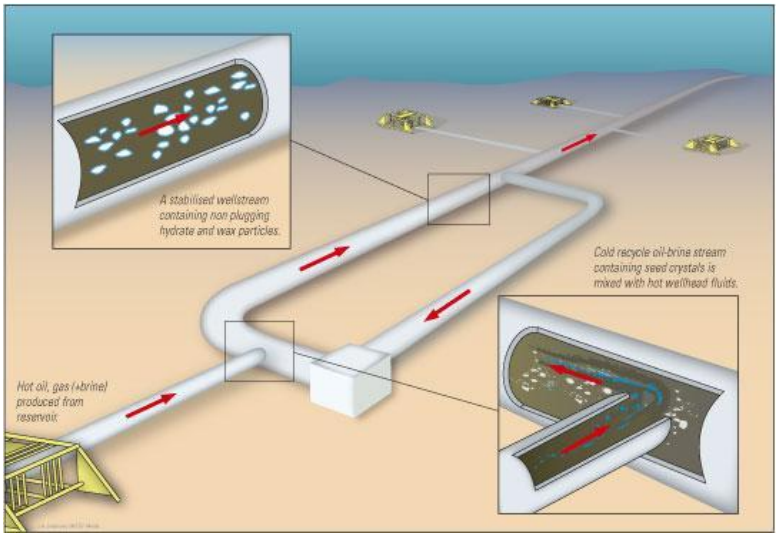

Figure 2.17 Mixing of hot well stream and cold recycle stream containing dry hydrate particles (SINTEF cold flow concept)

After water separation, fluid cools down to the hydrate stability temperature as it passes trough a bare pipe of the necessary length. The fluid phases may also be mixed before the reactor to provide a larger interfacial surface area. Chemicals such as corrosion, wax and asphaltene inhibitors can be added in this section if required. Further cooling takes place in the reactor and hydrate formation is promoted by adding cold fluid containing hydrate seed from a down stream splitter. All of the water should be converted to dry hydrate particles in the reactor then fluid stream enters a splitter where some of the cold hydrocarbon fluid and dry hydrate particles are recycled to the hydrate reactor. It is assumed that the dry hydrate particles will not dissociate to water

and natural gas until end of the transport where hydrate particles can be mechanically separate from the bulk liquid phase.

From a practical viewpoint, there are several challenges with this approach, for example: subsea pump(s), adjusting the recycled fluid flow rate and mixing pattern, degree of subcooling (i.e., fluid entry temperature to the loop), coping with changes in the produced fluid rates and characteristics (it is necessary to cope with changes in flow rate as sufficient cooling is required), application to saline produced water systems (possibility of converting all the water to hydrate, i.e., form dry hydrates), effective formation of seed hydrate particles, etc. The success of this concept depends on the questions such as: whether the dry hydrate particles will be able to retain their dry, non sticking nature particularly at the low points, e.g. bends; how the dry hydrate particles will be produced in day one; can this concept deal with shut-ins and restarts; etc. These significant problems are reflected in the absence of commercialisation of this technology after significant efforts by SINTEF and BP.

2.7.2. The NTNU Cold Flow concept

Norwegian University of Science and Technology (NTNU) with cooperation of Aker Engineering (now Aker Technology) has investigated the flow of hydrate particles in water and oil (diesel fuel) phases (Andersson and Gudmundsson, 1999 and 2000) though with a main focus on hydrate for storage and transport of natural gas, i.e. stranded gas or capturing associated gas either through pipe line (slurry hydrate) or non-pipe line (dry hydrate) methods e.g. FPSO (Floating Production, Storage and Offloading) (Gudmundsson et al., 1999 & 2002; Gudmundsson and Mork, 2001).

NTNU's research work on hydrate in water and hydrate in oil slurry suggests that the pressure drop will not be greater than that expected in flow of the carrying liquid by itself (water only or oil only) especially in turbulent flow regime. Furthermore, their results show that hydrate slurries are not likely to deposit on the pipe or on the hydrate formation reactor walls and therefore are not likely to block the pipeline. Based on these experiences, Gudmundsson presented the NTNU's cold flow hydrates technology aims for flow assurance in deepwater production. Basically in this concept, the liquid water produced with oil and gas would be converted to hydrate particles and then would flow with oil phase as slurry in three-phase flow (gas, liquid

and solid) (Gudmundsson, 2002). A schematic illustration of one set of the NTNU cold flow process has been shows in Figure 2.18.

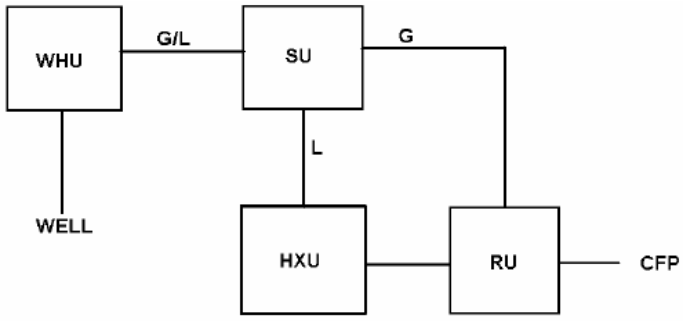

Figure 2.18 Schematic description of the NTNU cold flow process illustrating wellhead unit (WHU), separator unit (SU), heat-exchanger unit (HXU) and reactor unit (RU), feeding into a cold flow pipeline (CFP) (Gudmundsson, 2002)

The flow from a wellbore passes through several main units including wellhead unit (WHU), separator unit (SU), heat-exchanger unit (HXU) and reactor unit (RU) and leaves through a cold flow pipeline (CFP). The number of the processing sets (Su + HXU + RU) required in this concept mainly depends on the water cut and the gas to oil ratio (GOR). The well-stream (oil, produced water and gas) passes through the wellhead unit (required for subsea wellheads) and splits into gas and liquid phases in the separator unit. The liquid phase cools down in the heat exchanger unit before entering the reactor but the gas phase bypasses the heat exchanger. The hydrate formation reactor and rate of hydrate formation has been studied by Mork and Gudmundsson (Mork and Gudmundsson, 2002; Mork, 2002). It is possible to naturally cool down the system but to minimise the heat transfer surface, it is proposed to use active cooling for deep water production condition. However, the type and details of the active cooling have not been addressed in this concept.

Error! Reference source not found. shows some of the NTNU's results for water based hydrate slurry system. According to these results, in laminar flow, the frictional pressure drop expressed through the hydraulic gradient increases with increasing hydrate concentration. However, for turbulent flow, for all concentration, the slurry hydraulic gradient curve approaches the theoretical pure water curve. This means that the frictional pressure drop of turbulent water based hydrate slurry is identical to those of pure water without hydrates (Andersson and Gudmundsson, 2000). The same behaviour has been observed for higher concentration of water based hydrate, i.e. 32% slurry as well (Gudmundsson, 2002). Similar behaviour has been also reported for

diesel based hydrate slurries by this group as can be seen in Figure 2.20 and Figure 2.21 for 12.7 and 33.6 vol% slurry, respectively.

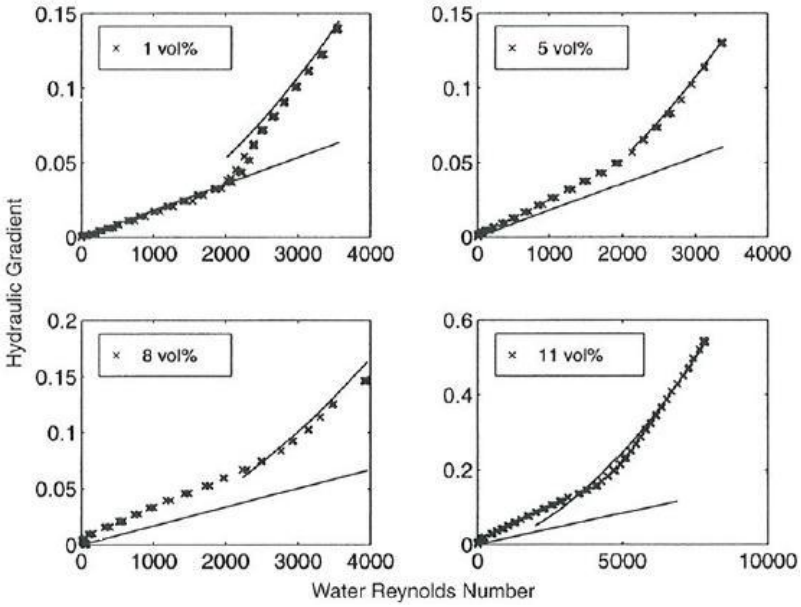

Figure 2.19 Slurry hydraulic gradient versus water Reynolds numbers. The hydrate concentration is increasing from top left to bottom right as indicated. The solid lines are the theoretical predicted laminar and turbulent water lines. (Andersson and Gudmundsson, 2000)

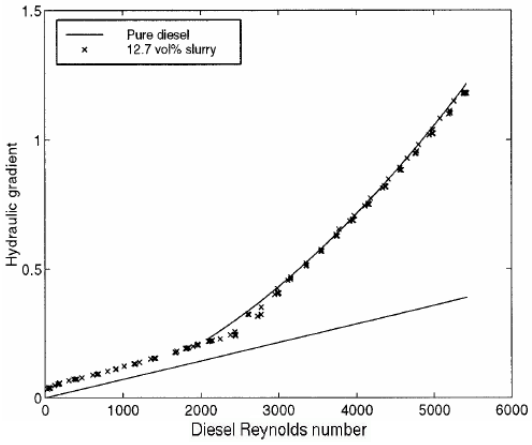

Figure 2.20 Hydraulic gradient for 1) pure diesel and 2) 12.7 % diesel-based hydrate slurry versus Reynolds number (Gudmundsson, 2002)

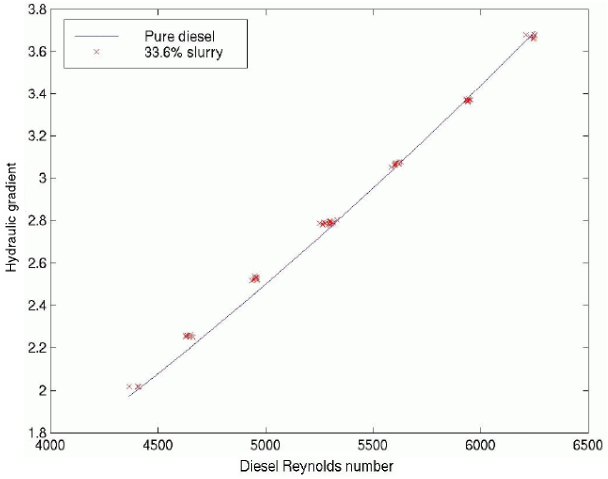

Figure 2.21 Hydraulic gradient curves for 1) pure diesel and 2) 33% diesel-based hydrate slurry. The turbulent regime is shown (Andersson and Gudmundsson, 1991)

It should be noted that the diesel based hydrate slurry systems in NTNU's studies were treated with an anti-agglomerant chemical named Emulfip 102b developed by IFP in

order to prevent formation of hydrate lumps. The reason explained in their paper for adding anti-agglomerant is that in the diesel based experiments, the water tended to separate from the liquid hydrocarbon phase and formed a water film on the pipe wall which later converted to hydrate and finally blocked the line by forming lumps of hydrate (Andersson and Gudmundsson, 1991). The authors have suggested making the pipe walls hydrophobic (oil-wetting) to prevent formation of water film on the walls. But as it was not possible to make this change in their laboratory set-up, they added the Emulfip 102b to stabilise the emulsion. This seems to be a draw back for NTNU's concept as their goal is to eliminate chemical usage because the Norwegian Pollution Authority (SFT) demands very restricted environmental laws e.g. all chemicals offshore must have 60^{+} biodegradability while none of the current commercialised anti-agglomerants meets this requirement (Kelland, 2006).

2.7.3. The Heriot-Watt University cold Flow concept – HYDRAFLOW

This ongoing research started in September 2005. The first phase of the project was supported by the Scottish Enterprise (SE) Proof of Concept Programme and an extensive experimental programme has been conducted, simulating various production scenarios and fluid systems mainly in small laboratory scale using autoclave type equipment and a limited number of tests in an in-house Flow Loop. The results are very promising and show that the concept is feasible. The second phase is a Joint Industrial Project (JIP) started on August 1, 2009 to generate additional Flow Loop large scale data.

The Heriot-Watt University cold flow concept proposed here, termed *HYDRAFLOW*, is a patented (Tohidi, 2006) chemical based wet cold flow assurance approach for preventing hydrate blockage. It allows gas hydrate formation but prevents solids agglomeration and lowers the viscosity of hydrate slurries using low doses (~ 1% by mass) of chemical anti-agglomerates where necessary (hence 'chemical based cold flow'). It is widely accepted that hydrate agglomeration is the main reason for plug formation and pipeline blockage; therefore, if agglomeration can be prevented by using Anti-Agglomerants, it can be possible to form hydrates and transport them as slurry without blockage. There are evidences that such situation occur in pipelines in Brazil. For instance, according to the Petrobras experience in Campos Basin, no hydrate plugging has been experienced in producing flow lines even during shutdowns and

restart operation. This behaviour has been explained by the presence of natural Anti-Agglomerants in their crude oils (Palermo et al., 2004). For crude oils that tend to form hydrate blockage, the use of anti-agglomerants is one of the methods used to effectively prevent agglomeration. Anti-Agglomerants are not new to the industry and have been detailed in Section 2.5.2 / AA.

Although *HYDRAFLOW* has parallels with other proposed cold flow concepts, is distinct in that rather than converting all the free water to hydrates. The objective is to minimise or completely eliminate the gas phase by converting it into hydrates (as opposed to dry cold flow concepts which aim to convert all the water phase into hydrates). If the produced water is insufficient for maximum gas conversion/hydrate formation, excess water can be added from other sources such as seawater (hence 'wet cold flow" as the presence of a free aqueous phase is desired). A number of benefits ensue from this concept; some of which are as followings:

Slugging: One of the problems associated with coexisting of gas phase and liquid phases (s) such as oil/gas/water mixture is 'slugging' where separated flow can occur; i.e. slugs of the liquid phase(s) can form in the pipe separated by pockets of gas. This unstable and intermittent flow presents many hazards and can impact seriously the economics of a hydrocarbon producing system. For example the gas phase behind a liquid slug becomes compressed because the transportation of a liquid slug requires a larger pressure behind the slug to keep it moving. The arrival of this compressed gas at the outlet of a pipeline or production platform creates a large gas surge threatening the reliable and safe operation of processing equipment. Significant CAPEX is currently invested in slug catchers and other means of reducing the instability due to slugging in current hydrocarbon production systems. By converting the gas phase into hydrates, the density difference between phases (i.e., gas/oil/water changes to hydrate/oil/water) will be greatly reduced. This reduction should help to alleviate pipeline slugging problems, meaning significant savings in CAPEX.

Adjusting slurry flow properties: It is also possible to adjust the amount of water to achieve optimised hydrate slurry concentration with respect to hydrocarbon transport and slurry viscosity. There could be various variations to this option, for example: 1) there may not be any need to add water and AA, if the slurry is non-blocking; 2) there may not be any need to add excess water and only AA should be added, 3) it might be

necessary to add water but no need for AA; 4) both water and AA should be added. If there is a need to add water, then a pump might be necessary.

Pressure recovery: Another potential benefit can come from pressure recovery in the system. In single or multi-phase flow the pressure within the system is reduced during uphill movement of the fluid (s). It is recovered in single phase flow during downhill movement. In the case of gas/liquid flow, pressure is not recovered in downhill movement as the gas phase is not compressed. Therefore, in single phase flow, hydrostatic pressure drop depends on the difference between inlet and outlet elevations, but in gas/liquid flow, the hydrostatic pressure drop is the summation of pressure changes caused by all uphills. Furthermore, in gas/liquid fluid flow the frictional pressure drop depends on the flow regime and the superficial gas and liquid velocities, which could be higher than single phase pressure drops. Finally, there is an element of acceleration pressure drop in systems containing gas, which is negligible in incompressible fluid flow.

Reduction in wax deposition problems: An additional benefit of the concept is that it could also potentially reduce wax deposition problems by: (a) providing solid seeds for wax nucleation in the flowing liquid phase rather than on pipeline walls and (b) abrasion of deposited wax by fast moving hydrate particles.

Reduction in corrosion: *HYDRAFLOW* might also reduce corrosion by eliminating/reducing H_2S concentration in pipeline due to small and round H_2S molecules being preferably locked up as hydrate formers in hydrate structures.

Shut-ins and restarts: In many cases the main risk of gas hydrate blockage occurs during shut-ins when the pipeline temperatures drop to very low temperatures and during start-up when the system is pressurised to start the fluid flow. The risks associated with hydrate blockages due to shut-ins/restarts could be minimised or prevented in *HYDRAFLOW* concept by forming stable hydrate slurries. In particular, it is widely understood that AAs can be used in shut-ins/restarts to prevent hydrate blockage problems.

Simple processing equipments: Finally, as an advantage over other forms of cold flow, this concept could eliminate the need for a hydrate reactor and/or the need for multiphase subsea/remote pumps for circulating hydrate 'seed' nuclei. In *HYDRAFLOW* concept, the subsea pipeline acts as the reactor, producing hydrate in oil

and/or water slurries and the pump is a single phase pump located in the receiving facilities.

HYDRAFLOW – Loop concept: *HYDRAFLOW* technology could offer further benefits when used in conjunction with a novel 'loop' pipeline concept being developed as part of this study. In the loop system, the recycled fluid phase plays the role of carrier fluid, collecting produced hydrocarbons from various wells (individual wells are connected to this loop at various points), reacting with the gas phase to form hydrates and transporting them as hydrate slurry in oil and/or water to the production unit before being separated and injected back into the loop (Figure 2.22). If necessary, the loop pipeline diameter can be gradually increased, to accommodate the extra fluid (wells) on its way to a destination.

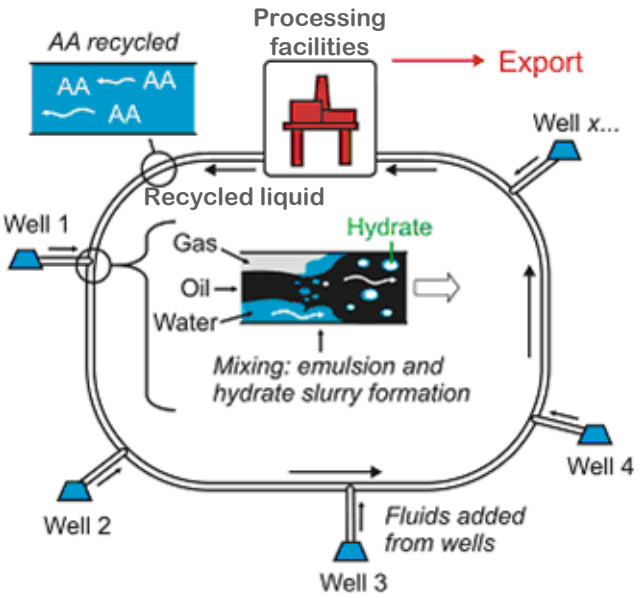

Figure 2.22 Illustration of the *HYDRAFLOW* pipeline 'Loop' concept.

When this slurry (hydrates + oil and/or free water) reaches to the receiving facilities onshore or on a platform, one can choose one of the following options depending on the specific conditions (after partial or total separation of free water phase):

- Dissociate the hydrates (by depressurisation and/or heating) and introduce the fluid system to a separator to recover the oil and gas
- Separate the hydrates and transport them (and hence the gas) as dry hydrates
- Mix the hydrates with oil and transport them as hydrates in oil slurry

- Where required mix the hydrates with extra water, i.e. to adjust the viscosity of slurry and transport them as hydrates in water slurry.

The objective of the 'Loop' concept is to recycle inhibitors, minimising the costs associated with various chemicals used in the oil industry (like corrosion, scale, wax and asphaltene inhibitors), and minimise their environmental impact. Furthermore, due to the partial closed loop nature of the proposed system and chemical separation, it should be possible to use low strength bio-degradable chemicals at high concentrations to improve their performance. The 'Loop' concept could also offer extra flexibility to the *HYDRAFLOW* concept for controlling the flow property and rheological behaviour of hydrate slurries by adjusting the amount of carrier fluids. For instance, there is a major challenge in gas condensate and natural gas systems as the amount liquid hydrocarbon and saline water in these systems is very low which can impair the efficiency of anti-agglomerants. In these cases, it could be possible to circulate a liquid hydrocarbon phase as carries fluid in the loop and also adjust the salinity of the aqueous phase.

The followings items address some enquiries about the *HYDRAFLOW* concept:

How much water has to be added to the system?

There are two opposing factors here. Increasing the amount of water (and liquid hydrocarbon, if necessary in gas condensate, natural gas or high GOR systems) will increase the total pipeline flow rate but will result in a low viscosity hydrate slurry, whereas, reducing the amount of water will have a positive impact on the total flow rate of the pipeline but will mean the hydrate content of the slurry is high hence high viscosity. The optimum range of water (and liquid hydrocarbon, if necessary) can and should therefore be determined by experimental means and/or integrated experimental and modelling approaches.

How hydrates can be separated/dissociated at the destination?

Various techniques can be used here, which are not the objective of this study. One option is to have a separator where the density difference between hydrates and water is used for their separation. It is also possible to introduce the incoming fluid to the top of a sieve tray; solid hydrates will remain at the top of the sieve tray whilst liquid phase will pass through and will be collected at the base of the separator. The collected water (part or all) and/or the water resulted from hydrate dissociation (part or all) could be recycled. The recycled stream may also contain liquid hydrocarbon to

improve the transportability of the hydrate slurries. Other separation techniques are also possible, for example in the case of ionic AAs, the application of ion exchanger units, and for polymeric AAs, membrane filtration units at destination may be considered. A process for degasification of hydrate slurry has also been patented by BP in WO2007/066071 (Argo et al., 2007) to which the reader is directed for detailed information.

2.7.4. HYDRAFLOW Economics

The objective of this section is to evaluate *HYDRAFLOW* economics compared to alternative techniques available. The benefits of this technique were explained in the earlier section, however, a summary of the benefits of this technique compared to alternative approaches, for economic evaluation purposes, are summarised below.

- Cold flow approach provides cost savings for selection of pipelines; i.e.: the diameter of the pipe required is smaller compared to other flow assurance techniques. The cold flow technique requires small amounts of chemicals to be injected, hence reduces the need for large pipe diameters for transferring thermodynamic inhibtors; however, the major source of cost-saving comes from the removal of the need for pipe insulation, as bare pipelines could be used. A bare steel pipeline (16") deployed subsea may cost around 0.5 Million USD per kilometre instead of around 1 Million USD per kilometre for insulated pipeline [Data gathered through several contacts/companies – 2006 costs]. The cost is obviously proportional to the length and diameter of the pipeline.
- The "Cold Flow" technique allows conversion of gas phase to hydrates; i.e.: creation of a fairly single phase flow and as a result pressure recovery in the system. Potential pressure recovery in the system will reduce the need for compression/pumping, hence reducing the CAPEX attached to it by reducing the size of compression equipments (pumps, compressors, etc.) required. Lower pressure drops could also result in higher overall recovery.
- By converting the gas phase into hydrates, the density difference between phases (e.g., water, oil, hydrates) will be greatly reduced, which should help to alleviate pipeline slugging problems, thus lowering CAPEX.

- From a final CAPEX view point and as an advantage over the other forms of cold flow, this concept could eliminate the need for a hydrate reactor and/or the need for multiphase subsea/remote pumps for circulating hydrate 'seed' nuclei. In *HYDRAFLOW* concept, the subsea pipeline acts as the reactor, producing hydrate in oil and/or water slurries and the pump is a single phase pump for circulating the liquid phase (after hydrate removal) located in the receiving facilities. Hence, the need for large multiphase pumps will be reduced. The *HYDRAFLOW* system, however, will need several components: The required components are pipeline for the pipe loop, a splitter and a pump. The size of the components required is normally small compared to the material/components required for other techniques.

- Shut-ins and restarts: In many cases the main risk of gas hydrate blockage occurs during shut-ins when the pipeline temperatures drop significantly and during start-up when the system is pressurised to start the fluid flow. The risks associated with hydrate blockages due to shut-ins/restarts could be minimised or prevented in *HYDRAFLOW* concept by forming stable hydrate slurries. In particular, it is widely accepted that anti-agglomerants can be used in shut-ins/restarts to prevent hydrate blockage problems. Cold flow reduces the number of interventions required for blockage removals/cleaning the pipes; hence reducing the OPEX and the shut-in times significantly. It has been well appreciated by the operators that reduction in the shut-in times results in added value/increased production.

- Cold Flow could potentially reduce wax deposition and consequently can reduce need for pigging. The pigging technique follows an easy concept and is being used in industry for long. The movement of pig in the pipe cleans the pipeline. Pigtraps are devices built into the pipelines to allow launching or removal of pigs from the pipeline. However, pigging requires shutting down the production, which results in lost production. Pigging can be expensive too. Pigs may cost from 50,000 USD to as high as 1,000,000 USD depending on the type of pig and the environment being used. Pigtraps can cost from 150,000 USD to 250,000 USD each for both receiver and launcher [Data gathered through several contacts/companies]. However, the cold flow technique significantly reduces the need for pigging, as mentioned earlier.

- *HYDRAFLOW* could have the extra benefit of minimising chemical and water treatment costs (this could include other chemicals, e.g., corrosion, scale, wax, asphaltene inhibitors) through aqueous phase recycling; this also helps to reduce the environmental impacts

The value of using *HYDRAFLOW* is the difference in Net Present Value (NPV) of the (oil) revenue and costs resulting from the application of *HYDRAFLOW* compared to other methods, once allowance has been made for risk and uncertainty issues connected to each method. The evaluation of the incremental cost and revenue are, however, complex. There are several input data required, some of which contain a large uncertainty in their value.

The benefits mentioned above are a summary of the added value which could be achieved by using *HYDRAFLOW* technique. However, it would be difficult to quantify the monetary value of this technology, as it is case dependent. Additionally, it would be difficult to put money on some benefits of *HYDRAFLOW* as the degree of added value for the benefits mentioned above is not well known, i.e.: carries some uncertainty. Hence, some advantages listed above can not be quantified accurately using commonly used economical evaluation techniques and requires more advanced qualitative methods such as "Real Options" which is out of the objective of this thesis. The "Real Options" theory was first used in finance and statistics and later developed in other disciplines. "Real Options" try to develop a range for the likely "added value" of a scenario. "Real Option Analysis (ROA) is often contrasted with more standard techniques of capital budgeting, such as NPV, where only the most likely or representative outcomes are modelled, and the flexibility available to management is thus ignored. The NPV framework therefore implicitly assumes that management will be passive as regards their Capital Investment once committed, whereas ROA assumes that they will be active and may/can modify the project as necessary (Harvey, 2002).

In the following sections it has been tried to compare the real cost elements for the current hydrate flow assurance techniques available. It should be highlighted that it is possible to make cases which show benefit for each technique compared to other ones; hence the monetary added value is very case-dependent. However, comparing the cost elements and the potential risk and uncertainty attached to each method helps to determine the potential added value for each technique; hence, selecting the best practice. The techniques which will be discussed are as below:

- Pipe insulation
- Thermodynamic hydrate inhibitors
- Low dosage hydrates inhibitors (LDHIs)

Pipeline insulation:

The insulation techniques are being used conventionally for heat loss/hydrate formation prevention. Pipe insulation has proven to add value; however its efficiency might not be sufficient enough compared to other techniques, considering the cost attached to it. The cost of insulation is a function of the pipe diameter and pipe length and can vary with the type of insulation. Pipe insulation in conjunction with other hydrate prevention techniques (e.g. methanol injection) can be used for increased efficiency. The insulation price of a thermal insulated pipeline is around 0.5-1 Million USD per kilometre depending on the pipe diameter and the material used [Data gathered through several contacts/companies - 2006 costs]. The environment where the pipe is installed also impacts the cost.

The insulation techniques are common in oil transportation systems with wax formation potential, so that insulation can prevent/reduce wax formation too.

Thermodynamic hydrate inhibitors:

Thermodynamic hydrate inhibitors are commonly used for hydrate reduction/prevention. Methanol and mono-ethylene glycol (MEG) are most common but other similar compounds are also sometimes used.

The cost of MEG is normally higher per unit volume compared to methanol. It is therefore only used continuously when it can be recovered or in special situations. However, regenerating glycol is associated with high CAPEX because of the equipments needed (Tvedt, 2005). Water need to be heated (boiled) for separating the MEG. This will require a large portion of heat, which again could be costly to acquire.

Instead, Methanol is normally used without regeneration, however, it normally evaporates to the gas phase and consumed in the process. Hence, large volumes of methanol might be required, even more than the volume of water in the oil. This means that large storing and transportation volumes will also be required which adds to the costs.

Worldwide methanol costs for hydrate inhibition are estimated at US$220 million annually [Data gathered through several contacts/companies]. In addition, severe financial investment/penalties are required/paid for large methanol storage capacity on offshore platforms and for greater than 50 p.p.m. methanol contaminations in refinery feedstock.

Methanol and MEG can cost around 1 – 5 USD per litre [Data gathered through several contacts/companies – 2006 cost]. As all the MEG cannot be regenerated, new MEG will need to be added, thus increasing the costs. This increases the costs of a MEG injection system as well as a costly extra pipeline being required.

The infrastructure for thermodynamic hydrate inhibiting systems is expensive. The cost of reinjection pipeline is a function of the length and diameter of other pipelines. The chemical injection pipelines will also require several equipments, valves, tanks for chemical storage, pumps, etc. The regeneration system depending on the size, infrastructure, etc. can cost 50-200 Million USD [Data gathered through several contacts/companies - 2006 cost].

Low Dosage Hydrate Inhibitors (LDHIs):

Low dosage hydrates inhibitors normally cost less than the thermodynamic hydrate inhibitors as no large storage tanks, no large pipelines and regeneration infrastructure is required. The chemicals can cost 7-10 USD per litre depending on the region it is being used, which is relatively expensive, however, one weight percent of chemical, or even less, added to the production line, is sufficient to prevent hydrate formation. The weight percent of inhibitor required (roughly 1%) compared to the required weight percent of methanol (30-60%) is quite low, which results in a reduced total cost for the application of these inhibitors.

Thermal insulation of pipeline with addition of chemicals can further add value. This practice is being used in industry. In fact, LDHIs can work in lower temperatures too. Hence, another advantage of LDHIs comes from the reduced need for pipe insulation. However, LDHIs may react with the oil and reduce the quality of oil, which is one of their drawbacks.

There are published examples of successful field application of LDHIs (Glenat, 2004). The benefit of using LDHIs instead of a usual MEG loop which requires to have specific process items such as MEG regeneration unit, etc. resulted in a savings of

around 50 Million USD (2003 costs) in investment, for a Middle-Eastern gas condensate field. The field production was around 2 Bcf/d of gas including around 40000 bpd of condensate [Data gathered through several contacts/companies – e.g.: Total].

It should be highlighted that *HYDRAFLOW* has several advantages, which listed earlier; a detailed cost calculation will be required in order to put money on all those elements, which is outside the objectives of this thesis. However, obviously, incorporating all the advantages of the *HYDRAFLOW* into cost calculation will result in a larger added value for this technology.

BP has done a series of cost calculations which shows a reduced CAPEX of up to 30 percent, and reduced OPEX of around 10 percent compared to LDHI and insulations for their cold flow technique. These cost savings can reduce the cost of subsea development in deepwater by the order of 100 Million USD (Tvedt, V., 2005). These numbers are case dependent and vary from a case to another. However, the cost of a cold flow hydrate prevention system is generally lower than other techniques as the components required, as explained above, are less and smaller in size and price.

Here, it was tried to give an overview of the cost elements attached to each hydrate prevention/reduction technique. Decision-making on the application of these techniques is not only a cost comparison issue. The operational issues, compatibility and flexibility to use, the quality and type of oil, the range of produced water-cut, etc. should all be taken into consideration when deciding on the best technique and developing a hydrate prevention/reduction technique screening tool. However, a quick comparison of the above-mentioned cost elements and benefits shows higher potential "added value" for the *HYDRAFLOW* compared to other techniques.

2.8. Summary

This chapter reviewed the existing gas hydrate flow assurance techniques and their limitations. New emerging Cold flow concepts including *HYDRAFLOW* as alternative solution for gas hydrate problems were also presented in this chapter. It was shown that there is a high potential for *HYDRAFLOW* to be implemented by the oil and gas industry due to its economical and technical benefits.

In order to design the production systems properly to implement this cold flow technology, it is critical to fully understand the rheological behaviour of hydrate

slurries in flowing and shut-in/restarts conditions. Risk management of hydrates in pipelines also requires better knowledge of how hydrates agglomerate and eventually form a plug in flow lines. A literature review on hydrate plugging and rheology and the effect of key variables on flow characteristics of hydrate slurries will be detailed in the next chapter. The experimental results on the demonstration of *HYDRAFLOW* concept, supporting the feasibility of the concept will be detailed in Chapters 5–7.

2.9. References

Alapati, R., Lee, J. and Beard, D., 2008. Two Field Studies Demonstrate that New AA LDHI Chemistry is Effective at High Water-cuts Without Impacting Oil/Water Quality. *Offshore Technology Conference*, Houston, TX, U.S.A., 5-8 May 2008.

Anderson, V. and Gudmundsson, J. S., 1999. Flow Experiments on Concentrated Hydrate Slurries. *Annual Technical Conference and Exhibition.* Houston, Texas, 3-6 Oct 1999.

Andersson, V. and Gudmundsson, J. S., 2000. Flow Properties of Hydrate-in-Water Slurries. *Ann. N. Y., Acad. Sci.*, **912** (Issue GAS HYDRATES: CHALLENGES FOR THE FUTURE), pp.322-329.

Anderson, B. J., Tester, J. W., Borghi, G. P., and Trout, B. L., 2005. Properties of Inhibitors of Methane Hydrate Formation via Molecular Dynamics Simulations. *Journal of the American Chemical Society*, **127**, pp.17852-17862.

Argo, C. B., Harper, R. N., King, D. C. and Willcox, P., 2007. *Process for Regasifying a Gas Hydrate Slurry*. World. Pat. 066071

Behar, E., 1994. *Gas Hydrate Seminar*. Trondheim, Norway, June 1992.

Behar, P., Kessel, D. and Sugier, A., 1991. Advances in Hydrate Control. *70th gas processors association conference*, San Antonio, 11-12 March 1991.

Blytas, G. C. and Kruka, V. R., 2001. World. Pat. 38695.

Borgund, A. E., Hoiland, S., Barth, T., Fotland, P., Kini, R. A. and Larsen, R., 2008. Critical Descriptors for Hydrate Properties of Oils: Compositional Features. *6th International Conference on Gas Hydrates*, Vancouver, British Columbia, CANADA, 6-10 July 2008.

Brustad, S, Loken K. P. and Waalmann J.G., 2005. Hydrate Prevention Using MEG instead of MeOH: Impact of Experience from Major Norwegien Developments on Technology Selection for Injection and Recovery of MEG. *Offshore Technology Conference*. Houston, TX, USA, 2-5 May 2005.

Claussen, W. F., 1951. Suggested Structures of Water in Inert Gas Hydrate. *J. Chem. Phys.*, **19**, pp.259-260.

Colle, K. S., Oelfke, R., H. and Kelland, M. A., 1999. U.S. Pat. 5874660.

Crosby, D. L., Rivers, G. T. and Frostman, L. M., 2005. U.S. Pat. 0261529.

Dahlmann, U. and Feustel, M., 2004a. *Additives for inhibiting the formation of gas hydrates*. US Pat. 0159041.

Dahlmann, U. and Feustel, M., 2004b. Corrosion and Gas Hydrate Inhibitors Having Improved Water Solubility and Increases Biodegradability. US Pat. 0166307.

Delion, A. S., Durand, J. P., Gateau, P. and Velly, M., 1998. Process for Inhibiting or Retarding the Formation and/or Aggregation of Hydrates in Production Effluents. US Pat. 5817898.

Denniel, S., Perrin, J. and Felix-Henry, A., 2004. Review of Flow Assurance Solutions for Deepwater Fields. *Offshore Technology Conference.* Houston, Texas, U.S.A., 3-6 May 2004.

Durand, J. P., Gateau, P., Delion, A. S. and Sugier, A., 1995. Method for Reducing the Agglomeration Tendency of Hydrates in Production Effluents. US Pat. 5434323.

Erstad, K., Hoiland, S., Barth, T and Fotland, P., 2008. Isolation and Molecular Identification of Hydrate Surface Active Components in Petroleum Acid Fractions. *6th International Conference on Gas Hydrates.* Vancouver, British Columbia, CANADA, 6-10 July 2008.

Fadnes, F.H.; 1996. Natural Hydrate Inhibiting Components in Crude Oils - Fluid Phase Equilibria. *ELSEVIER* **117** pp.186-192.

Freer, E. M., and Sloan, E. D., 2000. An Engineering Approach to Kinetic Inhibitor Design Using Molecular Dynamics Simulations. *Annals of the New York Academy of Sciences,* **912**, pp.651 – 657.

Frostman, L. M., 2000. Anti-Agglomerant Hydrate Inhibitors for Prevention of Hydrate Plugs in Deepwater Systems. *SPE Annual Technical Conference and Exhibition*. Dallas, Texas, 1–4 October 2000.

Genov, G. and Skaare, B.; 2008. Comparing Biodegradation Levels and Gas Hydrate Plugging Potential of Crude Oils using Whole-Oil Gas-Chromatography and Multi-Variate Analysis. *6th International Conference on Gas Hydrates (ICGH).* Vancouver, British Columbia, CANADA, 6-10 July 2008.

Gudmundsson, J. S., Andersson, V., Durgut, I., Levik, O.I., and Mork, M., 1999. NGH on FPSO – Slurry Process and Cost Estimate. *SPE Annual Technical Conference and Exhibition.* Houston, Texas, 3-6 Oct 1999.

Gudmundsson, J. S. and Mork, M., 2001. Stranded Gas to Hydrate for Storage and Transport. *International Gas Research Conference.* Amesterdam, 5-8 November 2001.

Gudmundsson, J. S., Mork, M., and, Graff, O. F., 2002. Hydrate Non-Pipeline Technology. *4th International Conference on Gas Hydrate.* Yokohama, 19-23 May 2002.

Gudmundsson, J. S., 2002. Cold Flow Hydrate Technology. *4th International Conference on Gas Hydrates*. Yokohama, 19-23 May 2002.

Haghighi, H., Chapoy, A., Burgess, R., Mazloum, S. and Tohidi, B., 2009. Phase Equilibria for Petroleum Reservoir Fluids Containing Water and Aqueous Methanol Solutions: Experimental Measurements and Modelling Using the CPA Equation of State. *J. Fluid Phase Equilibr.*, **278**, pp.109–116.

Haghighi, H., Chapoy, A. and Tohidi, B., 2009. Experimental and Thermodynamic Modelling of Systems Containing Water and Ethylene-glycol: Application to Flow Assurance and Gas Processing. *J. Fluid Phase Equilibr*., **276**, pp.24-30.

Harvey, C. R., 2002. Identifying Real Options. *Duke University*.

Hoppe, R., Martin, R. L., Pakulski, M.K. and Schaffer, T. D., 2006. Corrosion Mitigation with Gas Hydrate Inhibitors. *SPE Gas Technology Symposium.* Calgary, Alberta, Canada, 15-17 May 2006.

Huo, Z., Freer, E., Lamar, M., Sannigrahi, B., Knauss, D.M., and Sloan Jr., E.D., 2001. Hydrate Plug Prevention by Anti-Agglomeration. *Chem. Eng. Sci.* **56**, pp.4979-4991.

Irvin, G., Li, S., Simmons, B., John, V., McPherson, G., Max, M. and Pellenbarg, R., 2000. Control of Gas Hydrate Formation Using Surfactant Systems: Underlying Concepts and New Applications. *Annals New York Academy of Science*. pp.515-526.

ITI Energy, 2004. Foresighting Report – Maximing Value of Mature Oil and Gas Assets. Scotland, October 2004.

Kalogerakis, N., Jamaluddin, A. K. N., Dholabhai, P. D. and Bishnoi, P. R., 1993. Effect of Surfactants on Hydrate Formation Kinetics. *SPE International Symposium on Oilfield Chemistry*. New Orleans, 2-5 March 1993.

Karaaslan, U. and Parlaktuna, M., 2000. Effect of surfactants on hydrate formation rate. *Annals New York Academy of Science*, pp. 735-743

Kelland, M. A., 2006. History of the Development of Low Dosage Hydrate Inhibitors. *Energy and Fuels*, **20**, pp.825–847

Kelland, M. A., Svartaas, T. M. and Dybvik, L. A., 1996. *2nd International Conference on Gas Hydrates*, Toulouse , 7-9 June 1996.

Kelland, M. A., Svartaas, T. M. and Dybvik, L. A., 1995a. Studies on New Gas Hydrate Inhibitors. *SPE Annual Technical Conference.* Dallas, 22-25 October 1995.

Kelland, M. A., Svartaas, T. M. and Dybvik, L., A., 1995b. A New Generation of Hydrate Inhibitors. *SPE Annual Technical Conference in Dallas*, 22-25 October 1995.

Kini, R. A., Matthews, P. N., Surbramanian, S. and Creek, J., 2005. Changing the Focus of Hydrate Plug Prevention in the Oil Industry. *5th International Conference on Gas Hydrate.* Trondheim, Norway, 12-16 June 2005.

Klomp, U. C., Kruka, V.R., Reijnhart, R. and Weisenborn, A. J., 1995. *A Method for Inhibiting the Plugging of Conduits by Gas Hydrates*. WIPO Pat. WO 95/17579.

Kuliev A. M., et al., 1972. Surfactants Studies as Hydrate-Formation Inhibitors. *Gazov. Delo.* **10**, pp.17-19.

Kvamme, B., Kuznetsova, T., and Aasoldsen, K. 2005. Molecular Dynamics Simulations for Selection of Kinetic Hydrate Inhibitors. *Journal of Molecular Graphics and Modelling*, **23**, pp.524–536.

Larsen, R., Lund, A., Andersson, V. and Hjarbo, K. W., 2001. Conversion of Water to Hydrate Particles. *SPE Annual Technical Conference and Exhibition.* New Orleans, Louisiana, 30 September-3 October 2001.

Larsen, R., Lund, A. and Argo, C.B., 2003. Cold Flow - A Practical Solution. *11th International Conference "Multiphase 03", BHR group*. San Remo, Italy, 11-13 June 2003.

Larsen, R., Lund, A., Hjarbo, K. W and Wolden, M., 2009. Robustness Testing of Cold Flow. *20th International Oil Field Chemistry Symposium*. Geilo, Norway, 22-25 March 2009.

Leporcher, E.M., Peytavy, J.L., Mollier, Y. and Sjoblom, J., 1998. Multiphase Transportation: Hydrate Plugging Through Crude Oil Natural Surfactants. *SPE Annual Technical Conference and Exhibition*. New Orleans, Louisiana, 27-30 Sep. 1998.

Lund, A., Lysne, D., Larsen, R. and Hjarbo, K. W, 2004. *Method and System for Treansporting a Flow of Fluid Hydrocarbons Containing Water*. US Pat. 6,774, 276, B1.

Lund, A., Hjarbo, K. W, Larsen, R. and Lysne, D., 2000. Method and System for Treansporting a Flow of Fluid Hydrocarbons Containing Water. CA. Pat. 2 569 693.

Lund, A. and Larsen, R., 2000. Conversion of Water to Hydrate Particles – Theory and Application. 14th Symposium on Thermophysical Properties, Boulder, CO. USA, June 2000.

Makogon, Y. M., and Sloan, E. D., 2002. Mechanism of Kinetic Hydrate Inhibitors. *4th International Conference on Gas Hydrates.* Yokohama, Japan, 2002.

Metha, A. P., and Klomp U. C., 2005. An Industry Perspective on the State of the Art of Hydrates Management. *5th International Conference on Gas Hydrate.* Trondheim, Norway, 12-16 June 2005.

Matthews, P. N., Subramanian, S. and Creek, J. L., 2005. Method and System for Preventing Clathrate Hydrate Blockage Formation in Flow Lines by Enhancing Water Cut. US Pat. 0137432 A1.

Milburn, C. R. and Sitz, G. M., 2000. *Novel amines useful in inhibiting gas hydrate formation.* WIPO. Pat. 0078706.

Milburn, C. R. and Sitz, G. M., 2002. Novel amines useful in inhibiting gas hydrate formation. US Pat. 6444852.

Mokhatab, S., Wilkens, R. J. and Leontaritis, K. J., 2007. A Review of Strategies for Solving Gas Hydrate Problems in Subsea Pipelines. *Energy Source,* **29**(Part A), pp.39-45.

Mork, M., 2002. *Formation Rate of Natural Gas Hydrate – Reactor Experiments and Models*. Ph.D. Norwegian University of Science and Technology.

Mork, M. and Gudmundsson, J.S., 2002. Hydrate Formation Rate in a Continuous Stirred Tank Reactor: Experimental Results and Bubble-to-Crystal Model. *4th International Conference on Gas Hydrate*. Yokohama, Japan, 19-23 May 2002.

Ng, H.J., Chen, C.J. and Robinson, D.B., 1985. Effect of Ethylene Glycol or Methanol on Hydrate Formation in Systems Containing Ethane, Propane, Carbon Dioxide, Hydrogen Sulphide or a Typical Gas Condensate. GPA Research Report RR-92

Pakulski, M., 2000. European Pat. 6025302

Palermo, T., Mussumeci, A. and Leporcher, E., 2004. Could Hydrate Plugging Be Avoided Because of Surfactant Properties of the Crude and Appropriate Flow Condition? *Offshore Technology conference*. Houston, Texas, U.S.A., 3-6 May 2004.

Panchalingham, V., Rudel, M. G. and Bodnar, S. H., 2005a. Methods for Inhibiting Hydrate Blockage in Oil and Gas Pipelines Using Amide Compounds. US Pat. 0081432.

Panchalingham, V., Rudel, M. G. and Bodnar, S. H., 2005b. Methods for Inhibiting Hydrate Blockage in Oil and Gas Pipelines Using Amino Alcohols and Ester Compounds. US Pat.0085396.

Panchalingham, V., Rudel, M. G. and Bodnar, S. H., 2005c. Methods for Inhibiting Hydrate Blockage in Oil and Gas Pipelines Using Ester Compounds. US Pat. 0085675.

Panchalingham, V., Rudel, M. G. and Bodnar, S. H., 2005d. Methods for Inhibiting Hydrate Blockage in Oil and Gas Pipelines Using Betaines and Amine Oxides. US Pat. 0085676.

Panchalingham, V., Rudel, M. G. and Bodnar, S. H., 2006. Methods for Inhibiting Hydrate Blockage in Oil and Gas Pipelines Using Simple Quaternary Ammonium and Phosphonium Compounds. UK Pat. GB2422840.

Peysson, Y., Nuland, S., Maurel, P. and Vilagines, R.: 2003. Flow of Hydrate Dispersed in Production Lines. *SPE Annual Technical Conference and Exhibition*. Denver, Colorado, US, 5–8 October 2003.

Peytavy, J. L, Glenat, P. and Bourg Patrick, 2008. Qualification of Low Dose Hydarte Inhibitors (LDHIs): Field Cases Studies Demonstrate the Good Reproducibility of the Results Obtained from Flow Loops. *6th International Conference on Gas Hydrates (ICGH).* Vancouver, British Columbia, CANADA, 6-10 July 2008.

Pierrot, A., Doerler, N. and Goodwin, S., 1992. *Offshore Northern Seas Conference.* Stavanger, 28 August 1992.

Reijnhout, M. J., Kind, C. E. and Klomp, U. C., 1993. European Pat. 0 526 929 A1.

Ripmeester, J. A., Tsee, J.S., Ratcliffe, C.I., and Powell, B.M., 1987. A new Clathrate Hdrate Structure. *Nature*, **325** (6100), pp.135-136.

Rivers, G. T. and Down, H. H., 2004. Pat.0144732

Rivers, G. T., Frostman, L. M., Pryzbyliski, J. L. and McMahan, J. A., 2003. US Pat. 0146173.

Sinquin, A., Velly, M. and Durand, J. P., 1998. European Pat. 789132.

Sinquin, A., Bredzinsky, X. and Beunat.; 2001. Kinetic of Hydrates Formation: Influence of Crude Oils. *SPE Annual Technical Conference and Exhibition*. New Orleans, Louisiana, 30 September–3 October 2001.

Sloan, E.D. and Koh, C. A., 2008. *Clathrate Hydrates of Natural Gas*. 3rd ed. New York: CRC Press.

Sloan, E. D., 2005. A changing Hydrate Paradigm- from Apprehension to Avoidance to Risk Management. *Fluid Phase Equilibr*., 228-229, 67-74

Sloan, E. D., 2003. Fundamental Principles and Applications of Natural Gas Hydrates. *Nature*, **426**, pp.353-363

Sloan, E. D., 1998. *Hydrate Engineering*, Richardson, TX: Society of Petroleum Engineers Inc.

Sloan, E. D., Christiansen, R. L., Lederhos, J., Panchalingam, V., Du, Y., Sum, A. K. W. and Ping, J., 1997. U.S. Pat. 5639925.

Sugier, A., Bourgmayer, P. and Durand, J. P., 1993. Process for delaying the formation and/or reducing the agglomeration tendency of hydrates. US Pat. 5244878.

Sloan, E. D., 1995a. U.S. Pat. 5420370.

Sloan, E. D., 1995b. U.S. Pat. 5432292.

Sugier, A., Bourgmayer, P., Behar, E. and Freund, E., 1989a. *Method for Transporting a Hydrate Forming Liquid.* European Pat. 0323307.

Sugier, A., Bourgmayer, P., Behar, E. and Freund, E., 1989b. Process to Retard the Formation of Hydrates, or to Reduce Their Agglomeration Characteristics. European Pat. 0323774.

Sugier, A., Bourgmayer, P. and Stern, R., 1989c. Process for Delaying the Formation and/or Reducing the Agglomeration Tendency of Hydrates. European Pat. 0323775.

Takahashi, M. Moriya, H., Katoh, Y. and Iwasaki, T., 2008. Development of Natural gas Hydrate (NGH) Pellet Production System by Bench Scale Unit for Transportation and Storage of NGH Pellet. *6th International Conference on Gas Hydrate*. Vancouver, British Columbia, Canada, 6-10 June 2008.

Taxy, S., 2007. *Introduction to Flow Assurance*. Available at: <http://www.subseauk.org/documents/Stephane%20Taxy%20-%20DORIS.pdf> [Accessed 18 April 2008].

Tohidi, B., 2006. *Novel Hydrate Based Systems*. International Pat. WO 2006/048666.

Tvedt, V., 2005. Transportation of Petroleum in Subsea Pipelines - A Competitive Analysis. BSc. Norwegian University of Science and Technology.

Urdah, O., Bornes, A. H., Kinnari, K. J and Holme, R., 2004. Operational Experience by Applying Direct Electrical Heating for Hydrate Prevention. *SPE Production and Facilities*, **19**(number 3), pp.161-167.

von Stackelberg, M. and Muller,H. R., 1951. *Naturwiss,*, ***38***, p.456.

Wolden, M., Lund, A., Oza, N., Makogen, T.Y., Argo, C.B.and Larsen, R., 2005. Cold Flow Black Oil Slurry Transport of Suspended Hydrate and Wax Solids. *5th International Conference on Gas Hydrates.* Trondheim, Norway, June 13-16 2005.

Yolsim, J. and Englezos, P., 2008. The Effect of Surfactant on the Morphology of Methane/Propane Clathrate Hydrate Crystals. *6th ICGH*, Vancouver, British Columbia, 6-10 July 2008.

York, J. D and Firoozabadi, A., 2008. Comparing Effectiveness of Rhamnolipid Bio-Surfactant with a Quaternary Ammonium Salt Surfactant for Hydrate Anti-Agglomeration. *J. Phys. Chem.*, **112**, pp.845-851.

Chapter 3. Review of Hydrates Flow Behaviour

3.1. Introduction

A summary of hydrate plugging and rheology and the effect of key variables on flow characteristics of hydrate slurries are presented in this chapter.

3.2. Hydrate agglomeration and plug formation in flow lines

Hydrate particle agglomeration plays an important role in pipeline plug formation. It involves the cohesion of the growing crystals to form larger hydrate particles.

Austvik et al. have investigated the evolution of hydrate growth and their agglomeration. They have described hydrate plug formation in a gas/liquid hydrocarbon/water system using macroscopic scale observations (Austvik et al., 2000). The paper identifies the following five distinct stages in hydrate plug formation in pipelines: initial stage, first intermediate stage, agglomeration stage, second intermediate stage and the disintegrated stage. In the initial stage, hydrates are mainly small particles suspended in water with low agglomeration tendency. Sometimes at this stage, hydrate covers the droplets; however, they usually break to particles and release the confined water. As more hydrate forms, sticky hydrate particles agglomerate and forms lumps of hydrates in the bulk. Hydrates may also stick to the

pipe wall and develop a hydrate layer on the wall. These hydrate layers and lumps normally trap the free water in the pores and prevent further hydrate formation. There are different parameters affecting agglomeration and may lead to transportable hydrate slurry or plugs. When hydrate lumps are transported in the system, hydrates can form then on the surface of the lumps and reduces the gluing effect of the water phase. Reduced water wetting surface introduce a water flux from inside of the lumps to the surface due to capillary forces and therefore the trapped water in the lumps converts to hydrates. In this second intermediate stage, internal pressure changes and loss of water bridging cause a gradual disintegration of the plugs. And finally when the stickiness of the hydrate particles to the pipe wall and to other hydrate particles is lost, the disintegrated stage is reached. In this stage most of the water has been converted to powder-like hydrates.

Austvik's study seems to be the continuation of Alavik's works who described the appearance and characteristics of hydrate macrostructures as three main groups and the transition zones between each as in Table 3.1. The most notable contribution of Austvik was the identification that the agglomeration of hydrates is due to the water phase located between particles, which results in a glue-like effect; and the observation that during hydrate formation virtually all the free water is absorbed into the hydrate phase. The paper went on to claim that the gluing effect or water bridging is dominated by the capillary forces created by the different gases and liquids between the hydrate particles. As the water bridges are themselves converted into hydrate, the agglomerates break into smaller particles and powder like hydrates and are transported easily by the hydrocarbon phase.

Figure 3.1 also shows a simplified conceptual picture for hydrate plugging from a water-in oil emulsion which is an extension by Turner from the idea proposed by Lingelem et al (Lingelem et al, 1994) from Norsk Hydro. It is assumed that the oil phase is the dominated phase and forms water in oil emulsion in pipeline. Initially, a thin hydrate layer form around the water droplets. This layer growths and confines the water; however does not usually fully convert to hydrates. As more hydrates form, particles agglomerate together due to capillary attraction and therefore the viscosity of the system and the pressure drop in the pipe increases significantly. The point where aggregates become very large and stop the passage of the fluid is the indication of pipeline blockage (Sloan, 2008).

Table 3.1: Main Groups of Gas Hydrate Macroscopic Structures (Lund, 1994)

Macroscopic Structures	Common for the Group	Appearances Observed in Pipelines
1. Slurry-like hydrates	A liquid-like mixture of particles and water	– Milky liquid, Particles suspended in the water – Droplets covered with hydrates – High viscosity liquid
2. Transition slurry/slush	Hydrates flocs sticking together	– Partly soft hydrates, partly lumps – Depositions on the pipe wall
3. Slush-like hydrates	Hydrates forming larger flocs and lumps. Looking like wet snow	– Lumps filling most of the pipe cross-section area – Balls rolling on the pipe wall
4. Transition slush/powder	Hydrate lumps breaking up	– Hydrate lumps with a coral like surface – Gradually smaller hydrate lumps and flocs – Some depositions on the pipe wall
5.Powder-like hydrates	Hydrates with a powder-like appearance. Easily transported through the pipe	– Coarse grained powder – Gradually more fine grained powder

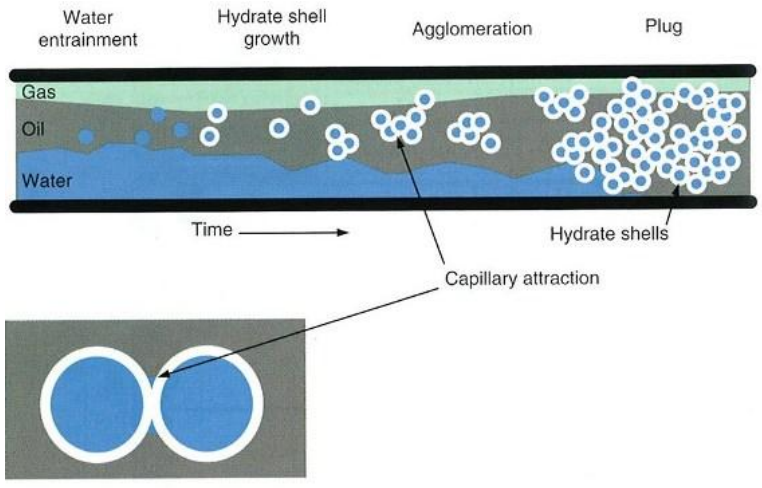

Figure 3.1: Hydrate plug formation in an oil dominated system (Sloan, 2008)

This water-oil emulsion concept may not be applied for gas dominated systems as the gas to liquid ratio is very high. Figure 3.2 gives a simplified conceptual picture for hydrate plugging in a gas dominated system which is again an extension from the idea proposed by Lingelmen et al. (Lingelem et al, 1994) from Norsk Hydro. Initially gas and an aqueous phase (due to both produced water and condensed water from the gas phase) are present in the pipeline. The pipe wall has a lower temperature than the gas due to heat transfer with the outside environment and therefore hydrates usually form on the pipe wall. As more hydrate forms and the deposition on the wall become thicker, the pressure drop in the pipeline gradually increases. At point E the deposits break away from the wall due to stress imposed by their weight and also by the passing fluid. Finally the detached hydrate particles stick together and form plug which stops production.

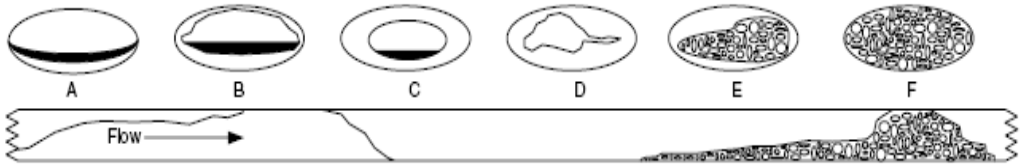

Figure 3.2: Hydrate plug formation in gas dominated system (Sloan, 2008)

3.3. Different type of forces involved in agglomeration of hydrates

The first work describing the effect of the capillary forces on holding the hydrate particles together was by Austvik et al., (2000) as detailed above. Camargo and Palermo (2002) proceeded to confirm the earlier work by Austvik and carried out a simple calculation based on existing theoretical correlations to express the capillary forces between hydrate particles using the expression:

$$F_a \approx 2\pi R \gamma_{wo} \cos\theta \qquad \text{Equation 3.1}$$

Where F_a is the adhesion force between hydrate particles (spheres of radius R), γ_{wo} is the water/oil interfacial tension and θ is the contact angle of the capillary liquid on the hydrate particle. This expression with a contact angle $\theta = 0$ (high hydrophobic hydrate surface) and an interfacial tension $\gamma_{wo} \approx 10$ mN/m shows that capillary forces would be of the order: $F_a/R > 50$ mN/m. This value is quite high compared with other interaction forces existing between hydrate particles, i.e. polymer-like forces ($F_a/R \approx 1$

mN/m) and van der Waals forces ($F_a/R \approx 0.1$ mN/m). It is proposed that some components of oil like asphaltenes adsorbed on the hydrate particles generate an attraction (polymer-like) force between hydrate particles that leads to a reversible aggregation process, responsible for the shear thinning behaviour and thixotropy shown by the hydrate suspensions. The van der Waals forces between two hydrate particles (assuming two sphere of same radius R) is given by the relation:

$$F_a = AR/12\ D^2 \qquad \text{Equation 3.2}$$

where A is the Hamark constant and D the distance which separates the two spheres.

The main conclusion gained from this work was that the attraction due to the capillary forces is significant and is responsible for the process of agglomeration; furthermore, changing the wettability of the hydrate is likely to reduce agglomeration.

Yang *et al.* (2004) described a method to directly measure the adherence forces of two hydrate particles. The work involved a micromechanical technique involving attaching hydrate particles to two small cantilevers and placing them together. The separation of the cantilevers results in the particles separating, and the adherence force is representative of the force applied on the cantilevers to separate the particles. Atmospheric tests were conducted with ice/*n*-decane and tetrahydrofuran hydrate/*n*-decane systems to measure the adherence forces as a function of temperature. The results showed that: an increase in roughness of hydrate crystals reduces the adhesion forces; and reducing the temperature below the freezing point of the particles results in a weakening of the adhesion forces, which is attributed to a reduction in a free water layer or a depression in freezing point of the capillary bridges.

3.4. Factors affecting hydrate aggregation and transportability in pipeline

It is critical to understand the effect of different factors and parameters influencing the hydrate flow behaviour in order to properly deploy novel flow assurance strategies and potentially reduce the risk of hydrate plug formation in pipeline and wellbore. While many variables control aggregation and transportability of hydrates, the major parameters are as follow.

Oil properties: Crude oils consist of mixtures of thousands of hydrocarbon compounds. As a result, each type of crude has distinct properties that affect the way oil behave. Oil chemical composition and oil interfacial tension with water are known

to play an important role in the potential of forming hydrate plugs though the difference in interfacial tensions can be attributed to the differences in chemical compositions. The effect of oil chemical composition, i.e. presence of natural anti-agglomerants, on plug formation tendency of crude oil has been detailed in chapter 2. Water/oil interfacial tension can alter hydrate agglomeration directly through its effect on capillary forces and indirectly through its effect on hydrate wettability and water droplet size. Smaller droplet size can be produced from a lower water/oil interfacial tension.

In the capillary bridge theory, liquid water wets the surface of hydrate particles and creates a liquid bridge between the particles when brought into contact. According to the Equation 3.1, the interfacial energy of the surrounding fluid substantially affects the adhesion force of hydrate particles. Therefore, one might consider reducing the interfacial energy of the oil and water, i.e. by injecting anti-agglomerants/surfactants, to reduce hydrate agglomeration.

Interfacial energy and Wettability: Recently, Høiland et al (2005) discovered that hydrate particles will prevent agglomeration into large aggregates and plugs if they are oil-wet and will agglomerate if they are water-wet. They invented a simple method to determine if an oil/water system is most likely to form water-wet or oil-wet hydrate particles. The idea is that if water-wet hydrates are to be formed, there must be a water volume fraction at which an oil continuous emulsion converts into a water continuous emulsion as soon as hydrates start to form. Conversely, if oil-wet hydrates are to be formed, there must be a water volume fraction at which a water continuous emulsion converts to an oil continuous emulsion. In their study, experiments were performed with 12 different crude oil/brine emulsions and the effect of Freon hydrate particles on inversion point was investigated. A reduction in the inversion point (volume fraction of water at which emulsion converts from being oil continuous to being in the inversion range) is attributed to water-wet hydrates, where as an increase is attributed to oil-wet hydrates. Only two oils were found to generate oil-wet hydrates and these two oils were the only oils that had shown low plugging tendency at realistic conditions.

Fotland et al. (2008) has described how interfacial tensions of water/oil, hydrate/water and hydrate/oil affect wettability and position of hydrate particles using wetting diagrams (e.g. Figure 3.3). These diagrams are graphical illustrations of all possible

wetting states. The upper left boundary (γ=0) is the situation where hydrate particle would resides entirely in the aqueous phase and would be strong water-wet. Conversely, lower right boundary (γ=180 & α=0) is the state of strong oil-wet hydrate particles and oil phase would cover hydrate surface. Any other points between boundaries of the wetting states are intermediate wet particles and are able to form stable water continuous or oil continuous emulsions depending on whether they are water-wet or oil-wet.

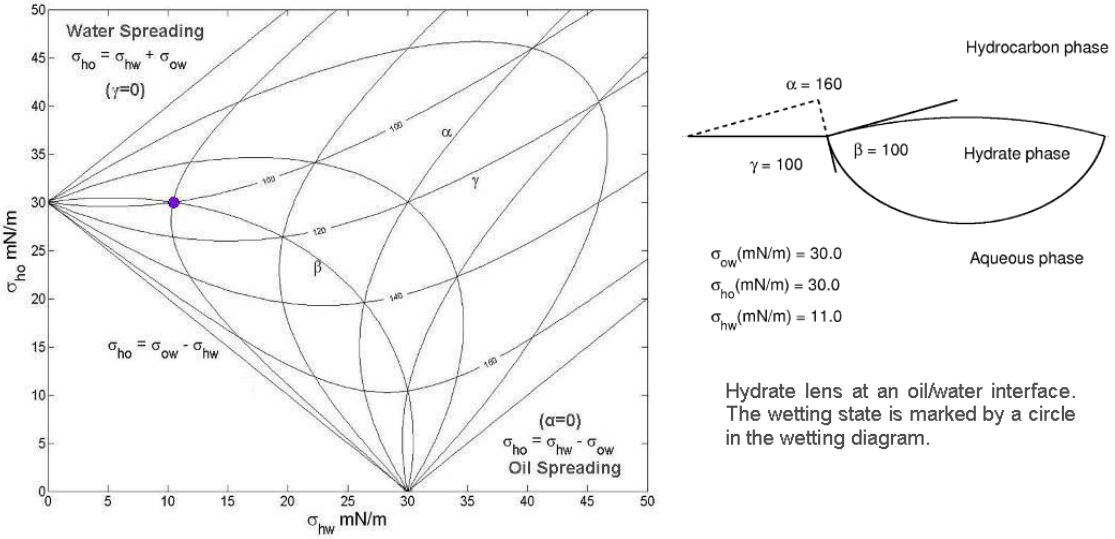

Figure 3.3: Wetting diagram for a hydrate lens in a system with oil/water interfacial tension of 30 mN/m (personal communication with Dr. Fotland).

Water droplet and hydrate particle sizes: Small droplets and hydrate particles are more difficult to break, and therefore have a lower probability to release any free water they might contain. This free water release is believed to be a key component of plug formation, by bonding hydrate particles together (Dellecase et al., 2008).

Boxall et al (2008) investigated the effect of droplet size on hydrate formation and agglomeration using a combination of Particle Video Microscope (PVM) and Focused Beam Reflectance Measurement (FBRM) techniques. Methane hydrate formation/dissociation were conducted for water in oil emulsions with three different size distributions of <5 μm, 5-15 μm and 20-150 μm. In the two smaller droplet size categories, hydrates were formed quickly and about 85% of the initial water was converted to hydrate. In the case of the largest droplet size experiments, the rate of hydrate formation was lower and less than 60% of the initial water was converted to

hydrate after 32 hours which might be attributed to diffusion barrier due to the tick hydrate shell. FBRM distribution before and after formation showed that significant agglomeration occurred for larger droplet sizes. However, showed little evidence of agglomeration for smaller size droplets (<15 μm).

Anti-agglomerants: It is widely accepted that anti-agglomerants have positive influence on the formation of flowable hydrates and reducing the size of water droplets as well as hydrate particles. According to Dellecase et al. (2008) results from a 2.9" ID flow loop with a model oil at 19 and 25% water cut, the addition of only 0.2% of anti-agglomerants was sufficient to emulsify all the water in the system (which otherwise segregates in less than one minute) and also prevent plug formation. It is not known whether the plug was prevented due to emulsification, the change in droplet size or some anti-agglomeration effect.

Taylor et al. (2008) tested Sorbitan monolaurant (Span 20) and poly-N-vinyl caprolactam (PVCap) to determine their anti-agglomerant potential by directly measuring the adherence forces of THF hydrate particles. The average adhesion forces between two hydrate particles were reduced by 85% with Span 20 and 75% with PVCap. Although the mechanism of the force reduction remains uncertain, they hypothesised that the PVCap polymer provided a short-range steric barrier by absorbing to the hydrate surface. They have also described that both these chemicals reduce the water-hydrocarbon interfacial energy, which would also decrease the strength of any capillary bridge acting between the hydrate particles.

Water cut: Dellecase et al. (2008) tested the effect of water cut on the transportability of hydrate slurry in a 2.9" ID flow loop at water cuts of 12.5, 25, 37.5, 50 and 100% for five different fluid and conditions (a total of 45 experiments). The risk of plug formation increased as water cut increased. It was observed that the transportability also depends on the interactions between hydrocarbon and aqueous phases, i.e. maximum water cut for which slurry flow remains transportable increases with the fluids forming stable emulsions and with velocity. However, at 50% water cut, all fluids resulted in line blockages. It should also be mentioned that these experiments were conducted with fresh water and transportability may improve with brines.

Liquid velocity and flow regime: Turner and Talley (2008) reported the liquid velocity as one of the most influential parameters for forming flowable hydrate. They tested a

Conroe crude (35% water cut) in a 4" ID flow loop and found that if the liquid velocity was greater than 1.7 m/s, a dispersed bubble flow was produced, which tended to form flowable hydrate. They explained that the increased velocity produces higher shear rate, which results in smaller water droplets and gas bubbles, larger reaction surface area, and rapid hydrate formation. Higher shear rate also results in breaking aggregates that may form.

Dellecase et al. (2008) also conducted few experiments in a 2.9" ID flow loop at velocities of 2.3, 3.9 and 7.2 ft/s. The results suggested that depending on the water cut, a minimum velocity is required to maintain the hydrate particles suspended as slurry. However, above a critical water cut (i.e. a water cut above which plugging will occur), an increase in velocity is not sufficient to prevent plugging and blockage forms.

It is not easy to isolate the effect of individual parameters influencing hydrates flow behaviour due to complexity and inadequate knowledge of aggregation process.

3.5. Rheological behaviour of hydrate suspensions

Rheology is defined as the science of deformation and flow of material (Van Vazer et al., 1963), is now recognised as an important field of scientific study. It provides properties such as viscosity, yield stress and dynamic modulus. A better understanding of the rheological behaviour of hydrate suspensions is essential for pipeline pressure drop calculation and consequently pipeline design. Rheology also gives insight into hydrate plugging concept.

The concept of viscosity can be used to characterise the behaviour of slurries, as long as they behave homogeneously. Viscosity is a property of the fluid, and can be defined as internal friction or as the resistance of the fluid during flow (Geankoplis, 1993). Isaac Newton defined viscosity by considering the model represented in the Figure 3.4, two infinitely planes (with area of A) and a fluid between them.

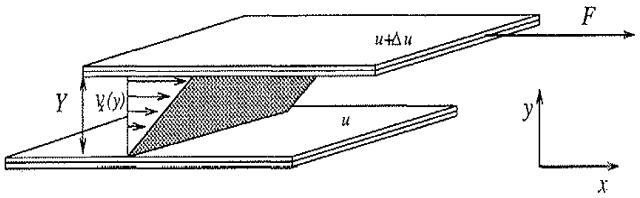

Figure 3.4: Illustration of fluid's resistance toward flow.

The upper plane has a constant velocity compared to the lower *plane*, resulted from the force F. Newton assumed that the force required to maintain this difference in speed was proportional to the velocity gradient. The general equation for the fluid can then be written as:

$$\tau = F/A = \mu\,(d\upsilon_x/dy) = \mu\,\dot{\gamma} \qquad \text{Equation 3.3}$$

Where τ is the shear stress (depends on the velocity gradient at the specific distance from the plates), $\dot{\gamma}$ is the shear rate (the rate of shear deformation) and μ is the Newtonian viscosity.

Fluids can be classified into different groups as illustrated in Figure 3.5 depending on how shear stress relates to shear rate in these fluids (Skelland, 1967).

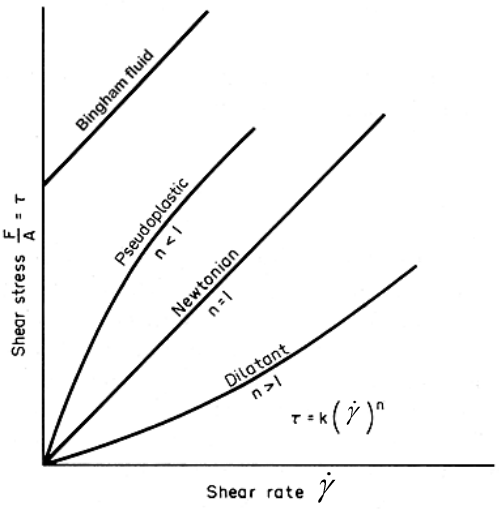

Figure 3.5: Flow Curves showing the concept of Newtonian and non Newtonian viscosities.

Liquid-solid mixtures are often considered as non-Newtonian fluids. The most common model, which can be used to describe non-Newtonian fluids and to determine the characteristics of the suspension are listed in Table 3.2.

In a suspension, the yield stress strongly depends on the particle size and its volume fraction. According to Barnes et al. (1989), yield stress is a result of microstructural reorganization in the stagnant mixture into a flowing mood. Generally, the rheological behaviour of the suspension should be determined by the shear stress vs. shear rate trends. The rheological behaviour of the suspension could be non-Newtonian (shear thinning or shear thickening) and even Newtonian. The relevant characteristic of shear

thinning fluids is a decrease in apparent viscosity with increasing deformation rate (shear rate). In contrast, for shear thickening fluid, an increase in the apparent viscosity is observed with increasing the shear rate.

Table 3.2: Common models describing flow behaviour of non-Newtonian fluids *

Power Law (PL)	$\tau = K\dot{\gamma}^n$	Equation 3.4
Bingham Plastic	$\tau = \tau_0 + \mu_B\dot{\gamma}$	Equation 3.5
Herschel-Buckley model (Yield Power Low)	$\tau = \tau_0 + K\dot{\gamma}^n$	Equation 3.6
Casson model	$\sqrt{\tau} = \sqrt{\tau_0} + \sqrt{\alpha\dot{\gamma}}$	Equation 3.7

* K: Consistency factor; n: flow index; τ_0: yield stress; μ_B: plastic viscosity; α: a function of particle diameter, particle volume fraction and adhesion force between particles

During the past decades several attempts were made to estimate the viscosity of emulsions and suspensions as a function of solid fraction. One century ago Einstein (1906) predicted that in the case of very diluted suspension of solid spherical non-interacting particles, the relative viscosity μ_r is:

$$\mu_r = 1 + 2.5\Phi \qquad \text{Equation 3.8}$$

where Φ is the volume fraction of solid particles and μ_r is relative viscosity which is defined as the ratio (μ/μ_c) between the emulsion viscosity, μ and the continuous phase viscosity μ_c. However this analysis was based on ignoring the intermolecular forces, and would work only on an ideal suspension. Later, Mooney (1951) developed an accurate functional equation based on strong mathematical modelling integrating interaction forces which was validated against published experimental data.

$$\mu_r = \exp\left(\frac{2.5\Phi}{1 - k\Phi}\right) \qquad \text{Equation 3.9}$$

where *k* is the constant self-crowding factor.

In 1985, Mills (1985) proposed a model to calculate the relative viscosity of flocculated suspensions. His equation which is well adapted to hard spheres of equal size is shown below:

$$\mu_r = \frac{1-\Phi}{\left(1-\frac{\Phi}{\Phi_{max}}\right)^2}; \quad \Phi_{max} = 4/7 \qquad \text{Equation 3.10}$$

where Φ_{max} is the packing concentration of randomly packed spheres.

Later, Camarago and Palermo (2002) modified Mills's equation and proposed to replace the real particle volume fraction (Φ) with an effective particle volume fraction (Φ_{eff}) due to the fractal structure of aggregates. Φ_{eff} is defined as below:

$$\Phi_{eff} \approx \Phi\left(\frac{d_A}{d_p}\right)^{(3-f)} \qquad \text{Equation 3.11}$$

In this equation, the porosity of the aggregates is taken into account by using a fractal dimension f, relating the number of particles N per fractal aggregate to characteristic lengths of the system (d_A: aggregate diameter; d_p: particle diameter; $N \approx (d_A/d_P)^f$). They first determined the aggregate diameter by balancing viscous and adhesive forces between the particles. Then, they use this aggregate diameter to calculate an effective volume concentration to determine the slurry viscosity.

The paper went on to compare model and experiments for two particle volume fractions of 0.134 and 0.274 for natural gas hydrate suspensions in an asphaltenic crude oil system. Two experimental devices were used: a double coaxial cylinder rheometer and a 2 in$\times$140 m flow loop. The results showed a good agreement between calculated and experimental data. At low volume fraction, hydrate suspensions behaved like a Newtonian system. On the other hand, for concentrated suspension, shear-thinning and thixotropy behaviour was observed because of a weak flocculation process between hydrate particles. They also described the rheological behaviour of the hydrate suspension at these two hydrate particle volume fractions by a Casson's like equation (Equation 3.7).

In another work from the same research group (Sinquin et al., 2004 and Peysson, 2005), effect of hydrate particles is analysed in terms of rheological properties of the system in the laminar regime and in terms of friction factor modification in the turbulent regime. In the laminar flow regime, prediction of the viscosity is as it mentioned above. In the turbulent flow regime, they measured friction factor for hydrate suspensions in two different oils, naphtha oil and condensate. An increase of the friction factor with water cut (and consequently hydrate concentration) was observed for both systems. This was attributed to an increase of the apparent roughness at the wall (due to particle deposition) or to the effect of solid particles itself in modifying the force balance by hitting at the wall. The rheological behaviour of hydrate slurries have also reported as Bingham fluid in some studies like Darbouret et al (2005) and Rensing et al (2008).

As it is reviewed in this chapter, rheology is often used as a common tool to characterise the flow behaviour of hydrate suspensions. Next chapter will describe the purposely-built apparatus which has been designed, built, calibrated and validated for studying the rheological behaviour and flow properties of hydrate slurries, i.e. viscosity, at high pressures.

3.6. References

Austvik, T., Li, X. and Gjertsen, L. H., 2000. Hydrate plug properties: Formation and removal of plugs. *Annals New York Academy of Science*, pp.295-303.

Barnes, H. A., Hutton, J. F. and Walters, K., 1989. *An Introduction to Rheology*. New York: Elsevier.

Boxall, J., Greaves, D., Mulligan, J., Koh, C. and Sloan, E. D, 2008. Gas Hydrate Formation and Dissociation from Water-in-Oil Emulsions Studied Using PVM and FBRM Particle Size Analysis. *6th International Conference on Gas Hydrates (ICGH*). Vancouver, British Columbia, CANADA, 6-10 July 2008.

Camargo, R. and Palermo, T., 2002. Rheological Properties of Hydrate Suspensions in Asphaltenic Crude Oil. *4th International Conference on Gas Hydrates*, Yokohama, 19-23 May 2002.

Darbouret, M. D., Cournil, M. and Herri, J., 2005. Rheological Study of a Hydrate Slurry for Air Conditioning Application. *5th International Conference on Gas Hydrates*. Trondheim, Norway, 12-16 June 2005.

Dellecase, E., Geraci, G., Barrios, L., Estanga, D., Domingues, R. and Volk, M., 2008. Hydrate Plugging or Slurry Flow: Effect of Key Variables. *6th International Conference on Gas Hydrates (ICGH*). Vancouver, British Columbia, CANADA, 6-10 July 2008.

Einstein, A., 1906. Eine neue Bestimmung der Moleküldimensionen. *Ann Phys*., **19**, pp.289-306.

Fotland, P. and Askvik, K. M., 2008. Some Aspects of Hydrate formation and Wetting. *Journal of Colloid and Interface Science*, **321**, pp.130-141.

Geankoplis, C., 1993. *Transport Processes and Unit Operations*. 3rd ed. London: Prentice Hall International, Inc.

Høiland, S., Askvik, K. M., Fotland, P., Alagic, E., Barth, T. and Fadnes, F., 2005. Wettability of Freon Hydrate in Crude Oil / Brine Emulsions. *Journal of Colloid and Interface Science*, **287**, pp.217-225.

Lingelem, M.N., Majeed, A.I. and Stange, E., 1994. *1st International Conference on Natural Gas Hydrates, Ann. NY Acad. Sci*. (Sloan, E.D., Happel, J., et al., eds.), **715**, 75 (As it is mentioned in Sloan and Koh, 2008)

Lund, A., 1994. Comments to Some Preliminary Results from the Exxon Hydrate Flow Loop. *Annals-New York Academy of Science*, **715**, pp.447-449.

Mills, P, 1985. Non-Newtonian Behaviour of Flocculated suspensions. *J. Physique Lett.*, **46**, pp.301-309.

Peysson, Y., 2005. Collision Process Between Particles in the Transport of Dispersed Hydrate in Production Lines. *5th International Conference on Gas Hydrates*. Trondheim, Norway, 12-16 June 2005.

Rensing, P. J., Liberator, M. W., Koh, C. A. and Sloan, E. D., 2008. Rheological Investigation of Hydrate Slurries. *6th International Conference on Gas Hydrates (ICGH)*. Vancouver, British Columbia, CANADA, 6-10 July 2008.

Sinquin, A., Palermo, T. and Peysson, Y., 2004. Rheological and Flow Properties of Gas Hydrate Suspensions. *Oil and gas Science and Technology – Rev. IFP*, **59**(No. 1), pp.41-57.

Skelland, A. H. P., 1967. *Non-Newtonian Flow and Heat Transfer*. New York: John Wiley & Sons, Inc.

Taylor, C. J., Dieker, L. E., Miller, K. T., Koh, C. A. and Sloan, E. D., 2008. Hydrate Particles Adhesion Force Measurements: Effect of Temperature, Low Dosage Inhibitors, and Interfacial Energy. *6th International Conference on Gas Hydrates (ICGH).* Vancouver, British Columbia, CANADA, 6-10 July 2008.

Turnet, D. and Talley, L., 2008. Hydrate Inhibition via Cold Flow – No Chemicals or Insulation. *6th International Conference on Gas Hydrates (ICGH)*, Vancouver, British Columbia, CANADA, 6-10July 2008.

Van Wazer, J. R., Lyons, J. W., Kim, K. Y. and Colwell, R. E., 1963. *Viscosity and Flow Measurement - A Laboratory Handbook of Rheology*. John Wiley & Sons, Inc.

Yang, S., Kleehammer, D. M., Huo, Z., Sloan, E. D. and Miller, K. T., 2004. Temperature dependence of particle-particle adherence forces in ice and clathrate hydrates. *Journal of Colloid and Interface Science*, **277**, pp.335-341.

Chapter 4. Experimental Equipments

4.1. Introduction

This chapter starts with a concise review of the apparati available for visual and rheological studies of hydrate suspensions and continues with the description, calibration and validation of our purpose-built Helical Tube Impeller (HTI) setup. Some examples will be also presented in this section. And finally, this chapter ends with the description of some other setups, which have been used in this study as complementary devices to prepare the materials for the main experiments or to support the results generated with the HTI setup.

4.2. Apparati available for visual and rheological study of hydrate suspensions

The performance of AAs is usually studied by testing their effect on the morphology and rheology of hydrate suspensions. Therefore, these equipments which are usually used to study the performance of AAs can be also useful to generate rheological data required for studying flow characteristics of hydrate suspensions. Many different methods are used for rheological studies of hydrate suspensions. The tests can vary in size and complexity, from small 10 ml rocking cells to pilot scale flow loops. The choice of the test is usually based on the suitability/availability of the equipment, and the added value of the information generated versus the cost of the test.

In this section, various laboratory equipments and techniques used in studying flow behaviour of hydrate suspensions are reviewed and compared. In general, there are three criteria and methods that can be used for this purpose; 1) visual observation, 2) assessment of hydrate plugging and deposition and 3) rheological measurements/characterisation of hydrate slurry.

4.2.1. Visual techniques

The most common visual testing techniques based on forming hydrates in optical cells. Optical cells usually consist of a window or a completely transparent cell at atmospheric or high pressures. The atmospheric tests involved the addition of chemicals such as tetrahydrofuran (THF), tetra-n-butylammonium bromide (TBAB) or ethylene oxide to water, which are hydrate formers at atmospheric pressures. High pressure hydrates tests can be seen in visual section of stirred tank reactors, rocking cells (Frostman 2000, Huo et al. 2001) and flow loops.

Glass micro-models (originally used to visualise the flow of reservoir fluids within simulated reservoir structures under high pressure conditions) were also discovered to be very useful for visualisation of hydrate experiments (Tohidi et al., 2001). Micro-model consists of two glass plates of which one has a pore structure or a small flow channel etched upon its surface. These plates are put against each other to form small channels and can be filled with solution at static or dynamic conditions and then pressurised and cooled to form hydrates. A simple diagram of a micro-model pore network can be seen in Figure 4.1. Figure 4.2 shows a diagram of flow channel alternatives to the pore structure arrangement.

The major advantages of the micro-model set-up compared to the other techniques include the magnification possible in the set-up, and the ability to see the hydrates through oil due to the small thickness of the sample (i.e., around 20 μ). However, water needs to be dyed (for example with methyl blue) in order to improve the contrast between water and other phases (i.e., gas, condensate and hydrate particles). This alters the interfacial tension (IFT) between water and hydrate particles and/or liquid hydrocarbon phase hence hydrate morphology and growth pattern. Another disadvantage of this set-up is its poor representation of real bulk condition. Heat and mass transfer are also limited by the narrow pore space and lack of mixing.

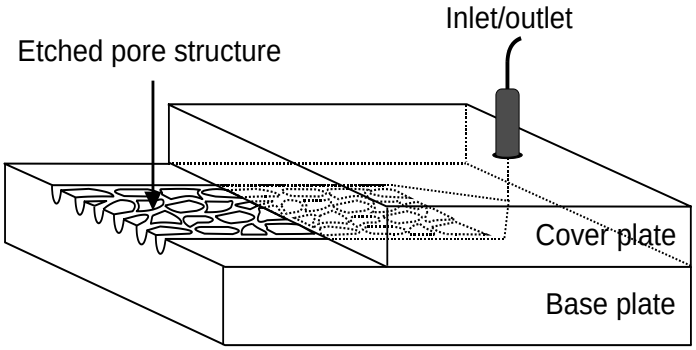

Figure 4.1 Basic glass micro-model pore structure network

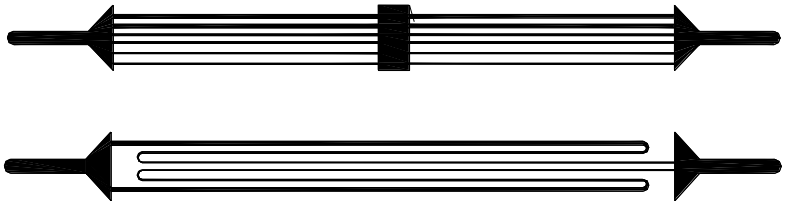

Figure 4.2 Micro-model multi-channel glass conduit

Focused Beam Reflectance Measurement (FBRM) is another relatively new technique and is used to measure various parameters during crystallisation and agglomeration, including particle number, particle size and particle size distribution. This technique can be applied to non-transparent solutions and direct particle size and distribution can be measured. FBRM has been applied to hydrate kinetics by the University of Calgary (Clarke and Bishnoi 2004, Clarke and Bishnoi 2005) in order to investigate and compare the growth development of hydrate crystals in emulsion with viscosity measurements. Colorado School of Mines (CSM) has integrated the FBRM with a particle video microscope (PVM). While the FBRM measures the quantitative tracking of the chord lengths, the PVM probe provides qualitative images of hydrate particle size and level of agglomeration (Sloan, 2008).

4.2.2. Plugging assessment techniques

A rolling-ball rocking-cell can be used to detect blockage caused by hydrates. The device consists of a stainless steel tube with a steel ball inside, attached to a rocking system to create a rocking movement. The tube is charged with a hydrate forming solution at the desired pressure and temperature conditions. The cell then rocks back and forth until it is plugged by a hydrate formation, which gives the time until blockage. Tests can be also conducted at atmospheric pressures with hydrate formers

such as THF and ethylene oxide. This type of test is commonly used for screening of AA inhibitors, and due to its simplicity and low cost is considered to be the unofficial standard test to evaluate AAs.

4.2.3. Rheological assessment techniques

Rheological measurements can be carried out in: rolling-ball rocking-cells, stirred tank reactors, viscometers and flow loop. Rheological measurements are considered to be more useful than the simple plugging assessment because more meaningful quantitative information can be gathered.

Rolling-ball rocking-cells: A rolling-ball rocking-cell can be also used to assess the rheological properties of hydrate slurries. As mentioned above, the device consists of a stainless steel tube with a steel ball inside on a rocking system. The velocity or travel time of the rolling ball from one end of the tube to the other can be used to calculate the viscosity of the hydrate slurry. At two ends of the tube, two magnetic sensors are placed to detect arrival of the ball.

Stirred autoclave reactors: A typical reactor consists of a stirred high-pressure cell with a pressure transducer, and temperature measuring device. These cells may have visual capabilities through a window and may be built out of sapphire glass (Kelland et al. 1994) or may involve THF testing at atmospheric conditions (Klomp et al. 1996). The fundamental difference in the application of stirred reactors involves the requirement to measure force exerted by the stirrer into mixing the hydrate slurry. Through the measurement of torque/power exerted by the stirrer it is possible to measure viscosity. Even though there are some limitations in the use of stirred tank reactors, they are still widely used due to their relative simplicity, reproducibility, cost and versatility (Sugier et al. 1989[a, b, c], Huo *et al.* 2001, Burgazli 2004).

More recently a miniature multi-cell system has been developed by Akzo Nobel (Oskarsson *et al.* 2005). The multi-cell system consists of 48 stirred high pressure cells with temperature, pressure and torque measurements. This is considered to be suitable for large scale screening of AA due to the number of tests that can be carried out at any one time.

Flow loops: Flow Loops are apparatus that provide a way of emulating conditions in a pipeline by re-circulating fluids in a small section of pipeline. Flow loops are widely

used for studying hydrate suspensions and LDHI chemicals for field application due to their ability to simulate the flow conditions in pipelines. The viscosity of the flowing solution can be accurately calculated from the measurement of pressure drop across a section of the loop.

Flow loops exist in many sizes from 1" ID and 20m long (mini-loop) to greater than 8" ID and hundreds of meters (pilot loop). Different designs of flow loops exist such as: Saturated flow loop, Multiphase loop (e.g. Exxon Mobile flow loop (Turner et al., 2005)), Gas lift loop (e.g. South West Research Institute (SWRI) and Saint Etienne School of Mines (Fidel-Dufour and Herri, 2002)) and Rotating wheel loop (Argo et al., (2002), Urdahl *et al.* (1995), Lund *et al.* (1996), Kelland *et al.* (2006a), Kelland *et al.* (2006b).

4.3. Helical Tube Impeller (HTI) autoclave cell for rheological studies

High pressure autoclave cells which are originally used for the measurements of KHI performance have been modified to generate rheological data, i.e. apparent viscosity, for investigating flow behaviour of hydrate suspensions and assessing AA performance. The cell (Figure 4.3) is cylindrical in shape and made of titanium. The cell volume is about 2400 ml and has a working pressure of up to 400 bar and can be operated between -30 and 50 ^{o}C. The equilibrium cell is held in a metallic jacket heated or cooled by a constant temperature liquid bath. The temperature of the cell is controlled by circulating coolant from a cryostat within the jacket surrounding the cell. A platinum resistance probe is placed inside the equilibrium cell and monitors the temperature; the probe is connected directly to a computer for direct acquisition. To achieve good temperature stability, the jacket is insulated with polystyrene board and the pipes (which connect it to the cryostat) are covered with plastic foam. The pressure is measured by means of a Druck pressure transducer mounted directly on the cell and connected to the same data acquisition unit. This system allows real time readings and storage of temperatures and pressures. The cell is also equipped with a magnetic stirrer with adjustable rotational speed and voltmeter/ampere-meter to measures the voltage and current needed to calculate the torque and the shear rate. The angular velocity of the stirrer ranges from 0 to 1200 rpm while the current is limited to ~ 4.7 A. The sensor signals are transferred to a real time PC-based data acquisition

system. As mentioned earlier, a special impeller called helical tube impeller (HTI) (Figure 4.4) has been also developed for mixing and torque measurement purpose.

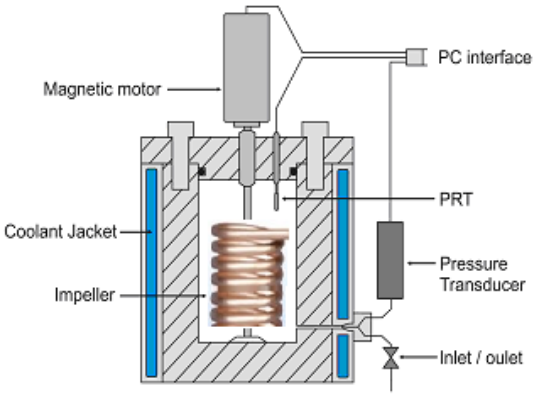

Figure 4.3 Schematic illustration of the HTI set-up used for slurry rheology studies.

Figure 4.4 Stainless steel HTI used for slurry rheology studies.

The impeller is a long tube coiled in helical shape. The idea is simulating a pipeline by pushing the pipe through the liquid (instead of pushing the liquid inside the pipe) and measuring the power applied to rotate the impeller at the desired rpm. The benefit of this set-up is that it provides viscosity data, as opposed to pass or fail of conventional rocking cells. To examine if fluid passes through the helical tube, a transparent HTI was made of polycarbonate and tested in a visual autoclave cell. Figure 4.5 clearly proofs this claim.

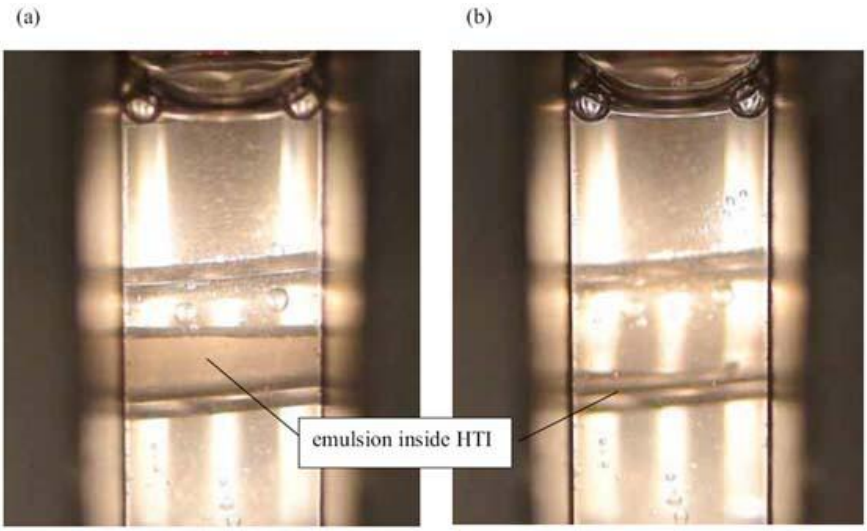

Figure 4.5 Fluid passing through HTI just (a) 2 seconds and (b) 4 seconds after stopping the impeller.

There are several advantages of the HTI over conventional impellers, including:

- The movement of the helical tube inside the fluid/slurry creates shear forces similar to those experienced in fluid flow inside a pipeline; though here the shear forces are both due to fluid movement inside and outside the helical tube.
- The flow from the HTI involves an upward movement of liquid as opposed to paddle impellers which push the liquid towards the wall of the cell and results in a layer of solid hydrate building up on the inside surfaces of the cell. This centrifugal force could cause separation of the phases and that a non-representative value for viscosity is measured. It should be mention that HTI can not completely eliminate the building up of hydrates to the wall but it is believed that the global apparent behaviour of the fluid will be similar to that of a pipeline. However, as it will be shown later the viscosity values can drop abnormally due to formation of a slippery hydrate layer on the wall, these data will be considered as non-representative. This conclusion has been reached by visual observations.
- The HTI produces axial fluid motion rather than radial one. Axial fluid motion is ideal for preventing vortex, while dispersing water droplets and hydrate particles evenly into the continuous phase.
- The HTI mixes the fluid/slurry in a less vigorous manner in comparison to conventional impellers and therefore by reducing the potential breakage of hydrate crystals, generates more representative results.
- The larger surface area of the HTI produces more stable torque measurements and consequently improves data interpretation.

4.4. Calibration of the HTI set up for viscosity measurements

Since the preliminary design and purpose of the experimental setup was not for use as a rheometer, calibration was required to determine the necessary parameters. For this purpose, Newton's equation which relates shear stress and velocity gradient by means of viscosity is used as follow:

$$\tau = \mu \left(\frac{d\upsilon_x}{dy}\right) = \mu \dot{\gamma} \qquad \text{Equation 4.1}$$

To determine the shear rate ($\dot{\gamma}$) and shear stress (τ) required for viscosity calculations, the angular velocity, voltage and amperage are measured. Shear rate can be calculated by the following equation as proposed by Metzner and Otto (1957). According to their equation, the shear rate is directly proportional to the angular velocity.

$$\dot{\gamma} = K_{SR}.\omega \qquad \text{Equation 4.2}$$

where ω is the angular velocity and K_{SR} is the shear rate constant number which depends on the design of the cell and impeller.

The shear stress is calculated from the following equation:

$$\tau = K_{SS}\frac{M}{L} \qquad \text{Equation 4.3}$$

where K_{SS} is shear stress constant number which depends on impeller and M and L are the torque and the effective length of the impeller respectively. The torque can be calculated using the following formulas:

$$P = M \times \omega = M \times 2\pi\Omega \qquad \text{Equation 4.4}$$

$$P = V \times I \qquad \text{Equation 4.5}$$

where V and I are the voltage and current which are applied to the motor to rotate the impeller. Combining Equation 4.1 to Equation 4.5 results in the following equation which gives the viscosity based on the parameters measured with HTI set up.

$$\mu = \frac{\tau}{\dot{\gamma}} = \frac{K_{SS}\frac{M}{L}}{K_{SR}.\omega} = K_{geo}\frac{VI}{L\omega^2} \qquad \text{Equation 4.6}$$

According to this equation, the viscosity is a function of the power applied to the mixer, the effective length of impeller and angular velocity of the motor. K_{geo} is a geometric constant which is specific of the impeller and cell.

It should be considered that the electrical input power, P_{el} (current and voltage) applied to the motor is not completely converted to the mechanical power, P_{mech} (speed and torque) consumed for mixing the fluid as can be seen in Figure 4.6. The losses that

arise are frictional losses and losses of the winding (resistance R). Iron losses do not occur in the coreless DC motors.

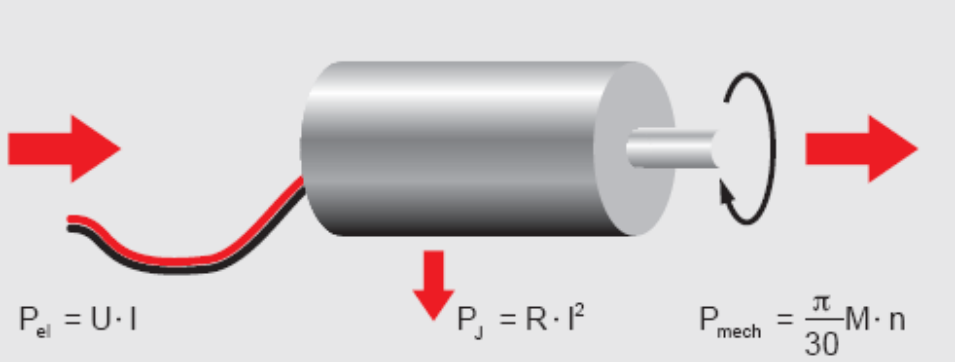

Figure 4.6 Power balance in the DC motors used in the HTI setups

The geometric arrangement of the magnetic circuit and winding defines in detail how the motor converts the electrical input power into mechanical output power. Two important characteristic values of this energy conversion are the speed constant k_n and the torque constant k_M. The speed constant combines the speed n with the voltage induced in the winding U_{ind}. Similarly, the torque constant links the mechanical torque M with the electrical current I. The following formulas apply:

$$n = k_n \times U_{Ind} \qquad \text{Equation 4.7}$$

$$M = k_M \times I \qquad \text{Equation 4.8}$$

The core statement of this proportionality is that the variables (i.e., torque and current) are equivalent for these DC motors. k_n and k_M are not independent of one another. The following applies:

$$k_n \times k_M = 3000/\pi \qquad \text{Equation 4.9}$$

Extensive calibration has been carried out for the helical tube setup involving testing different liquids with known viscosities. Water was used as one of the calibration fluids because its viscosity as a function of temperature and pressure is well known (Sengers and Kamgar-Parsi, 1984). For measuring the viscosity of water, the cell was loaded with distilled water and then the rotation speed of the mixer was increased step by step and at each step the required data such as temperature, pressure, current, voltage and rpm were recorded for about a minute to make sure that the recorded data

were steady. The K_{geo} has been tuned to fit viscosity measurements with the reference viscosity value of water at 21 ºC (0.9 cP from NIST, 2005) at different liquid volumes (expressed as percentage of the cell volume). Figure 4.7 shows the K_{geo} as a function of the liquid volume percentage of the cell equipped with HTI.

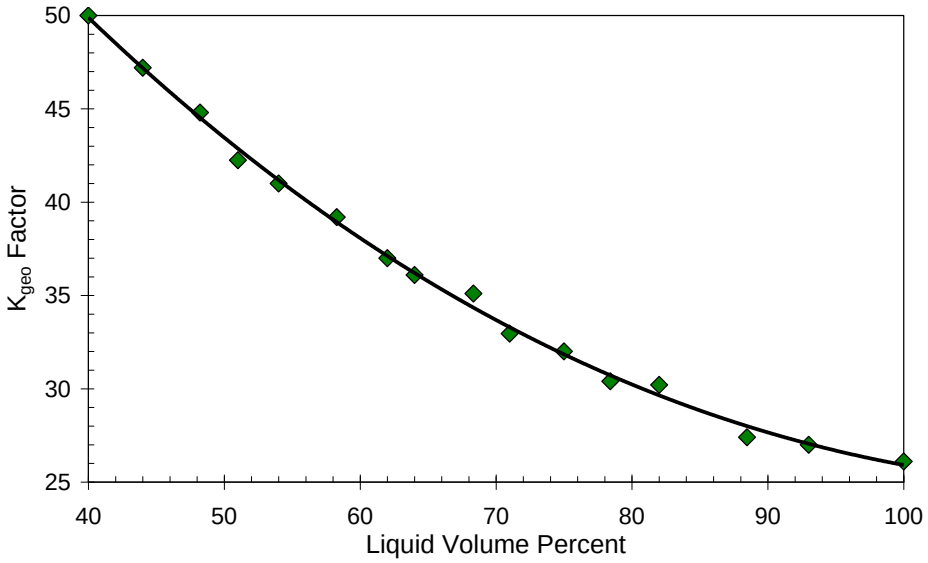

Figure 4.7 K_{geo} as a function of the cell liquid volume percent

As can be seen, the cell has been calibrated for liquid volume percentages above 40 because the impeller was not touching the liquid phase for lower values.

In calibration of the cell, it was necessary to consider that different liquids with different viscosities will have different effective liquid level with the same volume of liquid in the rig. This phenomenon is due to the effect of viscosity and the effect it has on the depth of vortex which will form in the rig as a result of the agitation. Therefore, several liquids with different viscosities have been used to drive a factor to correct the effective water height inside the rig. Figure 4.8 shows the final calibration curve for the HTI set-up used in this study. The maximum error in this calibration was 4 %.

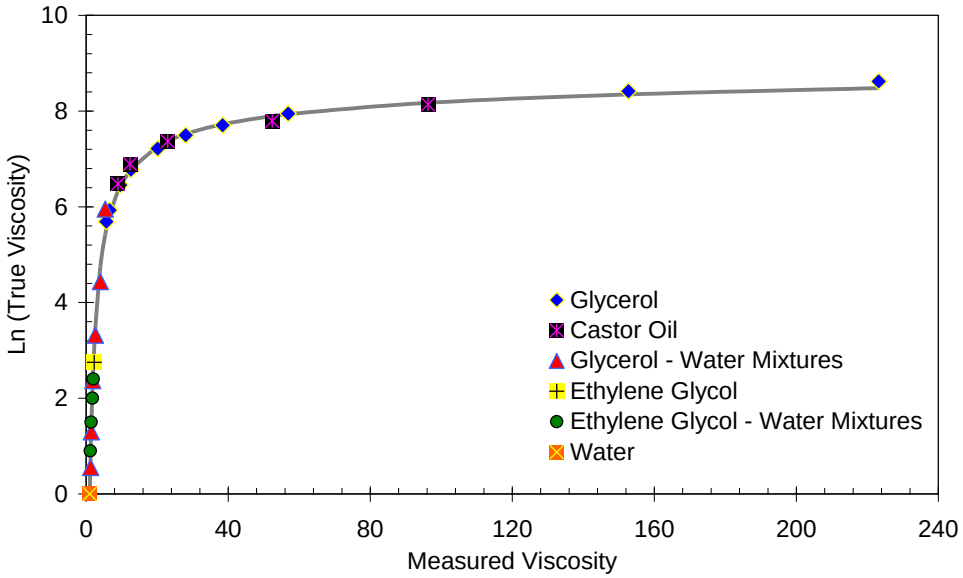

Figure 4.8 Viscosity calibration curve for the HTI setup. The Unit of viscosities in this curve is cP.

Figure 4.9 and Figure 4.10 show the viscosity of water and glycerol-water solution (88 mass%) which were measured with the HTI set up.

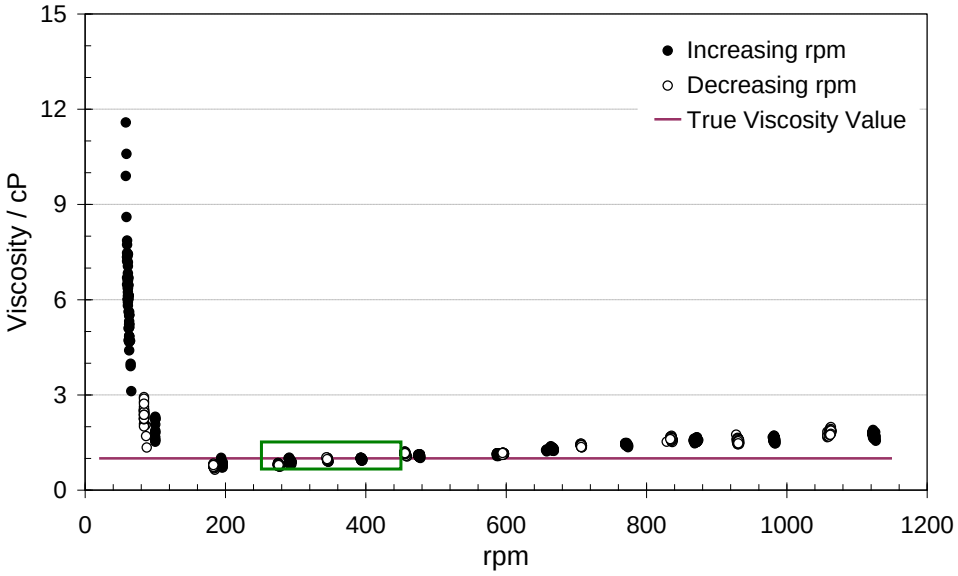

Figure 4.9 Viscosity of water at 22 ^{o}C measured with the HTI setup. The green rectangular shows the range of the rpm at which the HTI set up has been calibrated for viscosity measurements.

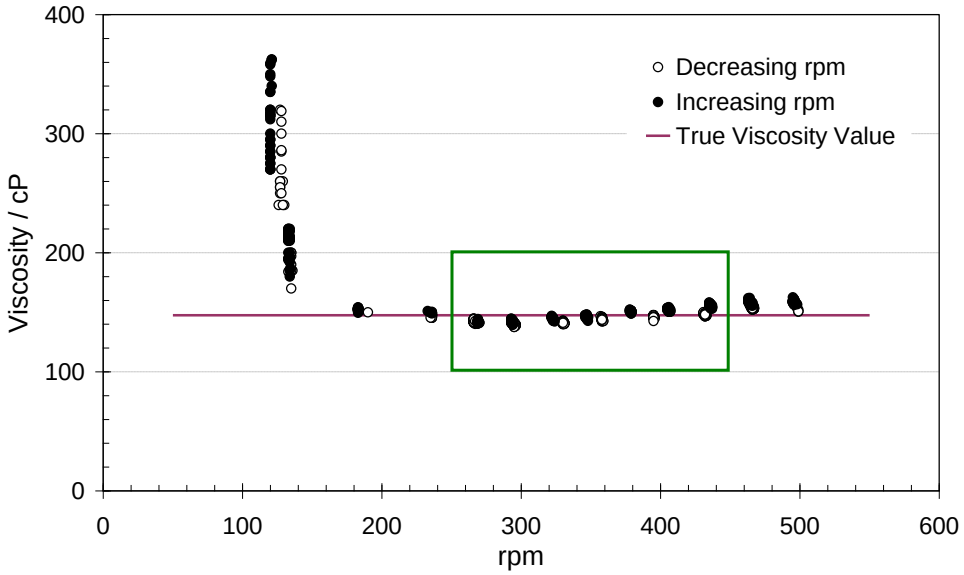

Figure 4.10 Viscosity of glycerol-water solution (88 mass%) at 22 ^{o}C measured with the HTI setup. The green rectangular shows the range of the rpm at which the HTI set up has been calibrated for viscosity measurements.

The green rectangular shows the range of the rpm at which the set up has been calibrated for viscosity measurements. The purple line shows the true viscosity value of the tested systems. As can be seen, the setup has been calibrated within the rpm range of 250 to 450. These rpms (shear rates) were chosen because of the following three reasons.

Firstly, the motor provides the highest level of efficiency and torque for mixing the fluids at this range of rpm (green rectangular in Figure 4.11). Comparing this figure with Figure 4.9 and Figure 4.10 illustrates the reason why the measured viscosity is higher than its true value at the two ends of the rpm ranges (approximately rpm<150 and rpm>450). The sharp decrease in the efficiency at $\eta<\eta_{max}$ corresponds to the sharp increase in the viscosity at rpm<150 and moderate decrease of efficiency at $\eta>\eta_{max}$ describes the linear increase of viscosity at rpm>450. Secondly, according to our visual experiments (Figure 4.12), these rpms would disperse better the liquid hydrocarbon/water phases without excess vortex. Minimum rpm of 250 is required to prevent phase separation. Higher rpms produce turbulent flow and vortex which can cause error in the viscosity measurements. Turbulent flow causes extra drag force on the impeller which will appear as an increase in viscosity value but does not reflect the true value of the fluid viscosity. And finally, higher rpms may breakdown hydrate crystals/particles and result in non-representative systems.

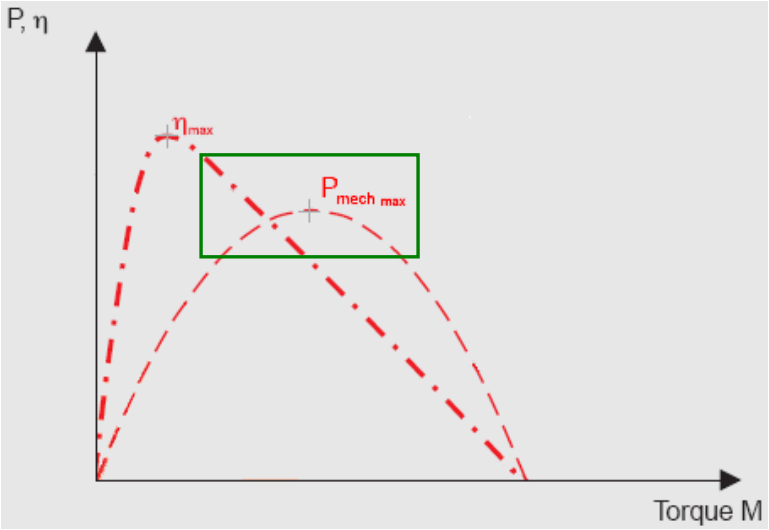

Figure 4.11 Mechanical output power and efficiency curve. The green rectangular shows the area at which the HTI set up has been calibrated for viscosity measurements.

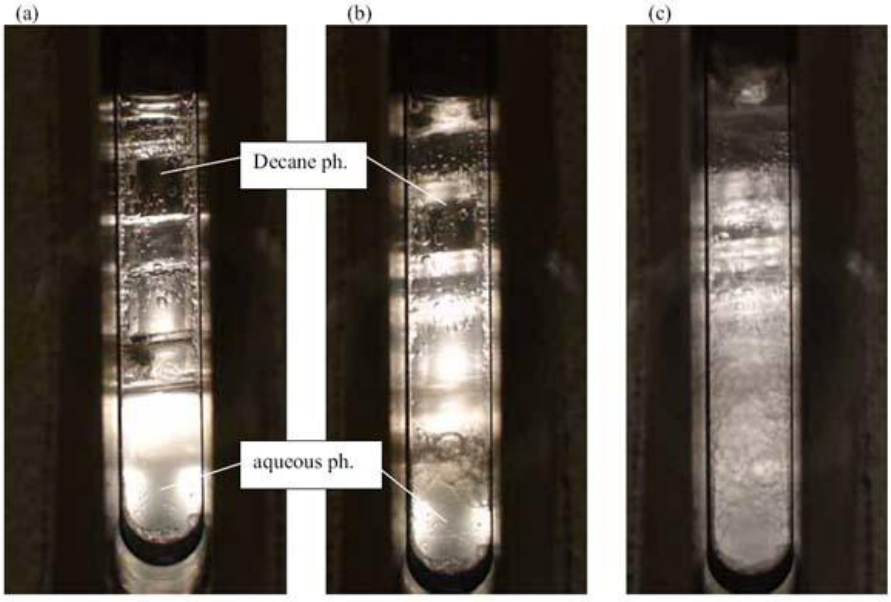

Figure 4.12 Decane and water phases in the HTI set-up during mixing process with (a) 50 rpm, (b) 150 rpm and (c) 250 rpm

Figure 4.13 is an example of viscosity measurement for water – oil – AA – salt – hydrate – natural gas system (water cut was 70%) using the HTI setup. As can be seen, it is possible to measure a reliable value for viscosity (235 cP) for this system because of the formation of a stable slurry.

Figure 4.14 is another example of viscosity measurement by the HTI setup. However, this plot differs significantly from Figure 4.14 demonstrating how the equipment can be used to characterise different fluid behaviours. This data would be typical of agglomerated high viscoelastic hydrates hence not suitable for transportation. As it will be detailed in the next chapters, in this type of systems the viscosity values are largely scattered. This is most probably due to large lumps of hydrate forming and breaking up in a random manner which is reflected in the large variation of viscosity at a given rpm. The fact is that when the dimension of the aggregates is similar to the dimension of the measuring device, i.e. the gap between the impeller and the wall or the inner diameter of the tube which the impeller is made of, the system does not represent the real behaviour of the fluid. In rheology to have the representative values, the gaps as a rule of thumb should be about ten times of the largest particle in the fluid (Mezger, 2006).

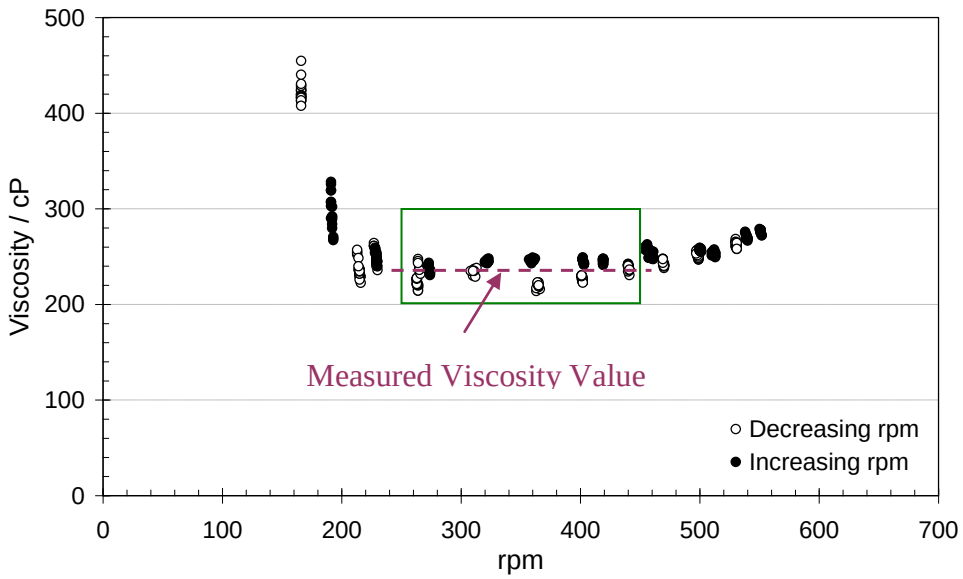

Figure 4.13 Viscosity of water – oil – AA – salt – hydrate – natural gas system (water cut was 70%) measured with the HTI setup.

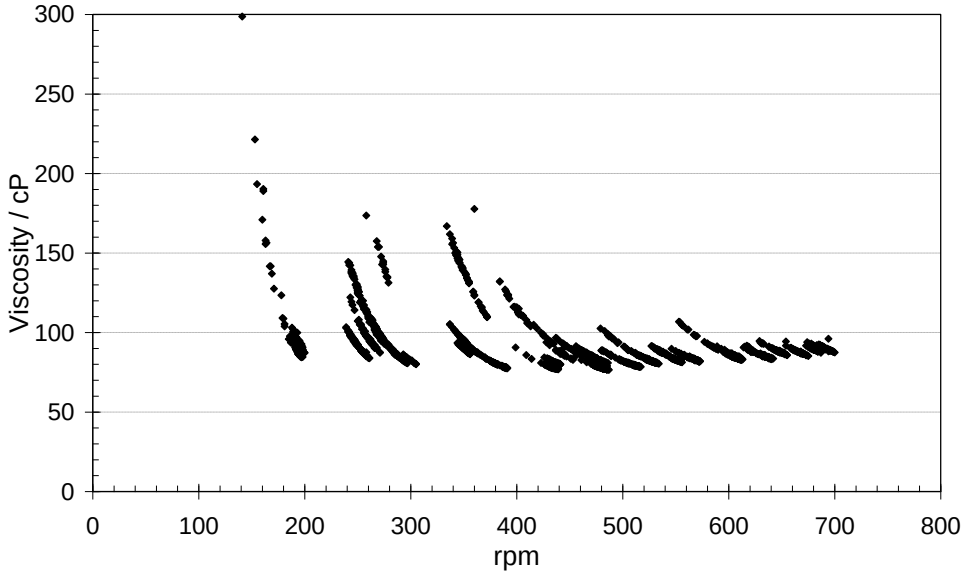

Figure 4.14 Viscosity of water – oil – hydrate – natural gas system (water cut was 70%) measured with the HTI setup

Figure 4.15 shows the different impellers designed and built for this study. Impeller (a) is the very first generation of HTI made of copper. Its inner diameter is ca. 8 mm. Impeller (b) has larger diameter however the setup with this impeller was vibrating due to its non symmetric shape, i.e. the ratio of pipe diameter to helical diameter was too big to build an even impeller. Vibration was shortening the life of the bearings of the magnetic stirrer. The stirrer axle is fixed at both bottom and top ends of the rig to minimise vibration. However, excess vibration can still cause damage to the stirrer bearings. Impeller (c) has the same diameter of ca. 8 mm and is made of stainless steel in order to be able to use it in the presence of salt and produced water. This impeller was used in almost all experiments unless otherwise stated. The transparent impeller (d) is made of polycarbonate and installed in a visual autoclave cell in order to facilitate visual observation. Impeller (e) which is smaller in helical diameter (ca. 45 mm in compare to ca. 125 mm of impellers (a) and (c)), is built for a smaller autoclave cell (300 ml in compare to 2400 ml of the main autoclave cell). The 300 ml cell was used for some experiments in which there was a limitation in the amount of fluid or chemical sample. The smaller cell was only used in the "AA partitioning and performance" experiments. And finally, impeller (f) was especially designed and built in-house for investigating the interactions between hydrate and wax.

(a)

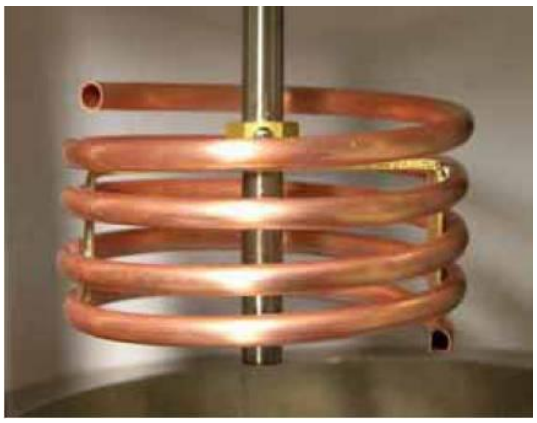

(b)

(c)

(d)

(e)

(f)

Figure 4.15 Different impellers designed and built in-house for developing testing technique and equipment

4.5. Validation of the HTI set-up and up-scaling in the C-FAR flow loop

Usually, development of new flow assurance concepts from laboratory to field involves several stages; initial laboratory tests are invariably conducted in autoclave or rocking cells, then the concept is tested in a pilot scale flow loop, which is considered to be most representative of production conditions. Many unknown factors exist in the transferability of data from laboratory scale to pilot scale, and further into field application. There is a desire to understand the factors involved with scaling-up from laboratory to pilot scale and further. This information may help in the design of better testing procedures and may result in improved testing method and procedures.

All the rheological experiments in this study were conducted in the 2.5 litres HTI set-up. Therefore, to examine the transportability of data from small scale to large scale experiments, a limited number of tests were conducted in an in-house flow loop (C–FAR (Centre for Flow Assurance Research)) using a diesel oil (composition given in Table A.5), a North Sea natural gas (composition given in Table A.6 and a commercial water soluble AA. Diesel was used as it was very difficult to find a supply of large quantities of crude oil for various reasons.

Three series of tests at 20% water cut (with and without AA at a flow velocity of 0.8 m/s and 0.3 m/s) were performed in parallel both in the C-FAR flow loop and in the laboratory high pressure kinetic rig. The flow loop set-up comprises of a 1" (2.5 cm) diameter, 40 m length loop driven by a Moineau pump system. The loop is housed in an environmental chamber, and can operate at pressures up to 200 bar (2,900 psia) from -15 to +20 °C. Figure 4.16 shows the schematic of the C-FAR flow loop.

Its viscometer is a horizontal 6 metre straight pipeline equipped with differential pressure transducers. Explaining the detail of flow loop is beyond the scope of this study and will not be detailed here. The flow loop experiments were carried out by another member of the research group and the results have been used for comparison. However, these experiments were designed and also carried out in the kinetic rig as part of this work.

Experiments in small and large scales were carried out under conditions as close as possible. For instance, the experiments were conducted in the absence of free gas phase because the flow loop is a saturated loop. For this reason, the kinetic rig was equipped with a high pressure piston-cylinder vessel to supply the required gas and

also maintain the pressure during the experiments. Water was injected to the piston side of the vessel using a HPLC pump to move the piston and to inject the gas from the cylinder side to the rig. In each experiment, similar to the flow loop tests, the kinetic rig was filled with the test liquids, and natural gas was then injected into the rig. After reaching the equilibrium at desired temperature and pressure, the system was cooled down to a target temperature. The temperature of the kinetic rig was set the same temperature to which hydrates had formed in the flow loop in order to have the same degree of subcooling.

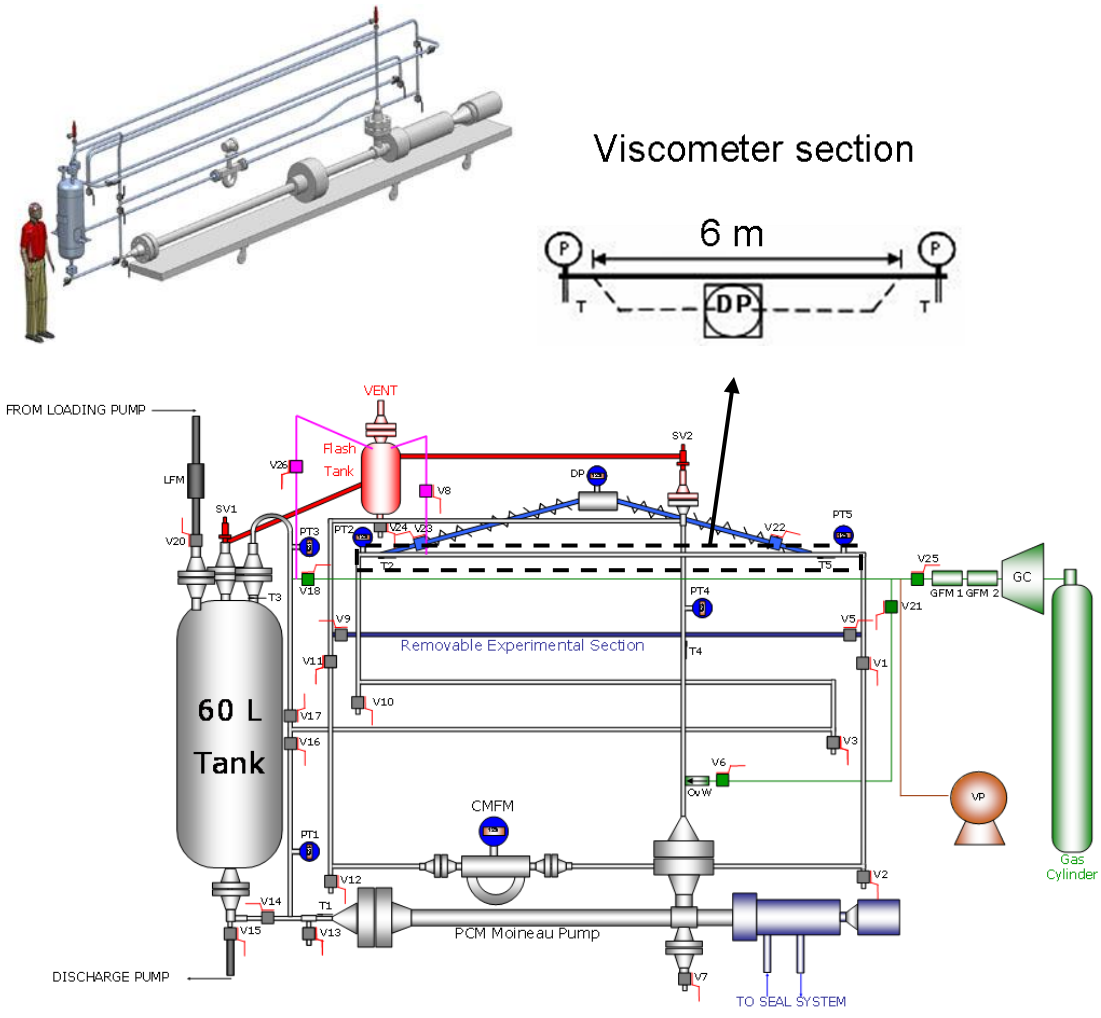

Figure 4.16 Schematic of the high pressure C–FAR flow loop

The mixing rate in the kinetic rig was controlled by adjusting the impeller angular velocity at a value to gives the same average fluid velocity as in the flow loop. The equation: $U=R.\omega$ can be used to relate the fluid average velocity to the impeller angular velocity assuming that the average fluid velocity in the rig is similar to that of

the linear velocity of the impeller. U, R and ω in this equation are the linear velocity, the diameter of the impeller and the angular velocity of the impeller, respectively. The velocity of the fluid in the flow loop was calculated from the Equation: $Q=A.U$ where U is the fluid velocity, A is the cross section of pipeline and Q is flow rate which is measured by a Coriolis flow meter. At the end of the test, when the system reached equilibrium following hydrate formation and no more gas was required to maintain the pressure, the viscosity of the systems were measured.

Typical results for a test (with AA at 0.8 m/s) are shown in the following figures. Figure 4.17 shows the cumulative gas consumption to maintain the pressure in the water – diesel – AA – natural gas – hydrate system.

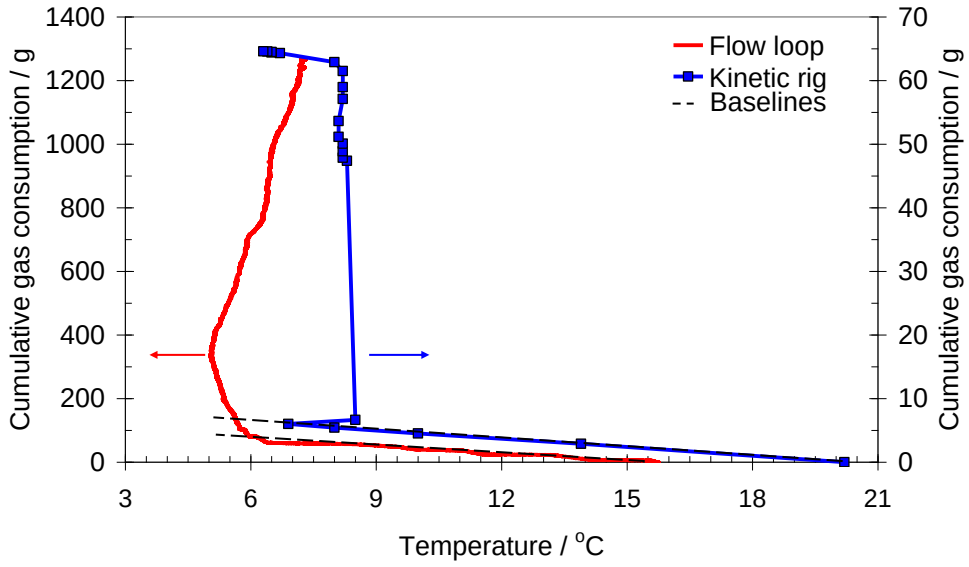

Figure 4.17 Gas consumption due to the temperature reduction and hydrate formation in the small scale kinetic rig with HTI and large scale C-FAR flow loop in a 20% water cut diesel-water-natural gas-AA system.

As can be seen, the gas consumption increased smoothly and linearly before hydrate formation due to temperature reduction and increased sharply when hydrates started to form. The base line in this curve predicts the amount of gas consumed due to temperature reduction, and the difference between the consumed gas and the base line gives the amount of gas consumed during hydrate formation. The amount of hydrate (mass% of the water present initially in the system converted to hydrate) in the system was calculated from *PVTX* relations. The total gas consumption was about 20 times more in the flow loop in comparison to the kinetic rig which is in agreement with the

volume ratio of two systems. As can be seen in this figure, hydrates started to form at about 6.5 ºC. The target temperature in the flow loop was set to 4 ºC, simulating seabed temperature. When hydrate formed, the flow loop system was still being cooled down; therefore the exothermic nature of hydrate formation was not pronounced in this system. However, after a while when cooling stopped, the temperature increased about 2 ºC because of the exothermic process of hydrate formation as well as the fluid friction due to the viscosity increase. The target temperature in the kinetic rig was set to reach approximately 6 ºC to have the same degree of subcooling as in flow loop. As can be seen in the figure, when hydrates formed in this system, the temperature initially increased due to hydrate formation and later decreased to about its previous value when hydrate formation was finished.

Figure 4.18 illustrates the amount of hydrate and viscosity changes versus time. Viscosity changes have been indicated by current (required for keeping rpm constant) and pressure drop in the kinetic rig and flow loop experiments, respectively. Both of these parameters are proportional to viscosity of the system. As can be seen, the two systems had very similar behaviour. The viscosity of both systems increased smoothly before hydrate formation (due to the temperature reduction) and also during the initial stage of hydrate formation. Viscosity steepened when about 40% of the initial water was converted to hydrates in both systems and kept increasing up to about 80% water conversion where finally started to decrease. This decrease in viscosity value can be attributed to rearrangement of the hydrate crystals.

Figure 4.19 presents the viscosity of the system at the end of the test when all the water was converted to hydrate in both systems. As can be seen, the viscosity values in the flow loop and the laboratory scale autoclave are very much comparable. The good agreement between viscosity measurements of hydrate slurries in laboratory setups and pressure drop measurements from flow loops have been also reported by Turner *et al.* 2005.

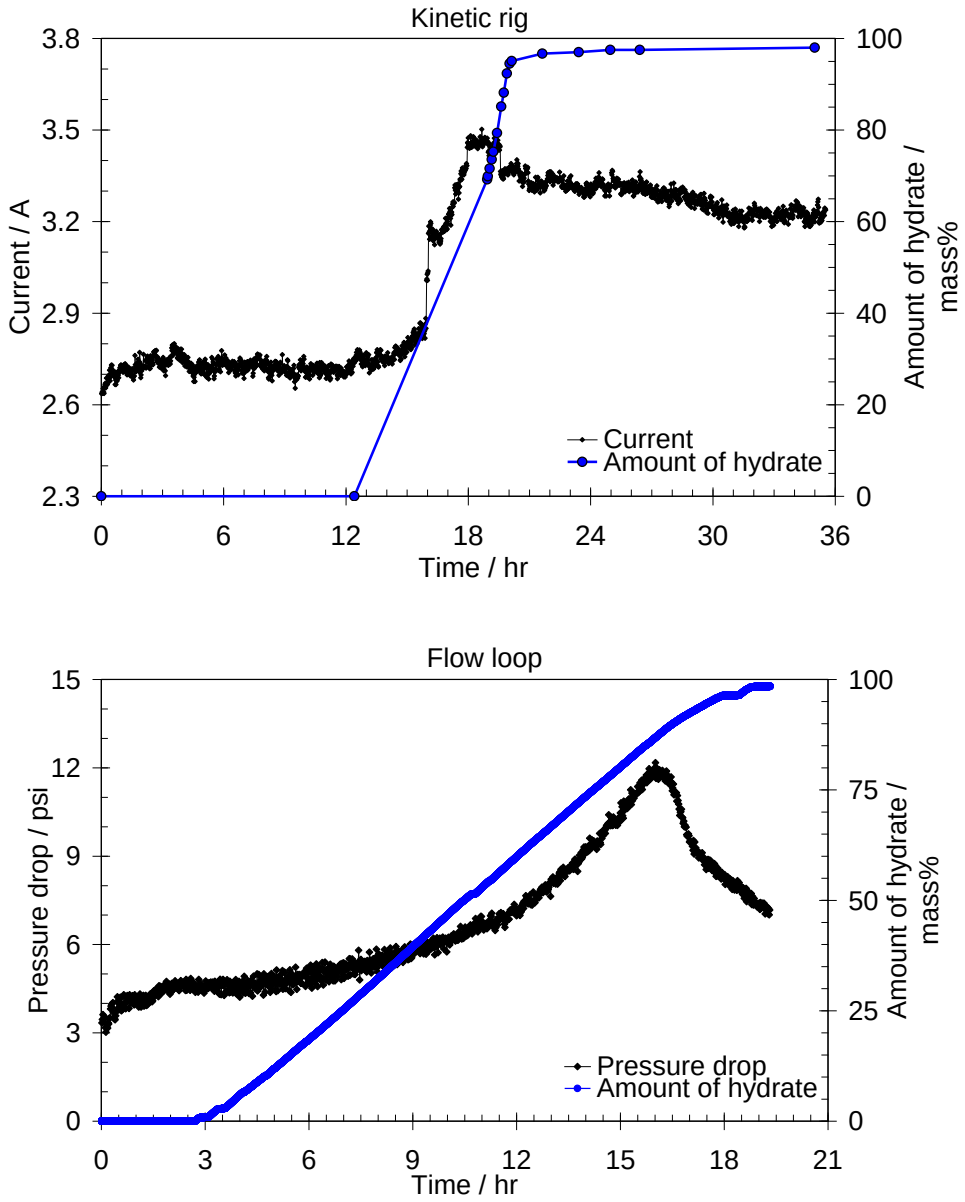

Figure 4.18 Amount of hydrate and viscosity indexes (pressure drop in the flow loop and current in the kinetic rig) in the small scale kinetic rig with HTI and large scale C-FAR flow loop in 20% water cut diesel-water-natural gas-AA system.

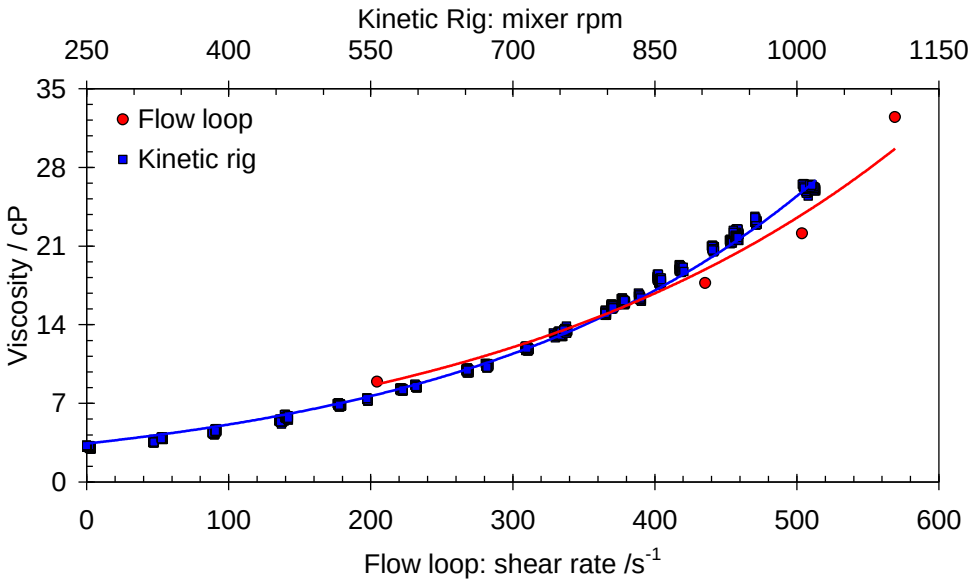

Figure 4.19 Viscosity of hydrate slurries in the small scale kinetic rig with HTI and large scale C-FAR flow loop in 20% water cut diesel-water-natural gas-AA system.

It should be mentioned that up-scaling is beyond the scope of this work and the only objective of these tests were to validate the HTI-set up with flow loop results.

4.6. Other experimental apparatus used in this study

The main experimental apparatus used in this study was the HTI setup. However, some other apparatus were also used as complementary devices to prepare the materials (piston-cylinder type rocking cell) for the main experiments or to support our results (visual cell) generated with the HTI setup. Descriptions of the two main set-ups used in this study in addition to the HTI-set up are given below. In some experiments, the set-ups had also been modified to meet the requirements of those particular tests; in these cases the modifications have been explained in the related experiments.

4.6.1. Piston-cylinder rocking cell

The piston-cylinder rocking cell (Figure 4.20) is a high-pressure rocking cell designed and built at the Centre for Gas Hydrate Research. The core of the set-up is a high pressure *Proserv* titanium piston-type vessel with a mixing metal shuttle. The maximum volume of the cell is 300 ml and the volume can be adjusted by displacing the piston. The cell is mounted on a horizontal pivot with associate stand for pneumatic controlled rocking through 180 degrees with adjustable rotation speed.

Rocking of the cell, and the consequent movement of the mixing shuttle within it, ensures adequate mixing of the cell fluid. The cell is held in a metallic jacket, which is heated or cooled by a constant-temperature liquid circulator. To achieve a good temperature stability, the jacket is insulated with polystyrene board and the pipes, which connect it to the cryostat, are also insulated with plastic foam. A platinum resistance probe is placed inside the cooling jacket and monitors the temperature. The cell pressure is monitored using a *Quartzdyne* pressure transducer. The temperature and pressure are recorded on a computer.

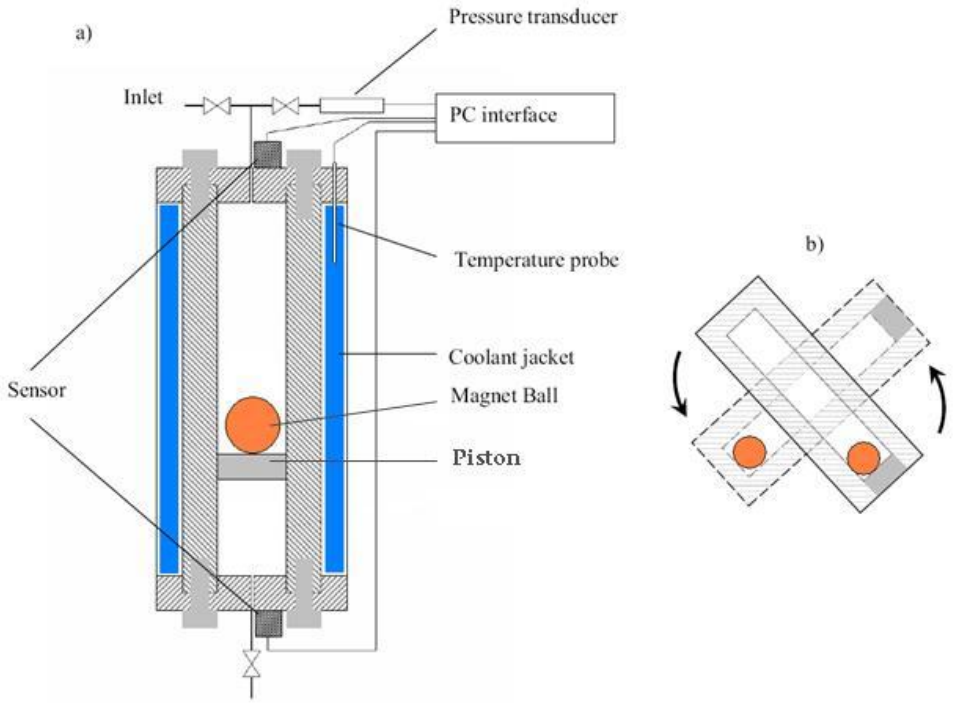

Figure 4.20 Piston-cylinder rocking cell (a) and the way of its movement (b)

4.6.2. Visual Apparatus

Visual experiments were conducted in an in-house built integrated rig (Figure 4.21) which combines visual and ultrasonic capabilities. However, ultrasound measurements were not conducted in this study. The cell is a high pressure kinetic rig equipped with the transparent HTI and fitted with two glass windows giving visibility to the central part of the cell. A magnifying camera is mounted for digital image and video capturing. The cell is held in a metallic jacket, which is heated or cooled by a constant-temperature liquid circulator. A platinum resistance probe is placed inside the cell and monitors the temperature. The cell pressure is monitored using a Druck

pressure transducer. The temperature and pressure are recorded on a computer. The cell volume is about 1750 ml.

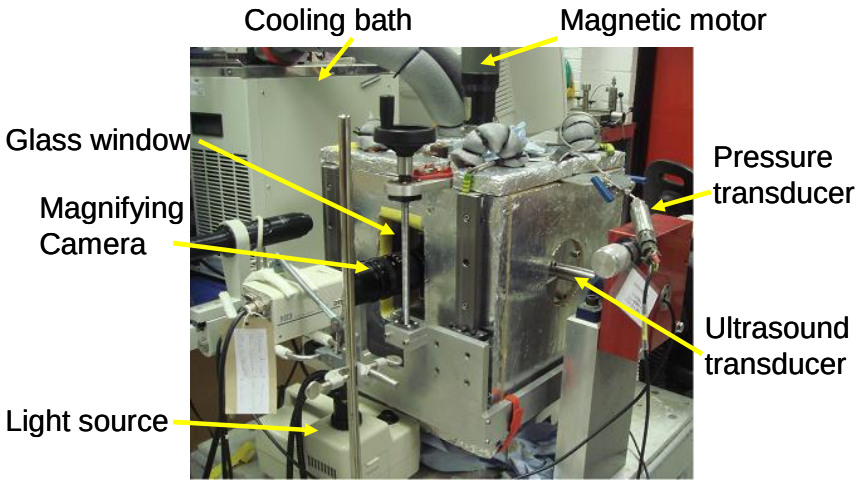

Figure 4.21 Picture of the Integrated rig used for visual studies

The results of all experiments were recorded by plotting temperature, pressure or calculated total gas consumption during hydrate formation and torque as a function of time.

4.7. Summary

This chapter covered description, calibration and validation of the in-house HTI-set up which has been used for rheological investigation of hydrate slurries in this study. The results confirmed that viscosity values in the C-FAR flow loop and laboratory scale HIP-set up are very much comparable, validating laboratory scale data.

In the next chapters, the HYYDRAFLOW concept will be demonstrated for different oil and gas systems at different operating conditions. The experiments consist of investigating rheological behaviour and flow properties of hydrate slurries using the HTI-set up.

4.8. References

Argo, C. B., Berger, R., Shoup, G., Fleyfel, F., Andersson, V. and Larsen, R., 2002, Selection of a Low Dosage Hydrate Inhibitor (LDHI) for a Gulf of Mexico Black Oil Tie-back Pipeline Application. *4th International Conferences on Gas Hydrates.* Yokohama, 19-23 May 2002.

Burgazli, C. R, 2004. *Gas hydrate inhibitors.* WIPO. WO2004/111161.

Clarke, M. A. and Bishnoi, P. R., 2004. Determination of the Intrinsic rate Constant and Activation Energy of CO_2 Gas Hydrate Decomposition Using In-situ Particle Size Analysis. *Chemical Engineering Science*, **59**, pp.2983-2993.

Clarke, M. A. and Bishnoi, P. R., 2005. Determination of the Intrinsic Kinetics of CO_2 Gas Hydrate Formation Using In-situ Particle Size Analysis. *Chemical Engineering Science*, **60**, pp.695-709.

Frostman, L. M., 2000. Anti-Agglomerant Hydrate Inhibitors for Prevention of Hydrate Plugs in Deepwater Systems. *Annual Technical Conference and Exhibition*, Dallas, 1-4 October 2000.

Fidel-Dufour, A. and Herri, J.-M., 2002. Formation and Transportation of Methane Hydrate Slurries in a Flow Loop Reactor: Influence of a Dispersant. *4th International Conference on Gas Hydrates.* Yokohama, 19-23 May 2002.

Huo, Z., Freer, E., Lamar, M., Sannigrahi, B., Knauss, D.M., and Sloan Jr., E.D., 2001. Hydrate Plug Prevention by Anti-Agglomeration. *Chem. Eng. Sci*., **56**, pp.4979-4991.

Kelland, M. A., Svartaas, T. M. and Dybvik, L. A., 1994. Control of Hydrate Formation by Surfactants and Polymers. *SPE 69th Annual Technical Conference*, New Orleans, 25-28 September 1994.

Kelland, M. A., Svartaas, T. M., Øvsthus, J., Takashi, T. and Chosa, J., 2006a. Studies on Some Alkylamide Surfactant Gas Hydrate Anti-Agglomerants. *Chem. Eng. Sci*., **61**, pp.4290-4298.

Kelland, M. A., Svartaas, T. M., Øvsthus, J., Takashi, T. and Chosa, J., 2006b. Studies on Some Alkylamide Surfactant Gas Hydrate Anti-Agglomerants. *Chem. Eng. Sci*., **61**, pp. 4048-4059.

Klomp, U. C. and Reijnhart, R., 1996. *Method for Inhibiting the Plugging of Conduits by Gas Hydrates*. WIPO Pat. WO 96/34177.

Lund, A., Urdahl, O. and Kirkhorn, S. S., 1996. Inhibition of Gas Hydrate Formation by Means of Chemical Additives-II: An Evaluation of the Screening Method. *Chemical Engineering Science*, **51**, pp.3449-3458.

Metzner A.B. and Otto R.E., 1957. Agitation of non-Newtonian fluids. *AIChE J*, **3**(No. 1), pp.3-10.

Mezger, T. G., 2005. *The Rheology Handbook*. 2nd ed. Vincentz, ISBN:3-87870-174-8

NIST Chemistry WebBook, NIST Standard Reference Database Number 69, June 2005 Release.

Oskarsson,H., Lund, A., Hjarbo, K. W., Uneback, I., Navarrete, R.C. and Hellesten, M., 2005. New Technique for Evaluating Anti-agglomerate Gas-Hydrate Inhibitors in Oilfield Applications. *International Symposium on Oilfield Chemistry*. Houston, 2-4 February 2005.

Sengers, J. V. and Kamgar-Parsi, B., 1984. Representative Equations for the Viscosity of Water Substances. *J. Phys. Chem*. Ref. Data. **13**(1), pp.185-205.

Sloan, E.D. and Koh, C. A., 2008. *Clathrate Hydrates of Natural Gas*. 3rd ed. New York: CRC Press,

Sugier, A., Bourgmayer, P., Behar, E. and Freund, E., 1989a. *Method for transporting a hydrate forming liquid*. European Pat. 0323307.

Sugier, A., Bourgmayer, P., Behar, E. and Freund, E., 1989b. Process to Retard the Formation of Hydrates, or to Reduce Their Agglomeration Characteristics. European Pat. 0323774.

Sugier, A., Bourgmayer, P. and Stern, R., 1989c. Process for Delaying the Formation and/or Reducing the Agglomeration Tendency of Hydrates. European Pat. 0323775.

Tohidi, B., Anderson, R., Clennell, M. B., Burgass, R.W., and Biderkab, A-B., 2001. Visual Observation of Gas Hydrate Formation and Dissociation in Synthetic Porous Media by Means of Glass Micromodels. *Geology*, **29**(9), pp.897-870.

Turner, D. J., Kleehammer, D. M., Miller, K. T., Koh, C. A., Sloan, E.D. and Talley, L. D., 2005. Formation of Hydrate Obstructions in Pipelines: Hydrate Particle Development and Slurry Flow. *5th International Conference on Gas Hydrates*. Trondheim, 12-16 June 2005.

Urdahl, O., Lund, A., Mork, P. and Nilsen, T-S, 1995. Inhibition of Gas Hydrate Formation by Means of Chemical Additives-I. Development of an Experimental Set-Up for Characterization of Gas Hydrate Inhibitor Efficiency with respect to Flow Properties and Deposition. *Chem. Eng. Sci*., **50**, pp.863-870.

Chapter 5. Demonstrating HYDRAFLOW Concept in Different Systems

5.1. Introduction

The aim of this chapter is to investigate the rheological behaviour and flow properties of hydrate slurries for various oil and gas systems in the presence or absence of AAs to determine the feasibility of transportation of hydrate slurries and demonstrate the *HYDRAFLOW* concept. Specific objectives are

- Examine the effect of AAs on the rheological behaviour of hydrate slurries
- Assess *HYDRAFLOW* for low and high GOR oil systems
- Investigate the effect of salt (NaCl) on the rheological behaviour of hydrate slurries
- Examine if produced water would have the same effect as sodium chloride on AAs to validate the work conducted on the effect of produced water on AAs, using sodium chloride aqueous solutions to represent produced water.

5.2. Experimental Setup and Materials

All experiments were conducted in the high pressure HTI-setup which is explained in Chapter 4.

The materials used were a North Sea crude oil (crude oil-1 with a composition given in Table A.1), a standard natural gas supplied by air products (composition given in Table A.6), deionised water, a commercial oil soluble AA, two different commercial water-soluble AAs (labeled AA1 and AA2), NaCl (Sigma Aldrich, ≥99%), a synthesised produced water (composition given in Table A.7).

5.3. Effect of AA on hydrate slurry viscosities

To examine the effect of AA on rheological properties, viscosity measurements were carried out on systems with identical initial gas/oil ratios and water cuts in the presence and absence of AA for various amounts of hydrates.

5.3.1. Experimental procedure

In each experiment, the desired volume of deionised water and oil (50% water cut) with or without AA (AA1) was preloaded into the cell, with a headspace left for gas. Natural gas was then injected into the cell until achieving a stable and desirable pressure at 20 ºC. When the system reached equilibrium, the viscosity of the system was measured at various mixing rates (in rev/min). The temperature was then reduced to 4 ºC, simulating seabed temperature and inducing hydrate formation. Once conditions had stabilised following gas dissolution and hydrate formation/growth, the slurry viscosity was measured at various rev/min (rpm) values, and the amount of hydrates (mass% of hydrate based on the total fluid) was calculated from PVTX relations. The amount of hydrate was increased by stepped gas injection. Following gas dissolution and hydrate formation, the viscosity of the system was then measured again at various rpms.

5.3.2. Results and discussions

The measured viscosity data for the tested water/oil/hydrate/natural gas system without and with AA present are presented in Figure 5.1. The results suggest that AAs reduce the viscosity of the system significantly. As can also be seen, increasing the amount of hydrates in both systems resulted in an increase of the viscosity, as one would expect.

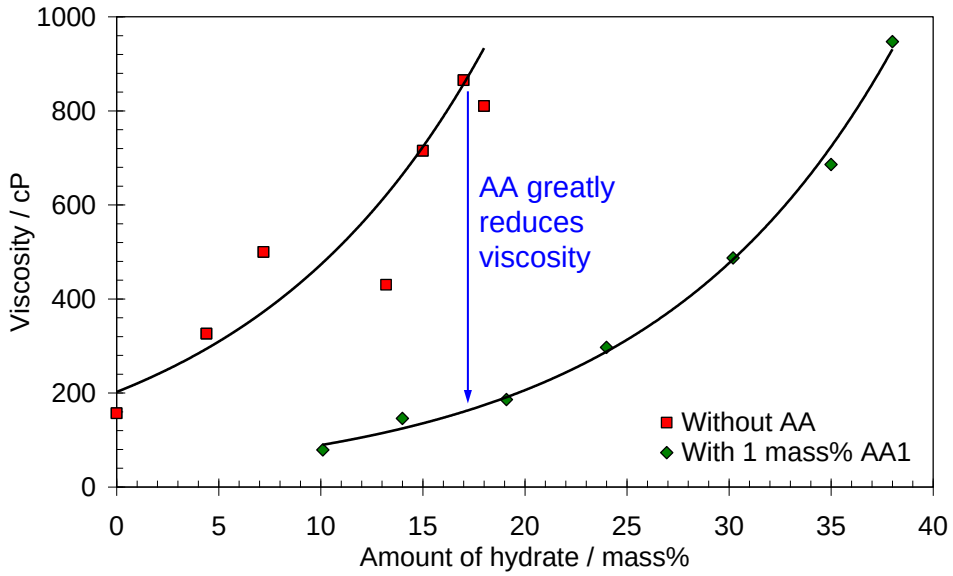

Figure 5.1 Viscosity versus mass% hydrate for comparable water/oil systems with and without AA present.

In the AA inhibited system, the viscosity values at various hydrate fractions form a quite regular trend which can be because of the formation of smooth hydrate slurry in which hydrate particles are well dispersed. The viscosity data for the untreated system (without AA) does not form a regular pattern. This can be attributed to the non-homogeneous nature of the formed hydrate particles. Hydrates might be unevenly distributed in lumps of different shapes and sizes inside the rig. In spite the scattering, there is still a clear trend. The black solid lines in this figure demonstrate the trends. As can be seen, the presence of AA reduces the viscosity of the system significantly (up to one order of magnitude).

5.4. HYDRAFLOW loop concept for low GOR oil system

A specific objective of this thesis was to assess the *HYDRAFLOW* 'loop' concept for both low and high GOR oil systems. Two series of experiment, i.e. without and with AA present, were conducted for low GOR oil system as detailed below.

5.4.1. Experimental procedure

In the 'loop' concept (Figure 2.22), the aqueous phase acts as the primary circulating carrier fluid to which reservoir fluids are added from wellheads at various points. To simulate this, a low GOR oil (GOR=60 vol/vol) was prepared in the laboratory and was added in steps (simulating flow from different wells) to the HTI-autoclave cell

which contained the 'carrier' fluid, as illustrated in Figure 5.2. For simplicity, the amount of fluid injected at various steps was identical, all above the bubble point, and all had the same injection rates.

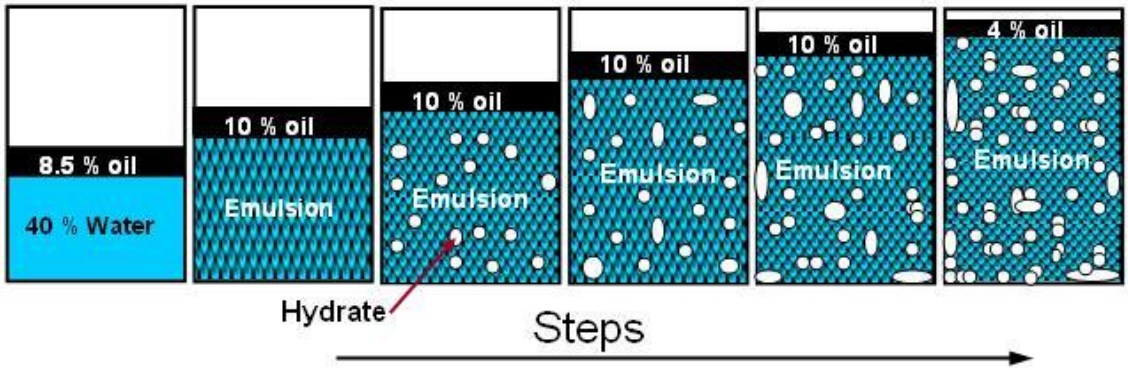

Figure 5.2 Schematic illustration of phase volumes at each oil injection step for low GOR 'loop' concept assessment experiments.

Initially the cell was preloaded with water (40 vol% of the cell) and oil (8.5 vol % of the cell) and the system was cooled down to 4 ºC (simulating seabed temperature) while the mixing was kept constant at 400 rpm. The low GOR oil was then added to the system (10 vol % of the cell); however the pressure of the system was too low to be inside the hydrate stability zone. Therefore more low GOR oil (another 10 vol % of the cell) was injected into the cell which resulted in hydrate formation. Once conditions had stabilised, the slurry viscosity was measured at various rpms. The amount of hydrates was increased by stepped injection of low GOR oil as shown in Figure 5.2. The same procedure was repeated in the presence of AA.

5.4.2. Results and discussions

Figure 5.3 shows the measured viscosity data for the tested low GOR oil system without and with AA present. The experimental points represent viscosity measurement and the amount of hydrates formed after each 10 vol% step-injection. The results suggest that the tested low GOR oil system can form transportable hydrate slurries both without and with AA present up to 45-50 mass% of hydrates. As can be seen, the amount of the hydrate formed at each step was higher for the system with AA present. This can be attributed to smaller water droplet sizes and larger surface area in the AA treated system. This system was blocked during the last step due to formation of large amounts of hydrates. Another point which should be mentioned here is that

adding 1 mass% AA to the system, reduces the viscosity of hydrate slurries significantly.

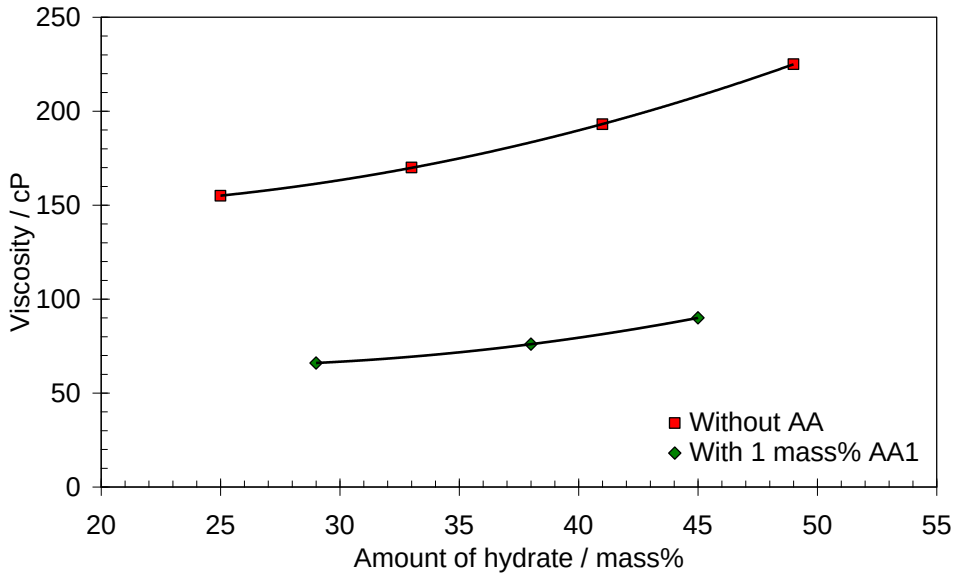

Figure 5.3 Experimental hydrate slurry viscosity for low GOR oil system simulating *HYDRAFLOW* 'loop' concept without and with AA present.

5.5. HYDRAFLOW loop concept for high GOR oil system

For high GOR 'loop' concept assessment, again tests were conducted both without and with AA present (AA1 and AA2).

5.5.1. Experimental procedure

As with the low GOR studies, for simplicity, the composition and volume of the fluids injected at various stages were identical (above bubble point and same injection rates). The tested high GOR oil was prepared in the laboratory with a GOR of 750 vol/vol.

Initially the cell was preloaded with deionised water (50 vol% of the cell) and the high GOR oil (5 vol% of the cell). The system was then cooled down to 4 ºC (simulating seabed temperature) while mixing at 400 rpm. Once conditions had stabilised following hydrate formation, the slurry viscosity was measured at various rpms. Increasing the amount of hydrate was achieved by stepped injection of the high GOR oil by a volume equivalent to 5 vol% of the cell at each step (Figure 5.4).

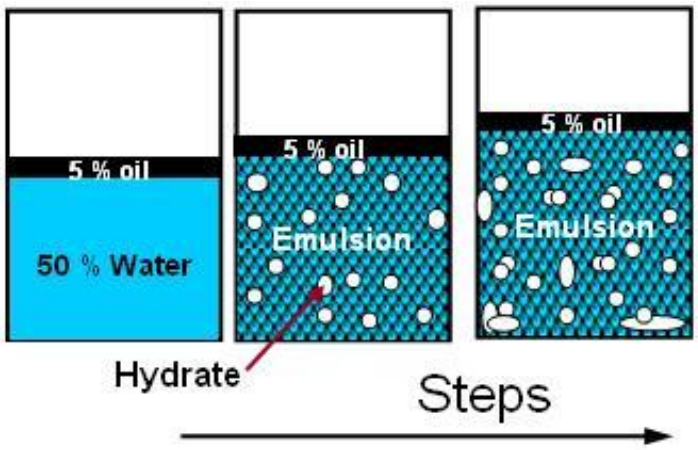

Figure 5.4 Schematic illustration of phase volumes at each oil injection step for high GOR 'loop' concept assessment experiments.

5.5.2. Results and discussions

For the system with no AA present, massive hydrate formation occurred upon cooling during the first step, which resulted in the blockage of the system. For AA systems, two different AAs were tested and in both series of the experiments, the systems were blocked at the third step of injection. As can be seen in Figure 5.5, more hydrates were formed at each step in the presence of AA2 and the viscosity of the system was also lower in this system.

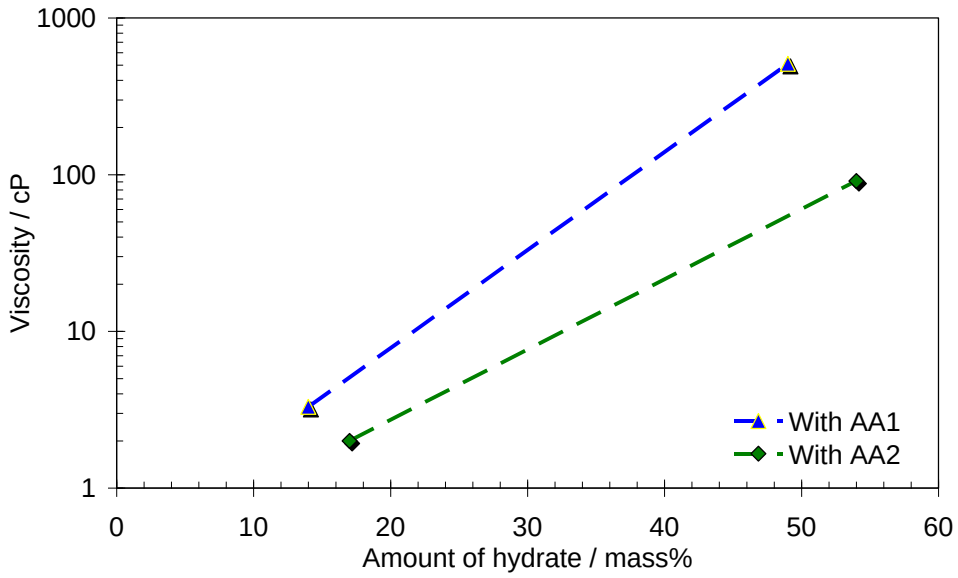

Figure 5.5 Experimental hydrate slurry viscosity for high GOR oil system simulating *HYDRAFLOW* 'loop' concept with AA present.

The results suggest that the tested high GOR oil system can form transportable hydrate slurries in the presence of suitable AA.

5.6. Hydrate formation and growth in different systems

A specific objective of this work was to investigate time-dependent behaviour of hydrate slurries. One of the important time-dependent challenges regarding hydrates is their formation and growth: how hydrates form and, once formed, how rapidly they will grow. Their growth can be controlled by heat and mass transfer.

On the molecular level, hydrate growth can be considered a combination of three factors:

- Kinetics of crystal growth at the hydrate surfaces
- Mass transfer of components to the growing crystal surfaces
- Heat transfer of the exothermic heat of hydrate formation away from the growing-crystal surfaces

It has been suggested that hydrate intrinsic kinetics plays a smaller role in hydrate growth in real systems than heat and mass-transfer effects (Sloan and Koh 2008). However, as it will be shown in this section, the degree of subcooling (or driving force) at which hydrate forms may affect the hydrate growth more than mixing and cooling rates. Subcooling can be considered as a latent factor in the kinetic of hydrates.

To investigate the effect of heat and mass transfer on hydrate formation and growth, different systems (e.g., low and high GOR oil systems) under different heat and mass transfer scenarios were investigated in this study. The principles can be extended to hydrate formation in a pipeline. The rate of mass transfer can be related to the regime of the flowing fluids in the pipeline. In addition, experiments were carried out at two different subcoolings to investigate the effect of driving force on hydrate growth.

As with rheological tests, two systems with different GORs (low GOR=60 vol/vol and high GOR=150 vol/vol) were studied in this section. The hydrate phase boundaries for these systems (Figure 5.6) were calculated with HWHYD software, which is an in-house PVT and hydrate predictive model.

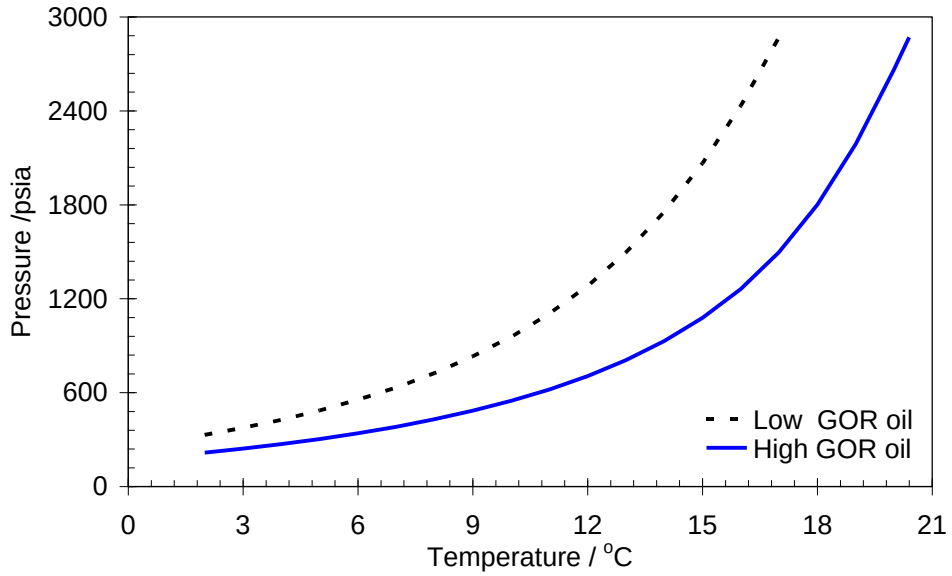

Figure 5.6 Phase boundaries of the tested low and high GOR oil systems (calculated using the HWHYD software).

5.6.1. Experimental procedure

Desired volumes of water, NaCl (4 mass% of the water), and AA (1 mass% of the water) were preloaded into the cell, with a headspace left to inject the low GOR or high GOR oil, depending on the experiment. The low GOR or high GOR oils were prepared in the laboratory (both oils were above their bubble points) and were added to the experimental cell. Addition of oil resulted in a water/oil emulsion with 43% water cut. When the system reached equilibrium at 20 °C, the system was cooled to the target temperature (at different cooling and/or mixing rates) to simulate various pipeline conditions. Temperature and pressure were recorded to monitor hydrate formation and growth rates. Once conditions had stabilized following hydrate growth, the experiment was ended and the system was heated to 40 °C and kept at this temperature overnight to remove hydrate memory. Different runs with different scenarios (different cooling and mixing rates and different subcoolings) were carried out for each system.

5.6.2. Results and discussions

To investigate the effect of heat transfer on the hydrate formation rate in low GOR oils; the system was cooled to 4 °C under two different cooling rates (1.7 and 4.8 °C/hr) at the same mixing rates (550 rpm). Hydrate formation rate is indicated by

means of pressure drop (i.e. gas consumption) in the cell. Figure 5.7 illustrates the hydrate formation rate in terms of pressure.

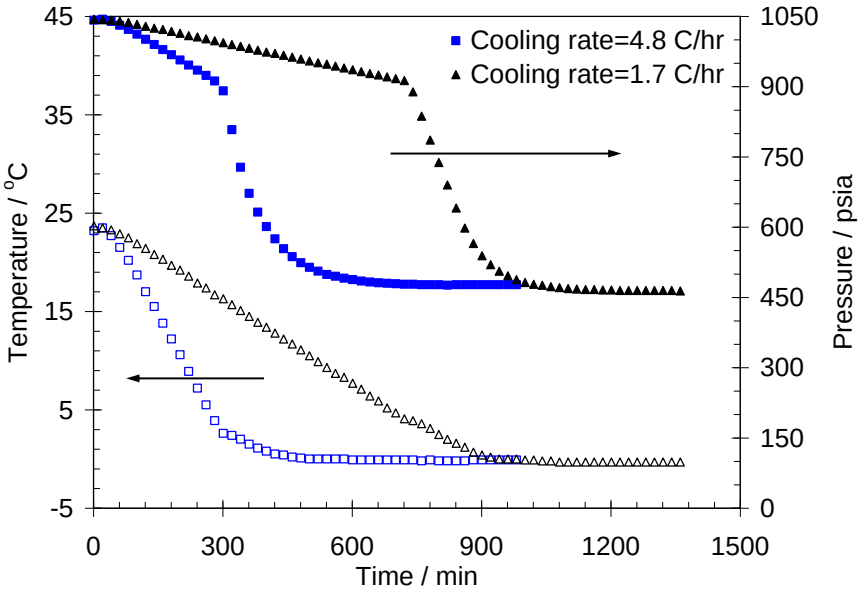

Figure 5.7 Hydrate growth (pressure vs. time) for low GOR oil/water/AA/salt/natural gas under two different cooling rates at 550 rpm. The full symbols are pressure profiles, and the open symbols are temperature profiles.

Under lower cooling rate, hydrate started to form at 4 °C and pressure dropped with a rate of 2.8 psi/min; under higher cooling rate, hydrate started to form at 2.5 °C with a pressure drop rate of 3.7 psi/min. The results show for these tests that the higher the cooling rate, the higher the initial hydrate formation rate.

To study mass-transfer effect on the hydrate formation rate, various tests were performed with a cooling rate of 1.7 °C/hr and different mixing rates. Figure 5.8 shows pressure and temperature profiles for mixing rates of 400, 550, and 770 rpm. The initial pressure drop rates of hydrate formation for all three systems were 0.94 psi/min, meaning that the tested mixing rates do not affect initial hydrate formation (and/or that 400 rpm is already greater than or equal to the minimum mixing rate to eliminate the effect of mass transfer).

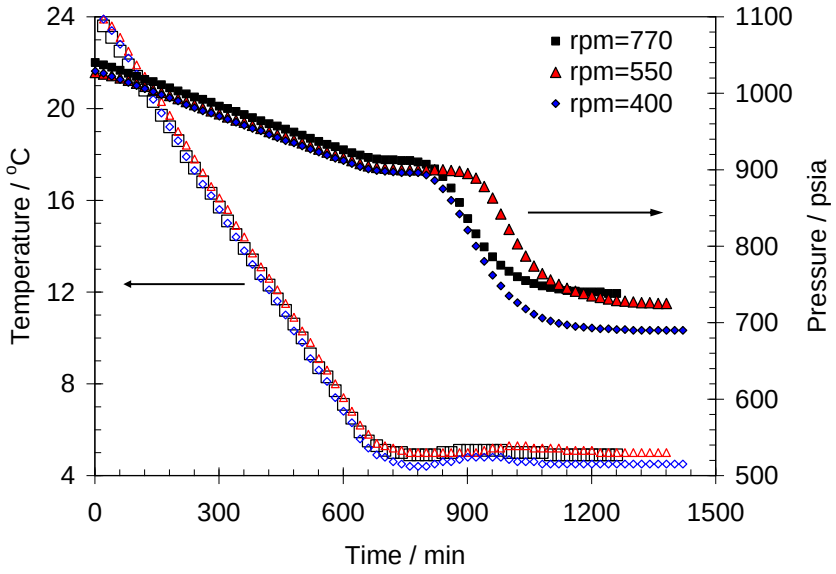

Figure 5.8 Hydrate growth (pressure vs. time) for low GOR oil/water/AA/salt/natural gas with different mixing rates. The full symbols are pressure profiles and the open symbols are temperature profiles

Three further experiments were performed to study the effect of degree of subcooling (driving force) and low mixing rates on hydrate formation rates. The mixer was switched off to minimize hydrate formation before reaching the stabilised target temperature (with respect to target degree of subcooling). In these experiments, the target temperatures were set to 3.5 and –2.5 °C to achieve 6 and 12 °C subcooling, respectively. Once the target temperature was achieved, the mixer was switched on, hydrate started to form, and the temperature of the system increased because of the exothermic hydrate formation process and the heat generated by the mixer. As can be seen in Figure 5.9, the degree of subcooling has a strong effect on the rate of hydrate formation; the rate of pressure drop because of hydrate formation changes from 0.7 psi/min for the system, which is 6 °C inside the hydrate formation zone to 19 psi/min for the system that is 12 °C inside the hydrate formation zone (constant mixing rate of 550 rpm, in both experiments).

To investigate the effect of mass transfer at lower mixing rates, one additional test was performed at 12 °C subcooling and a mixing rate of 350 rpm; the pressure drop rate decreased from 19 to 14 psi/min for the systems with mixing rate of 550 and 350 rpm, respectively (Figure 5.9).

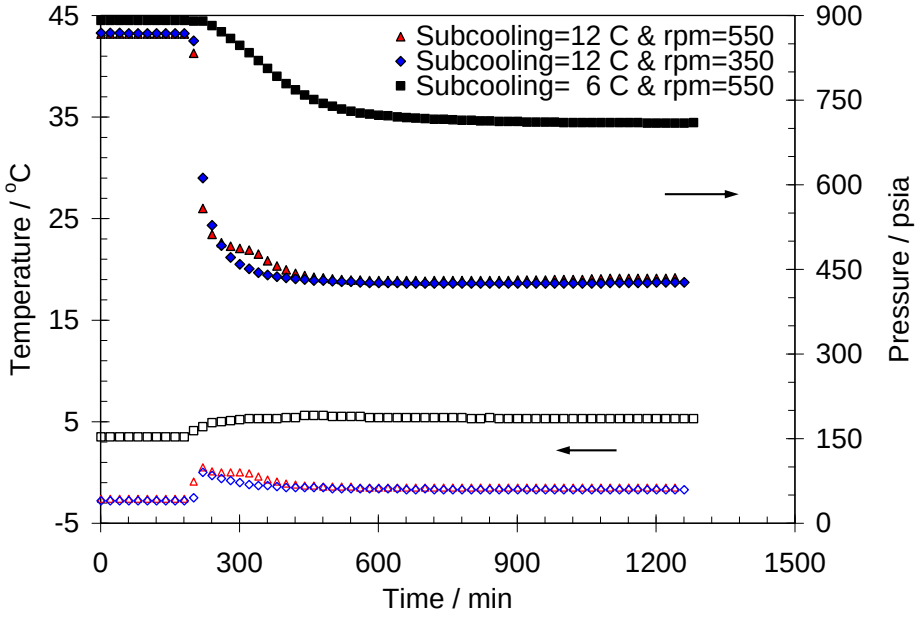

Figure 5.9 Hydrate growth (pressure vs. time) for low GOR oil/water/AA/salt/natural gas with different degrees of subcooling and different mixing rates. The mixer was switched off for the first 200 minutes. The full symbols are pressure profiles, and the open symbols are temperature profiles.

From all the experimental data, it appears that the effect of the degree of subcooling on the hydrate-formation rate is greater than mixing and cooling rates effects under the tested scenarios. However heat and mass transfer rates still have an effect on hydrate formation rates, as it will be detailed. Mass transfer (mixing rate) does not seem to have much effect on the hydrate formation rate at mixing rates greater than 400 rpm.

As with the low GOR studies, two experiments were performed to investigate the effect of cooling rate on the hydrate formation rate for a high GOR system. In the experiments, the system was cooled to 4°C with cooling rates of 1.7 and 4.8 °C/hr and a constant mixing rate of 550 rpm. Under the lower cooling rate, hydrate started to form at 4.5 °C with a pressure drop rate of 5.8 psi/min; under the higher cooling rate, hydrate started to form at 5 °C with a pressure drop rate of 11.4 psi/min. As with the low GOR system, the higher the cooling rate, the higher the initial hydrate formation rate.

To study the mass transfer effect on the hydrate formation rate, two experiments at 12 °C subcooling and mixing rates of 200 and 500 rpm were carried out. To remove the effect of heat transfer, the mixer was switched off to avoid hydrate formation before reaching the target temperature (4 °C). Once the target temperature was

achieved, the mixer was switched on, hydrate started to form, and the temperature of the system climbed from 4 to 10 °C. This could be because of both the exothermic nature of hydrate formation process and the energy loss because of friction. The initial pressure drop rate because of hydrate formation was 25.6 psi/min, with a mixing rate of 250 rpm and 82 psi/min with a mixing rate of 500 rpm.

The trends of mass and heat transfer effect on hydrate formation rate in high GOR oil systems are similar to those of low GOR oil systems. However, the rates of formation are higher in high GOR systems. Table 5.1 summarises the experimental hydrate-formation data at different conditions for low and high GOR oil systems.

Table 5.1 Experimental hydrate formation data for oil/water/salt/AA/natural gas system

#	T_i /°C	P_i /psia	Sub Cooling /°C	Mass Transfer		Heat Transfer (Cooling Rate) /(°C/hr)	Indication of Hydrate Formation Rate/ (psi/min)	Hydrate /%	T_f /°C	P_f /psia
				rpm_b	rpm_d					
Low GOR Oil										
1	4.4	905	4.5	400	400	1.7	0.94	7.3	4.5	690
2	5	900	4.5	550	550	1.7	0.94	6.4	5	725
3	4.9	909	4.5	760	760	1.7	0.94	6.7	5	693
4	4	890	5.5	550	550	1.7	2.8	13	–0.3	465
5	2.5	890	7	550	550	4.8	3.7	12.8	–0.2	477
6	3.5	890	6	0	550	T_{Bath} = constant	0.7	6	5.3	710
7	–2.6	867	12	0	550	T_{Bath} = constant	19	13	–1.5	435
8	–2.8	868	12	0	350	T_{Bath} = constant	14	14	–1.7	427
High GOR Oil										
9	4.2	2291	12	0	250	T_{Bath} = constant	25.6	42	4.6	1047
10	4.2	2291	12	0	550	T_{Bath} = constant	82	45	6.7	1195
11	12.5	2530	4.5	550	550	1.7	5.8	45	5.2	1076
12	12	2515	5	550	550	4.6	11.4	45	5.2	1078

T_f and P_f are final temperature and pressure, respectively, at equilibrium condition following hydrate formation.

T_i and P_i are temperature and pressure, respectively, just before hydrate formation.

rpm_b is the mixing rate before hydrate formation, rpm_d is mixing rate during hydrate formation.

T_{Bath} is the bath set-point temperature fixed at the start of the test to achieve the required target temperature in the cell. Target temperature depends on the target degree of subcooling in each test.

Figure 5.10 also compares the rates of initial hydrate formation in high and low GOR oil systems at similar conditions (Tests 7 and 10 and Tests 2 and 11 from Table 5.1) in terms of pressure drop rates. As can be seen, in the high GOR oil system hydrates form considerably faster than in the low GOR oil system.

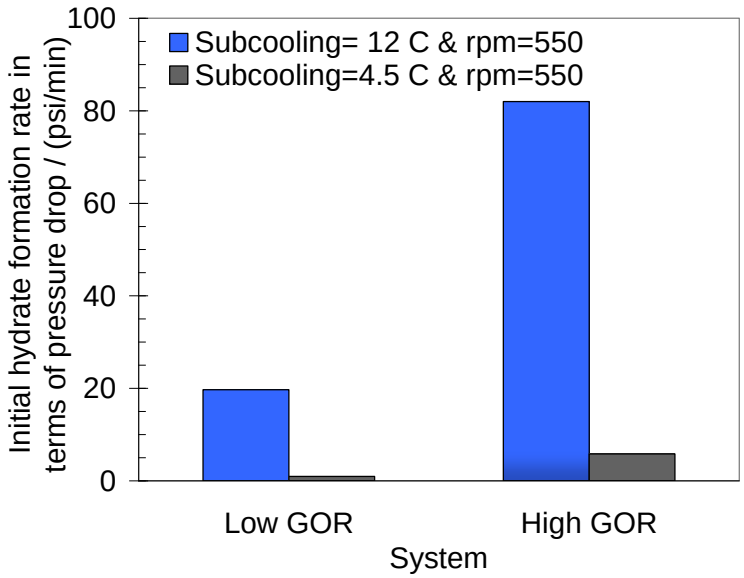

Figure 5.10 Initial hydrate formation rate in terms of pressure drop for low and high GOR oil systems at similar conditions.

The relative rates of pressure drop and, hence, rates of hydrate formation in this figure may be explained by:

- The presence of a liquid hydrocarbon phase may increase the interface between the hydrocarbon and water phases. In these systems there will be a higher surface area between the liquid hydrocarbon containing hydrate former gas and water, thus higher hydrate-formation rates.
- The higher hydrate formation rate seen in the high GOR oil system in comparison to the low GOR oil system can be attributed to the higher amount of hydrate former gas present in the system.

Figure 5.11 presents the effect of different parameters on the initial hydrate formation rate in terms of pressure drop in low and high GOR oil systems.

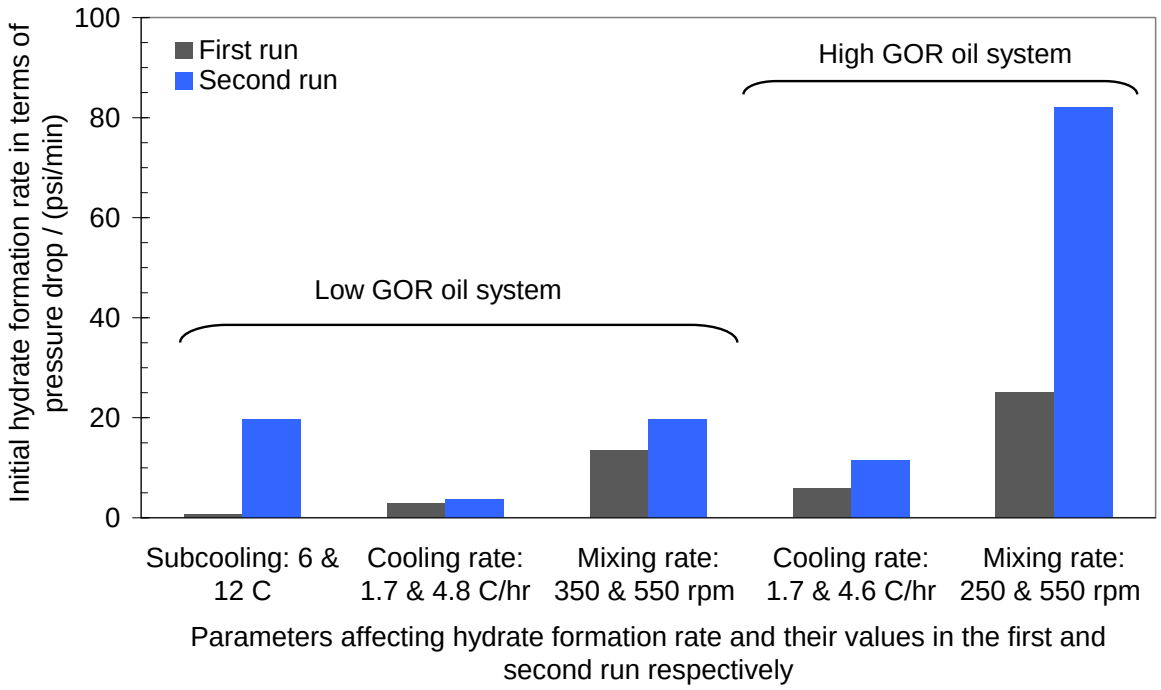

Figure 5.11 Effect of different parameters on hydrate formation rate in low and high GOR oil systems

From this figure, the following conclusions can be drawn:

- High GOR oil systems are more sensitive than low GOR systems with respect to changes in cooling and mixing rates.
- In the low GOR oil systems, increasing the degree of subcooling from 6 to 12 °C resulted in an increase in hydrate-formation rate by a factor of 28. Increasing the cooling rate from 1.7 to 4.8 °C/hr or the mixing rate from 350 to 550 rpm increased the hydrate-formation rate by almost 1.4 times.
- An increase in the cooling rate by an average factor of 2.8 resulted in an increase of hydrate formation rate in low and high GOR oil systems by factors of 1.3 and 2, respectively.
- An increase in mixing rate by an average factor of 1.8 has greater effect on hydrate formation rate than an increase in cooling rate by an average factor of 2.8.

5.7. Effect of salt on the performance of AAs and rheological behaviour of hydrate slurries

The production of oil and gas is usually accompanied with water, and the water cut typically increases as fields mature. The produced water is normally saline in nature and this could affect the hydrate phase boundary and the performance of different additives (e.g., thermodynamic hydrate inhibitors, AAs and KHIs). To examine the effect of salt on the performance of AAs and consequently on the rheological behaviour and flow properties of water/oil/hydrate slurries, viscosity measurements were carried out on low (20%) and high (60%) water-cut systems with varying concentrations of NaCl and different amounts of hydrates. Increasing the amount of hydrates in the system was achieved by step-injection of gas.

5.7.1. Experimental procedure

In each test, 60 vol% of the cell was preloaded with deionised water and oil (20% and 60% water cut), commercial water-soluble AA1 (1 mass% of aqueous phase), and NaCl (0, 2.5, and 5 mass% of aqueous phase for 20% water cut and 0, 3, and 7 mass% of aqueous phase for 60% water cut). The rest of the experimental procedure was similar to the stepped gas injection procedure described in Section 5.3.1.

5.7.2. Results and discussions

The measured viscosity data for low and high water-cut systems are presented in Figure 5.12 and Figure 5.13, respectively. Results demonstrate that the presence of salt can reduce the viscosity of hydrate slurries significantly at both high and low water cuts. In the other words, the presence of salt improves the performance of the tested AA. This may be attributed to the strength of the ion pairing in an aqueous phase of high ionic strength. Kelland (2006) reported that the quaternary AAs, designed and developed by the Shell US team, also performed extremely well in saline systems, coping with a subcooling of 20 °C. However, those AAs did not perform so well in fresh water. This effect may also be partly because of the hydrate inhibition nature of common salts.

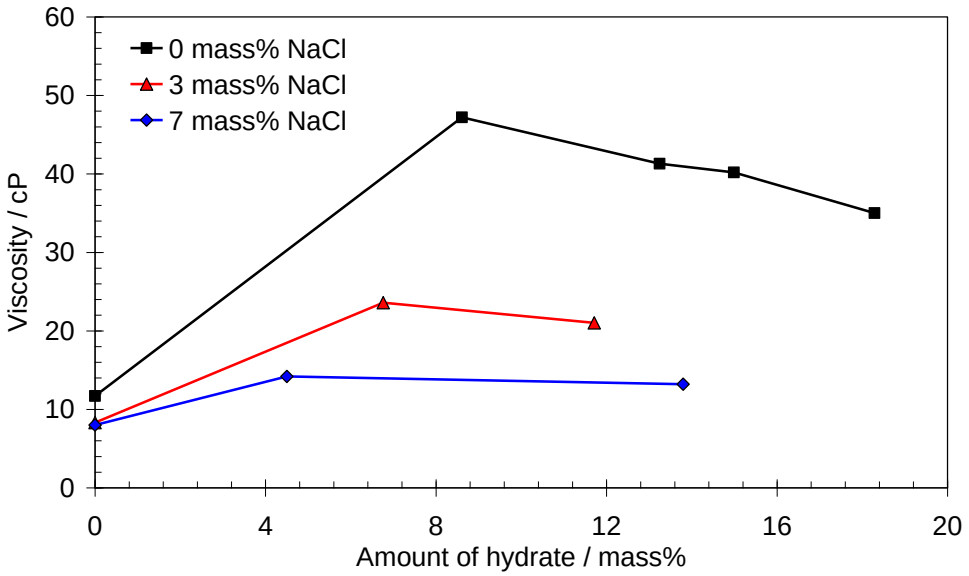

Figure 5.12 Effect of salt on the viscosity of water/oil/AA/hydrate/ natural gas slurries as a function of amount of hydrate (water cut 20%)

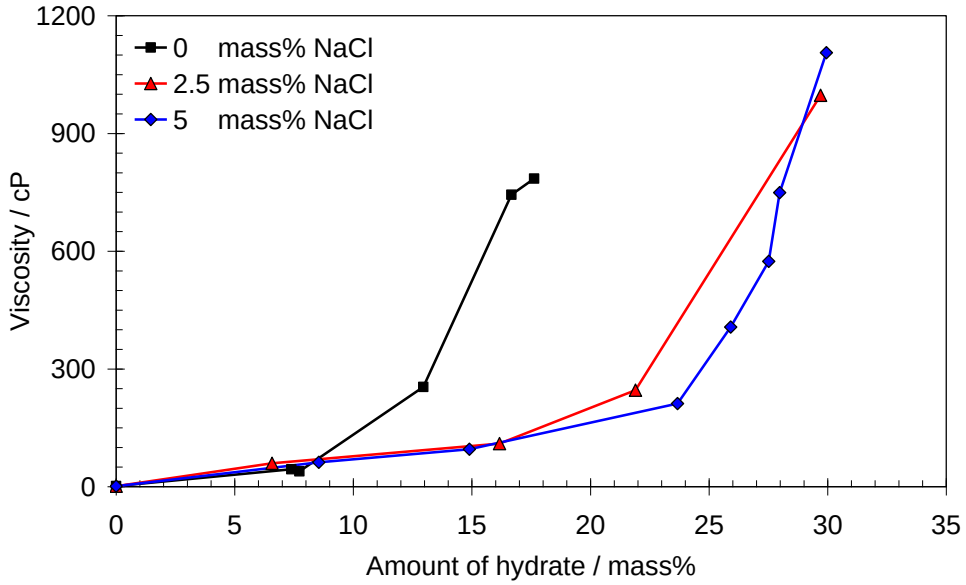

Figure 5.13 Effect of salt on the viscosity of water/oil/AA/hydrate/natural gas slurries as a function of amount of hydrate (water cut 60%)

Indeed, salt inhibits hydrate formation and shifts the hydrate stability zone to lower temperatures and higher pressures, and when hydrates do form, they take up only pure water and the salt concentration increases in the remaining aqueous phase. Therefore, salts reduce the amount of hydrate that can form. Furthermore, in general, in the presence of salts, the rate of hydrate formation at the same temperature and pressure conditions is slower in comparison with cases where no salt is present because of a

lower degree of subcooling (driving force). When hydrates form slowly, they have a lower tendency to agglomerate, but when they form rapidly, large masses of hydrate may agglomerate and increase the viscosity of the system.

Comparing Figure 5.12 and Figure 5.13 suggest that the viscosity of the high water-cut system is about one order of magnitude higher than that of low water-cut system. This also means that the tested water soluble AA is not very effective at 60% water cut. Virtually AAs only appear to work well in the presence of a hydrocarbon phase and they are limited to low water cut systems, which is of concern to maturing fields with increasing water cuts. This requirement may be related to w/o emulsion formation, but other reasons such as high slurry viscosity with high hydrate volume fraction are also cited in the literature (Kelland, 2006; Sloan, 2005). A recent study showed that a newly developed AA inhibitor is effective at water cuts as high as 80% (Alapati, 2008). An oil-soluble AA has been also evaluated successfully at both flowing and shut-in conditions up to 90% water cuts in this study as well. The results have been detailed in Chapter 6.

As shown in Figure 5.12, the viscosity of the low water-cut system rises when hydrate forms. However, the viscosity slightly decreases afterward as more hydrate forms. In addition to crystal size, distribution, shapes and the interaction among crystals, the viscosity of hydrate slurry is a function of the amount of hydrates and the viscosity of the carrier fluid. The sharp increase in the viscosity could be attributed to the high degree of subcooling required for initial hydrate formation, hence massive/irregular hydrate formation. The subcooling required seems to decrease with an increase in salt concentration, hence a reduction in the amount of hydrates formed (and the resulting viscosity increase). The decrease in the system viscosity despite the presence of more hydrates could be because of slow formation of hydrates (after the initial hydrates) as well as rearrangement of previously rapidly formed hydrates. Another factor to consider is the rheology of the carrier fluid (i.e., the remaining water-oil emulsion) considering the reduction in the free water fraction because of hydrate formation.

5.8. Effect of produced water on the performance of AAs and the rheological behaviour of hydrate slurries

In continuation of the work on the effect of NaCl on the performance of AAs and the rheological behaviour of hydrate slurries, it was decided to examine if produced water would have the same effect of NaCl on AAs to validate the work done with NaCl at low and high water cuts.

5.8.1. Experimental procedure

Two series of experiments were conducted in this part. The water cut was 70% in both series of experiments. One series was with sodium chloride brine as aqueous phase and the other one with a synthetic produced water representative of that found in the Gulf of Mexico (GoM) was used. The composition of the produced water is given in Table A.7. The reason for choosing a synthetic produced water from the GoM is that AAs are known to be used in this area (from personal communication with chemical service companies).

The experimental procedure is similar to that of the stepped gas injection procedure of explained in Section 5.3.1 but the system temperature was reduced to 2 ºC instead of 4 ºC because of the high concentration of salt.

5.8.2. Results and discussions

Figure 5.14 shows the rheological behaviour of the tested systems. As can be seen, there is apparently little difference between the viscosity values of the systems with produced water and sodium chloride. According to these results, produced water improved the performance of the tested oil soluble AA slightly more than the sodium chloride brine. However, this difference is within the uncertainty of our experiments.

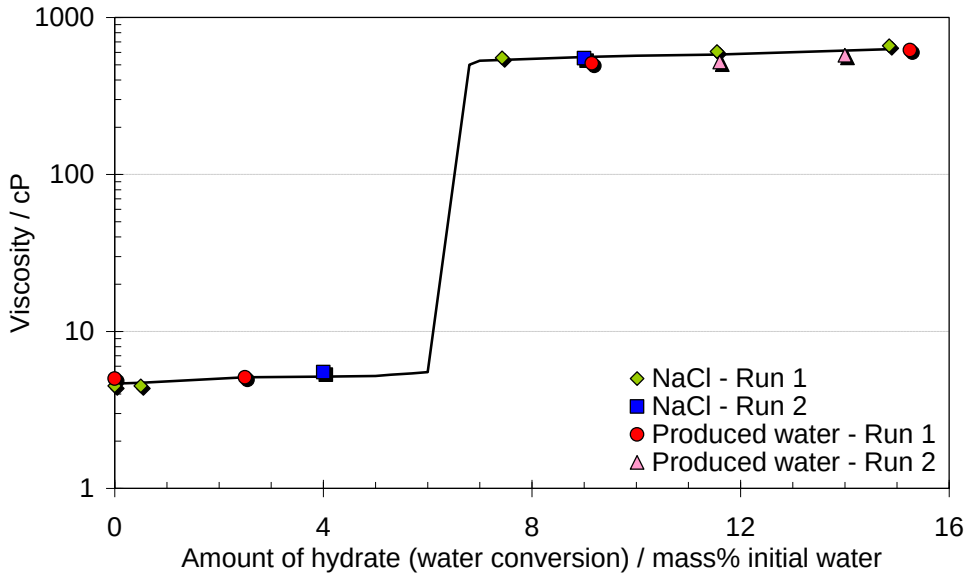

Figure 5.14 Rheological behaviour of the water–oil–salt–natural gas–hydrate system (70% water-cut). Amount of hydrate is in mass% of the initial water converted to the hydrate.

For all these experiments, it was observed that, the viscosity of the system initially increases slightly due to hydrate formation and then it steepens as it passes through 6 – 8 % hydrate concentration (mass % of the initial water converted to the hydrate). Viscosity keeps increasing slightly after this point. This observation has been illustrated in Figure 5.15.

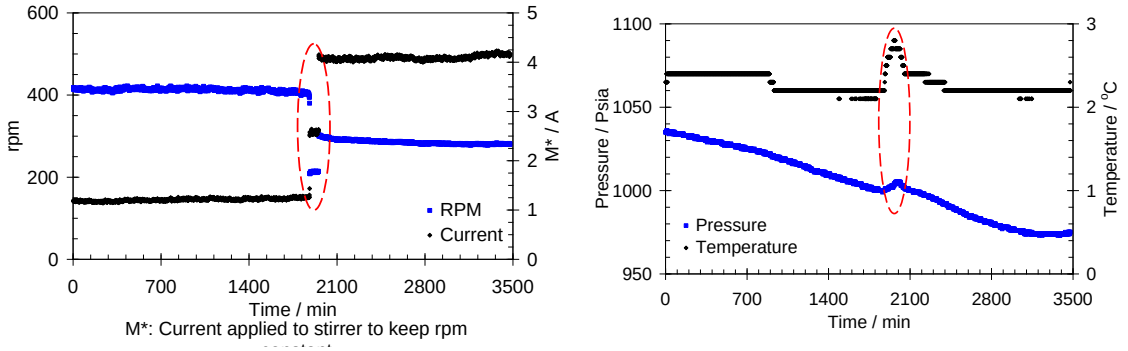

Figure 5.15 Strange behaviour of the water–oil–salt–natural gas–hydrate system.

As it is shown in these graphs, at about 1900 min, the system viscosity increased and the torque required to keep the rpm constant (at about 400), significantly increased and then the rpm dropped about 300 as the power of the mixer motor was not enough to keep it at 400. As a result, temperature and consequently pressure of the system increased at this point due to an increase in friction between impeller and fluid. Therefore, the bath set point was reduced to maintain the system temperature.

This point apparently could be the emulsion inversion point (emulsion inversion describes the change in emulsion type from O/W to W/O or vice-versa). As hydrates form, the amount of free water decreases in the system; this can lead to water-cut reduction in the remaining water/oil blend. It seems that in the tested system (70% water-cut), inversion happens when about 6 – 8 % of the initial water converts to hydrate and hence water-cut reduces to 55 – 60 %.

To examine if this was the inversion point, the system was heated up to 20 ^{o}C outside hydrate stability zone. However, the viscosity did not returned to the original value (system viscosity at 20 ^{o}C before hydrate formation) after hydrate dissociation meaning that the continuous phase was still oil. When the impeller was switched off and adequate time was given to the emulsion to destabilise, the viscosity returned to its original value. Table 5.2 summarises these viscosity values.

Inversion of the emulsion during the initial stages of hydrate formation has been observed by others for similar systems. For example, Fotland has related this phenomenon to the wettability of the hydrate particles (Fotland et al., 2008).

Table 5.2 Viscosity changes in the water–oil–salt–natural gas system due to inversion of emulsion

Condition	Viscosity / cP
Before hydrate formation at 20 ^{o}C	5
After dissociation of hydrate at 20 ^{o}C (Stirred)	150
After dissociation of hydrate at 20 ^{o}C (Half an hours after switching off the impeller)	150
After dissociation of hydrate at 20 ^{o}C (Seven hours after switching off the impeller)	5

5.9. Summary

This chapter examined the feasibility of hydrate slurries transport as well as the kinetic of hydrate formation in different low and high GOR oil systems. The effect of produced water on the rheological behaviour of hydrate slurries was also investigated here. The work conducted in this chapter confirms that:

- AAs can significantly reduce the viscosity of hydrate slurries, and therefore improving fluid transportability.
- *HYDRAFLOW* concept can be applied to the tested low GOR oil system both without and with AA present as supported by formation of transportable oil/hydrate/water slurries with viscosities suitable for pipeline transport.
- *HYDRAFLOW* concept can be applied to the tested high GOR oil in the presence of suitable AA as supported by the formation of transportable oil/hydrate/AA/water slurries with viscosities suitable for pipeline transport.
- In both low and high GOR oil systems, the amount of the hydrate formed at each step was higher for the system with AA present. This can be attributed to smaller water droplet size and larger surface area in the AA treated system.

- All studied parameters including degree of subcooling, heat transfer (cooling rate), and mass transfer (mixing rate) affected the kinetic (rate) of hydrate formation. However, any increases in the mixing rate above a certain value (400 rpm) did not change the hydrate formation rate in the low GOR oil system. The degree of subcooling had a more pronounced effect on hydrate formation rate than the mixing and cooling rate at all the tested conditions. Finally, the high GOR oil system showed more sensitivity to changes in the mixing and cooling rates.
- The presence of salt (NaCl) improved the performance of the tested AAs and the transportability of water/oil/hydrate in both low and high water cuts (20 and 60%).
- The viscosity of the high water-cut system was about one order of magnitude higher than that of low water-cut system. This also means that the tested water soluble AA is not very effective at 60% water cut (this limitation will be addressed in Chapter 6 where the *HYDRAFLOW* concept has been examined in adverse operating conditions).
- The tested AA was found to show equal or slightly better performance in presence of a multi-salt synthetic water as it does with NaCl.

The next chapter will demonstrate the *HYDRAFLOW* concept in conditions where other flow assurance solutions either cannot be applied or are not economically viable.

5.10. References

Alapati, R., Lee, J. and Beard, D., 2008. Two Field Studies Demonstrate that New AA LDHI Chemistry is Effective at High Water-cuts Without Impacting Oil/Water Quality. *Offshore Technology Conference.* Houston, TX, 2008

Fotland, P. and Askvik, K. M., 2008. Some Aspects of Hydrate formation and Wetting. *Journal of Colloid and Interface Science*, **321**, pp.130-141.

Kelland, M. A., 2006. History of the Development of Low Dosage Hydrate Inhibitors. *Energy and Fuels*, **20**, pp.825–847.

Sloan, E.D. Jr. and Koh, C.A., 2008. *Clathrate Hydrates of Natural Gases*, 3rd ed. Boca Raton, London, New York: Chemical Industries, CRC Press.

Sloan, E. D.,2005. A Changing Hydrate Paradigm- from Apprehension to Avoidance to Risk Management. *Fluid Phase Equilib*r., 228-229, 67-74

Sloan, E.D., 1998. *Clathrate Hydrates of Natural Gases*, 2nd ed, New YorkL: Marcel Dekker.

Chapter 6. Demonstrating HYDRAFLOW in Adverse Operating Conditions

6.1. Introduction

One major potential benefit of the *HYDRAFLOW* concept is that it may be used where other flow assurance solutions either cannot be applied or are not economically viable, e.g. at high watercuts (>50%) or under very high degree of subcoolings. In these cases, large amount of thermodynamic inhibitors will be required to either shift the hydrate phase boundary to conditions where KHIs can work or to achieve total hydrate inhibition at operating conditions.

For high watercut systems, the experimental results in the context of *HYDRAFLOW* concept presented in Chapter 5 showed that, for the tested AA, the viscosity of the oil/hydrate/AA/water slurries was not suitable for pipeline transport. Generally, it is believed that AAs are not effective at high water-cuts. However, very recently, some chemical companies claim that their AAs are effective up to 80-90% watercut. Therefore, in order to obtain a transportable slurry at watercuts >60 % the onus in this chapter was on testing suitable AAs for high water-cut systems.

In the case of high degree of subcoolings, e.g. across a choke with subcooling higher than 20 °C, ultra-deep offshore, permafrost and Arctic, systems may experience sub zero conditions and potential ice formation. Under this condition, the main concern is the impact of ice formation on AA performance at subzero conditions. The approaches which can be adopted to address this challenge have been also examined in this chapter.

6.2. High water cuts

Virtually AAs only appear to work in the presence of a hydrocarbon phase and they are limited to low water cut systems, which is of concern to maturing fields with increasing water cuts. This requirement may be related to w/o emulsion formation, but other reasons such as high slurry viscosity with high hydrate volume fraction are also cited in the literature (Kelland, 2006; Sloan, 2005). A recent study showed that a newly developed AA inhibitor is effective at water cuts as high as 80% (Alapati, 2008). However, the development of AAs still requires considerable R&D work before field application becomes commonplace.

In chapter 5, it was shown that the tested water soluble AA was not effective at high water cut. Therefore, it was decided to evaluate another AA which is claimed to be efficient at high water cuts. This AA is an oil soluble AA provided by a chemical service company.

The work on this topic involved the followings parts:

- Rheological investigation (viscosity measurements) of hydrate slurries in the presence and the absence of oil soluble AA at 70% and 90% water cuts
- Complementary visual studies of hydrate slurries in the presence and the absence of oil soluble AA at 90% water cut to support the rheological results
- Effect of shut-ins/restarts on the flow behaviour of hydrate slurries at different hydrate concentrations in the presence of AAs at 70% water cut

6.2.1. Experimental setups and materials

The experiments conducted in this section consist of two types (a) rheological studies and (b) visual observations. All rheological studies were conducted in the high

pressure HTI-setup and visual experiments were carried out in the Integrated rig. Both of these setups have been explained in detail in Chapter 4.

The materials used were two North Sea crude oils (crude oil-2 with a density of 871.5 kg/m^3 and composition given in Table A.2; crude oil-3 with a density of 900 kg/m^3 and composition given in Table A.3), a standard natural gas supplied by air products (composition given in Table A.6), deionised water, a commercial oil soluble AA and NaCl (Sigma Aldrich, ≥99%).

Crude oil-3 was only used in shut-in/restarts test because no more crude oil-2 was available.

6.2.2. Experimental procedure

6.2.2.1. Rheological experiments

In each test, 60 vol.% of the cell was pre-loaded with the test liquids (deionised water and oil with the desired water cut and where required 4 mass% NaCl and/or 1 mass% AA based on water). Natural gas was then injected until achieving the stable desired starting pressure at 20 ºC. Prior to cooling, the viscosity of the system was measured at various rpms. Temperature was then reduced to reach 4 ºC, simulating seabed temperature. This cooling induces hydrate formation. Once conditions had stabilised following gas dissolution and hydrate growth, the slurry viscosity was measured at various rpm. In the subsequent steps, additional gas was injected into the cell to evaluate the system at different hydrate concentrations. Following gas dissolution and hydrate formation, the viscosity of the system was then measured again at various rpms and the amount of hydrates calculated from *PVTX* relations. Figure 6.1 is an example of temperature and pressure profiles for one of the tested systems.

6.2.2.2. Visual observations

The experimental procedure of the visual tests is similar to that of the rheological study experiments but once the system reached equilibrium at the end of each gas injection steps, instead of viscosity measurements, images and videos of the system were captured through the glass window.

6.2.2.3. *Shut-ins/restarts experiments*

The procedure was similar to that of rheological studies but once conditions had stabilised at the end of each step of gas injection, the slurry viscosity was measured at various rpms and the system was shut in for 24 hours. The slurry viscosity was then measured again once conditions had stabilised following restart of the system.

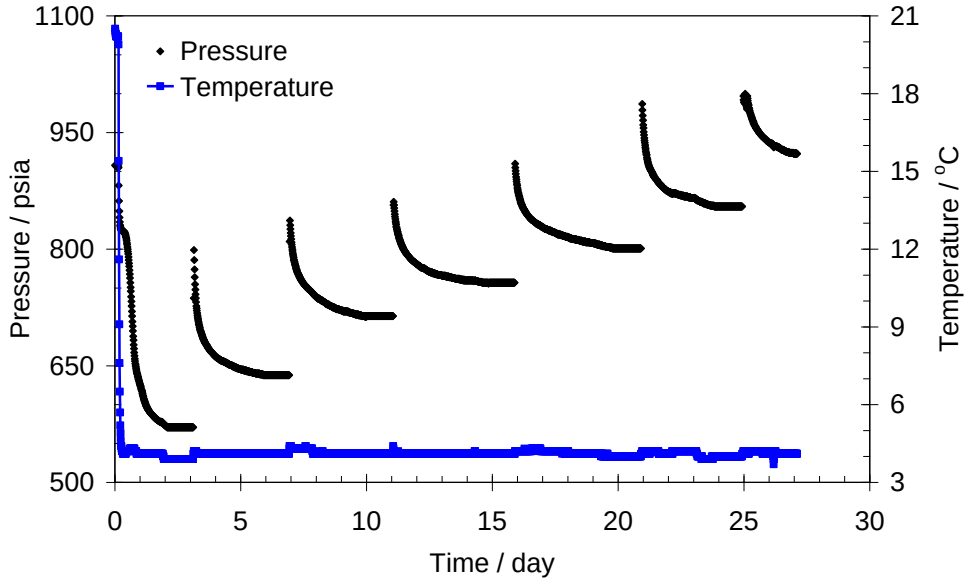

Figure 6.1 Typical temperature and pressure profile of the water–oil–natural gas–salt–AA–hydrate system in stepwise gas injection procedure.

6.2.3. *Results and discussions*

6.2.3.1. *Rheological experiments*

Figure 6.2 illustrates the rheological behaviour of the tested untreated system (water – oil – salt – natural gas – hydrate) with initial water cut of 70 %. This experiment was conducted five times. As can be seen, the viscosity data does not form a very regular pattern. This can be attributed to the non homogeneous nature of the formed hydrate particles. Hydrates might be unevenly distributed in lumps of different shapes and sizes inside the rig. Therefore, depending on the number, size, position and roughness of each the lumps, viscosity can vary from one run to another even for the same amount of the formed hydrate.

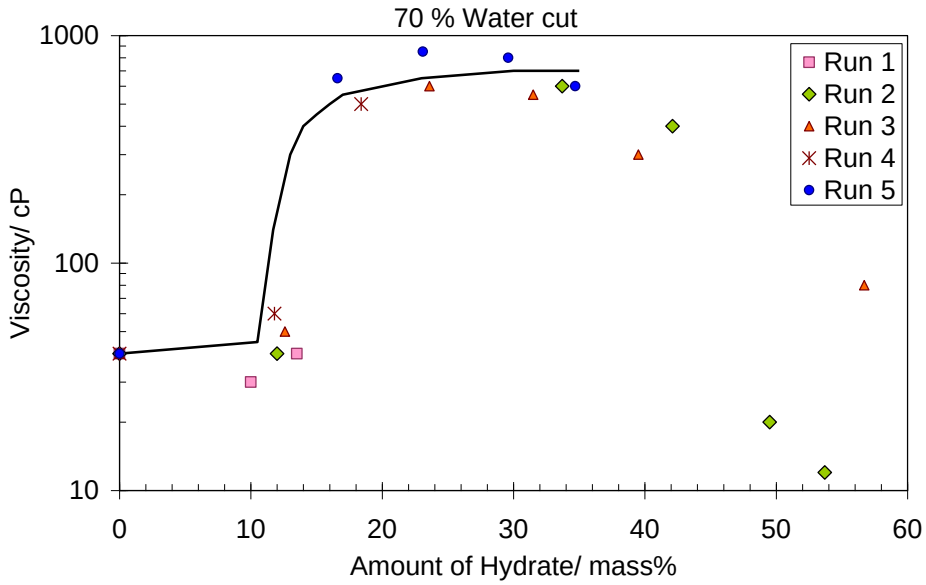

Figure 6.2 Rheological behaviour of the water–oil–salt–natural gas–hydrate system (70% water cut). Amount of hydrate is in mass% of the initial water converted to the hydrate.

In spite of scattering of the viscosity data, still there is a clear trend. The black solid line in Figure 6.2 demonstrates this trend. Initially, the viscosity of the system increases slightly due to hydrate formation and then it steepens as it passes through 10 – 15 % hydrate concentration (mass% of the initial water converted to hydrates). This point could be the emulsion inversion point. As hydrates form, the amount of free water decreases in the system; this can lead to water cut reduction in the remaining water/oil blend. It seems that in the tested system (70% water cut), inversion happens when about 10 – 15 % of the initial water converts to hydrates and hence water cut reduces to 55 – 60 %. Viscosity keeps increasing slightly after this point until either the system is blocked (due to high concentration of hydrate in the cell) or viscosity drops down significantly. The later could be explained by the fact that when a large amount of hydrate forms in the cell, they may build up on the walls and therefore, the impeller spins freely in the centre of the cell giving unrealistically low values for viscosity or hydrates form a cylinder around the impeller as shown in Figure 6.3.

Figure 6.3 An example of hydrate building up on the wall of the HTI setup

Unlike the system without AA, viscosity for the AA inhibited system has a regular trend which can be because of formation of smooth hydrate slurry in which hydrate particles are well dispersed in the system. Figure 6.4 compares the rheological behaviour of the water – oil – salt – natural gas – hydrate system without and with AA present. As can be seen, the presence of AA reduces the viscosity of the system significantly both with and without hydrate present.

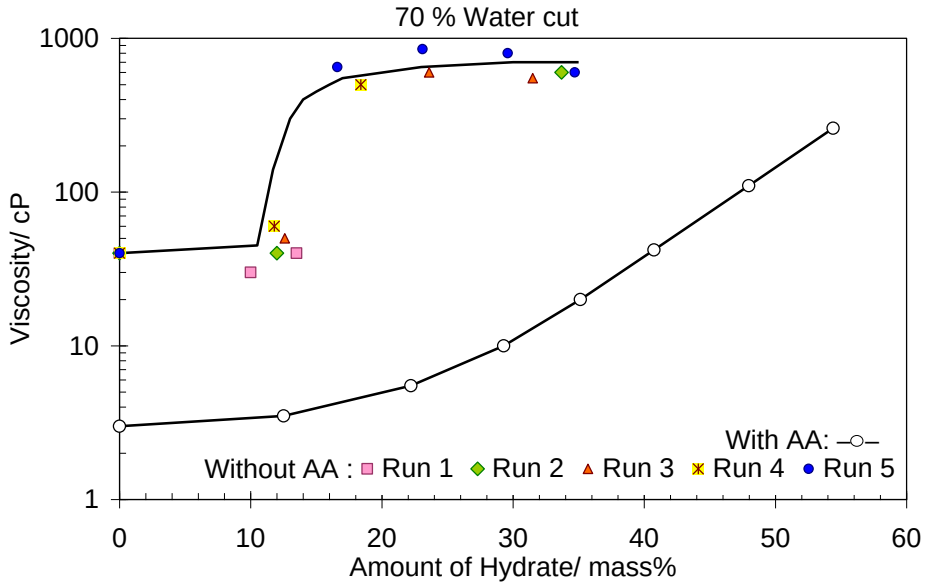

Figure 6.4 Rheological behaviour of the water–oil–salt–natural gas–hydrate system (70% water cut) without and with AA. Amount of hydrate is in mass% of the initial water converted to the hydrates.

As with the 70% water-cut system, two series of experiments without and with AA were conducted for 90% water-cut system (water – oil – salt – natural gas – hydrate). Figure 6.5 illustrates the rheological behaviour of the tested systems (with initial water cut of 90%) due to hydrate formation with and without the AA. Similar to the 70% water-cut systems, the viscosity data show a more regular trend in the AA inhibited system.

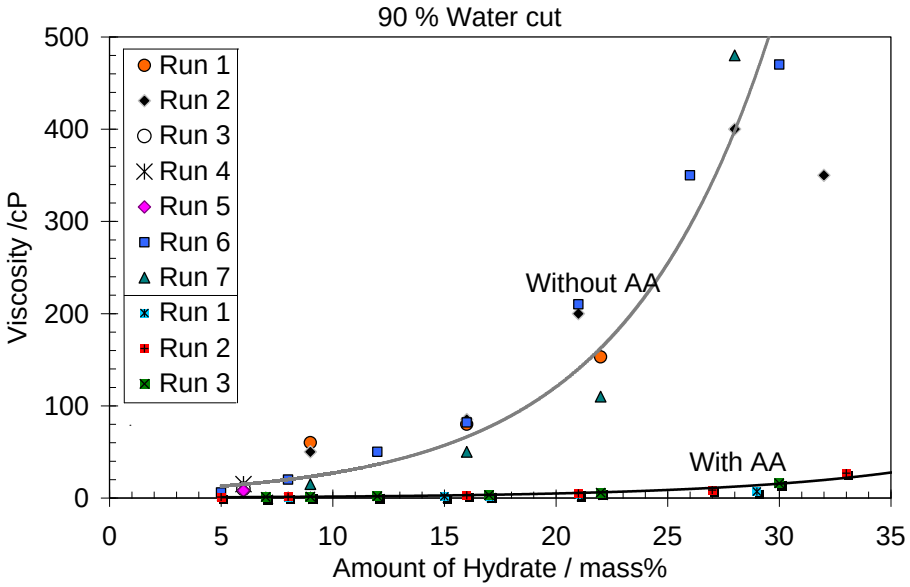

Figure 6.5 Rheological behaviour of the water – oil – salt – natural gas – hydrate system (90% water cut) without and with AA present.

As can be seen, the viscosity of the untreated and AA inhibited systems differ by one order of magnitude meaning that this oil soluble AA is very efficient, even at a water cut of 90%. In other words, the systems treated with this AA at high water cuts forms transportable oil/hydrate/water slurries as supported by the measured viscosity values.

Figure 6.6 and Figure 6.7 compare the rheological behaviour of the tested systems (without and with AA present respectively) at two water cuts (70 and 90 %). In both cases, the system is less viscous at higher water cut. This could be related to the larger volume of the free aqueous phase relative to the volume of hydrate which dilutes the system. It should be noted that the amount of hydrate in these figures are presented as mass of hydrate formed in order to have comparable data.

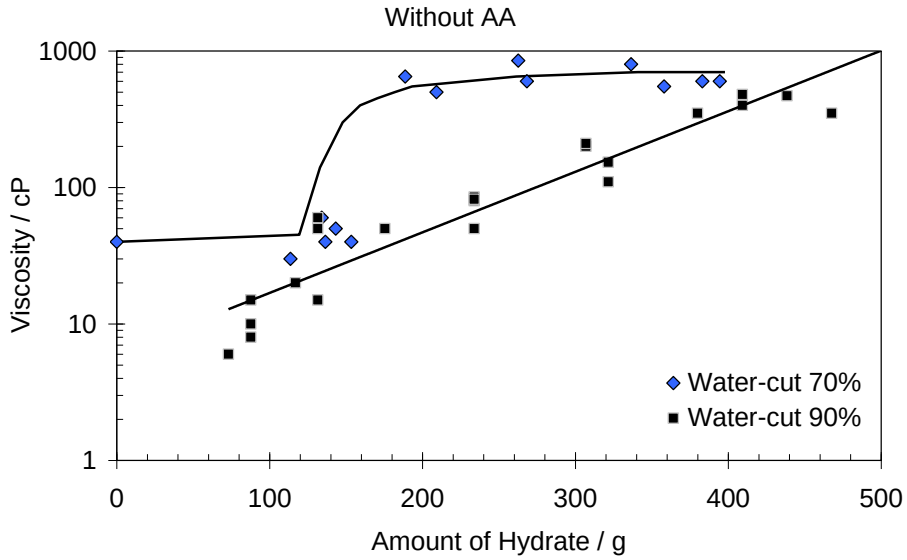

Figure 6.6 Effect of water cut on the rheological behaviour of the water – oil – salt – natural gas – hydrate system without AA.

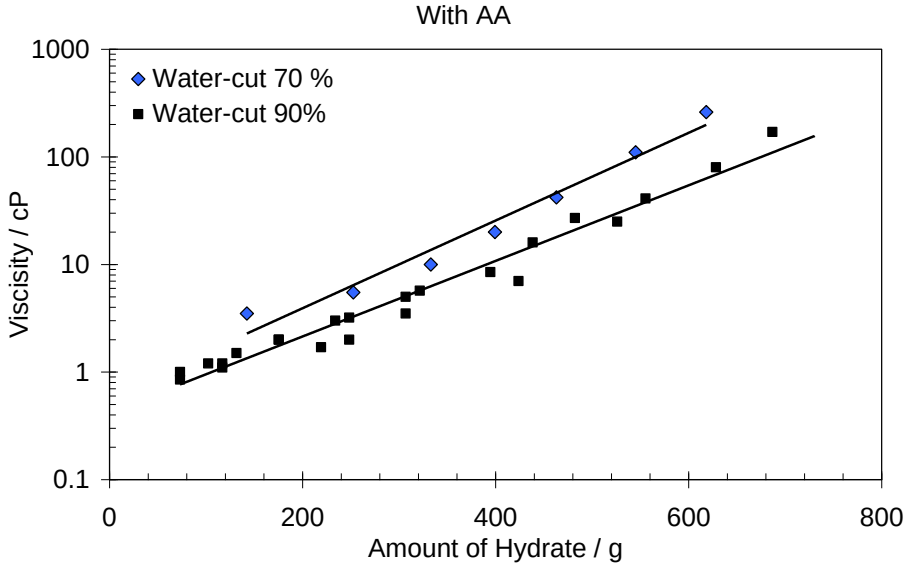

Figure 6.7 Effect of water cut on the rheological behaviour of the water – oil – salt – natural gas – hydrate system with AA.

6.2.3.2. Visual observations:

When investigating the hydrate slurry rheology and AA performance, visual data can help to gain a better understanding of hydrate particle morphology and AA mechanisms. Thus experiments have also been performed in a high pressure visual

set-up to complement viscosity measurements. Figure 6.8 shows hydrate formed in the water – oil – salt – natural gas system with and without the oil soluble AA present.

(a) Without AA and 0.5 % hydrate

(b) With AA and 0.5 % hydrate

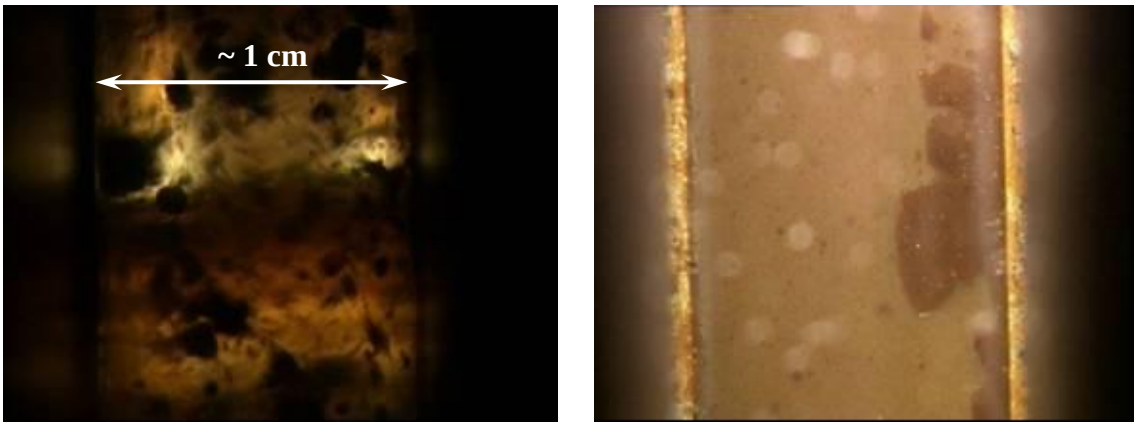

(c) Without AA and 20% hydrate

(d) With AA and 20% hydrate

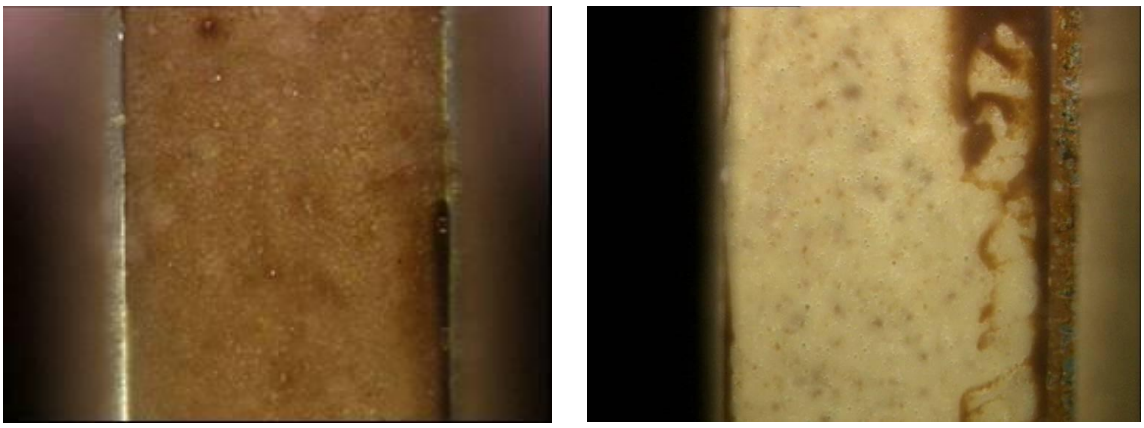

Figure 6.8 Hydrate formed in the water–oil–salt–natural gas–AA system (90% water-cut). Amount of hydrate (percentage of initial water converted to hydrate)

It is clear from the initial stage of hydrate formation (0.5% hydrate) that the AA reduces the size of hydrate particles significantly. At higher hydrate conversion values (20%), no large hydrate masses were observed in the AA inhibited system, only slurries of fine hydrate particles. In addition, the hydrate slurries could be shut-in and restarted without showing any sign of agglomeration. In the untreated system, hydrate particle sizes were much larger. Hydrates also built up in the recess of the cell window, and could only be dispersed gradually by increasing the mixing rate to very high values (1000 rpm). Visual results are consistent with viscosity measurements in that this AA is clearly performing well at high water cuts. However further work is

required to better understand the precise mechanism by which the AA prevents hydrate agglomeration which is beyond the scope of this study.

6.2.3.3. Shut-ins/restarts experiments:

Five shut-ins/restarts tests were carried out in this part with different amounts of hydrates (8, 15, 22, 30 and 45 mass% of initial water converted to hydrate) present in the system. Figure 6.9 is an example of the behaviour of the water – salt – oil – hydrate – oil soluble AA – natural gas system during shut-in (24 hour)/restart.

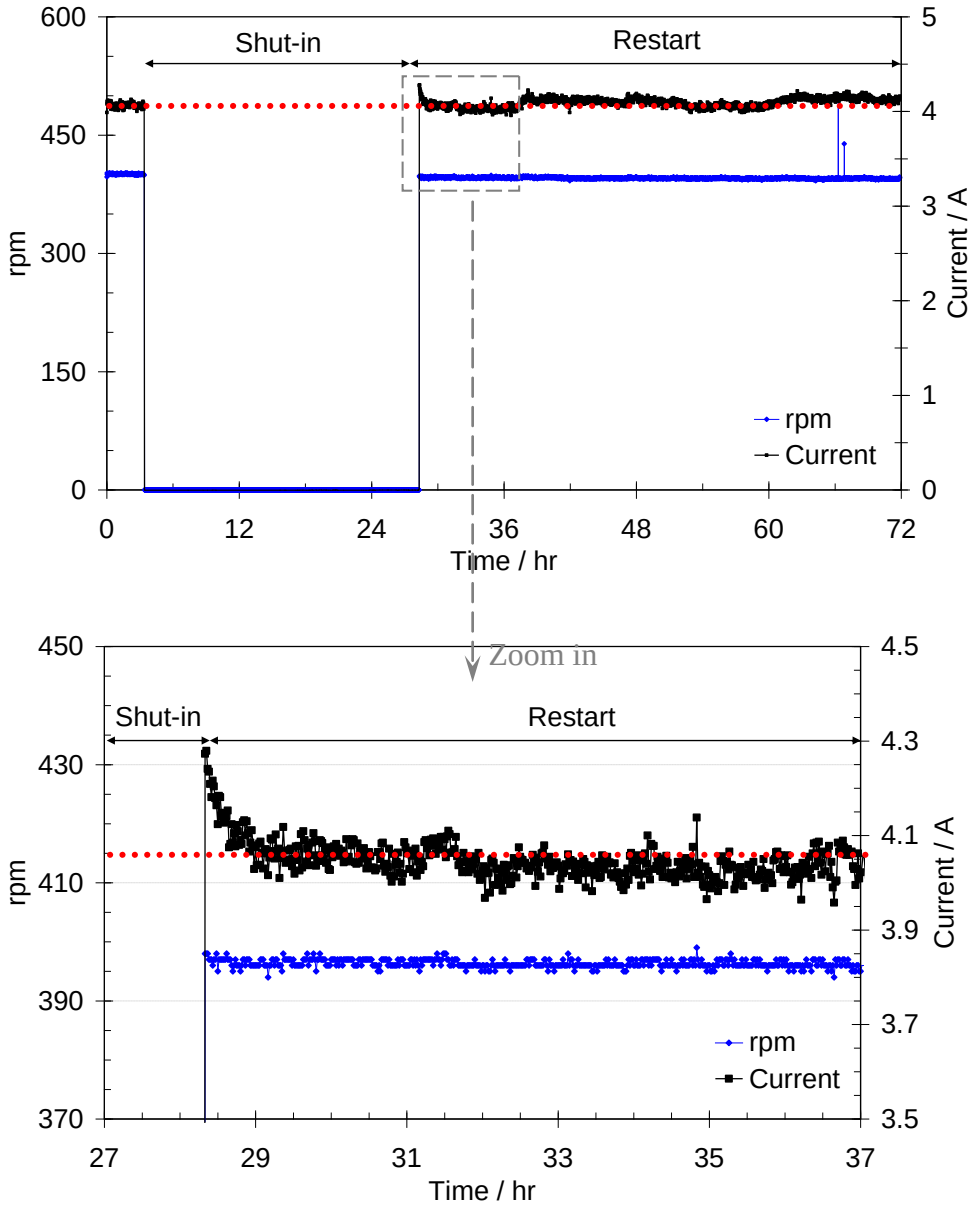

Figure 6.9 Behaviour of water–salt–oil–hydrate–oil soluble AA–natural gas system (30 mass% of initial water converted to hydrate) during shut-in/restart.

In this particular case, 30% of the initial water was converted to hydrate. However, for other hydrate concentrations similar behaviour was also observed. As can be seen, the current required to keep rpm constant, returned to its initial value before shut-in in less than 20 minute. The viscosities of the system before and after shut-in in this case were 650 and 660 cP respectively. This negligible change (1.5 %) in the viscosity is within the error range of the setup.

Table 6.1 summarises the viscosity and current values of the water – salt – oil – hydrate – oil soluble AA – natural gas system before shut-in and after restart.

Table 6.1 Specification of the water – salt – oil – hydrate – oil soluble AA – natural gas system before shut-in and after restart

#	H /%	Vis.$_b$/cP	Vis.$_a$/cP	rpm	Current$_b$/A	Current$_{ja}$/A	Current$_a$/A
1	8	5	5	400	1.06	1.14	1.06
2	15	160	155	400	2.62	2.73	2.62
3	22	350	350	400	3.76	3.88	3.76
4	30	650	660	400	4.08	4.28	4.07
5	46	920	935	310	4.65	4.78	4.65

H: Amount of hydrate (mass% of initial water converted to hydrate)
Vis.$_b$: Viscosity of the hydrate slurry before shut-in of the system
Vis.$_a$: Viscosity of the hydrate slurry once conditions had stabilised following restart of the system.
Current$_b$: Current applied to the stirrer to keep the rpm constant before shut-in of the system
Current$_{ja}$: Current applied to the stirrer to keep the rpm constant just after restart of the system
Current$_a$: Current applied to the stirrer to keep the rpm constant once conditions had stabilised following restart of the system

As can be seen, there is not significant changes in the viscosity values due to the shut-ins. Comparing the currents just after restart (Current$_{ja}$) with the stable currents before and after shut-ins (Current$_b$ and Current$_a$) shows that the current required to keep rpm constant, increased slightly after restart; however, it returned to its initial value before shut-ins for all hydrate concentrations. This initial negligible increase in current just after restart can be attributed to frictions/inertia and is normal even without hydrate present in the system. Therefore, it can be concluded that the tested oil soluble AA shows equal performance during shut-in/restarts as it does in flowing conditions.

6.3. High degree of subcoolings

Two preliminary tests were carried out in this part to investigate the rheological behaviour of hydrate systems inhibited by AAs at sub zero conditions. The idea was to provide some initial information based on which further systematic experiments can be

planed to demonstrate *HYDRAFLOW* concept at high subcoolings and subzero conditions.

Figure 6.10 shows the result of the first test. The fluid system was water and oil at 20% water cut with 1 mass% water soluble AA. The test procedure was stepwise cooling without maintaining pressure. The test fluid was preloaded to the HTI set up and natural gas was injected to the system up to stable pressure of 1550 psia at 26 ºC. The system was then cooled down step by step and at the end of each step when the system reached equilibrium, viscosity of the system was measured. Three zones can be identified in this graph. Zone 1 is only influenced by temperature reduction whereas in Zone 2, hydrate formation was the dominating factor. According to the pressure profile, hydrate mainly formed in Zone 2 because the slopes of the pressure drop were similar in Zone 1 (before hydrate formation) and Zone 3. The viscosity of the system in Zone 3 could be affected by rearrangement of hydrate particles and/or wax formation as well as temperature reduction. As can be seen, the water in the system was used up before system reached 0 ^{o}C.

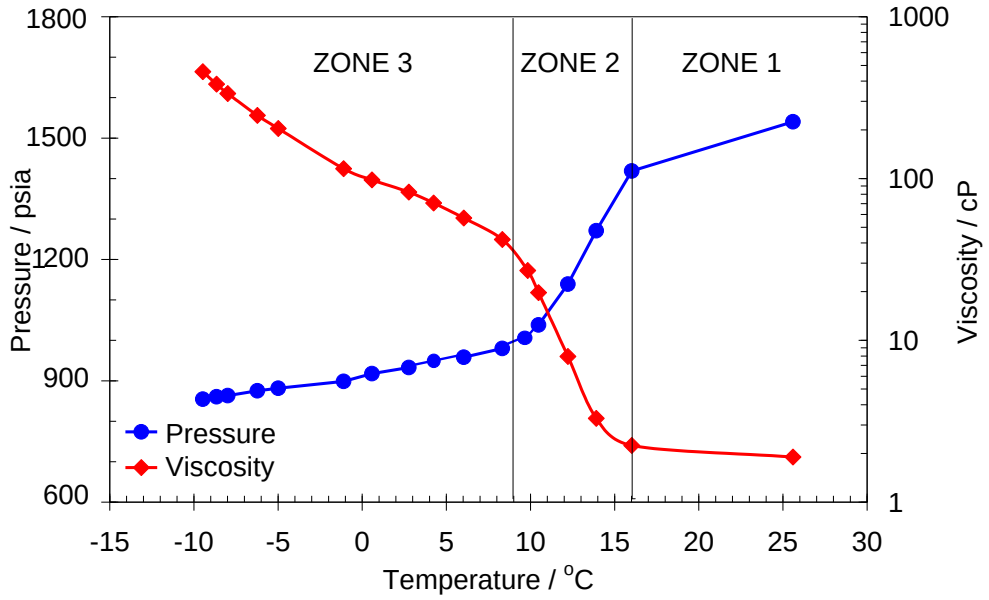

Figure 6.10 Viscosity and pressure of the water–oil–AA–natural gas system before and during hydrate formation (20% water cut)

The objective of the second preliminary test was to investigate the effect of ice on the viscosity of hydrate slurries. Therefore, the experiment was repeated at lower pressure (75 psia) to allow ice formation prior to hydrate formation. Figure 6.11 illustrates the

rheological behaviour of the system during cooling/ice formation and heating/ice melting. The viscosity of the system rises by a factor of 5 (from ~ 100 cP to ~ 500 cP) suggesting that the tested AA is not effective at subzero conditions and in the presence of ice. After ice melting, the viscosity of the system joins back to its initial value.

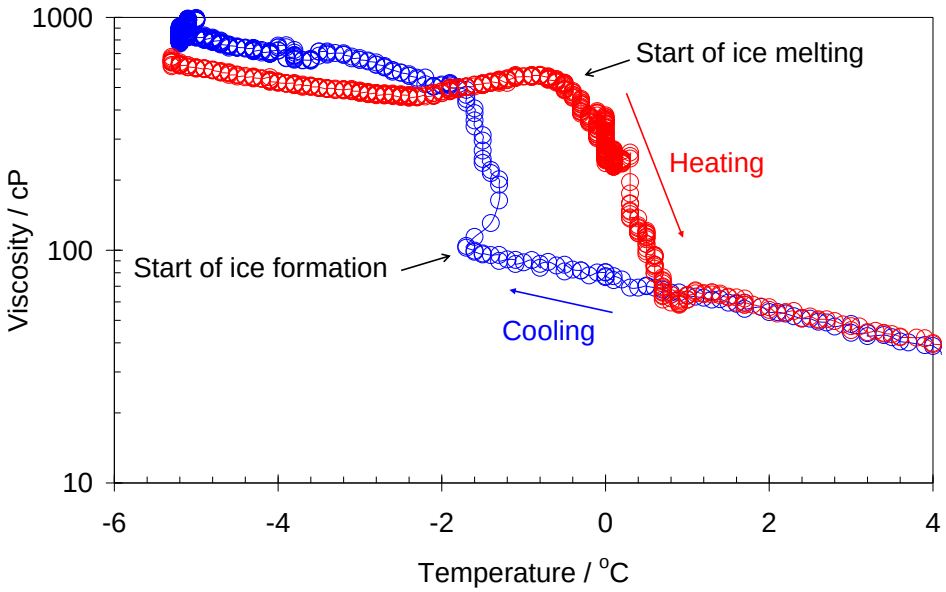

Figure 6.11 Viscosity of the water–oil–AA–natural gas system during ice formation and melting (at 20% water cut and 73 psia pressure).

To overcome the limitation of the negative effect of ice on AA performance, it was decided to investigate the effect of combining thermodynamic inhibitors and AAs on the rheological behaviour of hydrate slurries at subzero conditions. Methanol was selected for this purpose.

6.3.1. Effect of combining thermodynamic inhibitors and AAs on the rheological behaviour of hydrate slurries at subzero conditions

The tests consisted of measuring the viscosity of blends consisting of methanol at various concentrations (0, 5 and 20 mass% of the water), water and oil with 40% water cut (not considering methanol as part of aqueous phase in calculating water cut) and commercial AA (1 mass% of water). Two different AAs (water soluble and oil soluble) were tested in these series of experiments. All tests were performed at constant pressure (1050 psia).

6.3.1.1. Experimental setup and materials

All experiments were conducted in the high pressure HTI-setup as explained in details in Chapter 4. In these experiments, a high pressure piston cylinder was connected to the rig (Figure 6.12). Water was used to displace the piston and inject the gas into the high pressure rig to maintain the pressure. Water was injected using a HPLC (High Pressure Liquid Chromatography) pump.

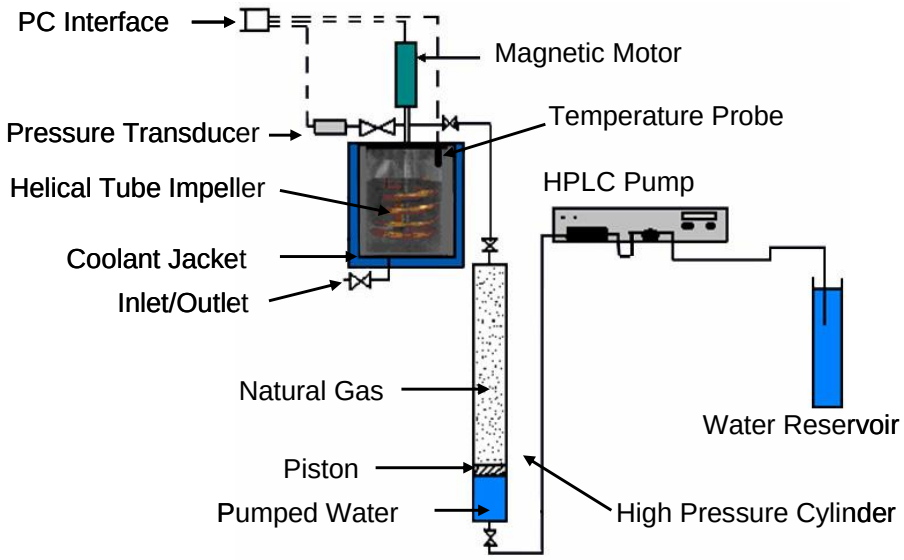

Figure 6.12 Schematic of the HTI-set equipped with a high pressure cylinder to maintain pressure in the cell.

The materials used were a blend North Sea crude oil (crude oil-4 with a density of 875.3 kg/m^3 and composition given in Table A.4), a standard natural gas supplied by air products (composition is given in Table A.6), deionised water, a commercial water soluble AA (w.s.AA), a commercial oil soluble AA (o.s.AA) and methanol (Aldrich, ≥ 99.9 %).

6.3.1.2. Experimental procedure

Three series of tests with varying concentrations of methanol (0 (blank test), 5 and 20 mass %) were conducted to investigate the effect of combining thermodynamic inhibitors and AAs on the rheological behaviour of hydrate slurries at subzero conditions.

In each test, 60 vol.% of the rig was preloaded with water and oil (40 % water cut), a commercial AA (1 mass % of water) and methanol (0, 5, 20 mass % of water). Natural

gas was then charged into both the cell and the high pressure piston vessel to achieve the required test pressure (1050 psia). The high pressure piston cylinder was then connected to the cell to maintain the pressure during the test. The system was kept at this condition (1050 psia and 22 ºC) for 3 hours to achieve equilibrium and to make sure there was no leakage in the system. The viscosity of the liquid was measured at the start of each experiment (at 22 ºC) then the system was cooled down to a temperature set point with a stirring rate of 400 rpm. The temperature of the system was decreased using steps of approximately 4 ºC down to the minimum achievable temperature of the cooling bath or until blockage of the system due to hydrate formation. The minimum temperature, which could be reached with the existing set-up, was -20 ºC. Lower temperature could be achieved by changing the bath (and the coolant if necessary). During the test, water was used to displace the piston and inject gas from the piston vessel into the rig to maintain the pressure. The volume of pumped water was recorded manually. At the end of each step, when the system reached equilibrium (no more water was needed to maintain the pressure) the viscosity was measured. Figure 6.13 is an example of the temperature, pressure and viscosity profile of the water – oil – natural gas – AA – methanol (20 mass%) – hydrate system in step-cooling procedure.

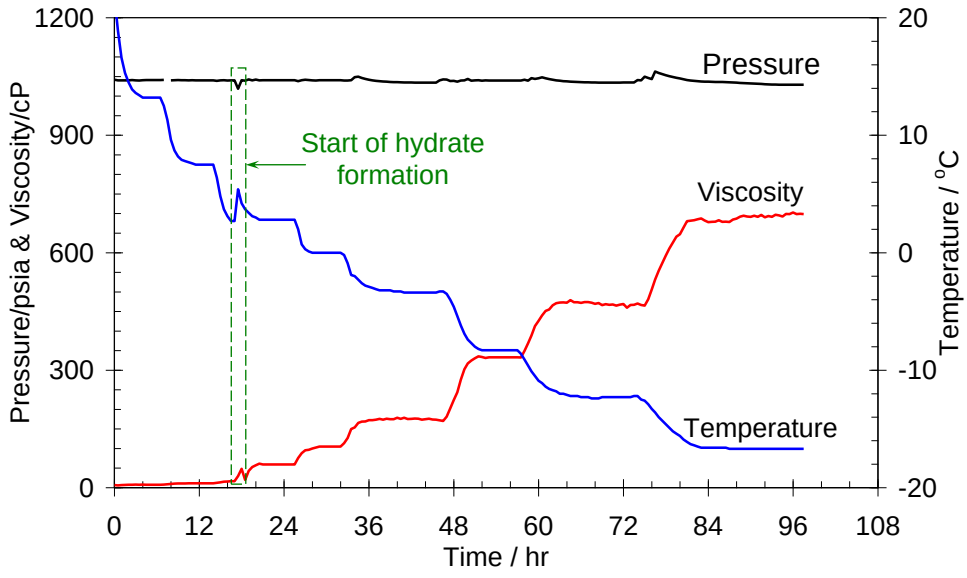

Figure 6.13 Typical temperature, pressure and viscosity profile of the water–oil–natural gas–methanol–AA–hydrate system in step-cooling procedure.(In this case, methanol concentration was 20 mass % and the AA used was water soluble)

In each experiment, the volume of the water pumped into the piston vessel (hence, the volume of gas inject into the experimental set-up) was measured and recorded before hydrate formation, and at the end of each step when the system achieved equilibrium. Measuring the consumed water before hydrate formation, made it possible to calculate and predict the amount of gas consumed due to the temperature reduction, gas solubility in the liquid, and the density changes. Figure 6.14 represents the cumulative gas consumption during one of the tests. The consumption increased smoothly and linearly before hydrate formation (due to temperature reduction and gas density change) and increased sharply when hydrate started to form. The base line of this curve predicts the amount of gas consumed due to temperature reduction, and the difference between the consumed gas and the base line gives the amount of gas consumed during hydrate formation. The amount of hydrate (mass% of the water present initially in the system converted to hydrate) in the system was calculated from *PVTX* relations.

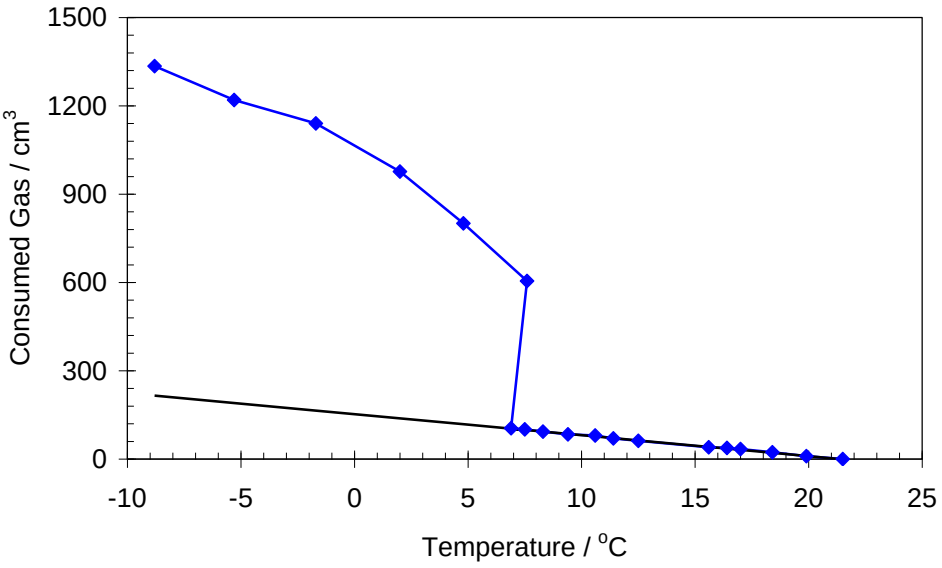

Figure 6.14 Cumulative gas consumption due to the temperature reduction and hydrate formation in the 5 mass% methanol–water–hydrate–AA (oil soluble)–oil–natural gas system.

6.3.1.3. Results and discussions

Figure 6.15 illustrates the effect of varying the concentration of methanol on the rheological behaviour of the tested water – oil – natural gas – hydrate system inhibited with the tested oil soluble AA at subzero conditions.

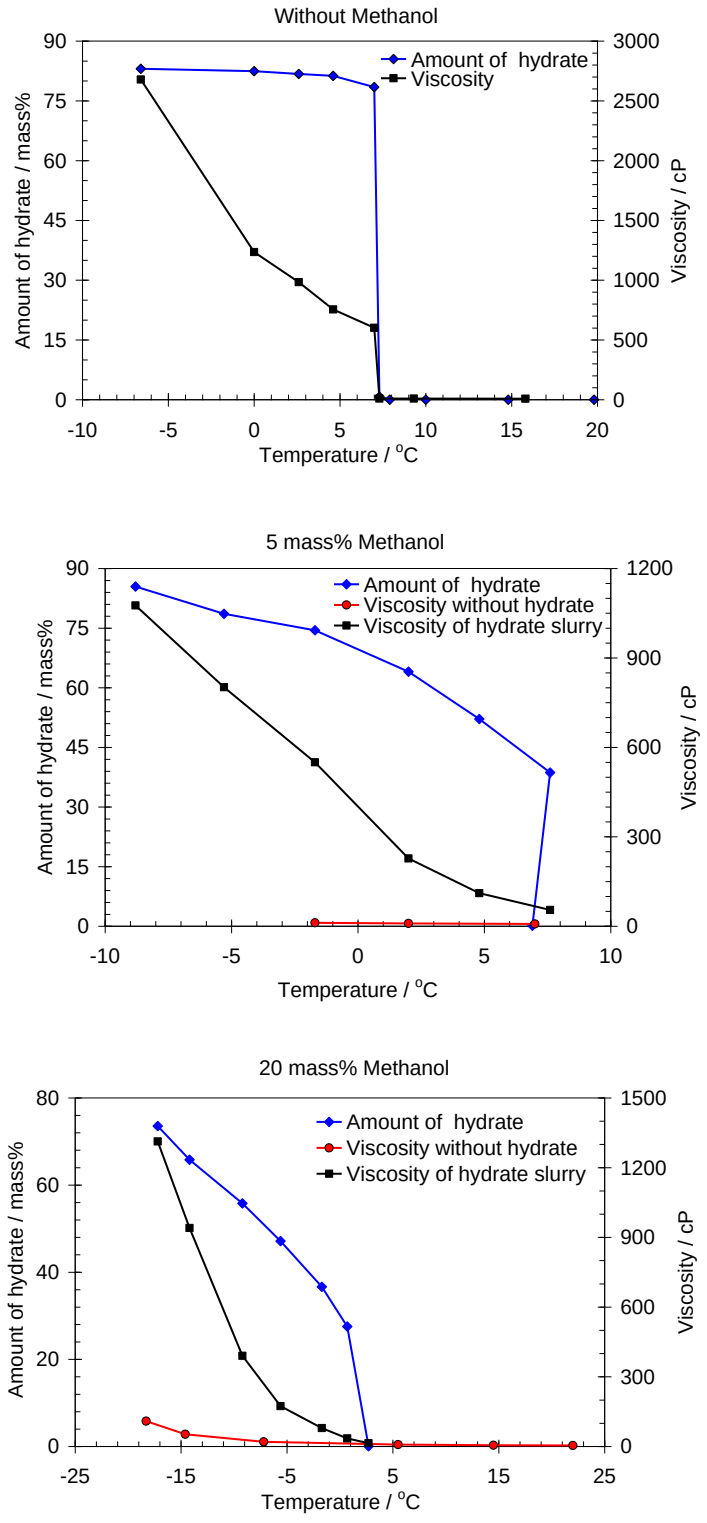

Figure 6.15 Effect of varying concentration of methanol on the rheological behaviour of water – oil – natural gas – hydrate system inhibited with an oil soluble AA

As can be seen, in the system without methanol, hydrate started to form at about 7 ºC and 80% of the water initially present in the system converted to hydrate at this temperature. As a result, the viscosity of the system rose sharply from 8 cP to 600 cP

at this point. Although the amount of the hydrate stayed relatively unchanged during the subsequent steps, the viscosity increased significantly. This could be due to agglomeration of hydrates, wax formation and/or the temperature reduction. The system viscosity sharply increased to 2680 cP as temperature fell below 0 °C. This could be attributed to ice formation. This result is in agreement with the results of the preliminary tests (with water soluble AA) confirming that the tested oil soluble AA is not efficient at subzero temperatures.

In the 5 mass% methanol system, hydrates started to form at 7 ºC and 39% of the water was converted to hydrate causing a viscosity increase from 9 cP to 55 cP. The viscosity of the system increased more in the subsequent steps as more hydrates were formed. Finally, the viscosity reached about 1080 cP at -8.5 ºC while about 85% of the water was converted to hydrate. This viscosity value is less than half of the viscosity of the system without methanol at about the same hydrate concentration (83.5%) and -6.6 ºC suggesting that adding 5 mass% methanol to the system improves the transportability of the system.

In the system with 20 mass% methanol, hydrates started to form at 2.7 ºC and the viscosity of the system increased from 15 cP to 35 cP with a 28 mass% water conversion.

An important point in these graphs is that in the untreated system almost all of the water was converted to hydrate during the first step of hydrate formation but in the system with 5 mass% methanol, 26–37% of water was converted in the first step. This means that amount of hydrate and consequently transportability of the fluid can be controlled by adding a few percent of methanol to the system.

These experiments were repeated for the same system but inhibited with a water soluble AA instead of the tested oil soluble AA at the same conditions. Very similar behaviours and trends were observed again. Table 6.2 summarises the effect of varying concentration of methanol on the rheological behaviour of the tested water – oil – natural gas – hydrate system inhibited with the tested water soluble AA at subzero conditions.

Table 6.2 Effect of varying concentration of methanol on the rheological behaviour of water – oil – natural gas – hydrate system inhibited with a water soluble AA

0 mass% methanol	Step	1	2	3					
	Temperature / ºC	9.6	6	3					
	Amount of hydrate/%	86.5	89.5	90					
	Viscosity / cP	640	1060	1500					
5 mass% methanol	Step	1	2	3	4	5	6	7	8
	Temperature/ºC	8.7	7.1	4.1	1.2	-2.3	-6.9	-10.6	-15
	Amount of hydrate/%	34.7	41.7	61	70.3	78.1	82	86	90.5
	Viscosity / cP	75	120	185	280	385	560	673	890
20 mass% methanol	Step	1	2	3	4	5	6		
	Temperature / ºC	2.7	0	-3.4	-8.3	-12.2	-17.2		
	Amount of hydrate/%	24.4	33.5	44.7	55.4	63.7	72.3		
	Viscosity / cP	60	90	135	270	385	650		

The viscosities of the tested systems inhibited with water or oil soluble AAs at different methanol concentration have also been presented as a function of amount of hydrate in these systems (Figure 6.16).

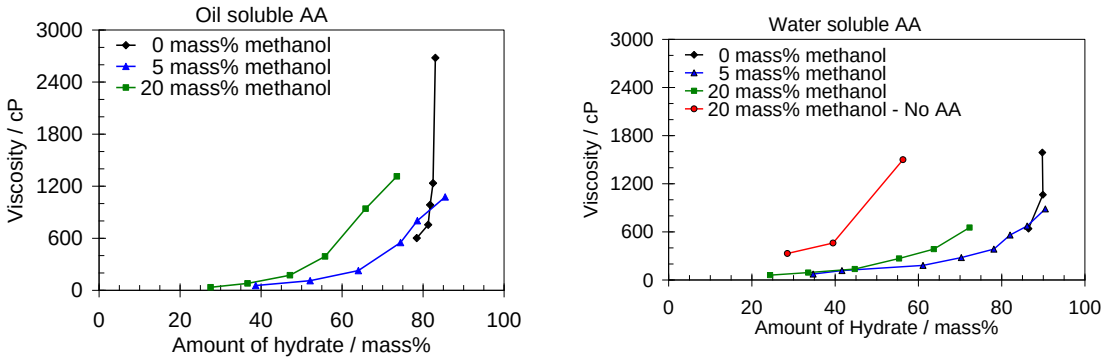

Figure 6.16 Effect of methanol concentration on the rheological behaviour of the water–oil–natural gas–hydrate system inhibited with an oil soluble or water soluble AA as a function of amount of hydrate

One might think that the untreated system has a comparable viscosity values with the systems inhibited with methanol especially at 80–90% water conversions. However, it should be noted that the system temperatures at these hydrate concentration were much lower in the systems with methanol than systems without methanol. The temperatures

at about 80–90% water conversions (viscosities of 600 – 1200 cP) was well above zero (3–9.6 ºC) in the absence of methanol while it was between -5 and -15 ºC for the system with 5 mass% methanol. In other words, it can be concluded that by adding only 5 mass% methanol to the tested hydrate slurry system containing AA, the viscosity of the system at subzero temperatures (-5 to -15 ºC) was reduced significantly near to the viscosity values of the system without methanol at the temperature range of 3–9.6 ºC and similar hydrate concentrations. This means that combining 5 mass% methanol and the tested AAs can improve the transportability of hydrate slurries at subzero conditions.

As can be seen in Figure 6.16, the viscosity of the system with 20 mass% methanol is higher than the system with 5 mass% methanol at the same hydrate concentration. This could be attributed to lower system temperatures for 20 mass% hydrates at the same hydrate concentrations or to the higher viscosity of the carrier fluid (water/oil/methanol/AA). The amount of aqueous phase (water + methanol) is also higher in the system with 20 mass% methanol.

According to these results and considering the fact that when hydrates do form, they take up only pure water and the methanol concentration increases in the remaining aqueous phase suggests that adding 5 mass% methanol should be enough to prevent the negative effect of subzero conditions on the rheology of hydrate slurry systems inhibited with AAs. Because the methanol concentration increases as temperature reduces and more hydrate forms; this can provide enough methanol required to prevent ice formation at lower temperatures.

To examine the efficiency of the AA, one more experiment was conducted without AA and with 20 mass% methanol (Figure 6.16). Comparing the experiments with 20 mass% methanol in the presence and absence of AA at equal amount of hydrate at the same temperatures, confirms that the tested AA works efficiently in this system.

It is also interesting to mention that the tested water soluble AA had better performance at higher hydrate concentrations compared to the tested oil soluble AA while the oil soluble AA showed slightly better performance at lower hydrate conversions. Figure 6.17 shows the comparison for the system with 5 mass% methanol. Similar behaviour was observed for the system with 20 mass% methanol.

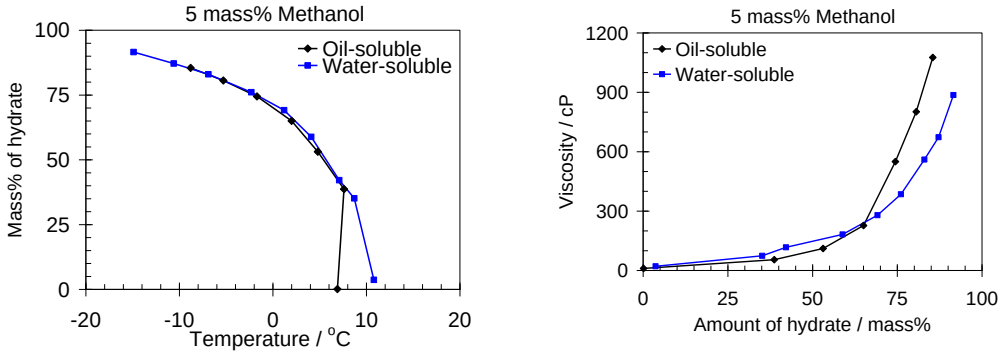

Figure 6.17 Comparison of performance of water and oil soluble AAs in the tested water–oil–natural gas–methanol system

As can be seen in this figure, water soluble AA promote hydrate formation. This characteristic has been frequently observed for the tested water soluble AA.

6.3.2. Effect of combining thermodynamic inhibitors and AAs on the rheological behaviour of hydrate slurries in the presence of salt at subzero conditions

The work conducted in the previous parts of this study confirmed that AAs perform more effectively in the presence of salt. Therefore, in the continuation of the rheological study of hydrate slurries with combining thermodynamic inhibitors and AAs at sub zero conditions, it was decided to assess the compatibility of the tested AAs and methanol in the presence of salt.

When studying the rheological behaviour of hydrate slurries, one of the principal parameters which may affect the results, is the kinetics of hydrate formation. When hydrate forms suddenly, i.e. at very high degree of subcooling, a large amount of water is converted to hydrate. If the rate of hydrate formation in this condition is very high, hydrate particles may stick together and form lumps of hydrate with different shapes and sizes which may results in a jump of the system viscosity. In contrast, the viscosity of the system could remain low if hydrates form at low rates. In this case, small amounts of hydrates may form in different parts of the system which do not necessarily form bulk of hydrate. The particles also have the chance to rearrange themselves. It was shown in Chapter 5 that the degree of subcooling at which hydrates form plays an important role in the rate of hydrate formation. Therefore, the rates of hydrate formation in different systems were measured at the same degree of subcoolings to have comparable results.

Following these tests, it is also interesting to see when hydrate forms when the systems are cooled down continuously with the same rate of cooling. Therefore another series of experiments was carried out to measure the onset of hydrate formation in each system.

In addition, a hydrate dissociation point for the tested water – oil – natural gas system was also measured. The measured dissociation data was used to predict the hydrate phase boundaries, which were required for calculating the degree of subcooling of the tested systems with different methanol concentrations and salt using the HWHYD software.

All experiments carried out in this section are divided into 4 parts as follows:

- Part 1: Measuring a hydrate dissociation point
- Part 2: Determining the onset of hydrate formation
- Part 3: Measuring the rates of hydrate formation and growth
- Part 4: Rheological study of hydrate slurries at subzero conditions – Effect of combining thermodynamic inhibitors and AAs in the presence salt

In each part, a number of systems (8 different systems) with varying methanol concentration (0, 5 and 20 mass% of water) and salt (0, 4 mass% of water) without and with AA (1 mass% of water) present were studied. The tested systems are as follow:

1) Water – oil – natural gas
2) Water – oil – natural gas – salt
3) Water – oil – natural gas – salt – oil soluble AA
4) Water – oil – natural gas – salt – oil soluble AA – 5 mass% methanol
5) Water – oil – natural gas – salt – oil soluble AA – 20 mass% methanol
6) Water – oil – natural gas – 20 mass% methanol
7) Water – oil – natural gas – salt– 20 mass% methanol
8) Water – oil – natural gas – salt – water soluble AA – 20 mass% methanol

All experiments of this section (25 series of experiments) were performed at 40% water cut (methanol was not considered as part of the aqueous phase in calculating water cut).

6.3.2.1. Experimental setup and materials

The experimental set up and the materials used were similar to the previous section (6.3.1.1). The salt used was NaCl (Sigma Aldrich, ≥99%).

6.3.2.2. Experimental procedure

Part 1: Measuring hydrate dissociation point

A dissociation point for the water – oil – natural gas system (40 % water cut) was measured using an isochoric step-heating technique (Tohidi et al., 2000). Once the cell was loaded with the desired components the mixing was started and the temperature was reduced to form hydrates. Hydrate formation was detected by a large pressure drop. The temperature was then increased with steps of 1 °C, slow enough to allow equilibrium to be achieved at each temperature step. At temperatures below the point of complete dissociation of hydrates, gas is released from decomposing hydrates, giving a marked rise in the cell pressure with each temperature step. However, once the cell temperature has passed the final hydrate dissociation point, and all clathrates have disappeared from the system, a further rise in the temperature will result only in a relatively small pressure rise due to thermal expansion of the fluids. This process results in two traces with very different slopes on a pressure versus temperature (P/T) plot, one before and one after the dissociation point. The point where these two traces intersect (i.e. an abrupt change in the slope of the P/T plot) is taken as the dissociation point.

Part 2: Determining the onset point of hydrate formation

In this part of the work, a series of experiments (8 experiments) were carried out to investigate the effect of salt, AAs and varying concentration of methanol on the degree of subcooling require to initiate hydrate formation. In each experiment, the test fluids were loaded into the cell and mixed for 3 hours to achieve equilibrium (at 14 ^{o}C and 1050 psia). The system was then cooled at constant cooling and mixing rates of 0.8 ^{o}C/hr and 500 rpm respectively. The idea was to provide a comparable heat and mass transfer condition for all systems. The cooling bath was programmed to cool each system for 40 hours to make sure enough time (to initially start hydrate formation/growth) is given to each system. Figure 6.18 is an example of temperature and pressure profiles for one of the tested systems.

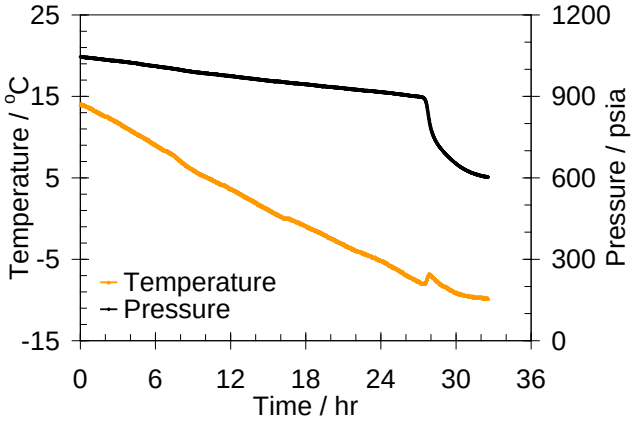

Figure 6.18 Typical temperature and pressure profile of the water-oil-NG-salt-AA (oil soluble)-20 mass% methanol system.

Part 3: Measuring the rate of hydrate formation and growth

The main objective of this part is to assess the effect of salt and different concentrations of methanol on the rate of hydrate formation at the same degree of subcooling (5–5.5 °C). Seven series of experiments were conduced at isobaric conditions (1050 psia). The test procedure is generally similar to that of the rheological tests at subzero conditions (explained in Section 6.3.1.2), but the difference is in the frequency of measuring the amount of pumped water used to displace the piston and inject gas from the piston vessel into the cell to maintain the pressure. In rheological tests, the amount of pumped water was measured at the end of each equilibrium step as shown in Figure 6.13. However, in these tests, the amount of pumped water was measured continuously every few minutes at the onset of hydrate formation until the system reached equilibrium at that step. The amount of pumped water for maintaining the pressure has been used to calculate the amount of injected natural gas to the system and consequently the amount of hydrate formed. Figure 6.19 is an example of consumed natural gas due to hydrate formation at the onset of hydrate formation for one of the tested systems. As can be seen, the system temperature increases as hydrate starts to form due to the exothermic process of hydrate formation. The black base line in this figure shows the gas consumption at the end of each equilibrium step before hydrate formation due to temperature reduction. Figure 6.20 shows the amount of hydrate (mass% of the water present initially in the system converted to hydrate) formed which is calculated using Figure 6.19. Hydrate formation rate has been indicated by means of amount of hydrate formed versus time.

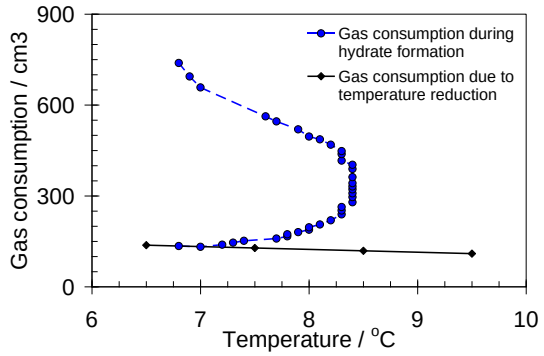

Figure 6.19 Cumulative gas consumption due to the temperature reduction and hydrate formation in the water–oil–natural gas–salt–hydrate system

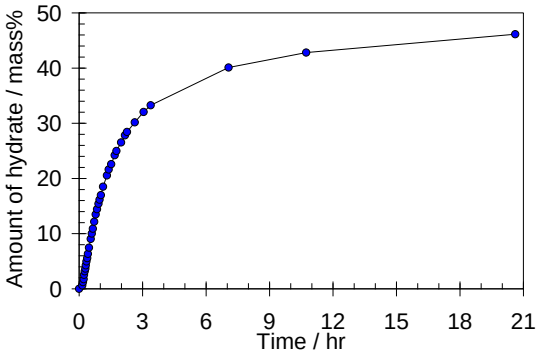

Figure 6.20 Rate of hydrate formation (mass% hydrate versus time) for the water–oil–natural gas–salt–hydrate system

Part 4: Rheological study of hydrate slurries at subzero conditions – Effect of combining thermodynamic inhibitors and AAs in the presence salt

The aim of these tests is to examine the compatibility of methanol, salt and the tested AAs at subzero conditions in terms of viscosity measurements. Again, seven series of experiments were conduced at isobaric conditions (1050 psia).

Following the measurements of hydrate formation rate as described in the previous section, when the system reached equilibrium (following hydrate formation at 5–5.5 ºC), viscosity of the system was measured at different rpms. The temperature of the system was then decreased by steps of 4 ºC. At the end of each step, when the system reached equilibrium (no more water needed to maintain the pressure) the viscosity was measured and the amount of pumped water was recorded. The steps were repeated down to the minimum achievable temperature of the cooling bath or until blockage of the system. The minimum temperature, which was reached in these series of tests, was -31 ºC (lower temperature could be achieved by changing the bath and the coolant). Figure 6.21 shows the cumulative gas consumption for the water – oil – natural gas – salt system. The red points are the equilibrium points at the end of each step and the blue points represent the gas consumptions during hydrate formation at the onset of formation which were measured in the previous part (Part 3) to calculate the rate of hydrate formation.

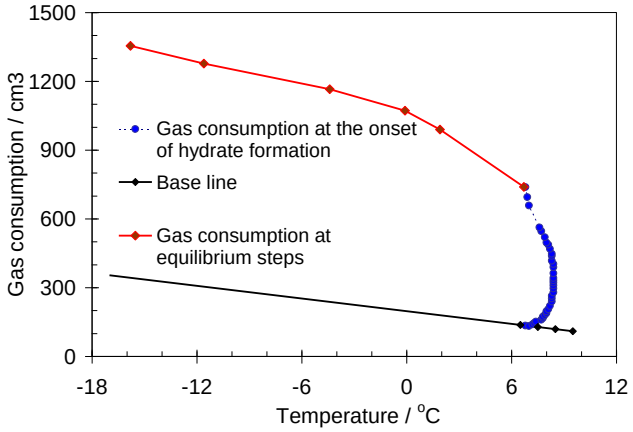

Figure 6.21 Cumulative gas consumption due to the temperature reduction and hydrate formation in the water – oil – NG – salt – hydrate system.

6.3.2.3. Results and discussions

Parts 1 & 2: Hydrate dissociation points and onsets of hydrate formation

Error! Reference source not found. lists the hydrate dissociation and formation (onset of hydrate formation) points for the tested systems at 1050 psia.

Table 6.3 Hydrate dissociation and formation data for the tested systems at 1050 psia

#	System	T_d / ºC	T_f / ºC	Subcooling (T_d-T_f) / ºC
1	Blank (Water – oil – natural gas)	13.4	4.8	8.6
2	salt	11.6	5.1	6.5
3	salt – oil soluble AA	11.6	3.1	8.5
4	salt – oil soluble AA – 5 mass% methanol	9.5	0.1	9.4
5	salt – oil soluble AA – 20 mass% methanol	3.2	-8	11.2
6	20 mass% methanol	5.5	-0.3	5.8
7	salt– 20 mass% methanol	3.2	-2.5	5.7
8	salt – water soluble AA – 20 mass% methanol	3.2	-1.1	4.3

T_d and T_f hydrate dissociation and formation temperatures at 1050 psia respectively

Hydrate formation points for all systems and hydrate dissociation point for the blank test (water – oil – natural gas) system were measured experimentally. Hydrated dissociation points for other systems were predicted using HWHYD software. As can be seen, salt and methanol shifts the dissociation points to lower temperatures. They also reduce the onset of hydrate formation temperature but not necessarily increase the degree of subcooling required for hydrate formation (comparing Test 1 with 2 and Test

1 with 6). According to this table (comparing Test 2 with 3), it might be concluded that the tested oil soluble AA delays hydrate formation while the tested water soluble AA promotes hydrate formation. This could be also confirmed by the increased induction times for the tested oil soluble AA and reduced induction time for the tested water soluble AA during the experiments measuring hydrate formation rates at the same degree of subcoolings.

Part 3: The rate of hydrate formation and growth

Figure 6.22 illustrates the effect of different inhibitors (salt, AAs and varying concentration of methanol) on the rate of hydrate formation and growth at the onset of hydrate formation (5.2 ^{o}C subcooling) at 400 rpm.

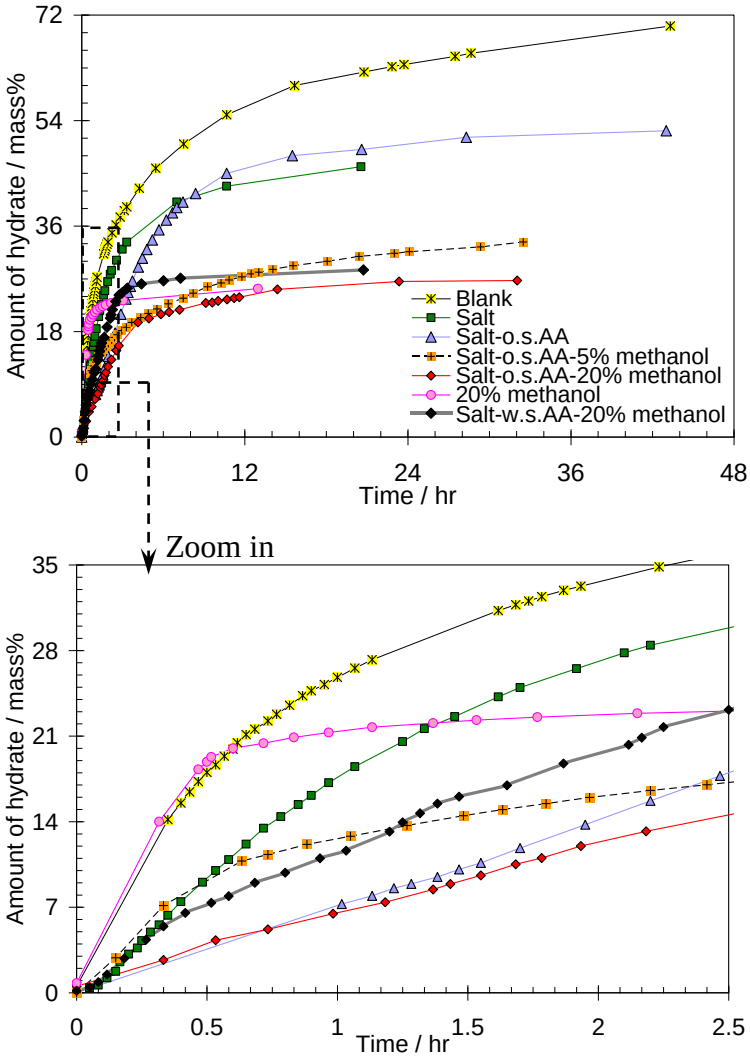

Figure 6.22 Effect of methanol, salt and AAs on the rate of hydrates growth (at 5.2 ºC subcooling and 400 rpm). The blank test is water– oil – natural gas with 40% water cut.

The amount of hydrate represents the mass% of water converted to the hydrate. The blank test is water – oil – NG system with 40% water cut. Water soluble and oil soluble AAs have been abbreviated to w.s.AA and o.s.AA respectively. The results suggest that the presence of salt reduced the rate of hydrate formation significantly (comparing Tests 1 and 2). For example during the first 40 minutes, 21.3 mass% water was converted to hydrate in the water – oil – natural gas system; while it was reduced to 12.5 mass% by adding salt (4 mass% NaCl). The amount of hydrates which can be formed at the same degree of subcooling had also been reduced in the presence of salt. This fact can be seen when the systems approached the equilibrium conditions and when the amount of the hydrate stayed relatively unchanged

The tested oil soluble AA in the presence of salt reduced the amount of hydrate formed within the first 40 minutes from 12.5 mass% for the water – oil – natural gas – salt system to 5 mass% for the water – oil – natural gas – salt – o.s.AA system (Tests 2 and 3). However, the amounts of hydrate formed at the equilibrium state in these two systems were comparable.

Tests 5 and 8 suggest that the rate of hydrate formation and growth in the 20 mass% methanol system with water soluble AA was higher compared to the same system with oil soluble AA. Comparing Tests 3 with 5 and 1 with 6 (Tests without and with 20 mass% methanol) suggests that the presence of methanol did not affect the rate of hydrate formation at the onset of hydrate formation. However, the amount of the hydrate which can be formed at the same degree of subcoolings was lower in the presence of methanol.

The degree of subcooling at which hydrate started to form in the system inhibited with 5 mass% methanol was higher (6.2 ^{o}C) than the other systems. Therefore the driving force for hydrate formation, which has a strong effect on the rate of formation, was not comparable in this system.

Part 4: Rheological studies

Figure 6.23 presents the amount of hydrate at different degrees of subcoolings and temperatures for the tested systems. The very first points after hydrate formation in these graphs (at a subcooling of 5.2 ^{o}C) are the equilibrium points of the Figure 6.22. For example, in the case of water – oil – natural gas system, 71 mass% of the water was converted to hydrate (subcooling of 5.2 ^{o}C). In the presence of salt, about 50

mass% and in the systems inhibited with 5mass% and 20 mass% methanol, about 36 and 25 mass% of the initial water were converted to hydrates, respectively. These means that hydrate concentration and consequently viscosity of the system can be controlled by salinity of the produced water and/or methanol.

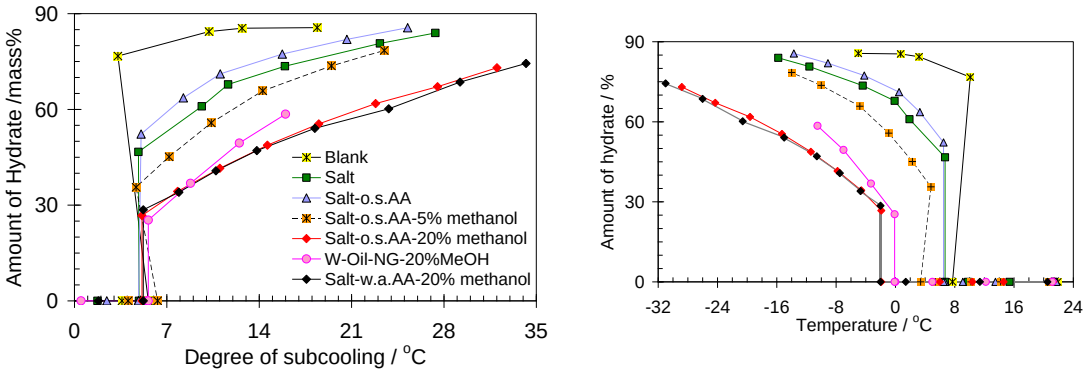

Figure 6.23 Effect of methanol concentration, salt and AAs on the amount of hydrates formed at isobaric conditions and same degree of subcoolings. The blank test is water – oil – natural gas with 40% water cut.

Figure 6.24 shows the effect of salt, AAs (water and oil soluble) and varying concentrations of methanol on the rheological behaviour of the water – oil – natural gas system. These results suggest that the presence of salt reduced the viscosity of the system with or without AAs present. Methanol also reduced the viscosity at the same temperature mainly because of the lower amount of hydrates formed. However, the presence of methanol increased the viscosity of the system at the same concentration of hydrate. This may be attributed to the lower temperature and/or viscosity of the carrier fluid (methanol increase the amount of aqueous phase and hence change the viscosity) and/or the higher rate of formation at the onset of hydrate formation (see Figure 6.22). Hydrates can agglomerate to each other and increase the viscosity of the system when massive quantities of them form suddenly.

It was not possible to measure a representative viscosity for the water – oil – natural gas and water – oil – natural gas – 20 mass% methanol systems at higher concentration of hydrate (represented by the open points). It can be due to the formation of massive bulks of hydrate in the absence of salt and/or anti-agglomerants. An average value of the scattered viscosities has been plotted in this graph.

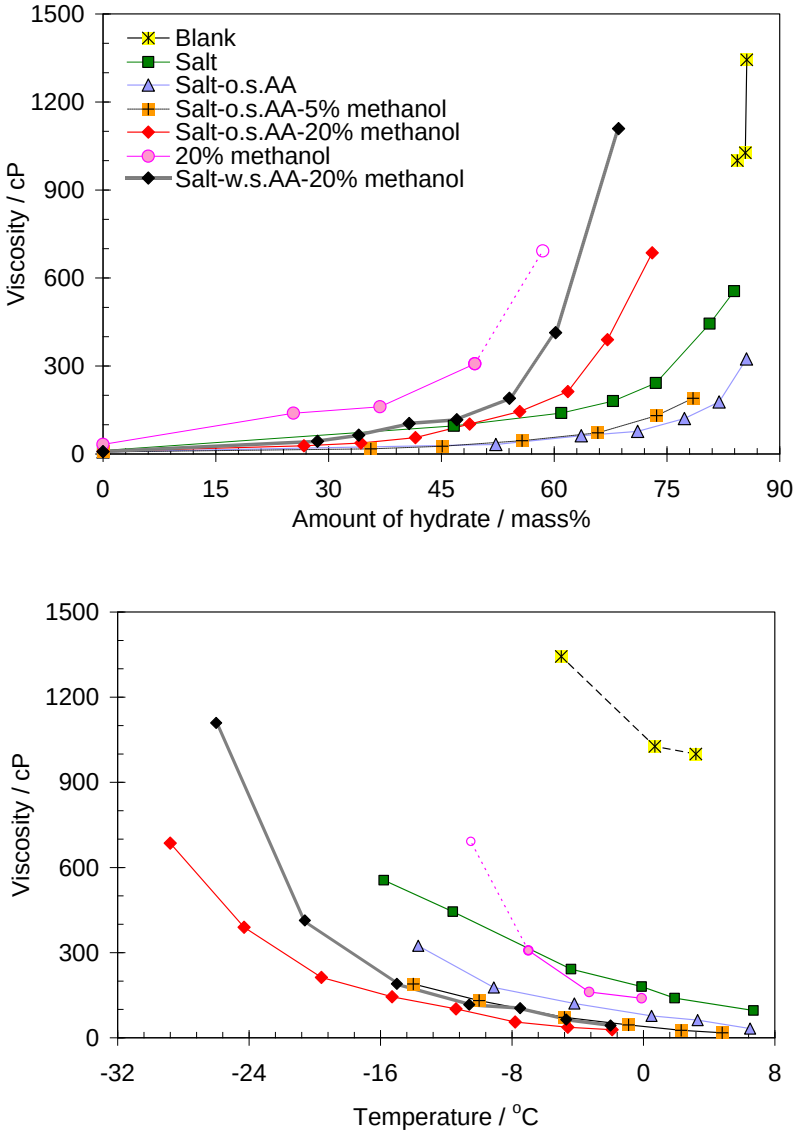

Figure 6.24 Effect of methanol, salt and AAs on the rheological behaviour of the water – oil – NG system as a function of temperature and amount of hydrate. The blank test is water – oil – natural gas with 40% water cut.

Effect of salt on the rheological studies of hydrate slurries at subzero conditions

Figure 6.25 illustrates the effect of salt on the rheological behaviour of the tested hydrate slurries (water – oil – natural gas – hydrate) inhibited with water soluble or oil soluble AAs and varying concentrations of methanol at subzero conditions. The first column shows the amount of hydrates and the second one shows the viscosity of the systems at different temperatures.

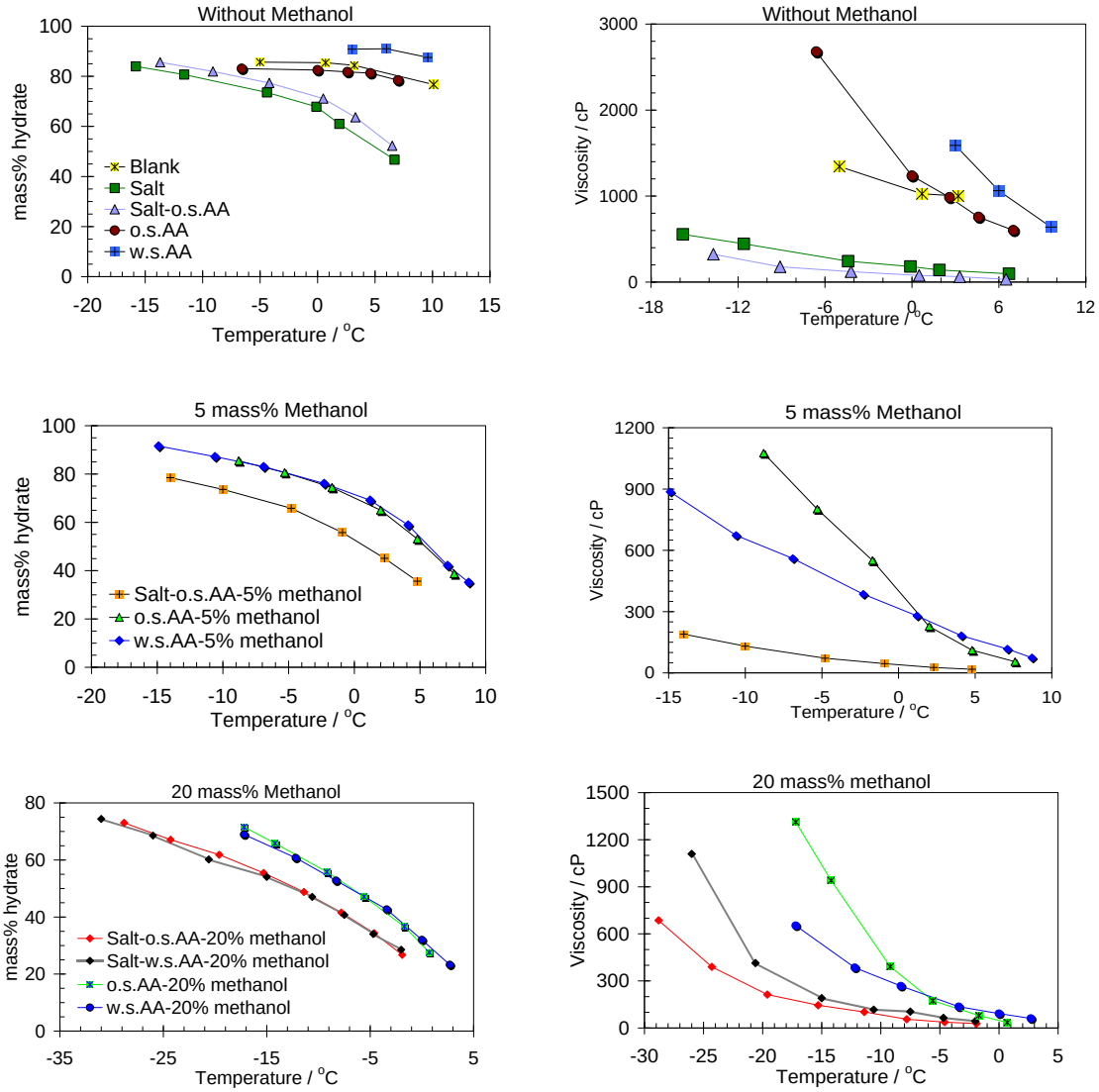

Figure 6.25 Effect of salt on the rheological behaviour of hydrate slurries (water – oil – natural gas – hydrate) in the absence and presence of methanol at subzero conditions. The blank test is water – oil – natural gas with 40% water cut.

As can be seen in the system without methanol, the performance of both AAs is very low or even worth than the blank system (water – oil – natural gas). However, adding salt to the system, improves the performance of the AAs. These results also show that the presence of salt without AA reduces the viscosity significantly. However, the viscosity has the lowest value in the presence of both salt and AA.

In the systems with methanol, the viscosities of the systems with salts are lower than the system without salts which might be attributed to a reduction in the amount of hydrates formed due to the presence of salts.

Figure 6.26 isolates the effect of 5 mass% methanol and 4 mass% salt (NaCl) on the viscosity of the water – oil – natural gas – oil soluble AA system. As can be seen, the amount of hydrate are similar for both systems while the viscosity of the system with 4 mass% salt is significantly lower than that of the system with 5 mass% methanol.

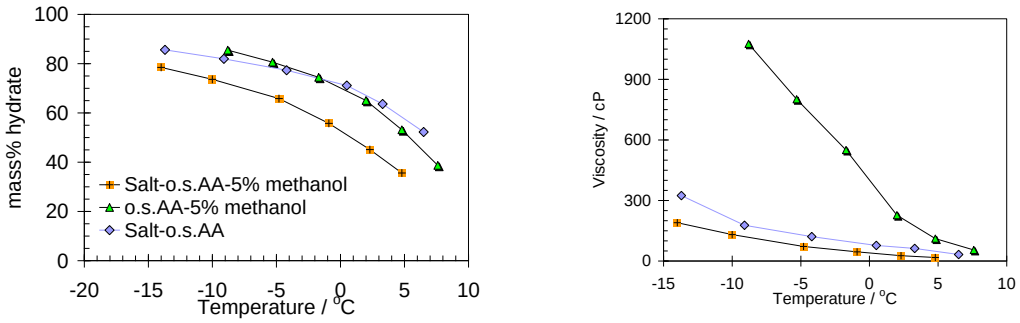

Figure 6.26 Comparing the effect of 5 mass% methanol and 4 mass% salt on the rheological behaviour of water –oil – natural gas – oil soluble AA system.

6.4. Summary

The main objective of this chapter was to demonstrate the *HYDRAFLOW* concept under conditions that other flow assurance solutions either cannot be applied or are not economically viable, e.g. at high watercuts (>50%) or under very high degree of subcoolings where systems may experience subzero conditions. The main conclusions of this chapter are as follow.

The experiments at high watercuts (70 and 90%) confirmed that:

- Presence of the AA reduced the viscosity of the system significantly both with and without hydrate present.
- In untreated systems, the viscosity data did not exhibit a regular pattern. This can be attributed to the non homogeneous nature of the formed hydrate particles. Hydrates might be unevenly distributed in lumps of different shape and size inside the rig.
- Unlike the system without AA, the viscosity for the AA inhibited system had a regular trend which can be because of the formation of hydrate slurry in which hydrate particles are well dispersed in the system.
- At both 70 and 90 % watercuts, the viscosity of the untreated and AA inhibited systems differed by one order of magnitude meaning that this oil

soluble AA is very efficient, even at a water cut of 90%. In other words, the tested AA inhibited systems at high water cuts forms transportable oil/hydrate/water slurries as supported by the viscosity values.

- The rheological behaviour of the tested systems (without and with AA present) at two water cuts (70 and 90 %) showed that the system is less viscous at high water cut. This could be related to high free aqueous phase to hydrate ratio which dilutes the system.
- Visual results were consistent with the viscosity measurements: this AA is clearly performing well at high water cuts. Visual observation at early stages of hydrate formation (0.5% hydrate) showed that the tested oil-soluble AA reduced the size of the hydrate particles significantly. At higher stages of hydrate conversion (20%), no lumps and no agglomeration were observed in the AA inhibited system, only fine slurry particles.
- The tested oil soluble AA shows equal performance during shut-in/restarts as it does in flowing conditions.

Experiments combining methanol and AAs at subzero conditions confirmed that:

- The tested AAs (water-soluble and oil-soluble) were not effective in the presence of ice at subzero temperatures.
- No antagonistic effect was observed between the tested AAs and Methanol.
- By adding only 5 mass% methanol to the tested hydrate slurry systems containing AA, the viscosity of the system at subzero temperatures (-5 to -15 ºC) was reduced significantly near to the viscosity values of the system without methanol at the temperature range of 3–9.6 ºC and at similar hydrate concentrations. This means that combining 5 mass% methanol with the tested AAs improved the transportability of hydrate slurries at subzero conditions.
- The viscosity of the system with 20 mass% methanol was higher than the system with 5 mass% methanol at the same hydrate concentration. This could be attributed to the lower system temperatures for the 20 mass% methanol system at the same hydrate concentrations or to the higher viscosity of the carrier fluid (water/oil/methanol/AA). The amount of

aqueous phase (water + methanol) is higher in the system with 20 mass% methanol compared to the system with 5 mass% methanol.

- According to these results and considering the fact that when hydrates do form, they take up only pure water and that the methanol concentration increases in the remaining aqueous phase suggests that adding 5 mass% methanol should be enough to prevent the negative effect of subzero conditions on the rheology of hydrate slurry systems inhibited with AAs.

Experiments combining methanol and AAs in the presence of salt at subzero conditions confirmed that:

- Rate of hydrate formation and also the amount of hydrate which can be formed at the same degree of subcooling were reduced in the presence of salt.
- The presence of methanol did not affect the rate of hydrate formation at the onset of hydrate formation. However, the amount of hydrates which can be formed at the same degree of subcoolings was lower in the presence of methanol.
- Presence of salt reduced the viscosity of the system with or without AAs present.
- Methanol reduced the viscosity at the same temperature mainly because of the lower amount of hydrates formed. However, the presence of methanol increased the viscosity of the system at the same concentration of hydrate compared to the similar system without methanol. This may be attributed to the lower temperature and/or viscosity of carrier fluid (methanol increase the amount of aqueous phase and hence change the viscosity) and/or the higher rate of formation at the onset of hydrate formation
- Comparing the effect of 5 mass% methanol with 4 mass% salt on the viscosity of the water – oil – natural gas – oil soluble AA system, showed that the viscosity of the system with 4 mass% salt is significantly lower than that of the system with 5 mass% methanol at the same hydrate concentrations.

- AAs can be deployed successfully at subzero condition in the presence of salt in system. In the absence of salt, the transportability of the fluid can be improved by adding few percents (5 mass% of water) of methanol to the system.

The next chapter will present a number of the practical aspects of the *HYDRAFLOW* concept.

6.5. References

Alapati, R., Lee, J. and Beard, D., 2008. Two Field Studies Demonstrate that New AA LDHI Chemistry is Effective at High Water-cuts Without Impacting Oil/Water Quality. *Offshore Technology Conference*, Houston, TX, 2008.

Fotland, P. and Askvik, K. M., 2008. Some Aspects of Hydrate Formation and Wetting. *Journal of Colloid and Interface Science*, **321**, pp.130-141.

Kelland, M. A., 2006. History of the Development of Low Dosage Hydrate Inhibitors. *Energy and Fuels*, **20**, pp.825–847.

Sloan, E.D. Jr. and Koh, C.A., 2008. *Clathrate Hydrates of Natural Gases*, 3rd ed. Boca Raton, London, New York: Chemical Industries, CRC Press.

Sloan, E. D., 2005. A changing Hydrate Paradigm- from Apprehension to Avoidance to Risk Management. *Fluid Phase Equilibr*. 228-229, 67-74

Sloan, E.D., 1998. *Clathrate Hydrates of Natural Gases*, 2nd ed. New York: Marcel Dekker.

Tohidi, B., Burgass, R.W., Danesh, A., Østergaard, K.K. and Todd, A.C., 2000. Improving the Accuracy of Gas Hydrate Dissociation Point |Measurements. *Ann. N.Y. Acad. Sci,*. **912**, pp.924–931.

Chapter 7. Practical Aspects of the HYDRAFLOW Concept

7.1. Introduction

Previous chapters demonstrated the *HYDRAFLOW* concept for different systems at different conditions. The results proved that the concept is viable (at least under laboratory conditions). This chapter will examine a number of added benefits of the concept. The specific objectives are:

- Demonstrating reduced wax deposition problems in the presence of hydrates
- Measuring partitioning of AA between phases (hydrate, water and oil) and examining the efficiency of the distributed AA in each phase for recycling purpose – Application of the *HYDRAFLOW* 'loop' concept
- Testing performance of biodegradable (green) AAs – Application of the *HYDRAFLOW* 'loop' concept

7.2. Reduced wax deposition problems in the presence of hydrates

Wax is composed of high molecular weight, highly saturated hydrocarbons that only contain hydrogen and carbon. Its solubility in crude oil strongly depends on

temperature and is slightly influenced by pressure. The wax appearance temperature WAT can vary widely from crude to crude, ranging from below 10 ºC to higher than 50 ºC. When the crude oil flows into the flow lines, the temperature may fall below the WAT, where solid wax starts to precipitate out of the oil phase. The wax crystals can deposit on the pipeline wall and restrict the production stream. One of the additional benefits of the *HYDRAFLOW* concept is that it could potentially reduce wax deposition problems by: (a) providing solid seeds for wax nucleation in the flowing liquid phase rather than on pipeline walls and (b) abrasion of the deposited waxes by fast moving hydrate particles. The reduction in wax depositions will reduce the need for pigging and/or other cleaning/maintenance methods, hence increasing the pipe longevity while reducing OPEX.

The mechanism of existing seed particles leading to preferential wax deposition on the seeds (hence helping to minimise wall deposition) has been examined by SINTEF/BP. Figure 7.1 illustrates their experimental set up and results.

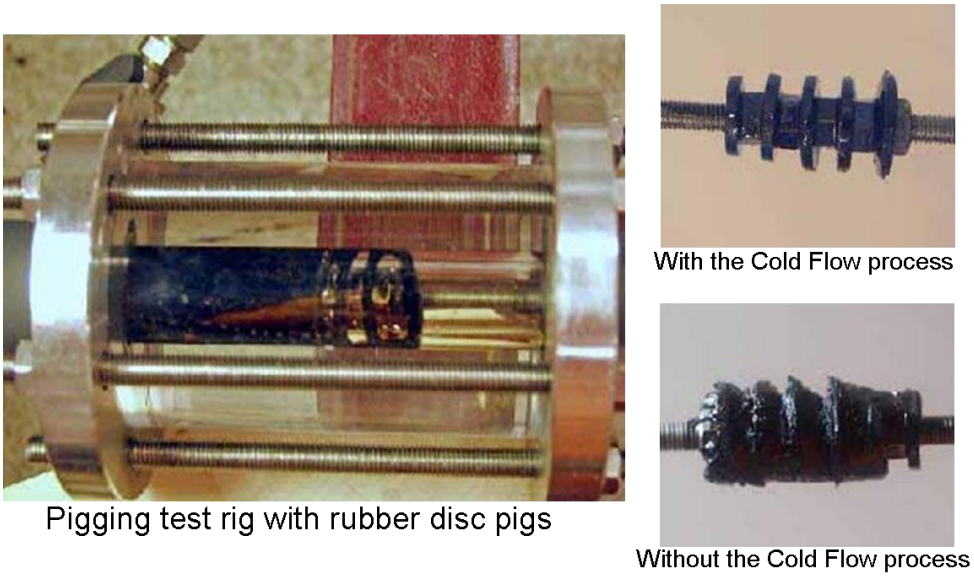

Figure 7.1 Pigging test rig and the pigs after experiments without and with the Cold Flow process. (Sintef/ BP)

The figure compares wax deposits pigged out after an experiment without the Cold Flow process and pigs with no wax deposits after an experiment with the Cold Flow process. SINTEF's Cold Flow concept has been explained in Chapter 2.

This part of the study focuses on examining the mechanism of wearing away of wax deposits from pipeline wall by flow of hydrate particles. Two methods named

"Pipeline wall segment ring" and "Mini tubes impeller" were used to investigate this mechanism.

7.2.1. Pipeline wall segment ring method

The experiments were performed in a purpose built, in-house equipment shown in Figure 7.2. It is originally a 2400 ml high pressure autoclave cell similar to that of the HTI-setup with a U-shape impeller. Ten mild steel inserts are held on the internal walls of the sample chamber between two stainless steel rings. The mild steel segments are cut to give a complete ring as shown in the figure. The test segments are made of mild steel in order to be of the same material as a standard pipeline. Model waxes are put on the surface of the segments before the experiments to simulate wax deposition. A waxy oil from India (with API=37, Wax Dissociation Temperature (WDT) = 69 ºC and pour point = 44 ºC) and a vacuum grease were used as two different model waxes to simulate hard and soft wax deposits, respectively.

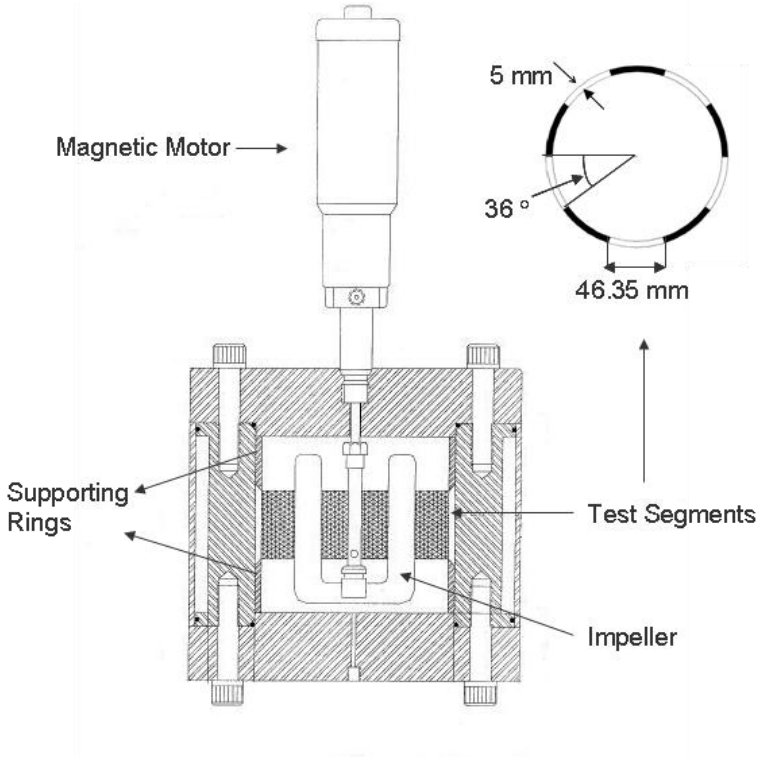

Figure 7.2 Schematic of the experimental setup used for wax deposition tests

Two experiments without (blank test) and with hydrate present were conducted for each wax as follow. At the beginning of each test, wax was put and trimmed on the internal surface of the inserts. Inserts were then weighed and mounted in the test

chamber as a ring between the two supporting stainless steel rings (images termed "before experiments" in the Figure 7.3 and Figure 7.4).

The cell was loaded with 1500 ml deionised water and then cooled down to 4 ºC to simulate seabed temperature. Nitrogen (below the hydrate stability zone of the system) for the blank tests or natural gas for the tests with hydrate was injected into the cell and the mixer was set at 350 rpm. The amount of hydrate formed was controlled by the amount of injected natural gas. In these tests, 20% of the water was converted to hydrate. The system was kept mixing at 350 rpm for 3 days, the system was then depressurised slowly and the inserts and rings were withdrawn carefully. The inserts were weighed again after drying. The weight difference of each insert before and after each test gives the amount of the wax which was removed from that particular insert. The inserts were marked with numbers.

The idea was to compare the amount of wax left on inserts for the systems without and with hydrates present. However, the quantitative comparison was not possible because the inserts rusted during the tests or the outer surface coatings were scratched when they were mounted in or taken out of the cell causing a large error in the results. Therefore, only pictures were taken in each test. Figure 7.3 and Figure 7.4 illustrate the results of the inserts covered with the tested model waxes (grease and waxy oil) before and after experiments without and with hydrates formed.

In the case of the soft wax, in the blank test (without hydrate formed) after experiment the wax was still coating the inserts, although there were some changes to the wax layer: the surface seemed porous which could be due to the gas bubbles penetrating and leaving the wax layer during pressurisation and depressurisation of the system. In the experiment with 20% hydrate, it can be clearly seen from the picture that the soft wax has peeled off from each insert, rolled upwards and now coating the upper supporting ring. This could be because of the upward movement of the hydrate particle flow driven by the vortex created by the stirrer.

Before Experiments

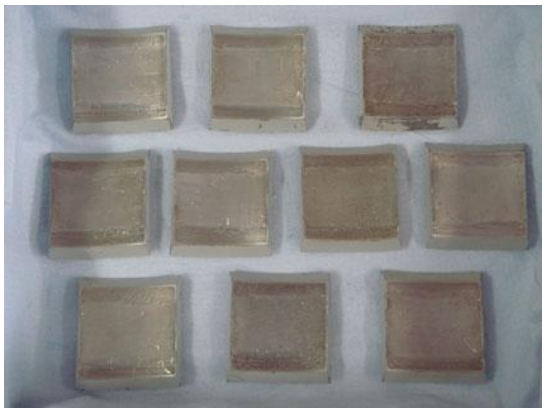
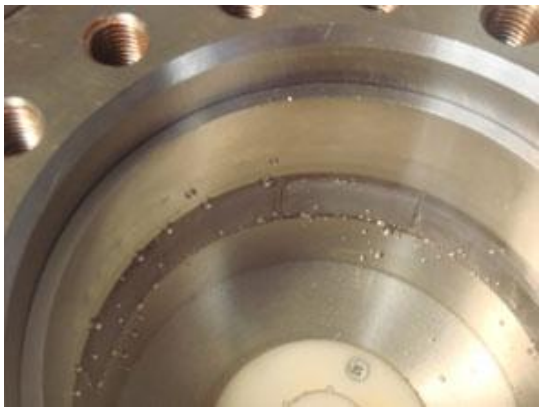

After experiments without hydrate formed (blank test)

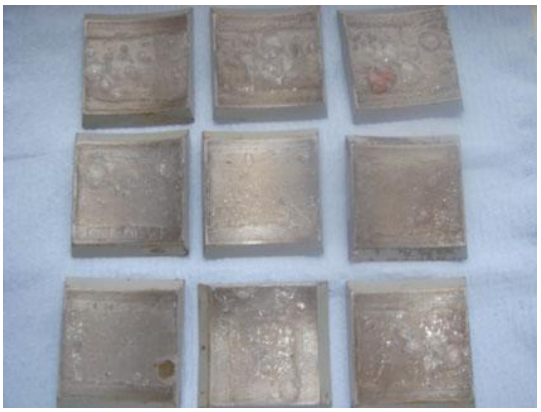


After experiment with 20% hydrate formed


Figure 7.3 Inserts covered with a model wax (grease) before and after experiments

Before Experiments

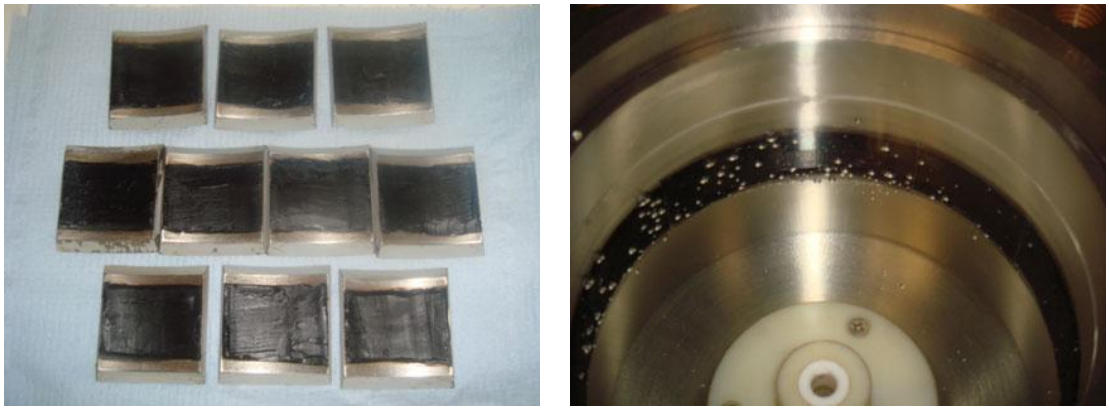

After experiments without hydrate formed (blank test)

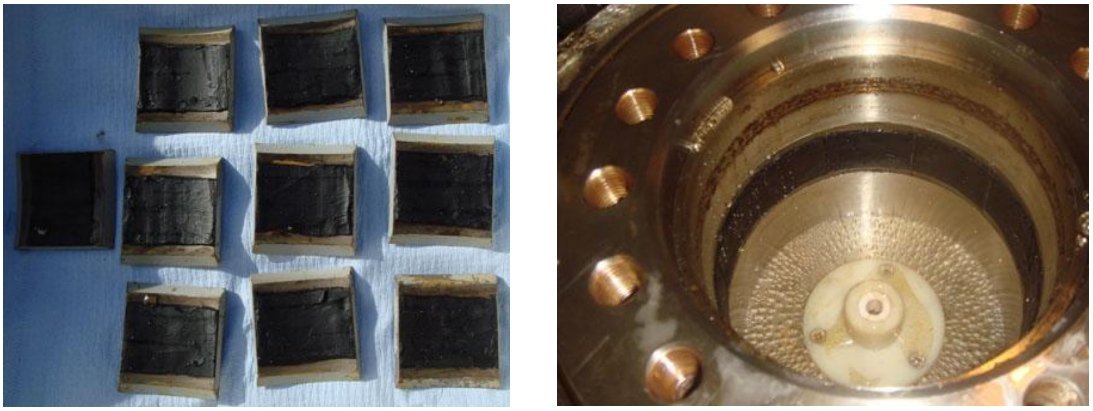

After experiment with 20% hydrate formed

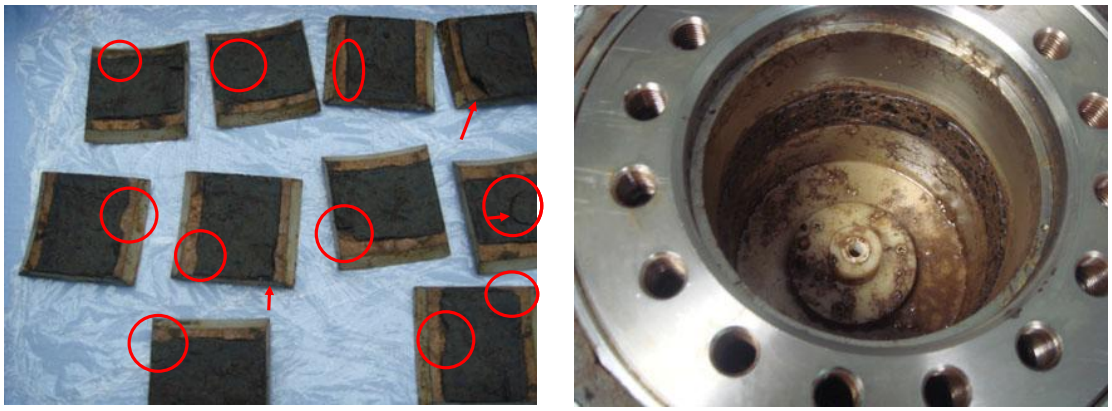

Figure 7.4 Inserts covered with a model wax (waxy oil) before and after experiments

As with the soft wax experiment, after the blank test, the hard wax was still attached to the inserts but unlike the soft wax case there was no visual indication of any change, i.e. porosity. This might be because the hard wax surface was not permeable to the gas. In the experiment with 20% hydrate, the hard wax was partially lifted from the

inserts (as indicated by red arrows in the images). There were also some cracks on the wax surface and some removal of wax on the edges (as indicated by red circles in the images). These effects could be due to the abrasion of wax layers by moving hydrate particles. A thin layer of brown sludge was also observed in the cell after the experiment which could be light components separated from the wax layers (Figure 7.4).

The results show that the presence of hydrates in the system can reduce wax deposition in the system. Therefore, as a next step it was decided to examine the effect of the hydrate concentration on the removal of wax deposition.

7.2.2. Mini tubes impeller

As with the "Pipeline wall segment ring" part, the main goal of these experiments was to investigate whether hydrate particles can remove wax deposits from the pipeline wall. A specific objective was to examine the effect of the hydrate concentration on the removal of wax deposits. Hard wax was selected for this purpose and a new device was designed and built in-house for this series of tests in order to eliminate the effect of vortex on the results. The Integrated rig as described in chapter 4 was modified. A special impeller called "*mini-tubes impeller*" was designed and built to simulate pipeline conditions and flow patterns as close as possible to oil and gas pipelines. It consists of four small tubes (2.5 cm internal diameter and 3 cm length) made of polycarbonate (Figure 7.5). The idea was to simulate pipeline condition by pushing the pipe through a liquid instead of pushing the liquid inside the pipe. The mini-tubes are designed straight and short in length in order to be able to cover the entire internal surface of the tube with waxes.

The experimental procedure is similar to that of the "*Pipeline wall segment ring*" method but the experiments were repeated with different amount of hydrate (12, 25 and 30 mass % of the initial water converted to hydrate). Each experiment was kept running for 7 days.

Before Experiments

After experiments without hydrate formed

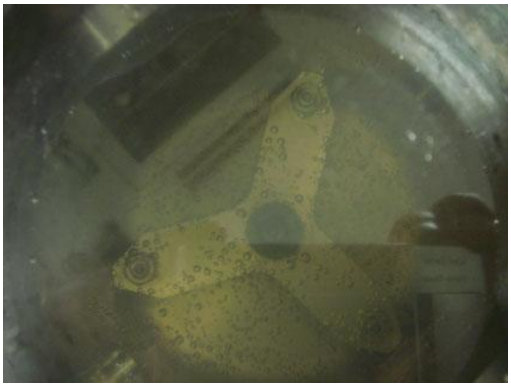

Figure 7.5 Mini tubes impeller and the experimental cell before and after experiments with no hydrate formed.

The experimental cell and the mini tubes impeller covered with wax before experiments and after the blank test without hydrates are shown in Figure 7.5. The results of the experiments with different hydrate concentrations are presented in Figure 7.6.

As can be seen in the images after the blank test and the test with 12% hydrate present, there was not any visual evidence of any change neither to the wax on min-tube surfaces nor in the test fluid. However, in the experiments with higher amount of hydrates (25 and 30%), wax deposits have been scrubbed off from the tube walls and impeller surfaces and some are now floating in the water (indicated by red arrows in the images). This seems to be due to abrasion of wax layers by moving hydrate particles. In the 30% hydrate case, even more wax was removed from the tube edges, exposing the transparent tube wall (pointed by red arrows in the image).

After experiments with 12% hydrate formed

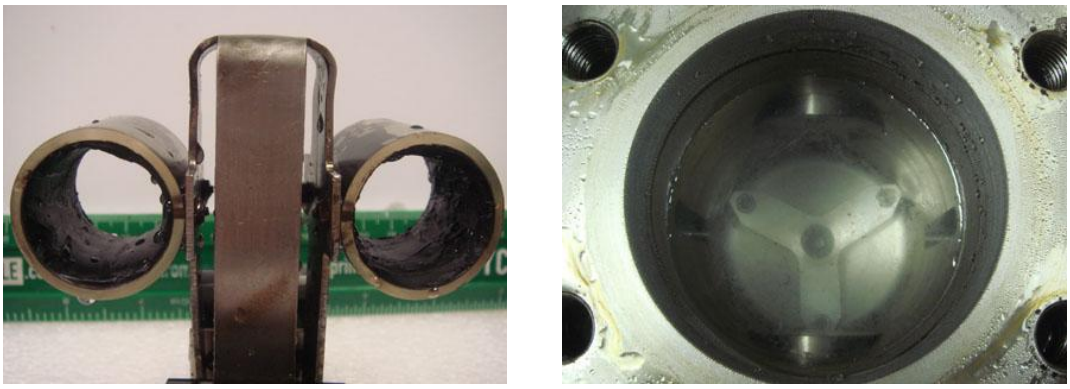

After experiments with 25% hydrate formed

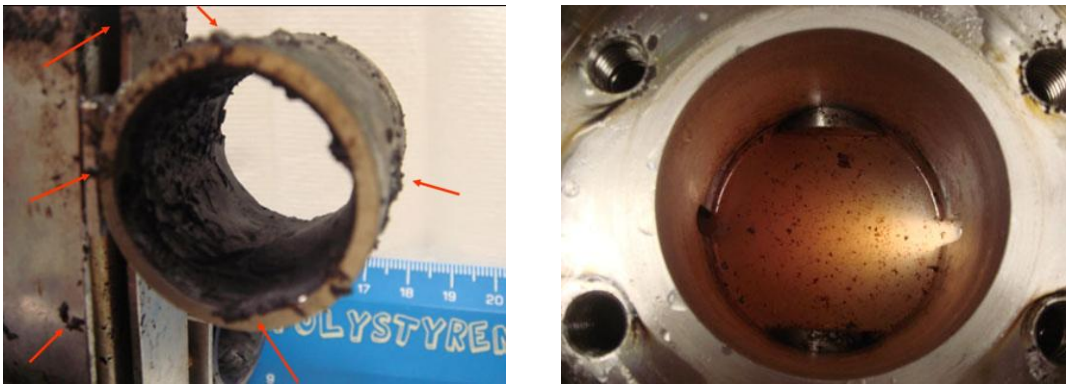

After experiment with 30% hydrate formed

Figure 7.6 Mini tubes impeller and the experimental cell after experiments with varying hydrates concentrations

Few practical issues worth mentioning:

- It is believed that wax depositions are initially soft and saturated with oil, gradual cooling and transfer of heavier compounds to the pipeline wall can result in wax hardening. In the case of heavy and waxy crudes, no serious wax

deposition problem is expected due to high viscosity of the oil. Therefore, conditions tested with soft wax could be more representative of real cases.

- It should be mentioned that in real cases waxes are initiated at higher temperatures than hydrates, therefore in conventional production pipelines there are section of the pipeline that could experience wax deposition without any hydrates to reduce/remove them, unless the *HYDRAFLOW*

The results of these two tests ("*Pipeline wall segment ring*" and "*Mini tubes impeller*") suggest that *HYDRAFLOW* can potentially reduce the wax problems in pipe lines.

7.3. Partitioning and efficiency of AAs – Application of the HYDRAFLOW 'loop' concept

The main objective of this experimental study is to assess the potential for recycling either whole or part of the AA in the context of the "*Loop*" concept. For this purpose, it is necessary to determine the distribution of AA components between different phases (oil, free water and hydrate). It is also important to assess the performance of the residual AA in the free water phase and of its components absorbed in the oil and/or hydrate phase(s). Depending on the results, different scenarios can be applied as follow:

- Separate the phases and recycle the free aqueous phase.
- Separate the phases, dissociate the hydrate phase and recycle the aqueous phase resulting from dissociation of the hydrates.
- Recycle a combination of the above, dissociate the hydrate and separate the oil and water phases and recycle the resulting aqueous phase, which is combination of the free water and the water from hydrate phase.

Additionally, some oil can be circulated in the "Loop" concept e.g. to improve the performance of AA for gas fields or high GOR system (AAs works more effectively in the presence of a liquid hydrocarbon phase). In this case, the amount and performance of AA components potentially transferred to the oil phase is also crucial.

The experimental work presented in this section is divided into 3 parts:

- Part 1 – Separating different phases including oil, free water and hydrate
- Part 2 – Determining AA distribution between different phases

- Part 3 – Examining the performance of the AA left in each separated phase

7.3.1. Experimental setups and materials

The materials used were a blend oil from the North Sea (low waxy oil with a density of 875.3 kg/m^{3,} composition given in Table A.4), an acidic oil from the North Sea (with a density of 900 kg/m^3 and composition given in Table A.3), deionised water, salt (>99% anhydrous NaCl (Aldrich)), a commercial water-soluble AA, natural gas (composition given in Table A.6). All the experiments were conducted with both the blend oil and acidic oil.

All "*phase separation"* experiments were conducted in the high-pressure piston-cylinder rocking cell described in section 4.5.1. All experiments of "*Performance of AA components in different phases*" were conducted in a 300 ml high–pressure autoclave cell similar to the HTI set-up described in Chapter 4. The helical tube impeller (e) from Figure 4.15 was installed in this cell. A high-pressure cylinder fitted with a piston was connected to the experimental cells to maintain the pressure during all experiments. Water was used to displace the piston and inject the gas into the high pressure cell to maintain the pressure inside the experimental rig. Water was injected using a HPLC (High Pressure Liquid Chromatography) pump.

7.3.2. Phase separation experiments

The phases separated in this part were used in the other experiments to determine and examine the distribution and efficiency of AA in different phases.

Several tests with varying concentration of AA (0, 1 and 4 mass% of water) and salt (0 and 4 mass% of water) were conducted in this part. Additionally, some tests with different initial pressure of natural gas were carried out to investigate the effect of amount of hydrate formed on the AA distribution in different phases.

The key point in the phase separation experiments is to avoid hydrate dissociation during phase separation process because it could affect the concentration of AA in the phases. Hydrate could dissociate when one of the phases is taken out from the experimental rig due to a reduction in the system pressure. To maintain the pressure, all the experiments were conducted in a high pressure cell with adjustable volume, which allows keeping constant pressure by reducing the cell volume while taking out the liquid phases.

The samples taken from the separated phases after hydrate formation are named free water, hydrate water and separated oil. Free water is the separated free water phase that was not bonded in the hydrate structure. Hydrate water is the water resulting from dissociation of the separated hydrate phase.

Test procedures: All tests were conducted in a rocking cell, which has a volume of 300 ml. The cell was filled with 210 ml of liquid (deionised water, oil (40% water cut), commercial AA (0, 1 or 4 mass% of the water depending on the specific experiment) and/or salt (0 or 4 mass% of the water)) in each test. Vacuum was applied to the cell, prior to the introduction of the natural gas to achieve the required pressure at 22 ^{o}C. The required pressure is defined as the pressure needed to convert the desired amount of the initial water into hydrates (desired conversion) depending on each test. The system was then kept at this condition for enough time (2 hrs) to achieve equilibrium and also to ensure there is no leakage in the system. The temperature was set to 4 ^{o}C and hydrates were formed during cooling. The cell was left rocking (to give a good mixing and speed up hydrate formation) while monitoring the pressure drop to ensure adequate hydrate formation. When the system reached equilibrium, the rocking was stopped and the cell was kept vertical with the inlet/outlet valve at the bottom.

In the case of the blend oil, which does not form stable emulsion and separates in couple of hours, the cell was left overnight to allow the separation of the phases (oil, hydrate and free water) due to density difference. Afterwards, liquids were taken out very slowly through a small valve at the bottom of the cell. In order to avoid hydrate dissociation during the liquid withdrawal, the cell pressure was maintained by reducing the cell volume by pumping water to the piston side of the cell to displace the piston.

The free water phase being the most dense phase is at the lowest part of the cell and comes out first. The second dense phase is hydrate, however could not pass through the very narrow space between the mixing shuttle and end of the cell and stays in. Therefore, the oil bypasses the hydrate phase and comes out next. After taking out the free water and oil phases, the pump was disconnected from the cell and the system containing mainly hydrate phase was heated up and hydrates were dissociated. At the end, the water resulting from the melted hydrate phase (hydrate water) was taken out from the cell.

In the tests with the acidic oil, which formed a stable emulsion in the presence of hydrate, the system was kept still for three days before taking out the liquids from the cell. However, the emulsion was stable even after this time and water did not drop out to give a separate layer. From the sample withdrawn from the bottom of the cell, it also appeared that there were two layers of hydrate/water/oil emulsion in the cell: hydrates were mainly in the upper layer while the water was mainly in the lower layer. The first layer came out as a slug of W/O emulsion whereas solid dissociating in the W/O emulsion were observed in the upper layer fluid. The upper part was also colder while leaving the cell. The two fluid samples were collected separately and the fluid in the vicinity of the interface of the two layers was discarded and not used to reduce the experimental error. The 2 samples (emulsions) separated overnight and the water released from the emulsion at top and bottom parts of the cell were considered as hydrate water and free water, respectively.

Results: Table 7.1 summarises samples obtained during these experiments. Each experiment was conducted 3–6 times in order to obtain enough samples for the further experiments.

The concentration of AA and/or salt (NaCl) was measured in Samples 1–15 except Samples 8 and 11 using analytical methods. It was not possible to analysis the oil samples with the methods used. However, the concentration of salt and AA absorbed to the oil phases can be calculated from mass balance. These concentrations have been also estimated from a qualitative method used for examining the performance of AA components remained in each phase. Samples 6–11 were used for examining the performance of AA.

Table 7.1 Samples obtained from phase separations after hydrate formation

Test ID	Oil phase	$C_{AA,i}$ / mass%	Hydrate %	$C_{S,i}$ / mass%	Phase	Sample ID
					Free water	—
1	Blend oil	4	100	4	Hydrate water	1
					Oil	—
					Free water	2
2	Blend oil	4	60	4	Hydrate water	3
					Oil	—
					Free water	4
3	Blend oil	1	75	4	Hydrate water	5
					Oil	—
					Free water	6
4	Blend oil	1	50	4	Hydrate water	7
					Oil	8
					Free water	9
5	Acidic oil	1	50	4	Hydrate water	10
					Oil	11
					Free water	12
6	Blend oil	0	40	4	Hydrate water	13
					Oil	—
					Free water	14
7	Blend oil	1	50	0	Hydrate water	15
					Oil	—

$C_{AA,i}$: Initial AA concentration in water before hydrate formation / mass% of water
$C_{S,i}$: Initial salt (NaCl) concentration in water before hydrate formation / mass% of water
Hydrate %: percentage of the initial water in the system converted to hydrate

7.3.3. AA distribution between different phases

AAs are multi–component commercial chemicals, of unknown composition due to confidentiality. It is therefore difficult to quantify the concentration of AA. Initial tests carried out in this laboratory, like conductivity or vaporisation measurements were not successful in measuring the AA distribution.

The concentrations of AA in Samples 1–7 from Table 7.1 were measured by the AA supplier using the QPI 086 methodology, "*Determination of amine and quaternary amine corrosion inhibitors in aqueous solution*". This technique is based on extraction using a bromophenol blue/bromocresol green indicator solution and absorbance

measurements using a UV/VIS spectrophotometer at a specific wavelength. This methodology has been explained in Appendix B. However, a brief description is as follow. A calibration curve was created using a series of calibration standards between 0.0004 and 0.004 mass% (4-40 ppm). The samples were then extracted in the same way as the calibration standards. The absorbances of these samples were blank corrected and the corresponding AA concentrations were obtained using the calibration curve. The samples with an initial AA concentration of 1 mass% were given a 250x pre-extraction dilution and those with a 4 mass% initial AA concentration a 1000x. This ensured that the results were likely to be within the calibration range.

Table 7.2 summarises the results of the AA concentration measurements using the UV/VIS spectrophotometer.

Table 7.2 Concentration of AA distributed in different phases following hydrate formation measured using a UV/VIS spectrophotometer method

Sample ID	$C_{AA,S}$ / mass%
1	3.13
2	4.49
3	3.56
4	1.05
5	0.72
6	1.12
7	0.62

According to these results, the concentration of AA in Sample 1, hydrate water (full conversion with an initial 4 mass% AA and 4 mass% salt) is 3.13 mass%. It suggests that some of the AA components were partially absorbed to the oil. Samples 2 and 3 are representative of the free water and of the hydrate phases respectively when approximately 60% of the initial water (with 4 mass% AA and 4 mass% salt) was converted to hydrate. The results show that the concentration of the AA components remained in the free water is greater than the concentration of the components absorbed in the hydrate phase. The colours of these samples in Figure 7.7 also support this result.

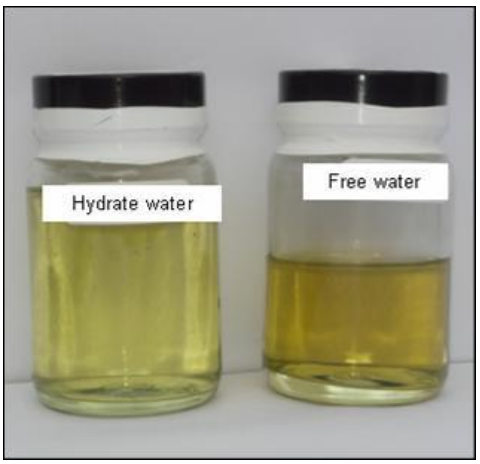

Figure 7.7 Free water and Hydrate water samples separated after hydrate formation process (Samples 2 and 3 from Table 7.1). Hydrate water is the water resulting from dissociation of the separated hydrate phase

The same behaviour can be seen in Samples 4-7 confirming that the AA concentration in the free water phase is higher than in the hydrate phase.

The weak point of this method is that it can measure the concentration of only one unknown analyte (AA or salt in this case) at a time. Therefore, it had been assumed that all the salt remained in the free water phase and that the concentration of salt in the hydrate water and oil was considered zero in these samples. The reason for this assumption is the fact that when hydrates do form, they take up only pure water and the salt concentration increases in the remaining aqueous phase. This assumption can be correct if the accuracy of the separation process is reasonable. To back up this assumption, Test 6 from Table 7.1 (with 4 mass% NaCl and without AA) was carried out and the resulting phases were separated in the same way as previous experiments. The salt concentration in these separated phases (Samples 12 and 13) were measured by evaporating the water. A three digit scale was used to weigh the solution and salt residue. Table 7.3 presents the results.

Table 7.3 Salt concentration in the free water and hydrate phases following hydrate formation and phase separation measured by evaporation

Separated phase	Sample ID	Salt (NaCl) concentration / mass%
Free water	12	6.45
Hydrate	13	1.19

As can be seen in this table, the salt concentration in hydrate water was not null. Considering the fact that hydrates exclude salts from the clathrate structure, these results suggest that the hydrate water is a combination of water released through hydrate melting and free water (brine) trapped amongst the hydrate particles. It was not possible to completely remove water from solid hydrates due to the level of the difficulty in separation and also the hydrophilic nature of hydrates. Even though the amount of the free water trapped in the hydrate matrix is small, it can still have a significant influence on the results. For example in this experiment, about 40% of the initial water (80.16 g) was converted to hydrate and therefore from a mass balance calculation, the salt concentration in the remaining free water and the water released from hydrate was expected to be about 6.48 and 0 mass% respectively if the phase separation was ideal. However, if about 7.2 g of the free water (with salt concentration of 6.48 mass%) remains in hydrate phase due to the difficulty in getting a complete separation, it will result in salt concentration of 1.19 mass% for hydrate water.

This experiment showed that the AA distribution results obtained using the UV/VIS spectrophotometer method may not be totally sound. Therefore, the concentrations of AA in Samples 9, 10, 14 and 15 from Table 7.1 were measured using a C–V (Conductivity–Velocity) device which is an industrial device patented by the Centre for Gas Hydrate Research at Heriot-Watt University (Tohidi et al., 2010).

The integrated C–V is a method for analysing an aqueous fluid containing one or more analytes with unknown concentrations. It is based on the measurements of the electrical conductivity and the sound velocity of the aqueous fluid under examination. The electrical conductivity of aqueous fluids depends on the concentration and activity of ions in the fluids. The ion concentration is proportional to the salt concentration, and its ion activity is strongly related to temperature, and impurity like non–electrolyte chemical additives. Therefore, electrical conductivity can be used as a parameter directly reflecting the concentrations of salts and hydrate inhibitors. Sound velocity in fluids is directly related to the fluid density, and the fluid density depends on the concentrations of salts and chemical additives. In the C–V device, sound velocity is measured and used along with the measured conductivity for determining both inhibitor and salt concentrations in pipeline aqueous fluids simultaneously. The device needs to be calibrated for each specific inhibitor at the desired range of salt and inhibitor concentrations.

Table 7.4 summarises the distribution of AA and salt between hydrate and aqueous phases measured by the C-V device.

Table 7.4 AA and Salt distribution in the free water and hydrate phases following hydrate formation and phase separation measured by the C-V device

Separated phase	Sample ID	AA concentration / mass%	Salt (NaCl) concentration / mass%
Free water	9	1.2	3.8
Hydrate	10	1.1	3.7
Free water	14	1.4	—
Hydrate	15	0.9	—

Samples 9 and 10 are the separated fluids following hydrate formation in the acidic oil/water/AA (initially 1 mass%)/salt (initially 4 mass%)/natural gas system. As it was mentioned before, this oil formed stable emulsion during the test with hydrate present and it is thought that water droplets and hydrate particles were almost evenly distributed in the emulsion. It was therefore expected to observe similar salt and AA concentrations for both free water and hydrate water because of the level of the difficulty in the separation.

Samples 14 and 15 were obtained from the Blend oil/water/AA (initially 1 mass%)/natural gas system. In this experiment about 50% of the initial water was converted to hydrate. As it was mentioned before, due to the difficulty in getting a complete separation of the free water, it was not possible to obtain an accurate mass balance. However, it is realistic to conclude that the AA concentration in the remaining free water is about 1.4 mass% and therefore a value of about 0.57 mass% is expected for the AA concentration in the hydrate phase assuming a perfect separation. It means that about 71% of the initial AA had remained in the free water and about 29% had bonded in the hydrate structure. However, the measured AA concentration in the hydrate water was about 0.9 mass% because it included some free water (with an AA concentration of about 1.4 mass%) which had been trapped in the hydrate structure. It has been assumed that the tested AA was not partitioning to the oil phase. This assumption will be demonstrated in the following section.

7.3.4. Performance of AA components in different phases

In this section the performance of AA components in the separated phases after hydrate formation was examined. The tests consist of measuring the power applied to the impeller to keep it rotating at 500 rpm using a 300 ml HTI–setup. The measured power is an indicator of the viscosity of the system. The higher is the required applied power to keep a constant rpm, the more viscous the system is. AAs work by affecting the rheological properties of hydrate slurries and reducing the viscosity of the system. Therefore, in a system containing a high performing AA, the viscosity of the system and the required applied power should be low. In order to quantitatively compare the results, three calibration tests with 3 concentrations of AA (0, 1 and 2 mass% of water) were carried out. Oil and water phases in these experiments depending on the specific test are summarised in Table 7.5.

Table 7.5 Materials used in each test for examining performance of AA

Test ID	Aqueous phase	Oil phase	C_{AA}/mass%	C_S/mass%
1	Deionised Water	Blend oil	0	4
2	Deionised Water	Blend oil	1	4
3	Deionised Water	Blend oil	2	4
4	Deionised Water	Separated oil (sample 8 from Table 7.1)	—	4
5	Free Water (sample 6 from Table 7.1)	Blend oil	—	—
6	Hydrate Water (sample 7 from Table 7.1)	Blend oil	—	—
7	Deionised Water	Acidic oil	0	4
8	Deionised Water	Acidic oil	1	4
9	Deionised Water	Acidic oil	2	4
10	Deionised Water	Separated oil (sample 11 from Table 7.1)	—	4
11	Free Water (sample 9 from Table 7.1)	Acidic oil	—	—
12	Hydrate Water (sample 10 from Table 7.1)	Acidic oil	—	—

C_{AA}: AA concentration / mass% of water
C_S: Salt (NaCl) concentration / mass% of water
—: The same quantity of AA and/or salt that existed in the samples obtained in the phase separation part.

Tests 1, 2, 3, 7, 8 and 9 are calibration experiments for systems containing the blend oil and the acidic oil. The oil phase in Tests 4 and 10 are the separated oil phase after hydrate formation (Samples 8 and 11 from Table 7.1) which represents the performance and concentration of the AA components absorbed in the oil phase. In the same way, the aqueous phases in Tests 5, 6, 10 and 11 are Samples 6, 7, 9 and 10 of Table 7.1 and represent the properties of AA component in the free water and hydrate phase, respectively.

Test procedure: All tests were carried out at constant pressure. In each test, 70 vol.% of the cell was pre-loaded with liquid phase according to Table 7.5 (40% water cut) and the headspace was left for gas. Then, natural gas was charged into the cell (and the high-pressure piston vessel) to achieve the required pressure (1500 psia). The high-pressure piston cylinder was then connected to the rig to maintain the pressure during the test. The system was kept at this condition (1500 psia & 22 ^{o}C) for 2 hours to make sure there was no leakage in the system. The system was cooled down to 2 ^{o}C with a stirring rate of 500 rpm. The voltage and current (power) applied to the stirrer were recorded to investigate the rheological behaviour of the system in each test. Figure 7.8 illustrates the amount of hydrate, current and temperature for one of the tests carried out (calibration test with 2 mass% AA and blend oil).

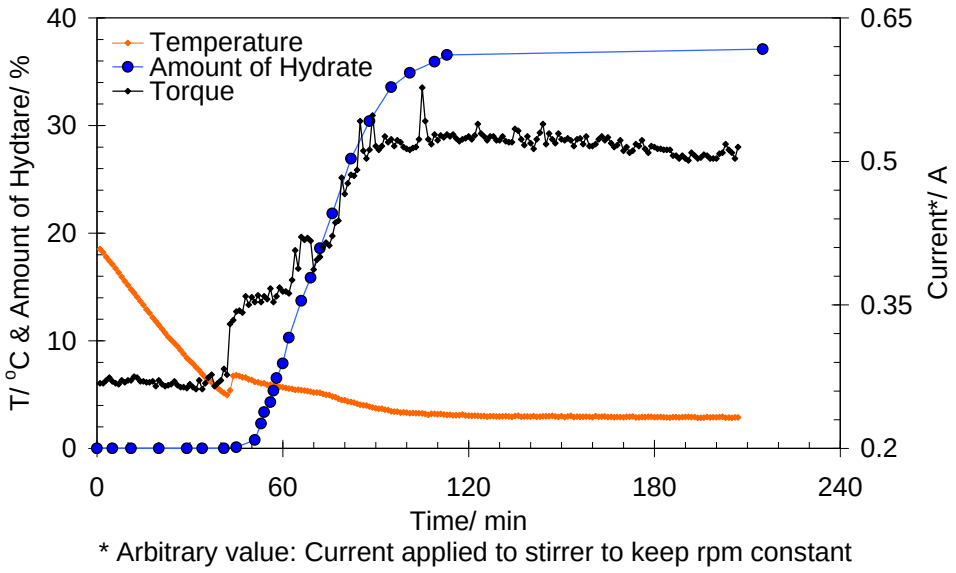

Figure 7.8 Behaviour of 2 mass% AA – deionised water – salt – Blend oil – hydrate – natural gas system (Test 3 from Table 7.5)

The behaviours are similar for all other tested systems. As can be seen, the power required to keep rpm constant increases with hydrate concentration and consequently the slurry viscosity increases in the system. This behaviour is more pronounced at the onset of hydrate formation. Temperature increases once hydrate starts to form because hydrate formation is an exothermic process.

During the test, water was used to displace the piston in the piston vessel and inject the gas into the rig to maintain pressure. The volume of pumped water was recorded at appropriate time intervals. It is therefore possible to calculate the amount of gas consumed due to the temperature reduction (gas solubility in the liquid and the density changes) and hydrate formation. Figure 7.9 represents a typical example of the cumulative gas consumption during one of the tests.

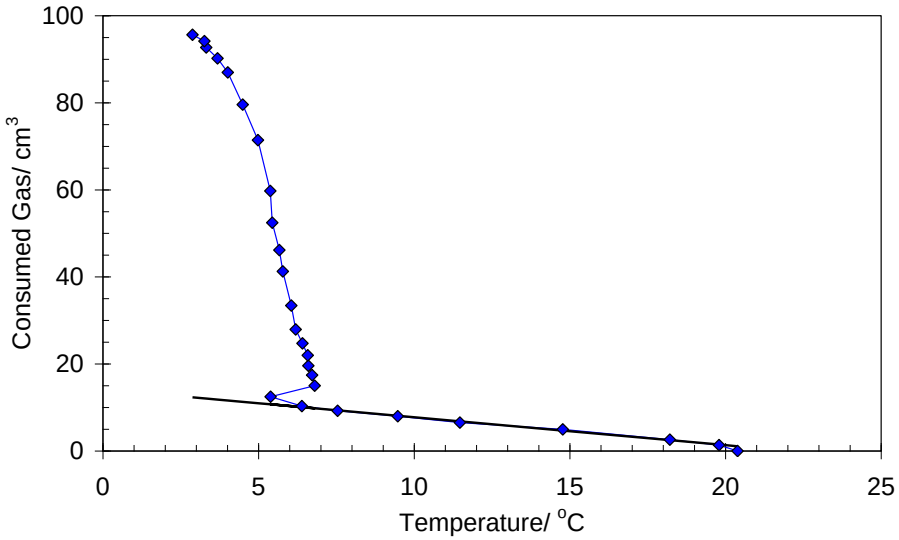

Figure 7.9 Cumulative gas consumption due to the temperature reduction and hydrate formation in "hydrate water"–Blend oil–hydrate–natural gas system (Test 6 from Table 7.5)

Results: Figure 7.10 shows the rheological behaviour of the systems listed in Table 7.5 as a function of the amount of hydrate in the system. The initial torque values at 0% hydrate are subtracted from the torque values to make them more comparable. The grey colour curves are rheological behaviour of the calibration test systems with varying concentration of AA (Tests 1, 2, 3, 7, 8 and 9 from Table 7.5).

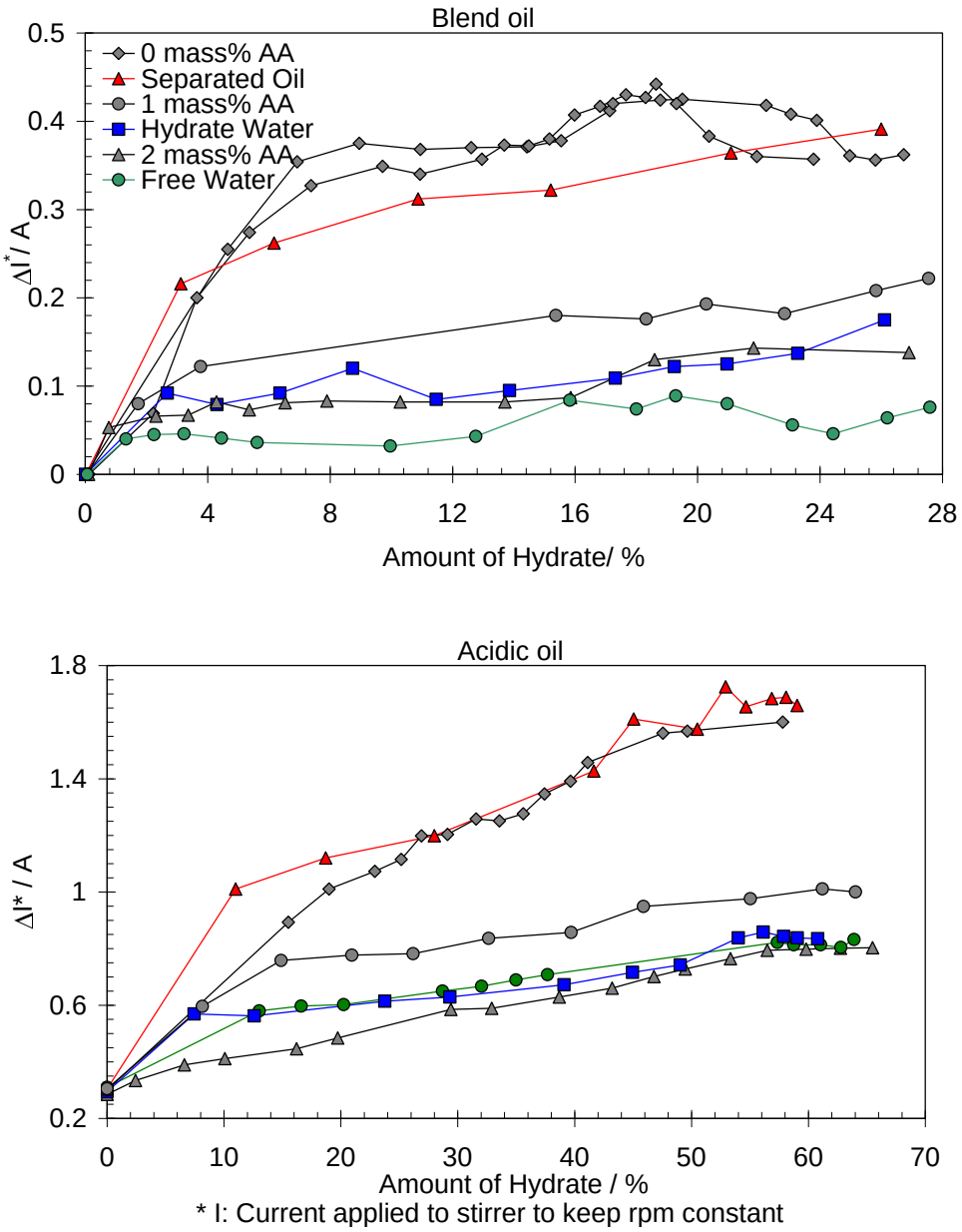

Figure 7.10 Performance of AA components separated/extracted from different phases (hydrate – water – oil) on a multiphase fluid system

The curves named "Separated Oil" (Tests 4 and 10 from Table 7.5) are representatives of concentration and performance of AA components absorbed in the oil phases. Their behaviour is similar to the calibration curves without AA; suggesting that the amount effective AA components entering oil phase is negligible. The curves named "Hydrate Water" are the results of the Tests 6 and 12 from Table 7.5 in which the aqueous phases were the hydrate water samples obtained from the previous phase separation tests. No extra salt and AA were added to these systems and therefore, they represent the behaviours of the AA components that were absorbed in the hydrate phases (or

adsorbed on the hydrate crystals) in the previous tests. And finally, "Free Water" curves represent the systems in which the aqueous phase was obtained from the free water samples collected from the phase separation tests. The anti-agglomeration effects of these systems are due to AAs remaining in the free water phase.

In the systems with the blend oil, as can be seen, the concentration of the residual AA in the free water phase is higher than the concentration of the tested AA components trapped in the hydrate phase. This can be due to higher concentration of AA components in these phases. In the case of the Acidic oil, the AA and salt concentration of the "Free Water" and "Hydrate Water" were also measured using the C-V device (Samples 9, 10 from Table 7.4). The results of the tests are in a good agreement.

7.4. Biodegradable (green) AAs – Application of the HYDRAFLOW 'loop' concept

As it has been described in Section 2.5.2, there is a major concern regarding the environmental impact of AAs which has limited their application. To a degree, this limitation can be addressed by exploring greener version of AAs. However, the cost of bio-surfactants is not comparable with chemical surfactants at the moment and also higher dosage of them is required compared to chemical AAs. This seems to be a major drawback for using bio-degradable AAs. In the *HYDRAFLOW* 'loop' concept, due to partial closed looped nature of the proposed system and the chemical separation, it should be possible to use low strength bio-degradable chemicals at high concentrations to improve their performance.

The objective of this part of the study is to test the performance of an organic compound from quaternary ammonium salt group as a potential green AA. The experiments consist of measuring viscosity of water – oil –natural gas–hydrate system without and with the potential organic AA. An additional experiment was carried out with the system inhibited with a commercial chemical AA for comparison.

Experimental materials, setup and procedure

The materials used were a North Sea crude oil (composition is given in Table A.2), a standard natural gas supplied by air products (composition is given in Table A.6), deionised water, water-soluble commercial AAs (1 mass% of water) and an organic compound from quaternary ammonium salt group (3 mass% of water). The experiments were conducted in the high pressure HTI-set up described in Chapter 4

and the test procedure was step-wise gas injection (explained in Section 5.3.1) and the water cut was 30%.

Results: Figure 7.11 presents the viscosities of the water – oil –natural gas – hydrate systems inhibited with a bio degradable potential AA and a commercial chemical.

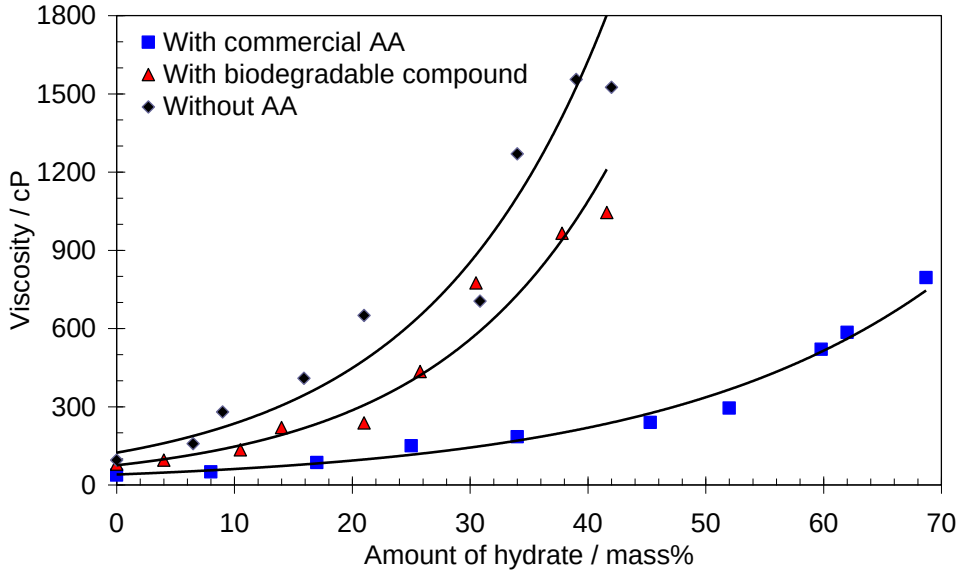

Figure 7.11 Rheological behaviour of the water–oil–natural gas–hydrate system without and with the commercial AA and tested biodegradable compound

As can be seen in this figure, the commercial AA reduced the system viscosity significantly. The tested biodegradable compound also improved the rheology of hydrate slurries comparing to the untreated system (blank test without AA). Especially, its effect is more pronounced at lower hydrate conversions. It should be mentioned that the performance of the tested biodegradable AA can be improved by using some synergic materials which are common to commercial AAs.

7.5. Summary

A number of practical aspects of the *HYDRAFLOW* concept were investigated in this chapter. The conclusions of this chapter are as follow.

The results of two methods used for wax experiments ("*Pipeline wall segment ring*" and "*Mini tubes impeller*") confirmed that:

- Hydrate flow can reduce the wax problems in pipelines. This can be mainly attributed to the abrasion of wax deposits by fast moving hydrate particles.

This effect gets more pronounced as hydrate concentration increases or the hardness of wax deposits decreases.

The experiments carried out for determining the performance and distribution of the tested AA components between oil, hydrate and free water, suggested that:

- The tested AA components absorbed in the oil phases were negligible.
- Hydrate phase incorporated some components of the tested AAs.
- The concentration of the residual AA in the free water phase was higher than the concentration of the tested AA components dissolved/trapped in the hydrate phase.
- Both AA components remained in the free water and those trapped in the hydrate phase showed higher performance compared to the fresh AA. This could be due to higher concentration of AA components in these phases.
- It was not possible to obtain very accurate mass balance for the AA components distributed between oil, hydrate and free water because of the difficulty in getting a complete separation of free water.
- In the case of the acidic oil, a stable emulsion was formed during the test with hydrate present and it is thought that water droplets and hydrate particles were almost evenly distributed in the emulsion. As a result, a similar salt and AA concentration for both free and hydrate water were measured due to the difficulty in separation.

The results of the tests investigating the performance of an organic compound from quaternary ammonium salt group as a potential green AA showed that:

- The tested biodegradable compound improved the rheology of hydrate slurries comparing to the untreated system (blank test without AA). Especially, its effect is more pronounced at lower hydrate conversions. However, it was not as effective as the tested commercial chemical AA. It should be mentioned that the performance of the biodegradable AA can be improved by using some synergic materials which are common for commercial AAs.

7.6. References

Tohidi, B., Yang, J. and Chapoy, A., 2010. Hydrate Monitoring System with Measurement of Sound Velocity and Electrical Conductivity. Pat. WO/2010/004289

Kelland, M. A., Svartaas, T. M. and Dybvik, L. A., 1996. 2nd International Conference on Gas Hydrates. Toulouse , 7-9 June 1996.

Kelland, M. A., Svartaas, T. M. and Dybvik, L. A., 1995a. Studies on New Gas Hydrate Inhibitors. SPE Annual Technical Conference. Dallas, 22-25 October 1995.

Kelland, M. A., Svartaas, T. M. and Dybvik, L., A., 1995b. A New Generation of Hydrate Inhibitors. SPE Annual Technical Conference. Dallas, 22-25 October 1995.

York, J. D and Firoozabadi, A., 2008. Comparing Effectiveness of Rhamnolipid Bio-surfactant with a Quaternary Ammonium Salt Surfactant for Hydrate Anti-Agglomeration. J. Phys. Chem., **112**, pp.845-851.

Chapter 8. Conclusions and Recommendations for Future Research

8.1. Conclusions

The lessons learned from this study could be used as valuable information on the feasibility of hydrate slurries transport and application of the *HYDRAFLOW* concept. The whole concept has been introduced and its main aspects have been investigated throughout the thesis. The *HYDRAFLOW* concept has been also compared with the current hydrate flow assurance techniques from both technical and economical viewpoints. An overview of the cost elements and the potential risk and uncertainty attached to each technique has been provided which helps to determine potential added value for each technique, hence, selecting the best practice.

With the particular aim of studying the flow properties of hydrate slurries, i.e. viscosity at high pressures, a purpose-built apparatus called the Helical Tube Impeller (HTI) setup was designed, built in house, calibrated and validated as part of this study. The HTI setup is a high pressure autoclave cell with a volume of about 2.5 litres equipped with a magnetic stirrer with adjustable rotational speed and voltmeter/ampere-meter to measures the voltage and current needed to calculate the torque, shear rate and viscosity. To examine the transferability of data from small scale to large scale experiments, a limited number of tests were performed in parallel both in the HTI set-up and in an in-house flow loop (C–FAR (Centre for Flow Assurance Research)). The

flow loop set-up comprises of a 1" (2.5 cm) diameter, 40 m length loop driven by a Moineau pump system.

To determine the feasibility of transportation of hydrate slurries in the context of the *HYDRAFLOW* concept, the aim of this thesis was to investigate:

- The rheological behaviour of hydrate slurries for various systems (low GOR and high GOR oil systems)
- The effect of AAs on the above systems
- The effect of degree of subcooling (or driving force), heat and mass transfer on hydrate growth rate, in different systems (e.g., low and high GOR oil systems) under different heat and mass transfer scenarios
- The effect of salt (NaCl) on the performance of AAs and consequently on the rheological behaviour and flow properties of water/oil/hydrate slurries at different watercuts (20% and 60%)
- The effect of produced water on the performance of AAs to validate the work done with NaCl (representing produced water) in this study
- The *HYDRAFLOW* concept in conditions where other flow assurance solutions either cannot be applied or are not economically viable, e.g. at high watercuts (>50%) or under very high degree of subcoolings
- The rheological behaviour of hydrate slurries at 70% and 90% water cuts without and with AA (oil soluble AA)
- Visual observation of hydrate slurries in the presence and absence of oil soluble AA at 90% water cut to support the rheological results
- The effect of shut-ins/restarts on the flow behaviour of hydrate slurries at different hydrate concentrations in the presence of AA
- The rheological behaviour of hydrate slurries at subzero conditions – Effect of combining thermodynamic inhibitors and AAs in the presence and the absence of salt
- The effect of different types of AAs (water-soluble and oil-soluble), salt (NaCl) and varying concentrations of methanol (0, 5 and 20 mass%) on the onset of hydrate formation and growth rate of hydrates

Additionally, a number of added benefits of the *HYDRAFLOW* concept were examined in this work. The specific objectives were to:

- Demonstrate reduced wax deposition problems in the presence of hydrates
- Measure the partitioning of AA between phases (hydrate, water and oil) and examine the efficiency of the distributed AA in each phase for recycling purpose – Application of the *HYDRAFLOW* 'loop' concept
- Test the performance of biodegradable (green) AAs – Application of the *HYDRAFLOW* 'loop' concept

The following conclusions were drawn from this study:

- Viscosity values of hydrate slurries in the C-FAR flow loop and laboratory scale HTI-set up are comparable, validating laboratory scale data.
- AAs can significantly reduce the viscosity of hydrate slurries, and therefore improving fluid transportability.
- The *HYDRAFLOW* concept can be applied to the tested low GOR oil system both without and with AA present as supported by the formation of transportable oil/hydrate/water slurries with viscosities suitable for pipeline transport.
- The *HYDRAFLOW* concept can be applied to the tested high GOR oil in the presence of a suitable AA as supported by the formation of transportable oil/hydrate/AA/water slurries.
- In both low and high GOR oil systems, the amount of hydrates formed was higher for the system with AA present. This can be attributed to smaller water droplet size and larger surface area in the AA treated system.
- All studied parameters including degree of subcooling, heat transfer (cooling rate), and mass transfer (mixing rate) affected the kinetic (rate) of hydrate formation. However, any increases in the mixing rate above a certain value (400 rpm) did not change the hydrate formation. The degree of subcooling had a more pronounced effect on hydrate formation rate than

the mixing and cooling rate at all the tested conditions. Finally, the high GOR oil system showed more sensitivity to changes in the mixing and cooling rates.

- The presence of salt (NaCl) improved the performance of the tested AAs and the transportability of water/oil/hydrate slurries in both low and high water cuts (20 and 60%).
- The tested AA was found to show equal or slightly better performance in presence of a multi-salt synthetic water (produced water) as it does with NaCl.
- In untreated systems, the viscosity data vs. amount of hydrates did not exhibit a very regular pattern. This can be attributed to the non homogeneous nature of the formed hydrate particles. Hydrates might be unevenly distributed in lumps of different shape and size inside the rig. Unlike the system without AA, the viscosity for the AA inhibited system had a regular trend which can be because of the formation of hydrate slurry in which hydrate particles are well dispersed in the system
- At both 70 and 90 % watercuts, the viscosity of the untreated and AA inhibited systems differed by one order of magnitude meaning that this tested oil soluble AA is very efficient, even at a water cut of 90%. In other words, the tested AA inhibited systems at high water cuts forms transportable oil/hydrate/water slurries as supported by the viscosity values. Visual studies of the tested oil-soluble AA were also consistent with the viscosity measurements. Visual observation at early stages of hydrate formation (0.5% hydrate) showed that the tested oil-soluble AA reduced the size of the hydrate particles significantly. At higher stages of hydrate conversion (20%), no lumps and no agglomeration were observed in the AA inhibited system, only fine slurry particles.
- The tested oil soluble AA shows equal performance during shut-in/restarts as it does in flowing conditions.
- The tested AAs (water-soluble and oil-soluble) were not effective in the presence of ice at subzero temperatures. By adding only 5 mass% methanol to the tested hydrate slurry systems containing AA, the viscosity of the

system at subzero temperatures (-5 to -15 ºC) was reduced significantly near to the viscosity values of the system without methanol at temperature range of 3–9.6 ºC and at similar hydrate concentrations. This means that combining 5 mass% methanol with the tested AAs improved the transportability of hydrate slurries at subzero conditions. The viscosity of the system with 20 mass% methanol was higher than the system with 5 mass% methanol at the same hydrate concentration. This could be attributed to the lower system temperatures for the 20 mass% methanol system at the same hydrate concentrations or to the higher viscosity of the carrier fluid (water/oil/methanol/AA). The amount of aqueous phase (water + methanol) is higher in the system with 20 mass% methanol compared to the system with 5 mass% methanol. According to these results and considering the fact that when hydrates do form, they take up only pure water and that the methanol concentration increases in the remaining aqueous phase suggests that adding 5 mass% methanol should be enough to prevent the negative effect of subzero conditions on the rheology of hydrate slurry systems inhibited with AAs.

- Rate of hydrate formation and also the amount of hydrate which can be formed at the same degree of subcooling were reduced in the presence of salt. The presence of methanol did not affect the rate of hydrate formation. However, the amount of hydrates which can be formed at the same degree of subcoolings was lower in the presence of methanol.

- Presence of salt reduced the viscosity of the system with or without AAs present. Methanol reduced the viscosity at the same temperature mainly because of the lower amount of hydrates formed. However, the presence of methanol increased the viscosity of the system at the same concentration of hydrate compared to a similar system without methanol. This may be attributed to the lower temperature and/or viscosity of carrier fluid (methanol increase the amount of aqueous phase and hence change the viscosity) and/or the higher rate of formation at the onset of hydrate formation

- Comparing the effect of 5 mass% methanol with 4 mass% salt on the viscosity of the water – oil – natural gas – oil soluble AA system, showed

that the viscosity of the system with 4 mass% salt is significantly lower than that of the system with 5 mass% methanol at the same hydrate concentrations.

- AAs can be deployed successfully at subzero condition in the presence of salt. In the absence of salt, the transportability of the fluid can be improved by adding few percents (5 mass%) of methanol to the system.
- Hydrate flow can reduce wax problems in pipelines. This can be mainly attributed to the abrasion of wax deposits by fast moving hydrate particles. This effect gets more pronounced as hydrate concentration increases or the hardness of wax deposits decreases.
- The hydrate phase incorporated some components of the tested AAs. However, the tested AA components absorbed in the oil phases were negligible. The concentration of the residual AA in the free water phase was higher than the concentration of the tested AA components dissolved/trapped in the hydrate phase.
- Both AA components remained in the free water and those trapped in the hydrate phase showed higher performance compared to the fresh AA. This could be due to higher concentration of AA components in these phases.
- The tested biodegradable compound improved the rheology of hydrate slurries compared to the untreated system (blank test without AA). Especially, its effect is more pronounced at lower hydrate conversions. However, it was not as effective as the tested commercial chemical AA. It should be mentioned that the performance of the biodegradable AA can be improved by using some synergic materials which are common for commercial AAs.

Overall, it was shown that there is a high potential for *HYDRAFLOW* to be implemented by the oil and gas industry due to its economical and technical benefits.

The results have shown that hydrocarbons can be transported in pipeline as hydrate slurries in low and high GOR oil systems. An industrial AA has been also successfully examined up to 90% watercuts. At subzero conditions, combining of 5 mass%

methanol and AA improved the transportability of hydrate slurries significantly. sever conditions where the hydrate viscosities were high

8.2. Recommendations for Additional Research

This thesis serves as a starting point for other researchers who wish to further investigate and understand the rheological behaviour of hydrates in pipeline and in particular the *HYDRAFLOW* concept as a risk management solution for hydrate problems in pipeline. Following issues are recommended for further studies.

- The results of this study showed that the *HYDRAFLOW* concept is viable in low and high GOR oil systems. It is recommended to expand the operation envelope of the concept into gas and gas condensate systems.
- The shut-ins/restart tests were carried only at high watercut (70%) which is one of the worse cases where hydrates can block the pipeline. It would be useful to conduct further tests in different systems or at different operating conditions.
- When studying the rheological behaviour of hydrate suspension in oil systems, it is recommended to investigate the effect of oil chemistry and emulsions on the viscosity of systems. In the *HYDRAFLOW* concept obtaining a transportable hydrate slurry can be obtained by finding suitable AAs for each type/group of oils/emulsions.
- To provide a very high level of confidence that the concept is viable at large scales, more experiments are needed to be conducted in flow loop.

Appendix A

A. 1 Oil composition (Oil 1)

Component	Mass%	Mole%
C_1	0.00	0.00
C_2	0.00	0.00
C_3	0.00	0.01
iC_4	0.00	0.00
nC_4	0.00	0.00
iC_5	0.00	0.00
nC_5	0.00	0.00
C_6s	0.02	0.05
C_7s	0.11	0.25
C_8s	0.54	1.07
C_9s	2.13	3.72
$C_{10}s$	3.42	5.38
$C_{11}s$	4.59	6.58
$C_{12}s$	6.34	8.30
$C_{13}s$	7.86	9.46
$C_{14}s$	8.71	9.66
$C_{15}s$	9.27	9.49
$C_{16}s$	9.09	8.63
$C_{17}s$	8.59	7.64
$C_{18}s$	8.43	7.07
$C_{19}s$	7.16	5.73
$C_{20}s$	6.61	5.06
$C_{21}s$	7.55	5.47
$C_{22}s$	3.85	2.70
$C_{23}s$	2.61	1.76
$C_{24}s$	1.69	1.10
$C_{25}s$	0.95	0.59
C_{26}^+	0.47	0.28

A. 2 Oil composition (Oil 2)

Component	Mass%	Mole%
C_1	0.00	0.00
C_2	0.00	0.00
C_3	0.00	0.02
iC_4	0.02	0.11
nC_4	0.05	0.22
iC_5	0.16	0.58
nC_5	0.15	0.54
C_6s	0.59	1.81
C_7s	2.21	5.90
C_8s	2.75	6.61
C_9s	2.33	4.96
$C_{10}s$	2.72	5.22
$C_{11}s$	2.78	4.87
$C_{12}s$	3.19	5.09
$C_{13}s$	3.87	5.69
$C_{14}s$	4.16	5.62
$C_{15}s$	4.40	5.49
$C_{16}s$	4.18	4.84
$C_{17}s$	3.76	4.08
$C_{18}s$	3.94	4.03
$C_{19}s$	3.61	3.53
$C_{20}s$	3.35	3.13
$C_{21}s$	3.11	2.74
$C_{22}s$	2.78	2.38
$C_{23}s$	2.69	2.21
$C_{24}s$	2.53	2.00
$C_{25}s$	2.65	2.02
C_{26}^+	38.02	16.31

A. 3 Oil composition (Oil 3)

Component	Mass%	Mole%
C_1	0.00	0.00
C_2	0.00	0.00
C_3	0.00	0.01
iC_4	0.00	0.02
nC_4	0.02	0.09
iC_5	0.01	0.07
nC_5	0.04	0.17
C_6s	0.11	0.43
C_7s	0.54	1.82
C_8s	1.10	3.28
C_9s	1.15	3.03
C_{10}s	1.54	3.68
C_{11}s	1.68	3.66
C_{12}s	2.08	4.14
C_{13}s	2.85	5.21
C_{14}s	2.96	4.98
C_{15}s	3.74	5.81
C_{16}s	3.04	4.38
C_{17}s	2.85	3.85
C_{18}s	2.90	3.69
C_{19}s	2.88	3.50
C_{20}s	2.79	3.24
C_{21}s	2.41	2.65
C_{22}s	2.34	2.49
C_{23}s	2.22	2.28
C_{24}s	2.10	2.07
C_{25}s	1.97	1.87
C_{26}^+	56.67	33.56

A. 4 Oil composition (Oil 4)

Component	Mass%	Mole%
C_1	0.00	0.00
C_2	0.00	0.00
C_3	0.00	0.00
iC_4	0.01	0.05
nC_4	0.02	0.07
iC_5	0.11	0.41
nC_5	0.07	0.26
C_6s	0.41	1.27
C_7s	1.55	4.15
C_8s	2.29	5.52
C_9s	1.98	4.23
C_{10}s	2.46	4.74
C_{11}s	2.57	4.52
C_{12}s	3.02	4.84
C_{13}s	3.63	5.36
C_{14}s	3.95	5.36
C_{15}s	4.35	5.45
C_{16}s	3.85	4.48
C_{17}s	3.38	3.68
C_{18}s	3.58	3.68
C_{19}s	3.10	3.04
C_{20}s	3.13	2.94
C_{21}s	2.80	2.48
C_{22}s	2.48	2.13
C_{23}s	2.44	2.02
C_{24}s	2.12	1.69
C_{25}s	1.97	1.51
C_{26}^+	44.72	26.14

A. 5 Diesel oil composition

Component	Mass%	Mole%
C_1	0.00	0.00
C_2	0.00	0.00
C_3	0.00	0.01
iC_4	0.00	0.00
nC_4	0.00	0.00
iC_5	0.00	0.00
nC_5	0.00	0.00
C_6s	0.02	0.05
C_7s	0.11	0.25
C_8s	0.54	1.07
C_9s	2.13	3.72
C_{10}s	3.42	5.38
C_{11}s	4.59	6.58
C_{12}s	6.34	8.30
C_{13}s	7.86	9.46
C_{14}s	8.71	9.66
C_{15}s	9.27	9.49
C_{16}s	9.09	8.63
C_{17}s	8.59	7.64
C_{18}s	8.43	7.07
C_{19}s	7.16	5.73
C_{20}s	6.61	5.06
C_{21}s	7.55	5.47
C_{22}s	3.85	2.70
C_{23}s	2.61	1.76
C_{24}s	1.69	1.10
C_{25}s	0.95	0.59
C_{26}^{+}	0.47	0.28

A. 6 Natural gas composition

Component	Mole%
C_1	88.83
C_2	5.18
C_3	1.64
iC_4	0.16
nC_4	0.27
iC_5	0.04
nC_5	0.04
CO_2	2.24
N_2	1.6

A. 7 Produced water coposition

Ion	Mg/L
Na^{+}	53300
Mg^{2+}	1823
Ca^{2+}	3895
Sr^{2+}	139
Ba^{2+}	131
Cl^{-}	94465
$HCO3^{-}$ *	283
$SO4^{2-}$ *	10

* Calcium carbonate and a little barium sulphate scales were observed in the synthetic brine; therefore, bicarbonate and sulphate ions were removed.

Appendix B

Determination of Amine and Quaternary Amine Inhibitor in Aqueous Solution

B.1 Introduction

This method is based on the fact that Beer's Law is valid for a chloroform extract of a dye transfer complex that forms between TROS corrosion inhibitors and mixed bromocresol dyes. This method was developed in-house.

B.2 Method

The concentration of the corrosion inhibitor in an unknown aqueous sample is determined as follows

1. Separate as much oil as possible from the sample using a separating funnel or centrifiguation. Avoid the use of filter paper as this may remove some of the corrosion inhibitor components.

2. Samples from gas lines may contain significant amounts of MEG or other glycols. It is recommended that such samples are diluted with water in aratio of 90% water to 10% sample in order to reduce any influence of the glycol on the analysis. Note that this of course will also dilute the corrosion inhibitor present but that this is probably tolerable for most gas line samples since the corrosion inhibitor concentration is likely to be fairly high anyway (ie hundreds of ppm). The calibration curve should also be obtained using the diluted solvent system.

3. Add 50 ml of the aqueous sample to a 250 ml separating funnel.

4. Add 10 ml of buffer/indicator solution (see Section 3) to the separating funnel.

5. Add 10 ml of chloroform to the separating funnel.

6. Place a stopper in the separating funnel and shake vigorously for 30 seconds.

7. Allow the layers to separate and draw off the chloroform layer (at the bottom) through a phase separation paper (Whatman IPS : to remove water droplets) into a 20 ml volumetric flask

8. Repeat steps 2.5, 2.6 and 2.7 with a further 10 ml of chloroform and draw it off into the same 20 ml volumetric flask.

9. Measure the absorbance of the chloroform extract against clean chloroform at 425 nm wavelength using 1 cm quartz cells in a UV/VIS spectrophotometer.

10. Obtain the absorbance for a blank sample, following steps 2.2 through to 2.8, using a corrosion inhibitor free sample of the water or MEG, or if this is not available, a sodium chloride solution of the same salinity as the sample water.

11. Subtract the blank absorbance reading from the sample reading to get the corrected absorbance reading for the test sample.

12. Prepare a calibration profile of corrected absorbance readings versus concentration by testing freshly made solutions of corrosion inhibitor covering a range of known concentrations. The solutions should be made up using a corrosion inhibitor free sample of the water, or if this is not available, a sodium chloride solution of the same salinity as the sample water.

13. The ppm of corrosion inhibitor is calculated using the calibration profile. The calibration profile (ie absorbance vs concentration) may be linear or curved. The calibration profile should be used directly. In other words, do not attempt to linearise a curved profile.

14. If the extract absorbance is too high for the calibration curve then either extend the calibration curve to higher concentration, or dilute the test sample and repeat the measurement.

B.3 Buffer/Indicator Solution

The buffer/indicator solution should be made up as follows:

50 mls of 0.2% w/v Bromophenol Blue in Methanol

50 mls of 0.2% w/v Bromocresol Green in Methanol

420 mls of 0.1 Molar Citric Acid

580 mls of 0.2 Molar Disodium Phosphate

Adjust the pH to 5.6 with citric acid or sodium hydroxide.

B.4 Notes

1. Some samples tend to produce solid material which attracts blue dye and then falls into the yellow chloroform layer. These solids can be removed from the chloroform layer by gentle agitation of the sample with a glass rod. This will ensure there is no contamination in the chloroform layer.

2. In water samples which contain solids (eg iron oxides, iron sulphides) it is possible that some corrosion inhibitor can adsorb onto the surface of the solid and so is possibly not detected by the colorimetric method. This would lead to an underestimate of the true residual concentration. One option for overcoming this difficulty is to adjust the pH of the buffer solution to 2 instead of 5.6. The lower pH is sufficient to dissolve many types of solid prior to the addition of chloroform. The lower pH has the effect of turning the buffer solution red instead of blue. Also it causes the blank absorbance values to be rather high at 425 nm. Nevertheless, development work shows that pH 2 still allows accurate measurement of residual quats.